O.K.

ISAS - INTERNATIONAL SCHOOL FOR ADVANCED STUDIES

Mechanisms controlling rhythmicity in the neonatal rat spinal cord *in vitro*

Thesis submitted for the degree of "Doctor Philosophiae"

Candidate:
Cristina Marchetti

Supervisor
Prof. Andrea Nistri

SISSA - SCUOLA
INTERNAZIONALE
SUPERIORE
STUDI AVANZATI
TRIESTE
Via Beirut 2-4

TRIESTE

TABLE OF CONTENTS

NOTE

Part of the data reported in the present thesis has been published in the articles listed below. In all cases the candidate personally performed the experimental work and data analysis, and contributed to paper writing.

Marchetti, C., Beato, M., & Nistri, A. (2001). Alternating rhythmic activity induced by dorsal root stimulation in the neonatal rat spinal cord in vitro. *J. Physiol.* **530**, 105-112.

Marchetti, C., Beato, M., & Nistri, A. (2001). Evidence for increased extracellular K^+ as an important mechanism for dorsal root induced alternating rhythmic activity in the neonatal rat spinal cord in vitro. *Neurosci. Lett.* **304**, 77-80.

Marchetti, C. & Nistri, A. (2001). Neuronal bursting induced by NK_3 receptor activation in the neonatal rat spinal cord in vitro. *J. Neurophysiol.* **86**, 2939-2950.

Marchetti, C., Pagnotta, S., Donato, R., & Nistri, A. (2002). Inhibition of spinal or hypoglossal motoneurons of the newborn rat by glycine or GABA. *Eur. J. Neurosci.* **15**, 975-983.

The work on metabotropic glutamate receptors has been done in collaboration with Dr. Giuliano Taccola.

ABSTRACT

The present study has investigated the rhythmic properties of spinal networks in the neonatal rat spinal cord *in vitro*, by means of intracellular recordings from single motoneurons and extracellular recordings from ventral roots.

The occurrence and basic characteristics of an alternating locomotor-like pattern, triggered by stimulating afferent dorsal root fibers, was described, suggesting that sensory inputs from the periphery can activate the spinal locomotor network. It was proposed that activation of the locomotor CPG could occur via an increase in extracellular K^+ and network neuron depolarization.

Furthermore, it was demonstrated that spinal networks could generate rhythms exhibiting a variety of different properties in terms of phase, frequency, and duration of patterns. Due to the importance of inhibitory transmission in shaping such rhythmic patterns, and the complex role that glycine and GABA seem to have in the developing central nervous system, the nature and function of Cl^- mediated synaptic transmission was investigated on motoneurons. To this aim, the glycinergic and GABAergic recurrent postsysnaptic potential (PSP) mediated by Renshaw cells was used to assess its impact on excitatory synaptic inputs from dorsal afferent fibers. Despite its depolarizing nature, the recurrent PSP consistently inhibited synaptic excitation of lumbar motoneurons.

Different patterns of rhythmic activity were obtained by activating certain classes of metabotropic receptors present in the spinal cord. In particular, tachykinin NK_3 receptors could trigger neuronal bursting, which outlasted the stimulus and appeared predominantly with alternation at segmental level and synchronous coupling between ipsilateral motor pools. Such bursting was accompanied by depression of GABAergic dorsal root potentials evoked by dorsal root stimulation and of the recurrent inhibitory PSP recorded from motoneurons, indicating the possibility that fully alternating pattern generation by the CPG was partly impaired due to a decrease in the efficacy of inhibition. Nevertheless, NK_3 receptor activation could facilitate fictive locomotor patterns, since they could operate synergistically with NMDA and 5-HT to trigger fully alternating locomotor-like rhythms. Furthermore, NK_3 receptor antagonism disrupted NMDA and 5-HT induced fictive locomotion.

Activation of glutamate metabotropic receptors elicited a wide range of effects. Group I receptors mediated depolarization and onset of oscillatory activity (via the subclasses mGluR1 and 5, respectively), which usually appeared synchronously at homosegmental and homolateral level. This type of rhythm represented another example of pattern that spinal cord networks could generate in addition to previously reported ones. While the role of group I metabotropic glutamate receptors in fictive locomotion was limited, they seemed to participate in regulating disinhibited rhythm, i.e. bursting induced by block of GABA and glycine receptors. In addition to an excitatory effect, group I receptors also reduced reflex responses, at least partly via facilitation of endogenous glycine transmission. Group II and III metabotropic glutamate receptors, on the other hand, were always inhibitory on spinal neurons and their bursting behavior. Experiments performed with selective agonists and antagonists indicated that group II and III receptors could modulate, and were involved in controlling, the duration and frequency of disinhibited bursts.

Thus, the present study broadened our current understanding of the rhythmic patterns generated by spinal networks and identified certain forms of oscillatory behavior as induced by activation of selective classes of transmitter receptors.

INTRODUCTION

1. RHYTHMIC ACTIVITY: A WIDESPREAD BEHAVIOR IN THE CENTRAL NERVOUS SYSTEM

The ability to generate rhythmic activity is widespread throughout the central nervous system (CNS). While it is present in developing neural networks in many areas of the brain and in the spinal cord, it is also a distinctive feature of several adult neural structures, where it is involved in a number of activities such as sleep, memory and locomotion. Given its importance, rhythmic activity has been widely studied in a variety of species at different developmental stages and in different experimental conditions. One common aim of these studies is the understanding of general principles which underlie the genesis of rhythmicity in a network. To this end, more specific issues can be addressed, such as investigating what classes of neurons generate activity, which mechanisms initiate and terminate this activity, and what are the factors involved in determining its spatio-temporal organization.

Rhythmic activity at different levels (from population of neurons to single cells) can be detected by a variety of recording techniques. For example, while electroencephalografic (EEG) recordings allow monitoring surface field potentials arising from the collective, synchronous, activity of a large number of neurons, intratissue extracellular recordings are used to detect electric field potentials generated by a limited number of closely spaced neural units. Furthermore, intracellular recordings (by means of sharp microelectrodes or patch-clamp electrodes) detect the time course of the membrane potential (or transmembrane current) of a single neuron.

1.1 Rhythmic patterns in the developing CNS

While rhythmic activity in the developed CNS is thought to be associated with a specific behavior or task performance of the animal, spontaneous activity of the developing nervous system is a widespread, but transient feature, believed to be important at the level of network circuitry, i.e. for network refinement of the initial connectivity (Katz & Shatz, 1996). This activity has been recorded from several developing neural circuits (Feller, 1999). Although

the structure of spontaneous activity differs in details, there is a global or "macroscopic" pattern: the spontaneous activity consists of rhythmic bursts of action potentials correlated across tens to hundreds of cells and occuring with a periodicity of the order of minutes. Examples of neural circuits that exhibit spontaneous action potentials are the retina (Galli & Maffei, 1988; Meister *et al.*, 1991; Feller *et al.*, 1996), the embryonic spinal cord (Landmesser & O'Donovan, 1984a Nishimaru *et al.*, 1996; see rest of INTRODUCTION) and the hippocampus (Ben Ari *et al.*, 1989; Gaiarsa *et al.*, 1990; Garaschuk *et al.*, 1998). In the latter case, early in postnatal development, spontaneous network-driven oscillatory events, termed giant depolarizing potentials (GDPs), occur synchronously over the entire hippocampus (Ben Ari *et al.*, 1989; Cherubini *et al.*, 1991). These events, which can be recorded either from hippocampal slices (Ben Ari *et al.*, 1989) or the intact hippocampus (Khalilov *et al.*, 1997), are generated by the interplay between GABA and glutamate (Ben Ari *et al.*, 1997; Bolea *et al.*, 1999).

It is useful to compare the different strategies used by the various periodically active networks as some general properties, but also important differences, emerge. For example, it has been proposed that local oscillator networks, present in the spinal cord, might function through basic mechanisms which are not specific to spinal networks but are inherent properties of many neural networks (Darbon *et al.*, 2002). Among such inherent properties, synaptic depression (O'Donovan & Rinzel, 1997; Staley *et al.*, 1998) and activity dependent changes in neuronal excitability (Maeda *et al.*, 1995; Sanchez-Vives & McCormick, 2000; Streit *et al.*, 2001) have been proposed to be critically involved in bursting.

1.2 Rhythmic patterns underlying brain activity

Several rhythmic patterns can be associated with different behavioral states. For example, different phases of sleep are accompanied by major changes in EEG recordings (reviewed by Steriade, 1994; Sejnowski & Destexhe, 2000): at the onset of sleep, brief episodes of 7-14 Hz synchronous spindling occurs in the thalamus and cortex, producing large-scale spatio-temporal coherence throughout the forebrain. These oscillations are generated in the thalamus as the result of synaptic interaction and intrinsic membrane properties of thalamocortical and reticular thalamic neurons connected in a recurrent loop by inhibitory and excitatory connections. During sleep, the low-amplitude, high frequency activity is replaced with high amplitude, low frequency rhythms called delta waves, having a frequency of 1-4 Hz. A delta-frequency rhythm can be generated in single cells by the interplay of two intrinsic currents of

thalamocortical neurons: the hyperpolarization-activated cation current (I_h) and the transient low-threshold Ca^{2+} current (I_T). A wide variety of other ionic currents with different voltage dependencies and kinetics contribute to shaping the amplitude and time-course of each burst of action potentials, as revealed both by biological experiments and computational modeling. Furthermore, synaptic connections are still obviously needed to ensure synchronization. Although it is thought that the purpose of the widespread activity that occurs in the brain during sleep might be memory consolidation, there is no consensus around this issue (Sejnowski & Destexhe, 2000).

Fast spontaneous oscillations (20-100 Hz) have also been recorded in aroused animals in several parts of the cortex and in the hippocampus (Jefferys *et al.*, 1996), suggesting synchronization between intracortical and cortical networks during the normal operation of the brain. Another important rhythm which has been recorded in the hippocampus, and in other cortical structures (Steriade, 2000) is the so-called theta rhythm (4-12 Hz). Although the theta rhythm in the hippocampus seems to be correlated to spatial exploration (Bragin *et al.*, 1995), also in this case no consensus has emerged on the relevance of this rhythm (Buzsaki, 2002).

In pathological conditions, such as epilepsy, paroxysmal synchronization of neural activity gives rise to rhythmic discharges in the hippocampus. Such synchronization is the result of an impairement of synaptic inhibition circuitry due to a decrease in fast synaptic inhibition (Fisher & Alger, 1984).

While important progress in the description and understanding of cellular and network oscillations of these systems has been achieved, the extreme complexity of the brain has so far precluded a satisfactory and widely accepted comprehension of the functional role of the various rhythmic patterns. In this respect, the spinal cord is a more advantageous system, in which oscillatory activity can be readily associated with basic rhythmic motor tasks, such as mastication, respiration and locomotion.

1.3 Pacemaker neuron driven *versus* network driven rhythmicity

There are two different mechanisms by which a network can generate rhythmic behaviors:

- Pacemaker neuron driven rhythmicity: one or more cells in the network possess the intrinsic ability to produce membrane potential oscillations due to a particular interplay between their voltage dependent conductances.

- Network driven rhythmicity: the elements of the network, when synaptically isolated, cannot oscillate and the ontogeny of rhythmic activity mainly relies on the pattern of connectivity between cells in the network.

It is worth noting that in the first case, synaptic connections are still necessary to ensure synchronicity within the network. Furthermore, in both mechanisms, the intrinsic membrane properties of a neuron will also affect the overall network activity, since they determine the input-output relation of every cell.

1.4 Functional role of rhythmicity in the spinal cord: motor behavior and definition of the Central Pattern Generator (CPG)

Contrary to many other areas in the CNS in which oscillatory activity does not have a clear connection to specific behavioral tasks, rhythmic activity generated by spinal networks are readily correlated to motor tasks such as mastication, respiration and locomotion. In the intact animal, activation of spinal cord circuitry is triggered by inputs coming from higher brain centers. Nevertheless, it has been shown that the basic features of locomotion can be generated also in the absence of descending inputs (Sherrington, 1898) or sensory feedback (Brown, 1911), indicating the presence in the spinal cord of a localized network, responsible for rhythm generation. Such network is termed Central Pattern Generator (CPG).

Whereas early progress toward the understanding of locomotor circuits originated from studies in the decerebrated or spinal cat *in vivo*, a detailed analysis of the electrophysiological and pharmacological properties of the CPG elements requires the use of *in vitro* techniques. The *in vitro* preparation is in fact more accessible, allowing greater control of the parameters involved, such as fine tuning of the use of pharmacological tools. When recorded *in vitro*, coordinated rhythmic patterns that give rise to locomotor activity are called "fictive locomotion" to indicate the absence if a real limb movement.

2. ORGANIZATION OF THE NEONATAL RAT SPINAL CORD

The spinal cord is the most caudal structure of the CNS and plays a major role in the motor functions of vertebrates. It is considered the lower station of a hierarchical motor system that includes the brainstem and the motor cortex. By receiving proprioceptive and sensory inputs from internal organs, muscles and skin, the spinal cord also plays a crucial role in relaying

and/or processing somatosensory information. Spinal networks are connected to supraspinal centers by ascending and descending pathways. Important relay stations are found in the brainstem and in the thalamus, while descending pathways involve, in addition to direct corticospinal tracts, the basal ganglia, the cerebellum and the brainstem.

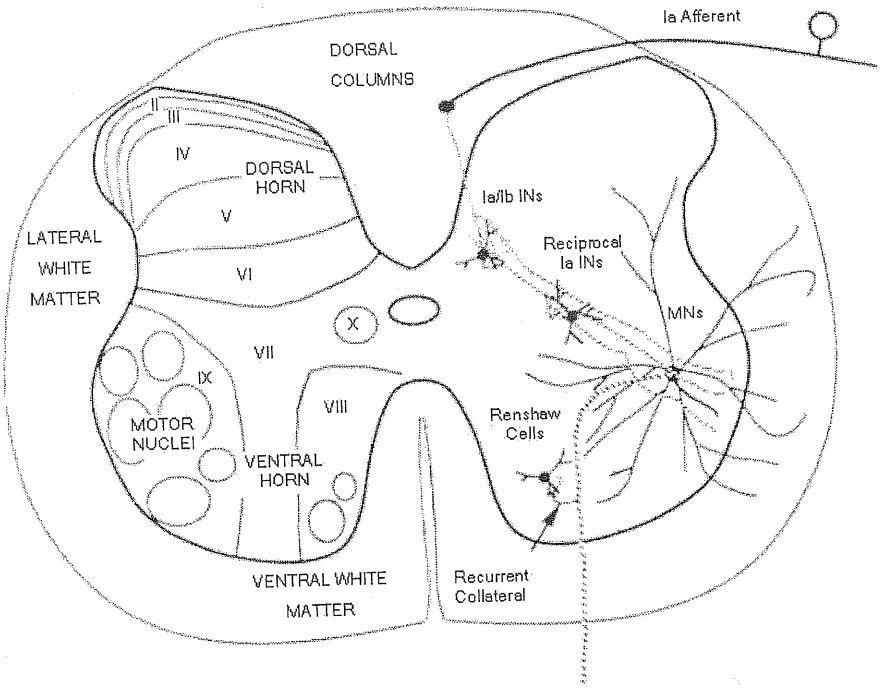

Figure I. Diagram of the spinal cord in cross section (adapted from Burke, 1990).

2.1 Laminar and Segmental Organization

The outer part of the spinal cord of the rat is formed by white matter that contains ascending and descending axons, located in the dorsal, lateral and ventral columns that run parallel along the rostrocaudal direction of the cord. The inner region is formed by gray matter that contains the cell bodies of the spinal neurons and the synaptic neuropile. A cross section of the spinal cord shows that the gray matter has a butterfly-shaped appearance, with the dorsal horns (elongated towards the region where the dorsal roots enter the cord), an intermediate region and two large ventral horns. The gray matter is divided into 9 laminae (I-IX) surrounding the central canal (X) region (Figure I), according to the morphological features of the cells located in each lamina (Rexed, 1952). The laminae superficially located in the dorsal horns (laminae I-IV) contain neuronal organizations that process incoming afferent

information. The functional identity of the many neurons in the intermediate portion of the gray matter (laminae V-VIII) are much less clearly delineated in terms of functions and morphology, although progress is being made (see Jankowska, 2001 for a review). The larger cells making up laminae VIII and IX are the output cells, namely motoneurons.

Along the rostro-caudal axis, the rat spinal cord is subdivided into cervical, thoracic, lumbar and sacral regions, which control movement of, respectively, forelimbs, chest, hindlimbs, and tail and sphincters. At the cervical and lumbar level, two enlargements are present where a higher density of motoneurons is located. All 4 regions are further subdivided into segments that in the rat are named as follows: cervical C1-C5, thoracic T1-T13, Lumbar L1-L6, and sacral S1-S4

2.2 Motoneurons

Motoneurons represent a special class of cells in the CNS since they not only innervate nonneural tissue (i.e. muscle fibers), but also have a precisely defined functional role, i.e. they provide the output of the CPG to muscles, in order to activate them. These properties allow motoneurons to be accessible and identifiable with electrophysiological recordings (through antidromic stimulation of the corresponding ventral root, VR), and thus endow the spinal cord preparation with great experimental advantage.

Motoneuron cell bodies and their dendritic extensions lie within the ventrolateral gray matter, clustered together in circumscribed motor nuclei; such nuclei are cigar-shaped, longitudinal structures located along the rostro-caudal axis of the ventral horn (Burke, 1981). There are two main kinds of motoneurons in mammals: *alpha* and *gamma*. *Alpha* motoneurons, characterized by a large somata and dendritic tree and fast (>60 m/s) conduction velocity of their axons, innervate extrafusal striated muscle fibers to produce muscle contraction. *Gamma* motoneurons, while having smaller somata and less branched dendritic tree, innervate intrafusal muscle fibers within muscle spindle receptors. Dendrites of both kinds of cell spread considerably (up to 2 mm, Cullheim *et al.*, 1987) outside the border of their nucleus, to invade both adjacent gray and white matter, where they receive synaptic contacts (Rose & Richmond, 1981).

2.3 Afferent fibers

Afferent fibers, whose cell bodies are contained in the dorsal root ganglia outside the cord, enter the spinal tissue at each segmental level through the dorsal roots (DRs). They are

classified on the basis of their conduction velocity (which is proportional to the fiber diameter; Hunt, 1954). As far as sensory fibers are concerned, group Ia afferents transmit information about muscle length (with the largest conduction velocity, 90-120 m/s in the adult cat), while group II afferents signal muscle length variation (slower, 35-75 m/s); also, group Ib arises from Golgi tendon organs and signals muscle tension (conduction velocity 70-90 m/s). Nociceptive fibers are classified according to their diameter and conduction velocity: Aβ>Aδ>C. With the exception of group C, all these afferents are composed by myelinated fibers. The synapses of primary afferents on spinal (or brainstem) neurons are thought to be always of excitatory type (Burke, 1990). The only fibers that are thought to impinge monosynaptically on motoneurons are group Ia fibers (these fibers also excite several classes of interneurons in the ventral and dorsal laminae).

2.3.1 The stretch reflex

Group I and II fibers are involved in several spinal reflexes that have been extensively investigated starting from the last century (reviewed by Baldissera *et al.*, 1981). The classical work by Eccles *et al.* (Eccles *et al.*, 1954) has cast light over several relatively simple spinal circuits, such as the stretch reflex. In this pathway, the stretching of a muscle excites Ia afferents that in turn excite motoneurons innervating the same muscle. This produces a positive feedback to contract the muscle. The stretch reflex can be recorded on motoneurons following activation of Ia fibers and consists of an excitatory monosynaptic reflex followed by a polysynaptic one. *In vitro* experiments have shown that the excitatory action is mainly mediated by the aminoacid glutamate, acting both on N-Methyl-D-Aspartate (NMDA) and non-NMDA receptor subtypes (Pinco & Lev-Tov, 1993a; Pinco & Lev-Tov, 1993b), although a slow serotoninergic component has also been observed (Elliott & Wallis, 1992). Activation of Ia fibers also produces a disynaptic inhibition in motoneurons innervating antagonist muscles, thus further facilitating contraction. This circuitry is known as the reciprocal inhibition pathway and is schematically depicted in Figure II.

2.3.2 Primary Afferent Depolarization (PAD)

Stimulation of afferents from antagonist muscles was found to reduce group Ia EPSPs in motoneurons without producing detectable IPSPs. This phenomenon is associated with a depolarization of the primary afferents (PAD) and is considered to be due to a presynaptic axo-axonic inhibition of the Ia terminals (Burke, 1990). Presynaptic inhibition in several

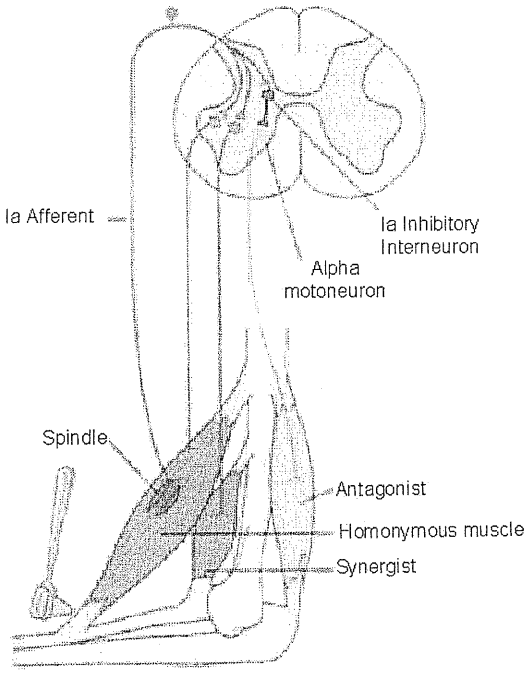

Figure II. Schematic view of the circuit mediating the stretch reflex.
Ia afferent fibers from muscle spindles make excitatory connections on two sets of motoneurons: alpha motoneurons that innervate the homonymous muscle from which they arise and motoneurons that innervate synergist muscles. They also act through inhibitory interneurons to inhibit the motoneurons that innervate antagonist muscles.

systems is fully abolished by the $GABA_A$ antagonists pixtrotoxin and bicuculline (Nistri, 1983; Sivilotti & Nistri, 1991) and is thought to be mediated by $GABA_A$ receptors that exert a depolarizing action on primary afferent terminals presumably due to the fact that the chloride equilibrium potential is more positive than the resting membrane potential in these terminals (Burke, 1990; Stuart & Redman, 1992). Although the precise mechanism by which PAD inhibits transmitter release is not known, the prevailing hypothesis is that it inactivates Na^+ channels sufficiently to block action potential invasion into the terminals (or reduce action potential amplitude), thereby suppressing transmitter release. Transmitter-induced membrane shunts and inactivation of Ca^{2+} currents may also contribute (Rekling *et al.*, 2000). Furthermore, an involvement of $GABA_B$ receptor subtypes, whose activation causes no depolarization in primary afferents, has also been shown, suggesting a role in presynaptic inhibition independent of PAD, but due to reduced influx of calcium in the terminals. These

mechanisms are not mutually exclusive, although there is much evidence in favor of a causal association between PAD and presynaptic inhibition (Burke, 1990).

2.4 Renshaw Pathway

The early studies by Eccles and co-workers (Eccles *et al.*, 1954) on cat allowed identification and characterization of another important pathway, i.e. the one mediated by Renshaw cells. Renshaw firstly described inhibition of motoneurons following antidromic activation of their axons. Upon such stimulation, axon collaterals branching from VRs monosynaptically excite Renshaw cells (through a cholinergic synapse), which in turn make synaptic connections on the same and related motoneurons. These connections have been shown to be mediated by the neurotransmitters γ-aminobutyric acid (GABA) and glycine in the adult cats (Cullheim & Kellerth, 1981) and, under certain conditions (see §2.5), in the rat (Schneider & Fyffe, 1992). In the intact spinal cord, Renshaw cells receive convergent excitatory post-synaptic potentials (EPSPs) from many neurons with different strengths (Burke & Rudomin, 1977; Baldissera *et al.*, 1981). This system provides a negative feedback, allowing fine tuning of the excitability of motoneurons.

2.5 Is the role of GABA and glycine transmitters developmentally regulated?

Although it is well accepted that GABA and glycine are inhibitory transmitters in the adult brain (Curtis & Johnston, 1974; Krnjevic, 1974), their role during early neuronal development is still debatable. GABA or glycine-mediated currents shift from depolarizing to hyperpolarizing in relation with the transmembrane Cl^- gradient that changes due to maturation of Cl^- transporters (Rivera *et al.*, 1999). An important question is whether this early depolarizing effect by GABA (or glycine) exerts an excitatory or inhibitory action on neonatal neurons, as data appears controversial even from the same region. For example, in the newborn rat hippocampus GABA is considered to be one major excitatory neurotransmitter (Cherubini *et al.*, 1991) acting synergistically with glutamate (Ben Ari *et al.*, 1997). Furthermore, GABA-evoked excitation can even be neurotoxic (Lukasiuk & Pitkanen, 2000). Conversely, on hippocampal pyramidal cells at postnatal (P) days 0-2 (Lamsa *et al.*, 2000), depolarizing $GABA_A$ receptor-mediated transmission is thought to be strongly inhibitory on glutamatergic transmission (Lamsa *et al.*, 2000).

On developing hypothalamic neurons, the action of GABA is biphasic with early inhibition followed by facilitation of excitatory events (Gao *et al.*, 1998). Furthermore, GABA-induced

excitation is regarded as the primary process to drive action potentials (Gao & van den Pol, 2001).

On brainstem motoneurons the effect of glycine or GABA shifts from depolarization to hyperpolarization during the first 2-3 postnatal weeks, together with changes in their receptor structure and associated channel kinetics (Rekling *et al.*, 2000; Singer & Berger, 2000). Parallel to these alterations, the reversal potential of glycinergic currents becomes very negative at P18 (Singer *et al.*, 1998).

In the spinal cord, GABA or glycine depolarizes P1-P3 motoneurons (Wu *et al.*, 1992; Gao & Ziskind-Conhaim, 1995), and cultured dorsal horn neurons (Reichling *et al.*, 1994; Wang *et al.*, 1994). Despite the depolarizing nature of these responses, they are thought to be inhibitory because of shunting of excitatory currents by the Cl^- conductance increase (Wu *et al.*, 1992; Gao & Ziskind-Conhaim, 1995; Singer *et al.*, 1998; see also Staley & Mody, 1992 for dentate gyrus granule cells). Furthermore, GABA-mediated depolarization of primary afferent terminals is responsible for presynaptic inhibition (Eccles *et al.*, 1963; see also § 2.3.2).

Even in the case of the spinal cord there are, however, reports of an excitatory role of GABA or glycine (Nishimaru *et al.*, 1996; Chub & O'Donovan, 1998). On young mouse spinal neurons, GABA apparently contributes more than glutamate to induction of action potentials (Gao & van den Pol, 2001).

In the present study, the question of whether, in neonatal rats, Renshaw cell mediated GABAergic or glycinergic transmission (see § 2.4) inhibits excitatory synaptic inputs to spinal motoneurons will be addressed (see RESULTS, § 2).

3. AN OVERVIEW OF SPINAL RHYTHMIC PATTERNS

3.1 From lamprey to mammals

To enable a cellular analysis of basic patterns of motor behavior in mammals, a number of *in vitro* preparations have been developed, usually taken from the embryonic or neonatal stage, because their brainstem-spinal cord is easier to maintain and oxygenate properly. These preparations, obtained from rat (for reviews, see Cazalets & Bertrand, 2000; Kiehn *et al.*, 2000; Lev-Tov & Delvolve, 2000) and mouse (Delvolve *et al.*, 1999) have provided valuable insights to the organization of pattern generators at several levels of the brainstem-spinal

cord, including the complex neuropharmacology of the locomotor network. Nevertheless, there is yet insufficient knowledge of the interneuronal connectivity (Grillner, 2000). For this reason, studies from lower vertebrates, such as the lamprey and the frog embryo, or from birds, like the chick embryo, have proven to be useful experimental models for higher vertebrate functions, since they can provide detailed information on some cellular processes involved in rhythmogenesis.

The isolated **embryonic chick spinal cord** is spontaneously active and produces episodes of rhythmic bursting lasting about 1 min, followed by 10–20 min of silence (Landmesser & O'Donovan, 1984b). Each episode comprises several cycles of activity in which flexor and extensor motoneurons discharge rhythmically. At the beginning of a spontaneous episode the activity of flexors and extensors is synchronized and only after some cycles alternation develops. The application of excitatory amino acids can turn the spontaneous episodes into a continuous pattern (Barry & O'Donovan, 1987). In this system, the ability to express rhythmicity has been found to be distributed along the rostrocaudal axis of the cord; yet, even a single, isolated segment can perform rhythmic activity. Experiments with selective lesions (Ho & O'Donovan, 1993) or application of specific antagonists (namely bicuculline, Sernagor *et al.*, 1995) show that rhythmogenesis and alternation are produced by anatomically distinct, but overlapping (O'Donovan *et al.*, 1998) networks.

Regarding studies on **mammalian locomotion**, much effort has been done to understand its ontogenesis, since the pioneer studies of Sherrington (Sherrington, 1898) and Brown (Brown, 1911). *In vivo*, locomotion can be studied by means of muscle fiber recordings (electromyograms) or nerve recordings (in which the activity of nerve branches supplying identified muscles is monitored). Locomotion is characterized by rhythmic bursts alternating between flexor and extensor muscles within one limb and with the controlateral limb. Details of the phase relationship and burst duration in each muscle subserving the ankle, the knee and the hip within one step cycle are far more complex (Rossignol, 1996; Kiehn & Kjaerulff, 1996). The area of the brainstem named mesencephalic locomotor region (MLR) plays an important role in the supraspinal control of locomotion. In fact, in the decerebrated cat, stimulation of the MLR can induce locomotion, the frequency of which depends on the stimulation intensity (Shik *et al.*, 1966). Also chemical stimulation of the brainstem by GABA antagonists (that induce bursting in neurons in the brainstem) can induce episodes of

locomotion, thus indicating that a descending excitatory input from the brainstem is converted into rhythmic pattern by a spinal pattern generator (Garcia-Rill *et al.*, 1985).
Following the observation that MLR stimulations could elicit locomotor patterns, further investigations were performed to clarify whether the descending locomotor command could be mimicked by pharmacological application of neurotransmitters. For the spinalized cat in particular, it has been found that the administration of the noradrenaline precursor L-DOPA (Grillner, 1981) or of the noradrenergic receptor agonist clonidine (Forssberg & Grillner, 1973) can evoke locomotion. On the contrary, serotoninergic agonists can facilitate and modulate locomotion, but fail to initiate it *in vivo* (Barbeau & Rossignol, 1991). Glutamate transmission plays a central role, since glutamate uptake blockers can induce fictive locomotion in cats and application of either NMDA or non-NMDA receptor antagonists block MLR-evoked locomotion (Douglas *et al.*, 1993; see also Beato *et al.*, 1997).
Another crucial result came from the observation that, when a mechanical contraint is applied to one hindlimb, fictive locomotion is impaired in the constrained limb, but can still be observed in the opposite limb (Edgerton *et al.*, 1976; Grillner, 1981). This evidence suggests that each synergistic group of muscle is subserved by an individual rhythm generator, producing rhythmic output even if the output of the other generators is impaired. According to this theory, different stereotypic motor behaviors would result from different coupling modes between such units.

3.2 The neonatal rat spinal cord as a model to study locomotor activity

The preparation of the neonatal rat spinal cord maintained *in vitro* was introduced by Otsuka and Konishi in 1974 (Otsuka & Konishi, 1974). This preparation remains viable for several hours when superfused with a saline solution that reproduces the composition of the cerebrospinal fluid. It has been used to study the central pattern generation since 1987, when Kudo and Yamada reported that bath application of NMDA induces locomotor-like activity in the spinal cord with attached hindlimbs. Since then, the isolated spinal cord of the neonatal rat has been used to study both the developmental aspects and the cellular bases of locomotor activity.

3.2.1 Recording techniques

In the original paper by Kudo and Yamada (Kudo & Yamada, 1987), the preparation consisted of the spinal cord with both hindlimbs attached and recordings were performed

with electromyograms from left and right tibialis anterioris and gastrocnemius. *In vitro* recordings from muscles show their exact phasing within a locomotor cycle, thus allowing a good comparison with muscle phasing in the intact animal (Kiehn & Kjaerulff, 1996; de Leon *et al.*, 1994; Gruner & Altman, 1980). Such an advantage can also be achieved with nerve recordings, typically obtained from branches of the sciatic nerve (femorotibialis and common peroneal) that innervate antagonist muscles (Cowley & Schmidt, 1994a; Cowley & Schmidt, 1994b). However the large majority of experiments uses ventral root recordings. A possible limitation of this technique is due to the fact that each ventral root contains axons from all the motoneurons at the same segmental level, although these motoneurons innervate different muscles. It is thus possible that some mixture of extensor and flexor activity could mask the rhythmic pattern when recording from ventral roots (Cowley & Schmidt, 1994b). Nevertheless, several studies have shown that the L1 and L2 ventral roots predominantly innervate flexor muscles, while L5 innervates extensor muscles (Kiehn *et al.*, 1992; Kiehn & Kjaerulff, 1998). As a consequence, recordings from homolateral ventral roots during fictive locomotion show that while L1 or L2 oscillate in alternation to L5, their phase relationship with L3 and L4 is usually less defined (Kiehn & Kjaerulff, 1996).

3.2.2 Chemically induced Fictive Locomotion

Studies run on decerebrated cats have demonstrated that electrical stimulation of the mesencephalic locomotor center elicits stepping movements which are the substrate of locomotor activity (Jordan, 1998). However, working on *in vivo* animals is difficult and poses problems for the identification of the cellular and network mechanisms responsible for locomotor patterns. These realizations prompted the use of chemically induced fictive locomotion generated by the rat isolated spinal cord (Kudo & Yamada, 1987). However, comparing patterns recorded from the *in vivo* adult animal (de Leon *et al.*, 1994) with those from neonatal rat *in vitro* preparations (Kiehn & Kjaerulff, 1996) should take into account the fact that neonatal rats cannot perform true locomotion until they are at least 12 days old (Brocard *et al.*, 1997), since ankle muscle at that age cannot yet sustain the weight of the body.

Experimental locomotor-like patterns in the neonatal rat spinal cord *in vitro* can be evoked by a wide variety of agents, such as excitatory aminoacids (EAAs) (Kudo & Yamada, 1987; Cazalets *et al.*, 1992), 5-HT (Cazalets *et al.*, 1990; Beato & Nistri, 1998), acetylcholine (Cowley & Schmidt, 1994a), dopamine (Kiehn & Kjaerulff, 1998) or high doses of

extracellular potassium (Bracci *et al.*, 1998). The most efficient way to elicit the locomotor rhythm from the isolated spinal cord is to use a mixture of EAAs and 5-HT (Sqalli-Houssaini *et al.*, 1993; Kiehn & Kjaerulff, 1996; Cazalets & Bertrand, 2000). Taking into account that glutamate, acetylcholine and 5-HT receptors are widely distributed in the spinal cord, the global effect of exogenous activation of one of these receptors may also include secondary activation of other receptors (e.g., a 5-HT induced glutamate release).

Although the exact role of each receptor system is presently unclear, several studies have been carried out to describe features of the locomotor pattern evoked by different agents (Sqalli-Houssaini *et al.*, 1993; Kiehn & Kjaerulff, 1996, Cowley & Schmidt, 1994a). In this case bath application of various excitatory agents like NMDA, 5-HT, acetylcholine or dopamine activated stable patterns of alternating ventral root discharges (fictive locomotion). Nevertheless, these studies are based on a non-physiological condition whereby the excitatory agents are applied to the entire spinal cord preparation, a circumstance clearly different from what occurs during physiological activity. Moreover, a feature of fictive locomotion is the latency (often several minutes) required to generate it, a time which extends beyond the delay to deliver the agonists to the tissue and raises questions concerning the widespread activation of transmitter receptors with perhaps subsequent, sustained elevation in intracellular Ca^{2+} or other metabolic changes not normally associated with real locomotion. Finally, the widespread activation of transmitter receptors might broaden network function by recruiting into firing patterns some groups of neuron not usually involved in locomotion. On the basis of these considerations it would therefore be very helpful to demonstrate that patterns analogous to those of chemically-induced fictive locomotion can be evoked by synaptic stimulation following activation of certain afferent fiber tracts. Previous investigations have however revealed that, while application of exogenous agonists can induce very stable and long lasting locomotor patterns, electrically induced locomotion is usually short lasting (Magnuson & Trinder, 1997). This issue requires further studies.

3.2.3 CPG Localization

An important issue for the understanding of spinal networks is the localization of the CPG responsible for locomotion. Data from several preparations point to the importance of ventral and intermediate areas for the generation of spinal rhythmic activity (Dai, 1990; O'Donovan *et al.*, 1994). In the neonatal rat spinal cord, in particular, Kjaerulff *et al.* (Kjaerulff *et al.*, 1994) found consistent activity dependent labeling during chemically induced locomotor

patterns in the region surrounding the central canal (lamina X) and in the intermediate gray matter (laminae VI-VII); furthermore they demonstrated the persistence of the locomotor rhythm even after complete surgical ablation of the dorsal horns (Kjaerulff & Kiehn, 1996). Patch clamp recordings have also been performed from rhythmically active interneurons located around the central canal (MacLean *et al.*, 1995; Raastad *et al.*, 1996; Raastad *et al.*, 1997) and in lamina VII (Raastad *et al.*, 1996; Raastad *et al.*, 1997) during locomotor activity. These studies have revealed that such interneurons receive a rhythmic synaptic input during fictive locomotion (MacLean *et al.*, 1995) that is composed of EPSPs and IPSPs (Raastad *et al.*, 1997), but did not allow to discriminate between areas that contain intrinsic elements of the CPG and areas that contain elements passively driven by the CPG.

Rhythmogenesis has been shown to be distributed along the rostro-caudal axis of the spinal cord in many species (Grillner *et al.*, 1998; Ho & O'Donovan, 1993; Kjaerulff & Kiehn, 1996; Kremer & Lev-Tov, 1997; Lev-Tov *et al.*, 2000; Roberts *et al.*, 1998).

In the neonatal rat, such a rostrocaudal distribution has been demonstrated by lesion experiments, together with bath-partition experiments (Kjaerulff & Kiehn, 1996; Kremer & Lev-Tov, 1997, see also Cazalets & Bertrand, 2000). Furthermore, hemisected preparations show flexor and extensor alternation (Kjaerulff & Kiehn, 1996; Kudo & Yamada, 1987; Cowley & Schmidt, 1997; Kremer & Lev-Tov, 1997), thus favoring the hypothesis of distributed CPGs that can be activated even if surgically separated from other components.

3.2.4 Can afferent inputs trigger the locomotor pattern?

As already pointed out in § 3.2.2, chemically induced locomotor activity, though yielding important information on the mode of operation of the CPG, represents a non-physiological condition. A functionally important issue is then to study whether descending inputs from the locomotor region of the brainstem or sensory signals ascending from the periphery would have the ability to trigger the activation of the CPG in an *in vitro* preparation.

Whereas fictive swimming is induced by activating certain sensory inputs to the spinal cord of the tadpole (Soffe, 1991) or lamprey (McClellan, 1984), comparable observations on the rat spinal cord *in vitro* are sparse. While electrical stimulation of discrete areas of the brainstem (Atsuta *et al.*, 1988; Atsuta *et al.*, 1990) or of the descending ventrolateral funiculus (Magnuson *et al.*, 1995; Magnuson & Trinder, 1997) can induce fictive locomotor patterns, there is only a preliminary report (Smith *et al.* 1988) that stimuli applied to a skin flap still attached to the rat isolated spinal cord can produce similar effects. On the other

hand, dorsal root stimulation has been reported to reset (Iizuka *et al.*, 1997) or partially entrain (Sqalli-Houssaini *et al.*, 1993) the locomotor rhythm induced by bath application of chemical substances.

In the present study the occurrence and the basic properties of an alternating locomotor-like pattern triggered by stimulating dorsal root fibers in the neonatal rat spinal cord *in vitro* will be described.

4. PROPOSED MECHANISMS FOR SPINAL RHYTHMOGENESIS

In the effort of clarifying the cellular and network mechanisms responsible for locomotor rhythms, it is important to discriminate between properties relevant for *rhythm generation*, i.e. the production of repetitive cyclical motoneuronal activity, versus *pattern generation*, i.e. the actual timing and coordination of agonist and antagonist muscles (Kiehn *et al.*, 1997). In this sense, the comparative study of different rhythmic behaviors expressed by different species or by the same network in different conditions, allows several important issues to be addressed.

4.1 Reciprocal inhibition, pacemaker neurons, gap junctions, plateau potentials

Following the original hypothesis by Brown (Brown, 1911), it had been proposed that pattern generation in the neonatal rat could result from **reciprocal inhibition** between antagonist pools of neurons. According to this model (half-centers model), rhythmogenesis and alternation are generated by a single mechanism (reciprocal inhibition), that keeps silent one pool while the other one is active. Models of the half center circuitry can account for rhythmogenesis in the lamprey spinal cord (Grillner *et al.*, 1995). Nevertheless, much evidence suggests that rhythm generation itself is not dependent on reciprocal inhibition and points to distinct mechanisms for rhythmogenesis and alternation. In fact, blocking glycinergic transmission (thought to be the principal mediator of reciprocal inhibition; Kiehn *et al.*, 1997; see also § 4.3) does not prevent rhythm generation in a wide variety of species (Soffe, 1989; Kudo *et al.*, 1991; Cowley & Schmidt, 1995; Bracci *et al.*, 1996a; Cohen & Harris-Warrick, 1984). Moreover, in the chick spinal cord, local application of bicuculline converts a flexor-extensor alternating rhythm into a synchronous one (Sernagor *et al.*, 1995). In the rat spinal cord, independent rhythmic discharge can be seen if one side of the cord is

selectively activated (Kjaerulff & Kiehn, 1997) or hemisected (Kremer & Lev-Tov, 1997). Recent experiments on the mouse spinal cord (Whelan *et al.*, 2000) have also demonstrated that each side of the cord is capable of independently generating rhythmic activity and coordinating the firing of flexor and extensor motoneurons.

Pacemaker neurons, i.e. cells provided with intrinsic membrane properties that allow the generation of rhythmic activity even in the absence of synaptic inputs, have been proposed to play an important role in spinal pattern generation as well as in respiration (Grillner *et al.*, 1991; Kiehn, 1991; Hultborn & Kiehn, 1992; Smith, 1997). According to this hypothesis, a group of cells might be able to transmit a rhythmic output to the rest of the network.

Neurons endowed with intrinsic TTX-resistant, NMDA receptor induced, oscillatory properties have been described in the lamprey spinal cord (Grillner *et al.*, 1991) as well as in the neonatal rat, at different laminar locations (Hochman *et al.*, 1994a; Kiehn *et al.*, 1996).

Recently, it has been proposed (Kiehn *et al.*, 2000) that motoneurons can be potentially important in generating rhythmic motor output, due to their ability to show pacemaker properties in the presence of NMDA. Furthermore, coordination of motoneuronal, but not interneuronal, populations would occur through **gap junctions**. This mechanism, though important in generating rhythmicity "locally" (i.e. at the level of motoneuronal population), cannot account for distant coordination of motor pools intersegmentally and ipsilaterally (see § 4.4).

The ability to generate **plateau potentials**, i.e. cellular depolarizations initiated by an external input but sustained by intrinsic membrane mechanisms, is another mechanism potentially involved in central pattern generation. This property can allow a neuron to amplify and/or prolong a synaptic signal (Kiehn, 1991). As in the case of pacemaker neurons, the ability to generate plateau potentials may depend on the presence of voltage dependent inward currents. Bistable firing and plateau-induced self-sustained firing (Kiehn & Eken, 1998) have been shown to occur in vertebrate motoneurons (reviewed by Hultborn & Kiehn, 1992; Kiehn & Eken, 1998) and interneurons (Kiehn *et al.*, 1996).

4.2 Rhythmicity: a balance between excitation and inhibition

4.2.1 Lower Vertebrates

A detailed knowledge of the balance between excitatory and inhibitory mechanisms necessary to generate rhythmic activity is known for lower vertebrates such as the lamprey

and the *Xenopus* tadpole. In the case of the lamprey spinal cord, for example, different cellular and network properties and several modulatory systems (GABA, 5-HT, mGluRs, and dopamine) act in concert to shape the rhythmic output of the network (reviewed by Grillner *et al.*, 1995; Wallen, 1997). Figure III summarizes the different factors that control the onset and termination of each burst in a network neuron. Briefly, reciprocal inhibition between left and right neuronal pools (mediated by contralaterally projecting, glycinergic interneurons) is a prominent feature of these circuits and is believed to play a crucial role in rhythmogenesis

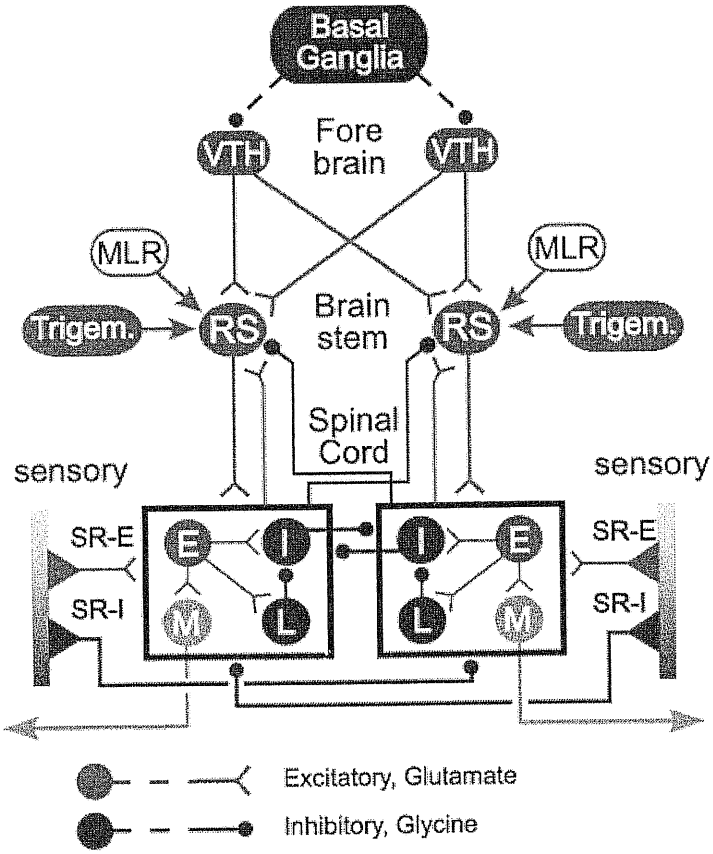

Figure III. Locomotor network of the lamprey. A schematic representation of the forebrain, brainstem and spinal components of the neural circuitry that generates rhythmic locomotor activity. All neuron symbols denote populations rather than single cells. The reticulospinal (RS), glutamatergic neurons excite all classes of spinal interneurons and motoneurons. The excitatory interneurons (E) excite all types of spinal neurons on the ipsilateral side, i.e. the inhibitory glycinergic interneurons (I) that cross the midline to inhibit all neuron types on the contralateral side, the lateral interneurons (L) that inhibit I interneurons, and motoneurons (M). The stretch receptor neurons are of two types; one excitatory (SR-E) which excites ipsilateral neurons and one inhibitory (SR-I) which crosses the midline to inhibit contralateral neurons. RS neurons receive excitatory synaptic input from cutaneous afferents (Trigem.), the mesencephalic locomotor region (MLR) and from the ventral thalamus (VTH), which in turn receives input from the basal ganglia. (from Grillner *et al.*, 2000).

(Grillner *et al.*, 1991). According to this view, when two (spontaneously active) pools of neurons are linked by reciprocal inhibition, alternating rhythmic activity is automatically generated: the onset of a burst results from disinhibition from the contralateral side in combination with a background excitatory drive that activates the different network interneurons. The E-interneurons further excite the other neurons of the network. In addition, depolarization may be enhanced by the activation of voltage dependent NMDA receptor channels and low-voltage-activated (LVA) Ca^{2+} channels. The activity is terminated when Ca^{2+} influx activates calcium dependent potassium channels (K_{Ca}) that, in turn, causes a progressive hyperpolarization and, furthermore, closure of NMDA receptors. Spike frequency adaptation due to K_{Ca}-dependent afterhyperpolarization can also contribute to burst termination (see Figure IV).

Like in the lamprey spinal cord, glycinergic reciprocal inhibition is thought to play a crucial role also in the pattern generation by the *Xenopus* (Dale, 1995).

4.2.2 Chick Spinal Cord

The chick spinal cord *in vitro* has provided important insights about mechanisms of spontaneously occuring rhythmic activity. Experiments performed by blocking different receptor classes (i.e. GABA/glycine, NMDA/AMPA or nicotinic acetylcholine; Chub & O'Donovan, 1998) indicate that rhythm generation is not based on a well-defined network but appears under various conditions and therefore is most probably produced by basic properties of developing neuronal networks. Such properties are proposed to be the degree of recurrent excitatory coupling in the network and activity-dependent synaptic depression (see § 4.2.4).

Recent experiments (Ritter *et al.*, 1999; Wenner & O'Donovan, 2001) have led to the hypothesis that transient depolarization and firing of motoneurons, originating from random fluctuations of interneuronal synaptic activity, activate R-interneurons (the avian homologue of mammalian Renshaw cells), which in turn trigger the recruitment of the remaining spinal interneuronal network.

Modeling studies have shown that hyperexcitability and activity-dependent depression of network excitability are sufficient to account for many features of spontaneous activity in the chick cord (Tabak *et al.*, 2000). Recently, it was shown that network excitability is transiently depressed after spontaneous episodes and recovers in the interval: after an episode, the

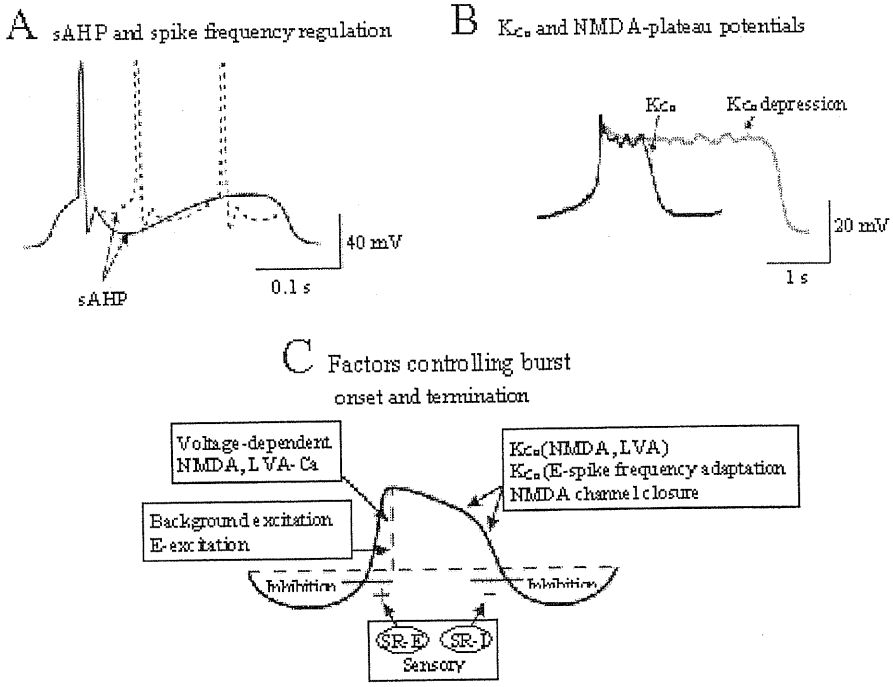

Figure IV. Spike frequency regulation, NMDA-plateau potentials and control of burst termination. (A) The amplitude of the slow afterhyperpolarization (sAHP) will determine whether one or several action potentials will occur during the phase of synaptic excitation in locomotor cycle. A large and long-lasting sAHP will make locomotor bursts shorter. (B) Ca^{2+}-dependent K^+ channels (K_{Ca}) not only cause the sAHP but will also promote the termination of NMDA-receptor induced plateau potentials. The control plateau (black trace) is markedly prolonged in the presence of the K_{Ca}-channel blocker apamin (gray trace). (C) Several different factors contribute to the initiation of the depolarizing phase, its maintenance, and its termination. In addition to conventional synaptic excitation, voltage-dependent NMDA receptors and low-voltage activated Ca^{2+} channels (LVA-Ca) are activated. Ca^{2+} will enter the cell through these channels, cause activation of K_{Ca}, and thereby a progressive hyperpolarization leading to closure of the NMDA channels. The initiation of the depolarizing phase is facilitated by activation of ipsilateral excitatory stretch receptor neurons (SR-E), while the termination of the depolarized phase is partially a result of activation of contralateral inhibitory stretch receptor neurons (SR-1). Abbreviation: E, excitatory interneuron. (from Grillner *et al.*, 2000).

amplitude of spontaneous and evoked synaptic potentials is transiently depressed (Fedirchuk *et al.*, 1999) and the membrane potential of spinal neurons is transiently hyperpolarized (Chub & O'Donovan, 2001). In addition, a positive correlation between episode duration and the preceding interval is observed, suggesting that episode termination occurs deterministically, when network excitability falls below a critical level (Tabak *et al.*, 2001). In contrast to the episode termination, the episode onset is stochastic, as no positive correlation between episode duration and the following interval duration is observed.

Although the physiological mechanisms for the recurrent excitatory feedback (synaptic connections or gap junctions) and for the depression (vesicle depletion, receptor

desensitization, etc.) can be different in developing networks of different tissues, spontaneous episodic activity might be generated by the same basic combination of recurrent excitation and activity-dependent depression.

4.2.3 Neonatal Rat Spinal Cord

Due to the complexity of the spinal cord in higher vertebrates, comparable understanding of the neuronal organization of the CPGs in mammals remains elusive.

One of the critical issues for understanding rhythmogenesis is whether rhythm is generated as an emergent property of network synaptic interactions, or from pacemaker-like neurons with intrinsic oscillatory bursting properties.

For example, in the case of respiratory networks, a hybrid pacemaker–network model, which would involve a combination of both types of mechanisms, has been proposed to underlie rhythm generation (reviewed by Smith, 1997; Smith *et al.*, 2000). It is also been recognized that the respiratory oscillator may be functionally plastic, i.e. capable of transformation between a state which favors pacemaker-like cellular oscillations and one in which network interactions are fundamental (Richter, 1996; Smith *et al.*, 2000).

In the intact spinal cord preparation, interneurons, which should belong to the CPG (see § 3.2.3), are not easily accessible to electrophysiological recordings; furthermore, due to a lack of detailed knowledge of network connectivity, interpretation of data from interneurons is difficult. Patch clamp recordings performed from rhythmically active interneurons located around the central canal (MacLean *et al.*, 1995; Raastad *et al.*, 1996; Raastad *et al.*, 1997) and in lamina VII (Raastad *et al.*, 1996; Raastad *et al.*, 1997), have revealed that such interneurons receive a rhythmic synaptic input during fictive locomotion that is composed of EPSPs and IPSPs. Although these studies provided useful information about the number of synaptic inputs received by such interneurons (Raastad *et al.*, 1996), it has not been possible to determine their exact functional role.

Furthermore, Kiehn *et al.* (Kiehn *et al.*, 1996) have found rhythmically active interneurons exhibiting intrinsic plateau or bursting properties (although in small percentage, about 12%), while most interneurons were synapticallly driven. Also, NMDA induced, TTX-resistant slow voltage oscillations, are present (Kiehn *et al.*, 1996; Hochman *et al.*, 1994a; Hochman *et al.*, 1994b), but they don't seem to be necessary to generate the locomotor rhythm. In fact, the observation that fictive locomotion can persist after removal of extracellular magnesium (Kiehn *et al.*, 1996) or in the presence of NMDA antagonists (Beato *et al.*, 1997), two

conditions which should have impaired the operation of NMDA–dependent pacemaker neurons, suggest that such intrinsic properties are not essential for spinal pattern generation. Recently, similar results have been found in the mouse spinal cord (Whelan *et al.*, 2000), in which, although NMDA receptors again contribute to rhythmogenesis and to the excitatory drive of motoneurons, they are not fundamental for the production of rhythmic activity or left/right alternation. Their primary role might be to facilitate the propagation of information within the network rather than generating the rhythm itself.

4.2.4 Synaptic depression

Since local oscillator networks might function through basic mechanisms not specific to spinal networks, synaptic depression has been suggested to be a determinant mechanism for burst termination.

In the intact spinal cord of the neonatal rat spinal cord (Lev-Tov & Pinco, 1992; Pinco & Lev-Tov, 1993a) as well as in slice cultures of embryonic spinal cord (Streit *et al.*, 1992), frequency dependent synaptic depression has been shown to be a prominent feature. In the spinal cord of the chick embryo as well as in hippocampal slices, refractory period following bursts have also been attributed to synaptic depression (O'Donovan & Rinzel, 1997; Staley *et al.*, 1998; Fedirchuk *et al.*, 1999, Tabak *et al.*, 2001) from which the network slowly recovers.

In contrast with these findings, synaptic depression does not seem to account for burst termination in disinhibited rhythm elicited in the intact neonatal rat spinal cord, since a burst with the same characteristics as spontaneous ones can be elicited at *any* time during the silent period, and entrainement of bursts can occur up to 0.25 Hz (Bracci *et al.*, 1997, Rozzo *et al.*, 2002a). A recent finding also showed that in dissociated cultures, synaptic depression does not account for burst termination (Darbon *et al.*, 2002). Furthermore, by analyzing the amplitude of postynaptic currents recorded in interneurons that were active during fictive locomotion, Raastad *et al.* (Raastad *et al.*, 1997) inferred that depression (or facilitation) had little importance for the information transfer.

4.2.5 Organotypic slice cultures

The hypothesis that rhythm generation might be due to the presence of intrinsically active interneurons (without pacemaker properties) which give rise to a patterned activity due to their connectivity is also supported by studies on organotypic spinal slice cultures. This

preparation has the advantage of higher accessibility to interneurons while still displaying some of the basic features of rhythmic behavior (Ballerini & Galante, 1998; Ballerini *et al.*, 1999). It must be noted though that while this preparation is useful to study mechanisms of rhythmic bursting (able to produce muscle contraction, Tscherter *et al.*, 2001), it lacks ability to generate left/right alternation.

The use of organotypic slice cultures have allowed addressing the question of whether, within a "local" oscillatory network, specific wiring arrangement is crucial in determining the ability to generate rhythms and to test the hypothesis that rhythmic phenomena might rely on recurrent excitation in a random excitatory network with frequency dependent synaptic depression (Senn *et al.*, 1998; O'Donovan & Rinzel, 1997; Tabak *et al.*, 2001). In this case, burst initiation would depend upon neurons which spontaneously discharge in the absence of synaptic input (Latham *et al.*, 2000a) and which have been found in spinal cultures (Legendre *et al.*, 1985; Latham *et al.*, 2000b). It has been further proposed (Latham *et al.*, 2000a; Latham *et al.*, 2000b; Streit *et al.*, 2001) that the percentage of such cells in a network determines the transition from steady firing to bursting.

Multisite recordings on organotypic cultures show that patterns of rhythmic activity seen in spinal cultures under various conditions can be reproduced in randomised networks (i.e., networks which are formed *in vitro* from a random initial distribution of their elements; Streit *et al.*, 2001). Furthermore, intrinsically active cells (showing neuronal discharge in the absence of synaptic transmission) have been found at a high percentage of locations where bursts start, suggesting they initiate bursts (Tscherter *et al.*, 2001).

These findings led to the hypothesis that network parameters, rather then a specified architecture of the network, are responsible for burst generation and maintenance (Streit *et al.*, 2001; Darbon *et al.*, 2002). However, such parameters do not seem to involve synaptic inhibition (Darbon *et al.*, 2002), but rather intrinsic spiking of some neurons, recurrent excitation of the network and auto-regulation of neuronal excitability (probably due to hyperpolarization of the neurons which give rise to a refractory period). This result is in line with findings related to disinhibited rhythm in the intact spinal cord (Bracci *et al.*, 1996a; Ballerini *et al.*, 1997; Rozzo *et al.*, 2002a; see also § 4.2.6).

It is also worth noting that intrinsically active neurons, while providing a source of activity to the network, do not determine its bursting pattern, which is a network phenomenon based on recurrent excitation.

Given these local circuits, the CPG could then be assembled by coupling them with mutual excitatory and inhibitory connections. Furthermore, specific pacemaker cells would not be essential for bursting because burst sources could be recruited at many sites in the network by a general increase in excitability. This result is in line with Bracci *et al.* (Bracci *et al.*, 1998) which showed that a general increase in network excitability leads to rhythm generation.

4.2.6 Disinhibited Rhythm

In the neonatal rat spinal cord, network-driven rhythmic bursting arises spontaneously when applying saturating concentrations of strychnine and bicuculline, which block, respectively, GABA and glycine receptors. This rhythm, called disinhibited rhythm, is of course unphysiological for the neonatal rat spinal cord; however, blocking fast, chloride-mediated inhibition largely simplifies the rhythmogenic network. Furthermore, disinhibited rhythmicity, by using excitatory connections only, resembles the early type of collective network burst (Sernagor *et al.*, 1995).

Thus, the disinhibited rhythm represents a useful model to elucidate the cellular mechanisms responsible for the generation and expression of spontaneous rhythmic bursting. In this case, evidence for the crucial role of the electrogenic Na^+ pump in determining spinal rhythmogenesis was shown (Ballerini *et al.*, 1997; Rozzo *et al.*, 2002a), in line with the hypothesis proposed by Streit *et al.* (Streit *et al.*, 2001) of an "auto-regulation" of neurons for burst termination. Also in the case of disinhibited bursting, it is suggested that onset is caused by synchronous firing of a certain number of spontaneously active cells recruiting most other neurons via recurrent excitation (Rozzo *et al.*, 2002a).

To comprehend the role of inhibition in the genesis of the fictive locomotor pattern, it is important to answer the question of whether disinhibited rhythm and fictive locomotion are generated by the same network (Bracci *et al.*, 1996b; Nishimaru & Kudo, 2000). Evidence favors this hypothesis, as Bracci *et al.* (Bracci *et al.*, 1996a; Bracci *et al.*, 1996b) found that disinhibited bursting shares with locomotor patterns the same sensitivity to block of either class of ionotropic glutamate receptors (Beato *et al.*, 1997; Bracci *et al.*, 1996a; Bracci *et al.*, 1996b) and the same anatomical location (Bracci *et al.*, 1996b; Kjaerulff & Kiehn, 1996). In addition, rhythm could be accelerated by 5-HT (Bracci *et al.*, 1996a), known to be involved in the generation of fictive locomotor patterns (Cazalets *et al.*, 1992), and a strong synergy between disinhibited rhythm and locomotor pattern was demonstrated with the use of the split bath configuration (Beato & Nistri, 1999). Recently, it has been objected (Nishimaru &

Kudo, 2000; Kiehn *et al.*, 1997) that the data of Bracci *et al.* (Bracci *et al.*, 1996a) was obtained with bicuculline and strychnine at non-specific concentrations for $GABA_A$ and glycine receptors, suggesting that further investigation at the cellular level is needed to solve the question. However, the interpretation of the data given by Bracci *et al.* (Bracci *et al.*, 1996a) is strongly supported by evidence that the effects of bicuculline are mimicked by the $GABA_A$ antagonists penicillin and picrotoxin, and that they do not change by increasing concentrations of strychnine from 1 to 10 μM (Bracci *et al.*, 1996b).

Observations made on the organotypic spinal slice culture have further supported the possibility that a common network is involved in generation of the two rhythms. In fact, it has been shown that bursting induced both by disinhibition or by increased excitability are composed of similar waves and are spread over the same areas of the slice (Tscherter *et al.*, 2001).

4.3 Alternating patterns: a balance between excitation and inhibition

During locomotion, appropriate sequencing of motoneuronal rhythmic firing is ensured by the temporally coded (excitatory and inhibitory) synaptic inputs provided by the CPG circuitry.

A variety of experimental evidence from a wide range of preparations indicates that glycinergic transmission plays a central role in reciprocal organization of the locomotor pattern. In the tadpole (Soffe, 1987) and in the lamprey spinal cord (Grillner *et al.*, 1991), left/right alternation is thought to be mediated by intersegmental glycinergic commisural interneurons, projecting directly to the rhythm-generating interneuronal network on the contralateral side of the cord. In the models describing rhythm generation in these species (half center models), alternation and rhythmicity are generated by the same network/mechanism (Grillner *et al.*, 1995), although it has also been shown that strychnine can eliminate alternation during fictive swimming in the lamprey (Cohen & Harris-Warrick, 1984).

In the chick spinal cord, pattern generating networks seem to utilize distinct (but overlapping) mechanisms for rhythmogenesis and alternation (O'Donovan *et al.*, 1998). According to this model, various rhythm generators, present within the entire spinal cord, directly excite motoneurons, whereas temporal phasing of these inputs is mediated via separate interneuronal circuits, driven by the rhythm generators. Alternation is thought to occur

because sartorius motoneuron firing is shunted or voltage-clamped by its GABAergic synaptic drive at the time of peak femorotibialis discharge (O'Donovan *et al.*, 1998).

In the rat embryonic spinal cord *in vitro* (Kudo *et al.*, 1991), NMA-induced rhythmic activity emerges synchronously between left and right sides at embryonic day (E) 15.5, turning into alternating at E18.5. At the intermediate stage, E17.5, the activities of the two sides occur independently. All together, this data reveals the presence of rhythm-generating circuits on each half of the spinal cord. Furthermore, evidence for interaction through midline connections of these rhythm-generating circuits comes from the effects of blockers of inhibition on different rhythms. In fact, while bath-application of strychnine (or bicuculline) does not affect NMA-induced rhythmic activity when this is expressed synchronously at embryonic day E16.5, at E18.5 alternated activity is synchronized by the same drug. In addition, at E17.5, strychnine synchronizes independent left and right patterns, thus indicating that an excitatory interaction between the right and left rhythm generators exists at this stage, but that a strychnine-sensitive inhibitory mechanism masks the interaction between them (Kudo *et al.*, 1991).

In the neonatal rat spinal cord, intracellular recordings, performed with the longitudinal split bath configuration, have shown (Kjaerulff & Kiehn, 1997) that motoneurons receive a mainly glycinergic rhythmic synaptic inhibition from the contralateral half of the locomotor network. Furthermore, blocking glycine receptors with strychnine during locomotion in the neonatal rat (Kudo *et al.*, 1991; Cowley & Schmidt, 1995), and in the cat (Noga *et al.*, 1993) disrupts left/right alternation or mid-cycle inhibition. It also causes co-activation of flexor and extensor muscles in legged animals.

Nevertheless, the source of inhibitory drive during locomotion is unknown. In fact, Ia interneurons, which are rhythmically active during locomotion (Pratt & Jordan, 1987) and have appropriate reciprocal connections to provide inhibition of antagonist muscles (Jankowska, 1992), do not seem to be part of the rhythm-generating network (Pratt & Jordan, 1987), although they might be important in shaping the final motoneuronal output. Potential candidates are instead the commisural interneurons that project segmentally to the contralateral side (Silos-Santiago & Snider, 1992) since lesioning of their axons abolishes left/right coordination in the neonatal rat (Kjaerulff & Kiehn, 1996; Kiehn *et al.*, 1997).

The role of the neurotransmitter GABA is less clear. In the embryonic chick spinal cord, $GABA_A$ receptors have been shown to be involved in flexor extensor alternation of the spontaneous motor rhythm (Sernagor *et al.*, 1995). In the neonatal rat, data are more

controversial. While Cazalets *et al.* (Cazalets *et al.*, 1994) showed that pharmacological block of $GABA_A$ receptors with bicuculline up to 10 μM and of $GABA_B$ receptors with phaclophen (up to 100 μM) did not change the left/right relationship, Cowley and Schmidt (Cowley & Schmidt, 1995), on the other hand, found that higher concentrations (10-25 μM) of bicuculline do convert drug induced fictive locomotion into synchronized bursting.

The possibility that both GABA and glycine are involved in left/right alternation is supported by the fact that these neurotransmitters can be co-released from individual synaptic vescicles onto inhibitory synaptic sites of motoneurons (Jonas *et al.*, 1998; Nishimaru & Kudo, 2000). In addition, Gao and van den Pol (Gao & van den Pol, 2001) found that in the developing rat spinal cord, the onset of glycinergic transmission is delayed with respect to GABAergic one, with glycine receptors becoming predominant at birth. It is thus possible that there are developmental switches from GABAergic to glycinergic inputs during the perinatal period, when extensive synaptogenesis occurs (Gao & van den Pol, 2001).

Experiments performed on the neonatal rat spinal cord by Kremer and Lev-Tov (Kremer & Lev-Tov, 1997) support the more general idea that phase relation between left and right hemicords during the locomotor rhythm may be determined by an interplay between inhibitory and excitatory cross-coupling pathways. These authors show that decreasing the cross-excitation with the non-NMDA receptor blocker CNQX prevents strychnine from transforming a left/right alternating rhythm to a bilaterally synchronous rhythm. This suggests that, under normal circumstances, lumbar segments of the cord are controlled by a strong reciprocal inhibition and a much weaker cross excitation, but this balance can be altered by pharmacological manipulations.

Furthermore, as already pointed out in § 4.2.6, pharmacological block of GABAergic and glycinergic inhibition elicits spontaneous network-driven rhythmic bursts that, unlike those of fictive locomotion, appear synchronously in all lumbar ventral roots (Bracci *et al.*, 1996a). These bursts, although displaying different characteristics in terms of frequency, amplitude and duration, with respect to fictive locomotion (Bracci *et al.*, 1996a), indicate the ability of the rat spinal cord to generate patterned activity in the absence of fast synaptic inhibition. This study further shows that ionotropic glutamate receptors mediate rhythmic activity and the excitatory synaptic connections between the left and right side of the spinal cord.

4.4 Role of motoneurons in rhythm generation

It is widely accepted that locomotor pattern generation requires coordination of the activity across many neurons in the central pattern generator. Nevertheless, motoneurons are endowed with intrinsic and conditional membrane properties that can have a role in shaping the final motor output of the CPG (Kiehn *et al.*, 2000). Recent studies have revealed a complex picture in which motoneurons can express nonlinear responses, such as plateau potentials and endogenous oscillatory properties (Kiehn, 1991; Kiehn *et al.*, 2000), which can be influenced or even made explicit by neuroactive substances expected to be released during locomotor activity (Kiehn, 1991).

In fact, it has been shown that the generation of plateau potentials by motoneurons in various species is promoted by a range of metabotropic neurotransmitters such as 5-HT (Hounsgaard & Kiehn, 1989), noradrenaline (Conway *et al.*, 1988; Lee & Heckman, 1996), acetylcholine or glutamate (Svirskis & Hounsgaard, 1997; Delgado-Lezama *et al.*, 1997).

It has been further suggested that motoneurons might actually play an active role in coordinating a local motor output (Tresch & Kiehn, 2000). Attention to this matter has been brought up by the fact that NMDA receptor-mediated voltage oscillations were shown to persist after block with TTX of action potential-mediated synaptic transmission in all vertebrates investigated, i.e. the lamprey (Wallen & Grillner, 1987), the chick (Moore *et al.*, 1999), the turtle (Guertin & Hounsgaard, 1998), the tadpole (Prime *et al.*, 1999) and the neonatal rat (MacLean *et al.*, 1997; Schmidt *et al.*, 1998).

Recently, Tresch and Kiehn (Tresch & Kiehn, 2000) have shown that TTX-resistant rhythmicity requires the simultaneous expression of NMDA-induced oscillatory properties in individual motoneurons and of coupling across motoneurons by means of gap junctions. The latter is necessary to synchronize these oscillations and is not capable of producing coordinated oscillations by itself. Although this study suggests an important role for gap junctions in coordinating motoneuronal populations locally, the activity of interneuronal networks remains crucial for the generation of fictive locomotion, which implies the distant coordination of motor pools both intersegmentally and ipsilaterally (Tresch & Kiehn, 2000).

4.5 Coupling between local oscillators

Although precise knowledge of the CPG connectivity is still lacking, the wealth of data coming from different species, experimental preparations, and techniques used, allows to hypothesize that the CPG is made of local oscillators, distributed rostrocaudally and

segmentally, and connected by excitatory and inhibitory synapses. Can these local oscillators be differentially coupled to produce rhythms with different characteristics? This question requires two steps to be answered: 1) Can the strength of such excitatory and inhibitory connections be varied? 2) How does varying such strengths affect the coordinated output of the network?

One way of testing this hypothesis is to change the strength of synaptic connections by applying receptor antagonists.

An interesting possibility is however that endogenous transmitters, active via G-protein coupled receptors, might be locally released to modulate excitation or inhibition in a differential fashion. This arrangement would provide network plasticity and may disclose additional patterns of rhythmicity. Hence, the experimental activation or block of certain classes of metabotropic receptors in the intact spinal cord may be a useful tool to explore variable functional coupling between oscillators.

5. Role of metabotropic receptors in the spinal cord

5.1 Tachykinergic NK_3 receptors

5.1.2 Receptor structure, function and localization

Tachykinins are a family of peptides which share the common C-terminal sequence Phe-Xaa-Gly-Leu-Met-NH_2, that is crucial for their interaction with specific receptors and for producing most of their biological effects (reviewed by Gao & Peet, 1999). The first and best known peptide of this family, substance P, was discovered as early as 1931 by Von Euler and Gaddum, but more than 50 years elapsed before two other mammalian tachykinins, neurokinin A and neurokinin B, were discovered (see Maggio, 1988 for review). Their role as neurotransmitters and neuromodulators is now well accepted (Rekling *et al.*, 2000).

Three receptor subtypes, designated NK_1, NK_2 and NK_3, were identified on the basis of marked differences in the rank order of potencies of agonist peptides in different tissues, with substance P being the preferred agonist for the NK_1 receptor, neurokinin A for the NK_2 receptor and neurokinin B for the NK_3 receptor (Regoli *et al.*, 1994). The existence of these three receptor subtypes has been confirmed by the cloning and sequencing of three distinct genes from mammalian sources (see the review by Gao & Peet, 1999 for references).

Tachykinins elicit a wide range of responses from many types of cell, and have been implicated in a wide variety of biological actions such as pain transmission, neurogenic inflammation, smooth muscle contraction, vasodilatation, secretion and activation of the immune system.

In many systems, tachykinins have been shown to activate phospholipase C, which is coupled to the receptor via a G-protein. Cellular responses result mainly from the subsequent formation of inositol 1,4,5-trisphosphate (IP_3) and diacyl-glycerol, which in turn lead to the release of calcium within the cell.

The three mammalian tachykinins are widely distributed throughout the central and peripheral nervous systems (Otsuka & Yoshioka, 1993; Rekling *et al.*, 2000) and their expression is developmentally regulated (Rekling *et al.*, 2000). In the immature rat spinal cord, it has been found that, while NK_2 receptors are minimally present (as shown by ligand binding and electrophysiological studies; Baranauskas *et al.*, 1995), this preparation does contain NK_1 and NK_3 receptors (Otsuka & Yoshioka, 1993), which however differ in their distribution. In fact, NK_3 receptors are diffusely present throughout the spinal gray matter (Beresford *et al.*, 1992; Linden *et al.*, 2000; Mileusnic *et al.*, 1999; Seybold *et al.*, 1997) while NK_1 receptors are most abundant in the deep layers of the dorsal horn (Liu *et al.*, 1994; Ogawa *et al.*, 1985).

5.1.2 Role of NK_3 receptors in spinal rhythmicity

Recently, Barbieri and Nistri (Barbieri & Nistri, 2001) have found that selective activation of NK_3 receptors, in the neonatal rat spinal cord, elicits a novel type of intense, long-lasting bursting, which is usually not induced by activation of other tachykinin receptors (Fisher *et al.*, 1994). Furthermore, interaction of tachykinins with the locomotor network has been demonstrated in several species, since substance P can accelerate fictive locomotion in the rat (Barthe & Clarac, 1997) and fictive swimming in the lamprey (Parker *et al.*, 1998), although it cannot *per se* elicit these activities. As substance P is a broadly acting agonist effective on all three major classes of receptors (although with a marked preference for NK_1), one possibility is that simultaneous activation of receptors mediating contrasting actions could prevent the onset of the CPG activity. Alternatively, the pathways expressing tachykinin receptors may have only a minor involvement in the locomotor network.

The present study will aim at clarifying the basic properties of bursting evoked by NK_3 receptor activity, its segmental distribution and its potential interaction with the activity generated by the locomotor CPG of the neonatal rat spinal cord in vitro.

5.2 Metabotropic Glutamate Receptors (mGluRs)

Glutamate is the principal fast excitatory neurotransmitter mediating spinal rhythmicity (Cazalets *et al.*, 1992; Bracci *et al.*, 1996a; Beato *et al.*, 1997). In addition, it also modulates neuronal excitability by activating a large family of metabotropic receptors.

5.2.1 Receptor structure, function and localization

Metabotropic glutamate receptors (mGluR) are a class of G-protein coupled receptors, mediating a variety of effects. There are at least eight subtypes of mGluR (mGluR1 to -8) that can be divided into three groups (groups I, II, and III) on the basis of sequence homology and pharmacological profiles (reviewed by Pin & Duvoisin, 1995). Group I mGluRs (mGluR-1,5) are coupled to phospholipase C (PLC), which is responsible for increasing the synthesis of inositol 1,4,5-trisphosphate (IP_3), and triggering intracellular Ca^{2+} release. Group II (mGluR-2,3) and group III mGluRs (mGluR-4,6,7,8) are negatively coupled to adenylyl cyclase, which inhibits the formation of cAMP (Pin & Duvoisin, 1995).

Metabotropic glutamate receptors are widely distributed in the CNS, with a heterogeneous distribution of mGluR subtypes in different areas (Cartmell & Schoepp, 2000).

The extensive electrophysiological research on mGluRs has been recently reviewed by Anwyl (1999): overall, activation of mGluRs results in a large number of cellular actions, including inhibitory (and potentiating) actions on K^+ and Ca^{2+} conductances, presynaptic modulation of transmitter release, modulation of AMPA and NMDA receptors-mediated responses, activation of non-selective cation channels, and mediation of excitatory and inhibitory postsynaptic potentials. Furthermore, the differential cellular localization of receptor subtypes suggests that the precise placement of receptors is a crucial factor contributing to the control of neuronal excitability (Rekling *et al.*, 2000).

Within the rat spinal cord, detailed studies have addressed the distribution of distinct mGluRs. In situ hybridization experiments show that the mGluR1 signal is the strongest amongst all mGluRs and is widely distributed with gradual decline in intensity during postnatal development (Berthele *et al.*, 1999). mGluR5 transcripts are, instead, predominantly located in the superficial dorsal horn. Immunohistochemical data indicate that mGluR1

receptors are found in the ventral horn (including motoneurons) and deep dorsal horn while mGluR5 receptors are chiefly present in lamina I and II, and absent from motoneurons (Alvarez *et al.*, 2000). A very similar distribution is found also in the human spinal cord in which mGluR1 have the highest distribution in lamina VIII and IX while mGluR5 are mainly in dorsal horn (lamina I, II). Class II receptors are also mainly in lamina II while glia is generally very weakly immunoreactive (Aronica *et al.*, 2001). Comparable data on group III receptor localization in neonatal rat spinal cord are not yet available.

5.2.2 Role of mGluRs in the spinal cord

Several studies have examined the functional role of mGluRs in the lamprey spinal cord. Presynaptic inhibitory modulation of reticulospinal EPSPs in gray matter neurons is mediated by mGluRs (Krieger *et al.*, 1996; Kettunen *et al.*, 2002), and a modulation of the lamprey spinal locomotor network has been demonstrated (Krieger *et al.*, 1998). The class I agonist DHPG enhances the postsynaptic membrane action and locomotor output evoked by NMDA (Krieger *et al.*, 2000) probably by facilitating Ca^{2+} influx and EPSPs (Takahashi & Alford, 2002). Furthermore, the broad spectrum agonist trans-ACPD (t-ACPD) generates a slow rhythm with either phase alternation or synchrony, perhaps dependent on the extent of modulation of inhibitory transmission (Aoki *et al.*, 2001).

On the rat spinal cord, class I mGluRs increase motoneuron excitability at postsynaptic level (Dong & Feldman, 1999) while class II and III receptors act presynaptically to depress synaptic inputs (Pinco & Lev-Tov, 1993a; Cao *et al.*, 1995; Cao *et al.*, 1997; Dong & Feldman, 1999). Analysis with broad spectrum agonists and antagonists indicate that mGluR activation also contributes to nociceptive dorsal root-induced reflex in young rats (Boxall *et al.*, 1996). It is however noteworthy that the action of class I receptors on rat spinal neurons remains controversial as DHPG has been reported to enhance NMDA and AMPA transmission (Jones & Headley, 1995; Ugolini *et al.*, 1999), but in a non-selective way (Jones & Headley, 1995). Furthermore, mGluR5 activity is reported to enhance GABAergic transmission and NMDA receptor mediated responses, giving an overall inhibitory action (Dang *et al.*, 2002).

ACPD or DHPG applications have been found to increase excitability of turtle dorsal horn neurons (Russo *et al.*, 1997) and motor neurons (Svirskis & Hounsgaard, 1998) by facilitating plateau properties, possibly through the involvement of an L-type calcium conductance. This

action by ACPD is however rather weak when compared with that of 5-HT or muscarine (Hornby *et al.*, 2002).

The role of class I, II and III mGluRs in rhythmic activities expressed by the neonatal rat spinal cord *in vitro* is thus unexplored. Question arise regarding: (a) whether mGluR activation by endogenous glutamate released during rhythmic patterns contributes to rhythmic discharges; (b) whether activation of certain classes (or subclasses) of mGluRs yield an electrophysiological signature observed as a distinctive change in network or single cell properties.

6. AIMS OF THE PRESENT STUDY

While several aspects regarding the phenomenology and characterization of spinal rhythmicity are well established, various issues concerning the mechanisms of activation of the locomotor network and the role of different classes of receptors are yet to be investigated. The aim of this thesis is to shed light on several of these issues which are summarized below.

i. Although it is well established that the CPG can function in the absence of inputs from afferent fibers, selective activation of the CPG by dorsal root stimulation should represent a more physiological condition with respect to bath-application of drugs. As an extension, the identity of the mechanism which could trigger CPG activation in the presence of patterned stimuli was investigated.
ii. Given the importance of GABA and glycine receptors in determining alternated rhythmical activity, and the diverse role (inhibitory/excitatory) they seem to play in different parts of the neonatal CNS, the function of these receptors was explored on neonatal motoneurons.
iii. While several aspects regarding the role of ionotropic receptors in locomotor patterns have been investigated, the function of metabotropic receptors in spinal rhythmicity has received much less attention. Although a wealth of data is available at cellular level for receptors such as tachykininergic and glutamatergic metabotropic receptors, an understanding of the importance of synaptic connectivity and membrane properties in producing the final output of neuronal networks requires bridging the gap between effects at the cellular and network levels. For this reason, the role of several classes of

metabotropic receptors, i.e. tachykinergic NK_3 receptors and class I, II and III metabotropic glutamate receptors was investigated in relation to:

- their ability to elicit rhythmical activity in the neonatal spinal cord
- their relationship with other known patterns of rhythmicity, i.e. fictive locomotion and/or disinhibited bursting
- their direct action on motoneurons

These receptors are expected to play a role in spinal rhythmicity as their activation relies on neurotransmitters commonly released in the network when generating rhythmic activity. In the case of glutamate, for example, the functioning of at least one class of ionotropic receptors is required in order to generate both fictive locomotion (Beato *et al.*, 1997) and disinhibited rhythm (Bracci *et al.*, 1996a).

Furthermore, the possibility of differentially modulating synaptic connections by activating these receptors should allow to reveal different modes of spinal network rhythmicity (see § 4.4), which in turn rely on different coupling strength between local oscillators.

METHODS

1. Tissue Preparation

The spinal cord, from low cervical segments to *conus medullaris*, was isolated from neonatal rats (0-6 days old, P0-P6). Animals were firstly anaesthetized with intraperitoneal injection (0.2-0.4 ml) of urethane solution (10%). As soon as the animal lost the withdrawal reflex, it was rapidly decapitated with scissors. The forelimbs and the ventral part of the chest were removed and the animal was eviscerated in order to expose the ventral side of the vertebral column. The remaining skin was also removed and the body was washed in cooled (4° C) oxygenated artificial cerebrospinal fluid (ACSF, see below for composition) and fixed by pins with the ventral side upon the sylgard bottom of a Petri dish containing ACSF at the same temperature. The solution contained in the dish was continuously oxygenated and was replaced every 3-4 minutes during the dissection. A complete laminectomy was performed in the rostrocaudal direction under the microscope. Meningeal tissue was removed from the ventral side, while dorsal and ventral roots were cut as close as possible to the dorsal root ganglia. Remaining meningeal tissue present on the dorsal side of the spinal cord was also removed.

2. Recording Chamber

After dissection, the spinal cord was pinned to the sylgard bottom of a recording chamber made of plexiglass (internal volume ~3 ml) and was continuously superfused with ACSF. Perfusion was fed by a peristaltic pump that delivered ACSF to the recording chamber, via a small tubing, parallel to the rostrocaudal axis of the spinal cord and ACSF outflow was drained via a small channel. Constant flow rate was ensured by a flow spacer placed between the pump and the chamber to damp fast oscillations in the fluid level. Flux was maintained between 5 and 7 ml/min. All neurochemicals were applied via the perfusion system. The time

necessary to completely exchange the solution in the bath was estimated using ACSF stained with phenol red and found to be less then 3 minutes. Composition for both dissection and recording was (in mM): NaCl 113, KCl 4.5 mM, $MgCl_2 7H_2O$ 1, $CaCl_2$ 2, NaH_2PO_4 1, $NaHCO_3$ 25 and glucose 11, gassed with 95% O2-5% CO2, pH 7.4. Experiments were performed at room temperature.

3. Recording Techniques

3.1 Extracellular Ventral Root Recordings

Ventral root recordings were performed with miniature monopolar suction electrodes made from heat pulled glass capillaries. Electrode tips were fire polished and the size of their tip was selected to (a) allow entry of the entire ventral root and (b) provide a tight fit of the ventral root. Roots were sucked in the electrode by applying gentle negative pressure with a syringe connected to the apical end of the pipette. When the root was entirely inside the electrode, further negative pression was delicately applied in order to obtain a seal between the tip of the pipette and the ventral surface of the spinal cord. Electrical contact was achieved by filling the pipette with Krebs solution and connected via an Ag/Ag-Cl micropellet (Harvard Apparatus, UK) further connected to a custom made low-noise DC-coupled amplifier.

DC-coupled ventral root recording is a suitable method to detect not only fast firing activity but also slower membrane potential variations of the population of motoneurons from which the recording is made. Under these conditions, firing activity usually appeared as a biphasic signal, and slow polarization changes, that took place simultaneously in a large population of motoneurons, preserved the same polarity as those observed with the intracellular technique (Bracci *et al.*, 1996a).

Signals were also displayed on-line on a Gould chart recorder, digitized and recorded on DAT tape for further off-line analysis.

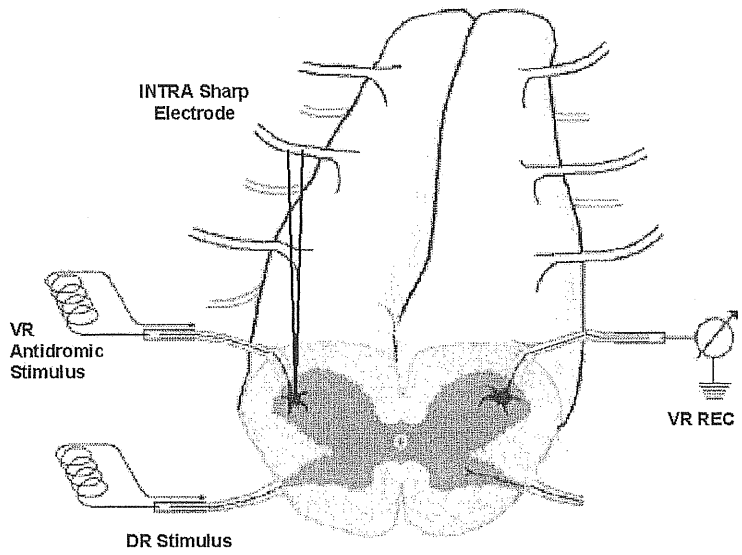

Figure V. Schematic representation of the intact spinal cord *in vitro*, during simultaneous intracellular and extracellular recordings (section view). Motoneurons were identified by means of antidromic stimulation of the corresponding ventral root and recorded with sharp electrodes. Extracellular ventral root recordings were made with suction electrodes. Electrical stimuli were delivered to dorsal roots to monitor DR evoked reflexes.

3.2 Intracellular Recordings

Intracellular recordings from motoneurons were performed with sharp glass electrodes filled with intracellular solution and connected via a 0.1× headstage (Axon Instruments) to an amplifier (Axoclamp 2A, Axon Instruments). Intracellular solution was one of the following: (a) KCl 3 M (b) KCl 3 M+ QX-314·Cl^- 30 mM (c) $KMeSO_4$ 2 M+ QX-314·Cl^- 20 mM. Electrode resistance varied between 30MΩ and 70MΩ for KCl-filled electrodes and between 70 MΩ and 120MΩ for $KMeSO_4$-filled ones. Experiments were performed in current-clamp mode.

3.2.1 Motoneuron Impalement

As the sharp electrode was lowered through the ventral horn of the spinal cord, the following stimulation protocol (delivered at a frequency of 0.5 Hz) allowed motoneurons to be identified: a negative-current step (10 ms, 0.1 nA) for monitoring electrode resistance,

followed, with a 100 ms lag, by a pulse stimulus (0.1 ms) applied to the ipsilateral homologous ventral root (antidromic stimulation).

When the electrode was in proximity of the motor nucleus, antidromic stimulation evoked a short latency (~2 ms) biphasic field potential due to a synchronous motoneuron firing (Fulton & Walton, 1986), while an increase of electrode resistance was used a diagnostic sign that the tip of the electrode was in contact with the membrane of a motoneuron. A this stage, the "clear" command on the amplifier was applied, in order to facilitate penetration into the membrane.

3.2.2 Current –Clamp recording

Current-clamp experiments were performed in bridge mode. After motoneuron impalement, ventral root stimulation elicited a short latency (<2 ms) all-or-none overshooting antidromic action potential (Fulton & Walton, 1986). Only cells in which this kind of response could be consistently elicited were considered for analysis.

Electrode capacitance was compensated (in Discontinuous Current Clamp (DCC) mode at 1.5-2.0 KHz). Motoneuron input resistance was constantly monitored by injecting a negative current pulse (20-50 ms); it was then calculated as the ratio between the steady state hyperpolarization induced by injection of the pulse and the amplitude of the current injected (0.1-0.2 nA). Bridge balance was routinely monitored and compensated whenever necessary.

To monitor the voltage dependence of single cell responses, current-voltage (I-V) curves were performed. In this case, successive hyperpolarizing (-0.1 to -0.9 nA, with 0.1 nA interval) and depolarizing (0.1-0.9 nA) current steps, were delivered at 0.2 Hz.

3.2.3 Recurrent Post-Synaptic Potential Recording

In several experiments, it was necessary to record the Renshaw cell mediated recurrent post-synaptic potential (rPSP, see INTRODUCTION § 2.4). Although sharp electrodes allow very little diffusion of the intracellular solution into the cell (especially when compared to whole-cell patch clamp technique), $KMeSO_4$ (2 M)–filled electrodes were nevertheless used, to avoid any disruption of the Cl^--mediated rPSP. Furthermore, in order to avoid interference of the rPSP measurement by the antidromic action potential afterhyperpolarization (AHP), motoneuron spike was blocked by adding the sodium channel blocker QX-314·Cl^- (20 μM) to the intracellular solution.

4. Electrical Stimulation

4.1 Dorsal and Ventral Root Stimulation

Miniature bipolar suction electrodes were used in order to deliver single or repetitive electrical stimuli to either dorsal roots or ventral roots. Such electrodes were made from thin (1.5 mm diameter) glass capillaries and contained a silver wire inside and another one wound around. Electrode tip diameter was chosen to closely fit the root to be stimulated. Square electrical pulses (0.1 ms duration, 0.5-20 V amplitude) were applied via a Digitimer stimulator to either VRs in order to antidromically activate motoneurons, or to DRs to activate afferent fibers. For each preparation, intensity of stimuli delivered to DRs was expressed in terms of threshold (Th), defined as the minimum intensity able to elicit a detectable response in the homolateral VR. On a sample of preparations used for repetitive stimulation protocols, the average threshold was Th=1.8±0.9 V, n=25.

4.2 Afferent Volley Measurements

Tests were carried out to monitor the afferent volley induced by DR stimulation. For this purpose, stimuli were delivered at the distal end of the L5 DR, while a 3 M NaCl-filled microelectrode was inserted at the site of entry of the dorsal root into the cord. In accordance with Fitzgerald (Fitzgerald, 1988) and our histology experiments (see § 7), two negative-polarity peaks were detected with conduction velocities of 1.0±0.6 and of 0.34±0.07 $m \cdot s^{-1}$ (n=5). The second (delayed) peak appeared with stimuli of about 1.6×Th. Maximal volley amplitude was observed with 10×Th stimuli. No fatigue of volley peaks was observed with stimuli up to 10×Th at 10-20 Hz for 120 s.

5. Experimental Configurations

5.1 Extracellular Recordings

During extracellular experiments, the spinal cord was placed ventral side up and one or two pairs of VRs were used for recording, usually L2s and/or L5s (see Figure VI). In all experiments, a stimulating electrode was also placed, usually on a L5 dorsal root, in order to continuously monitor the DR reflex during the experiment.

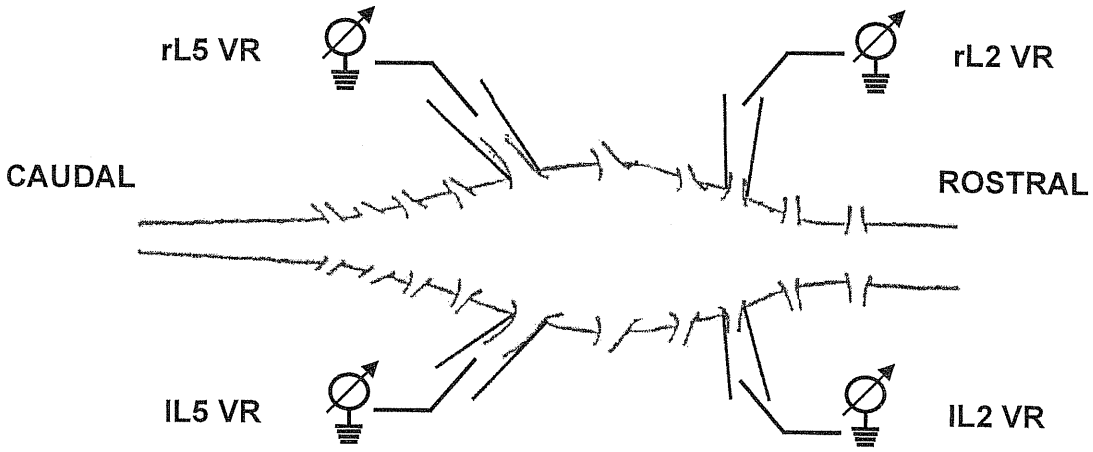

Figure VI. Simultaneous extracellular recordings from four ventral roots. Two pairs of ventral roots (L2 and L5) were usually recorded to monitor homosegmental and homolateral phase difference. In all experiments, a stimulating electrode was also placed usually on an L5 dorsal root.

5.2 Simultaneous intracellular and extracellular recordings

Intracellular recordings from single motoneurons (usually from lumbar L3 to L5 segments) were obtained simultaneously with extracellular recording of two or three VRs. In this experimental configuration, the spinal cord was rotated with respect to the extracellular one. This allowed the ventrolateral part, containing the motor nuclei, to be more accessible to the microelectrode that was lowered vertically by means of a micromanipulator. Furthermore, two electrodes were used to deliver, respectively, orthodromic stimuli through a DR homolateral to the motoneuron, and an antidromic stimuli to the VR used for motoneuron identification.

6. VIABILITY OF THE SPINAL CORD

After dissection, the viability of the spinal cord was ascertained before any further testing. In healthy preparations, single pulse stimulation (0.1 ms duration, 1-15 V) intensity delivered to one dorsal root elicited a reflex response from the ipsilateral ventral root at the same segmental level. If this response was absent, the preparation was discarded. Spinal cord preparations could usually be maintained *in vitro* for >12 hours without apparent sign of rundown of electrophysiological properties. For this purpose, the DR reflex was continuously monitored. Reliability of single cell recordings was continuously monitored by checking

input resistance and response to antidromic stimulation. These recordings could be kept stable for up to 9 hours.

7. Histology of Dorsal Roots

To verify whether the two conduction velocities measured with the afferent volley corresponded to two distinct fiber populations in the afferent dorsal roots, an histological study was undertaken. To this aim, two kinds of staining techniques were applied to dorsal root slices: a) Hematoxilin-Eosin to stain nuclei and cytoplasm, respectively and b) Luxol Fast Blue, to stain for myelin.

Slice preparation was done in the following way: after spinal cord dissection from two P0 and P3 rats, L2, L4 and L5 dorsal roots were extracted and fixed in liquid formalin, then sucrose (20% in PBS), frozen, and kept at –20° until further use (which took place within a couple of days). 14 μM thick slices were cut with a cryostat, mounted on glass gelatin-coated slides and allowed to dry for two hours.

a) ***Hematoxilin-Eosin staining*:** after having rinsed slides in water for 1 minute, ematoxilin-eosin staining was carried out by incubating slides for 15 minutes in ematoxilin at room temperature. After rinsing for 10 minutes in running water, coverslips were further incubated in eosin for 1 minute, at room temperature. Subsequently, after being rinsed in bidistilled water, slices were dehydrated with successive (2 minutes long) washes in ethanol solutions of increasing concentrations (70%, 96%, 100%). They were then rinsed with two 4-minute washes in Xylene (Fluka), and mounted with Eukit (Fluka).

b) ***Luxol Fast Blue staining*:** after incubation in ethanol for 2 minutes, slices were kept in a Luxol Fast Blue solution (Luxol Fast Blue, 1 g; Methanol, 1000 cm^3; 10% acetic acid) for two hours at 60°C. Subsequently, slides were washed in alcohol (70%) and tap water.

In both cases (a and b) slices were then analyzed under a 20× Zeiss Axiophot microscope and images were acquired with a camera.

Figure VII shows a slice stained with luxol fast blue. Therefore, the darker staining indicates myelination. These fibers were about 10% of the area of the slice (n=2).

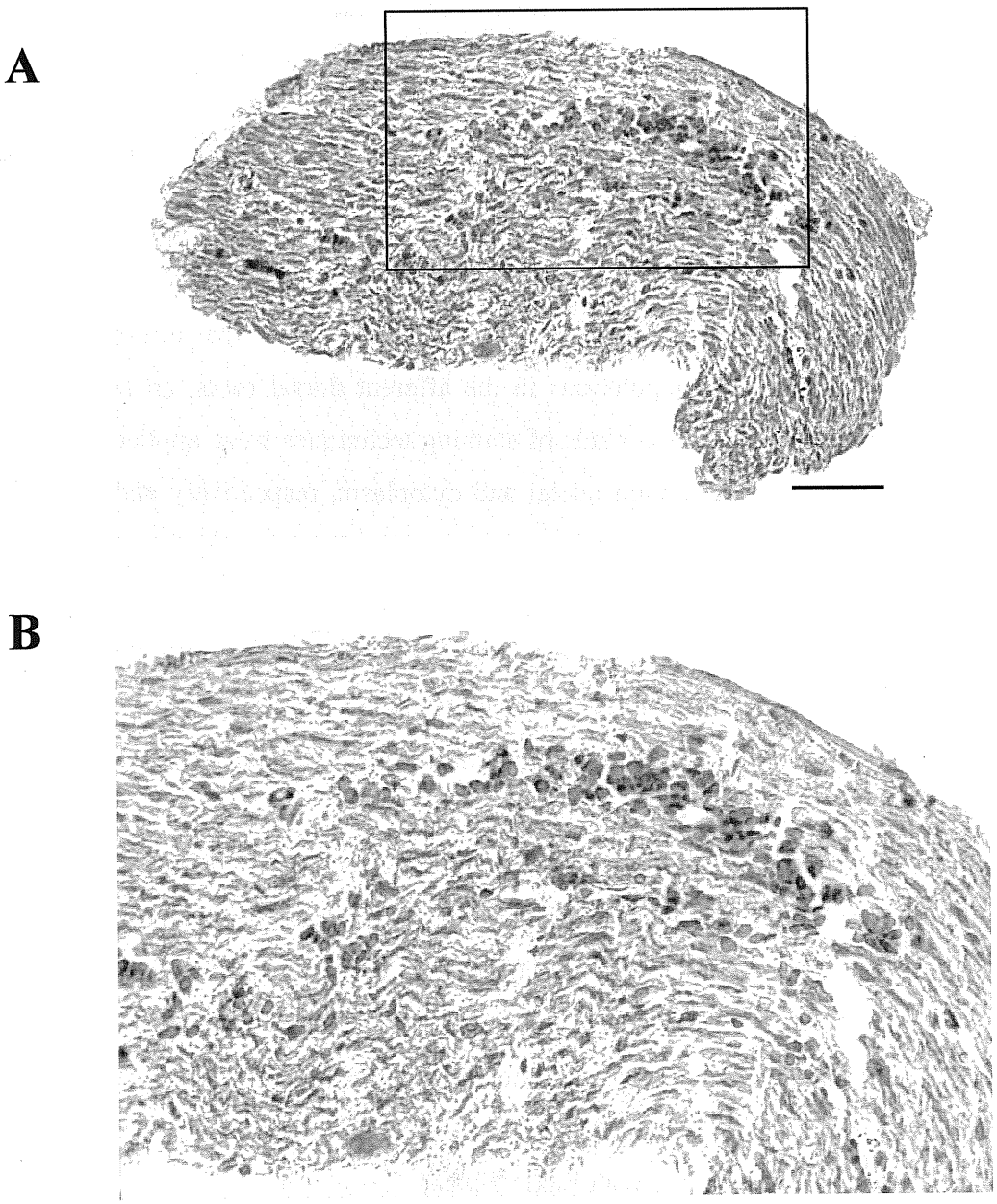

Figure VII. A. Section of an afferent L5 dorsal root, from a P3 rat, stained for myelin, with Luxol fast Blue (calibration bar: 100 μM, 20x). B. Enlargement of the area outlined in panel A.

8. DRUGS

Drugs were bath applied via the superfusion solution. Stock solutions of the agents (usually at concentrations 10^3 higher than the final ones) were made in distilled water and frozen in small aliquots (≤ 1ml volume). The final concentration was obtained by dissolving an amount of the stock into the ACSF. Drugs were usually dissolved in distilled water. Concentration of drugs that were dissolved in dimethylsulphoxide (DMSO) was such that DMSO concentration in batch was <0.02%.

9. DATA ANALYSIS

All data were stored on a DAT tape recorder (MicroData Instruments), digitized at 10 kHz and played back for off-line analysis.

9.1 Definition of measured parameters

9.1.1 Analysis of oscillatory activity

Quantitative analysis of oscillatory activity (fictive locomotion induced either chemically or electrically; activity induced by NK_3 receptor or mGlu receptor activation), required the definition of some basic parameters. Figure VIII shows the method used for measuring the cycle period (T): the trace was first low-pass filtered (10 Hz cut off frequency) and baseline (line a) was calculated taking the average of 100 ms during the quiescent phase between two cycles. Another line (line b) was placed at 3 times the standard deviation (SD) of the baseline noise. The onset of each cycle was determined by the first (ascending) crossing of line b with the trace, while the end of the cycle was fixed at the second ascending crossing. When the phase relationship between two ventral roots was calculated, the same operation was applied to both traces. The phase shift was determined as the latency between the two consecutive onsets in the two analyzed roots (ΔT in Figure VIII). Within each cycle, the quantity $\Phi=2\pi\cdot\Delta T/T$ was defined as the phase shift expressed in radians (or degrees), so that 2π indicates synchronicity and π complete alternation. This quantity was used to assess whether phase relationship between bursts in each ventral root was giving rise

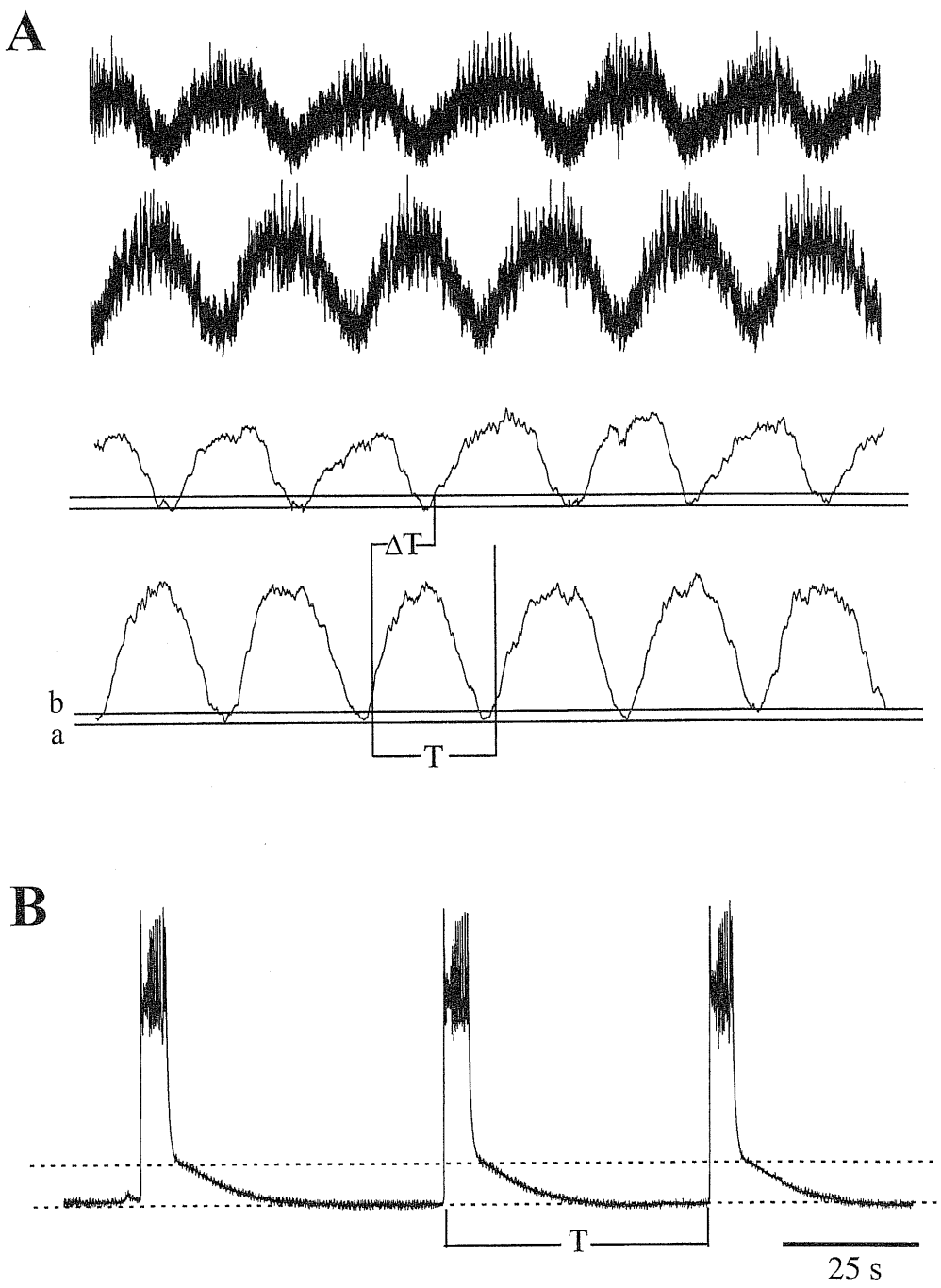

Figure VIII. Definition of parameters measured during rhythmic activity. A. Fictive locomotion rhythm. B. Disinhibited rhythm.

to activity compatible with locomotion and whether fictive locomotion was preserved during various pharmacological treatments. When periods and phase shifts were analysed in chemically induced oscillatory acivity, a collection of at least 10 cycles were selected at

random, averaged and expressed as mean ± SD (standard deviation). Often, during electrically induced oscillations, a smaller number of oscillatory cycles was present, and therefore analysed.

9.1.2 Analysis of disinhibited rhythm

During disinhibited rhythm, bursts appeared as episodes of sustained membrane depolarization. Burst period was defined as the time between the onset of two consecutive bursts. Burst duration was calculated from the onset of the burst to when the signal had a marked change in slope (see Figure VIII). When this was not a clear point, burst duration was measured as the time in which membrane potential was above a certain threshold, set at 5-25 times the standard deviation of the baseline noise (measured over 0.5-1 s during the quiescent period immediately before the onset of a burst), depending on signal-to-noise ratio conditions. Intraburst oscillations period was measured as the peak-to-peak time interval.

9.1.3 Analysis of Single Cell Recordings

Measurements of motoneuron input resistance was carried out by averaging at least ten traces in which a hyperpolarizing step was delivered through the recording electrode. Input resistance was then calculated as the ratio between the averaged voltage response and the applied current (usually 0.1-0.2 nA).

Similar measurements were performed to generate I-V curves, in which the averaged voltage responses to hyperpolarizing and depolarizing steps was plotted against amplitude of injected current.

In the case of recurrent depolarizing potentials measurements, at least ten responses were averaged and measured in terms of peak amplitude, rise time, decay time, time-to-peak and area. Rise time and decay time was measured between 10% and 90% of peak amplitude. In certain cases, decay time was also estimated with a monoexponential fitting carried out with Chebychev algorithm, provided by Axograph Software.

9.2 Linear Statistics Analysis

Data was expressed as mean ± SD (standard deviation) while "n" denoted the number of experiments used to calculate the mean and SD.

Before assessing statistical differences between groups, a normality test was performed to select using parametric or non–parametric tests.

For comparison between two groups, the following tests were performed depending on data: Student's *t*-test (paired or unpaired) for normally distributed data or Wilcoxon Signed Rank or Mann Whitney for non-normally distributed data. For multiple comparisons, ANOVA (ANalysis Of VAriance) tests were used (ANOVA on ranks, in the case of non-parametric data), followed by a post-hoc test (Tukey test). Accepted level of significance was p= 0.05.

9.3 Circular Statistics Analysis

Strength of coupling between activity of different VRs was analysed with methods of circular statistics (Drew & Doucet, 1991; Kjaerulff & Kiehn, 1996). In the following subsections, the parameters and the statistical test (Rayleigh test) used for this analysis are explained. A program in Matlab was written to calculate numeric values for the parameters, test significance and generate a graphical output, representing the Rayleigh vector on a phase plot (see Figure IX).

9.3.1 Rayleigh Test

To calculate the strength of coupling between the activity of different VRs (usually left/right and L2/L5 pairs), first phase was calculated as $\Phi_i = 2\pi \cdot \frac{\Delta T_i}{T_i}$ (see § 8.1.1) for each cycle *i*, and the mean phase defined as:

$$\Phi = arctan\left(\frac{Y}{X}\right)$$

being:

$$X = \frac{\sum_{i=1}^{n} \cos \Phi_i}{n} \qquad Y = \frac{\sum_{i=1}^{n} \sin \Phi_i}{n}$$

R was then defined as the concentration of values around the mean:

$$R = \sqrt{X^2 + Y^2}$$

and ranges between 0 and 1. This vector can also be represented graphically by the length of the vector.

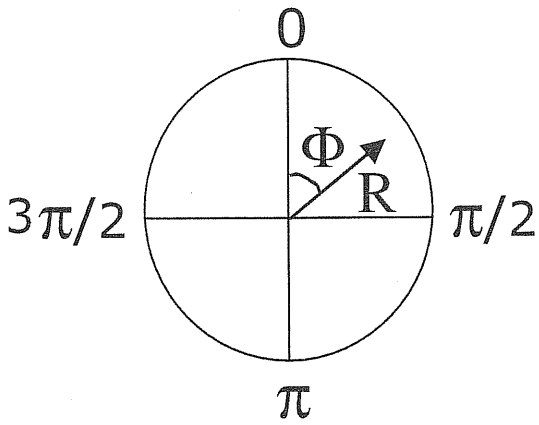

Figure IX. Circular phase diagram, representing for Rayleigh vector. Φ indicates the mean phase value and is graphically represented by the angle of the vector (0-2π). R indicates the concentration of phase values around the mean (ranging betweeen 0 and 1) and is represented graphically by the length of the vector.

When phase values are highly concentrated around the mean value, $R \rightarrow 1$, i.e. coupling is strong. On the contrary, when phase values are uniformly distributed around the 0-2π circle, $R \rightarrow 0$, i.e. there is no coupling between activity in two VRs.

Furthermore, to illustrate variability of the data, the value R can be used to calculate an angular deviation (in radians):

$$s = \sqrt{(-2 \ln R)}$$

Statistical significance of these values can be assessed with the Rayleigh test (Drew & Doucet, 1991). In this test, the null hypothesis is that R, the concentration of phase values around the mean, is not sufficiently high to state that phase coupling is present.

In the Rayleigh distribution, given n vectors Φ_i, $i=1...n$, randomly distributed in [0,2π], the probability that r< R_0 is:

$$P(r < R_0) = 1 - e^{-R_0^2/n}$$

To test whether the distribution of our variable $R_o = R$ is uniform, i.e. to test our null hypothesis, it is sufficient to calculate the quantity $e^{-R_0^2/n}$ and reject uniformity if it falls short of the chosen level of significance (usually 0.05).

9.3.2 Small sample Modification

When n is small (as it sometimes was in the analysis of electrically induced oscillations), there is a substantial discrepancy between the distribution of R (the concentration of phase values around the mean) and the Rayleigh distribution for r. In this case, rather than applying precise mathematical expressions for the distribution of R (Kluyver's formula, 1906), which presents computational difficulties, one can take the asymptotic expansion of the formula (Durand & Greenwood J.A., 1958). To this end, the test variable is first redefined as $Z = n \cdot R^2$ and it will be compared to a critical value Z_0. To calculate Z_0:

$$P(r < R_0) = P\left(\frac{r^2}{n} < Z_0\right) = 1 - P\left(\frac{r^2}{n} \geq Z_0\right) = 1 - Q$$

(being Q the accepted level of significance) and the expansion carried out:

$$P\left(\frac{r^2}{n} < Z_0\right) = 1 - e^{-Z_0^2/n} = 1 - e^{-Z_0}\left[1 + c_1\left(Z_0, Z_0^2\right)\cdot\frac{1}{n} + c_2\left(Z_0, Z_0^2, Z_0^3\right)\cdot\frac{1}{n^2} + O\left(\frac{1}{n^3}\right)\right]$$

from which:

$$P\left(\frac{r^2}{n} > Z_0\right) = e^{-Z_0}\left[1 + c_1\left(Z_0, Z_0^2\right)\cdot\frac{1}{n} + c_2\left(Z_0, Z_0^2, Z_0^3\right)\cdot\frac{1}{n^2} + O\left(\frac{1}{n^3}\right)\right]$$

Reversing to find Z_0 through subsequent substitutions of $O(1)$, $O(\frac{1}{n})$,... one can rewrite the equation to:

$$Z_0 = a_0 + \frac{a_1}{n} + \frac{a_2}{n^2} + \frac{a_3}{n^3} + O\left(\frac{1}{n^4}\right)$$

where the constants a_0, a_1,... depend only on the accepted level of significance Q:

$$a_0 = -\ln P\left(\frac{r^2}{n} > Z_0\right) = -\ln Q$$

$$a_1 = \frac{\left(2a_0 - a_0^2\right)}{4}; \qquad a_2 = \frac{\left(12a_0 - 3a_0^2 - a_0^3\right)}{4}; \qquad a_3 = \ldots$$

Usually the first two terms of the series provide a substantial improvement and it is not needed to calculate terms of the order of $1/n^3$.

For an accepted level of significance of Q=0.05, a_0=2.99573, a_1= -0.74574, a_2= -0.24805, which, given n, allows the calculation of Z_0.

If $Z\ (= n \cdot R^2) > Z_0$, there is significant modulation of the variable R, i.e. there is significant coupling between phases.

RESULTS

1. FICTIVE LOCOMOTOR PATTERNS CAN BE EVOKED BY DORSAL ROOT STIMULATION

In the neonatal rat spinal cord, rhythmic locomotor-like patterns can be elicited by bath-applied excitatory substances like NMDA (Kudo & Yamada, 1987), serotonin (Cazalets *et al.*, 1992; Beato *et al.*, 1997) or high potassium (Bracci *et al.*, 1998). Although this approach has yielded important insights into the mode of operation of the fictive locomotor network, persistent bath application of these excitatory substances to the entire spinal tissue represents a non-physiological condition (see INTRODUCTION § 3.2.2, 3.2.4). One way to try to overcome this problem and a functionally important issue to investigate is whether inputs from the periphery would have the ability to trigger the activation of the locomotor CGP. In the present study, the occurrence and the basic properties of an alternating locomotor-like pattern triggered by stimulating dorsal root fibers are described.

1.1 VR oscillations induced by DR stimuli

Fig. 1 A shows an example of activity induced by applying a 12.5 s train of 2 Hz stimuli (2xTh) to left L5 DR. During the stimulation train a gradual baseline depolarization developed, upon which oscillatory activity (with action potential firing on top of each oscillation) emerged. The period (T) of this pattern was 1.0 ± 0.2 s measured for 9 cycles. This oscillatory activity outlasted the stimulus train and presented typical alternation between contralateral VRs and intersegmental VRs (for example left L2 was in antiphase with left L5). In order to quantify the pattern alternation, the phase of this activity was expressed in polar plots as shown in Fig. 2 for 18 preparations. Individual data points refer to single preparations stimulated within the 0.5-10 Hz and 1.3-10xTh range. In each panel data (from left/right VRs or from cranial/caudal homolateral VRs) were grouped around 180° indicating that they occurred in antiphase. In particular, mean values were 186±17° (left/right L2), 180±20° (left L2/L5), 182 ±21° (right L2/L5), and 182±19° (left/right L5). The Rayleigh test

showed that for each one of these root pairs the coupling strength (expressed as R values; see METHODS § 9.3) was significant (R=0.92±0.28 for left/right L2; R=0.91±0.30 for left L2/L5; R=0.89±0.30 for right L2/L5; R=0.92±0.28 for left/right L5; $p<0.005$ for each pair; number of cycles from each preparation was 5-15).

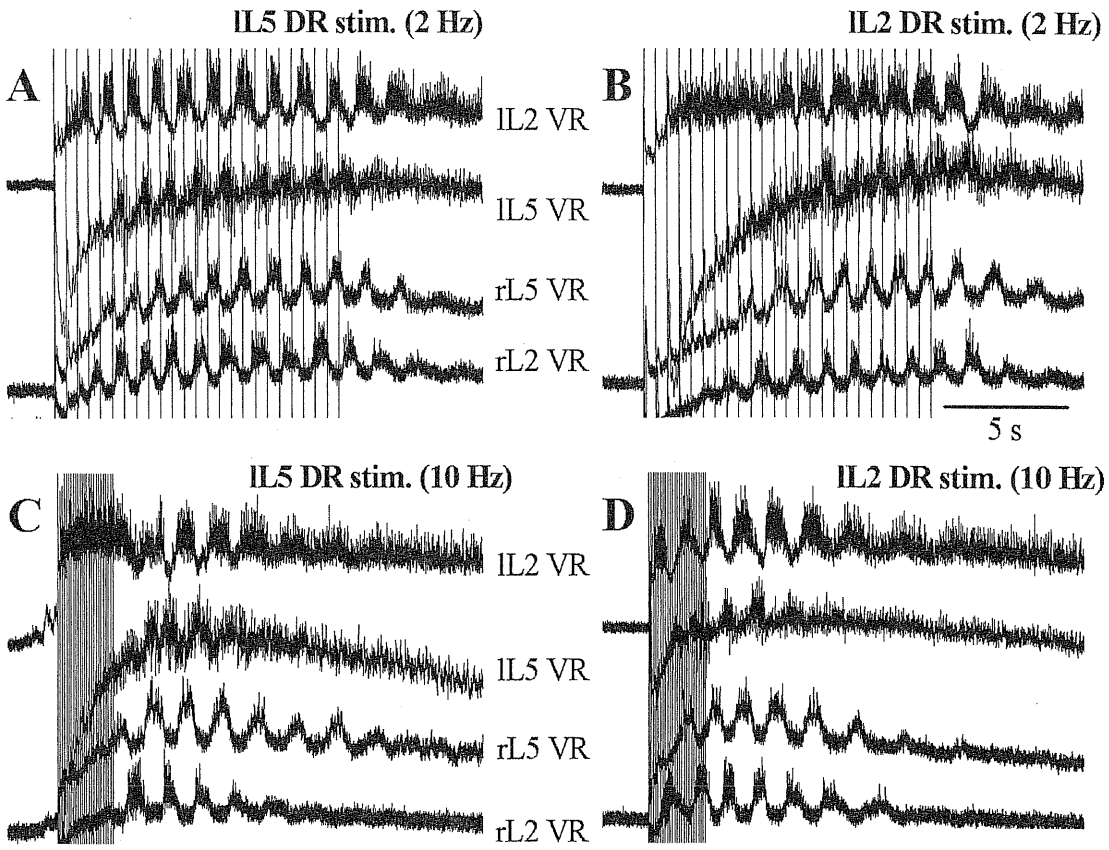

Figure 1. Locomotor-like patterns induced by different stimulation protocols. Each panel shows DC records of responses from pairs of VRs (left, l, or right, r, of L2 and L5 segments) in the same preparation. Oscillations are in alternation between contralateral VRs and between intersegmental VRs of the same side; they are not time-locked with the stimuli (applied at constant intensity=2xTh; stimulus artifacts are shown as large deflections) and persist when the train is over. A: L5 DR is stimulated with 2 Hz train (25 pulses), T=1.0±0.2 s. B: stimulation of left L2 DR with a 2 Hz train, T=1.25±0.3 s. C: stimulation of left L5 DR with a 10 Hz train, T=1.25±0.3 s. D: stimulation of left L2 DR with a 10 Hz train, T=1.25±0.3 s. Baseline traces are shown for left VR L2 and right VR L5 only.

Fig. 1 B shows that, on the same preparation shown in Fig. 1 A, a similar pattern of oscillatory activity (T=1.25±0.3 s; 7 cycles) was observed when the stimulus train (2 Hz) was applied to left L2 DR. Still on the same preparation it was also possible to evoke an oscillatory pattern when stimulating left L5 or left L2 DRs at higher frequency (10 Hz; same

intensity; T values=1.25±0.3 s, 5 cycles in either case) as shown in Fig 1 C and D. The pattern of activity illustrated in Fig. 1 was elicited in 42/54 preparations. DR stimuli were ineffective to elicit oscillatory activity from twelve spinal cord preparations, eight of which did generate fictive locomotor patterns with bath-application of NMDA (4-6 μM) and serotonin (5-8 μM) (see also Kjaerulff & Kiehn, 1996; Beato *et al.*, 1997) while the remaining four were insensitive to these chemical agents as well. Since DR stimuli evoked alternating patterns in the large majority of preparations, the electrophysiological characteristics of this effect were further explored.

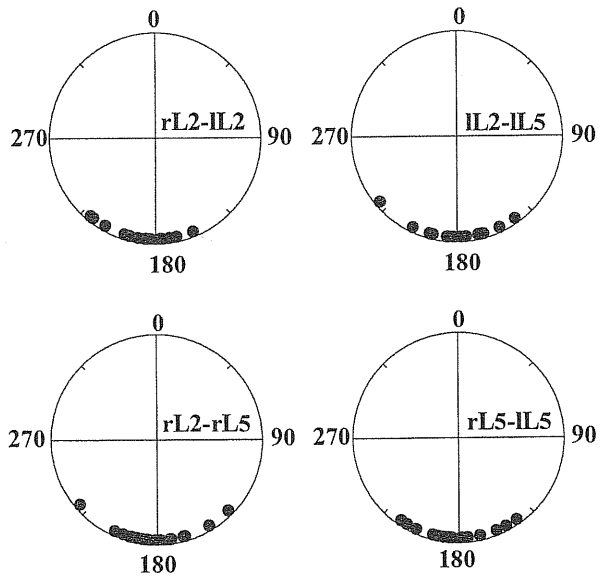

Figure 2. Phase plots of oscillatory activity induced by DR stimulation. Distribution of oscillatory phase values (expressed as degrees; see METHODS) recorded for pairs of VRs following DR stimuli (0.5-10 Hz and 1.3-10xTh). Each data point represents the mean result (averaged from 5-15 cycles) from a single spinal cord preparation. Grouping of data around 180° indicates phase lock between responses from each pair of VRs.

1.2 Characteristics of DR stimuli to induce alternating patterns

We first tested how the oscillatory pattern might have changed with varying intensities of DR stimulation. As indicated by the histograms of Fig. 3 A, period (calculated for the first 5-10 cycles; 0.5-4 Hz stimulus rate) weakly depended upon stimulus intensity because a significant (one way ANOVA followed by Tukey test; $p<0.05$) decrease was found only

when strong (≥10×Th) pulses were applied (compared against the 1.3x, 1.8x and 5xTh groups; *n*= 12). We next explored the relation between oscillatory period and stimulation

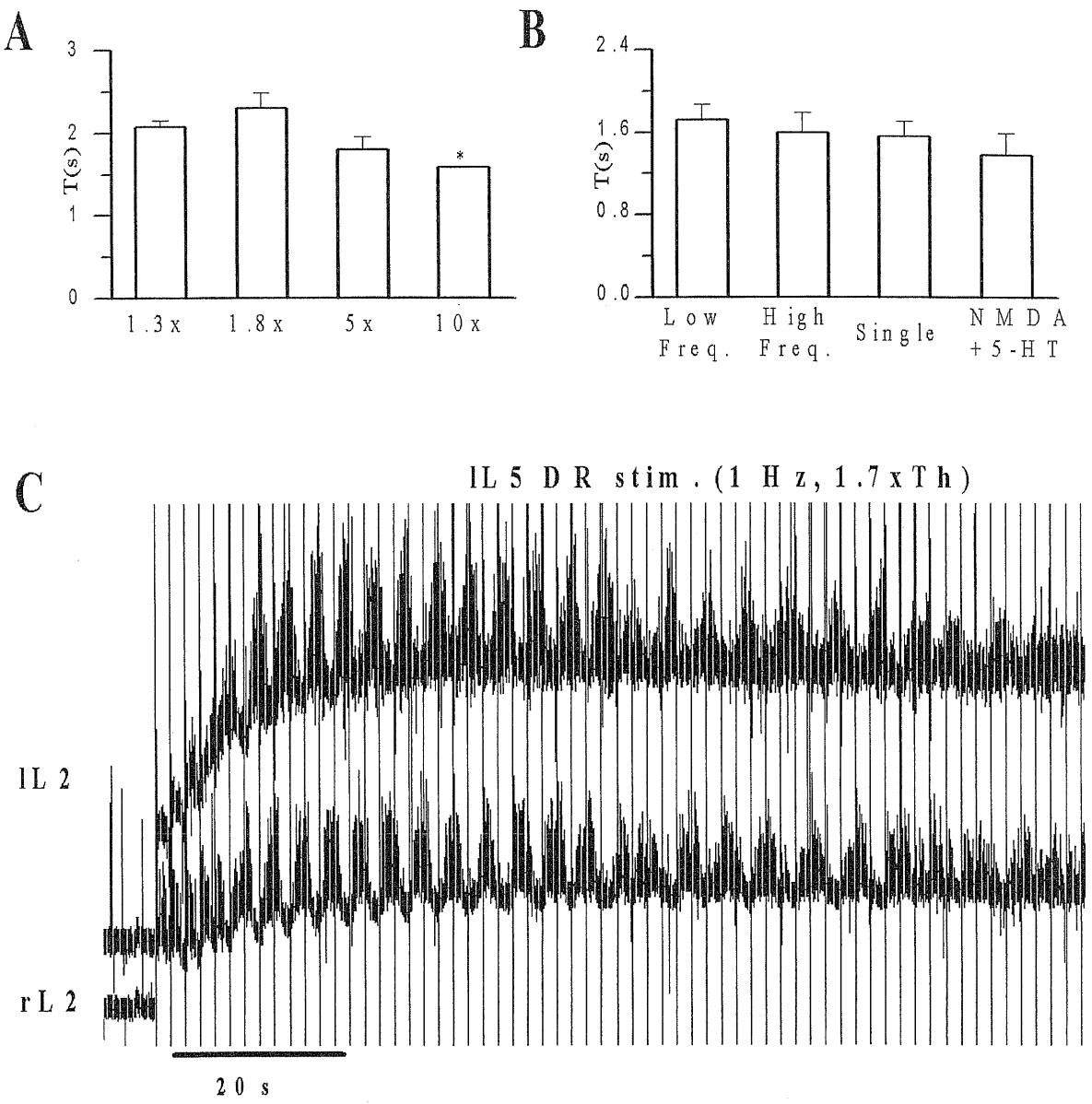

Figure 3. Effects of changing intensity and/or frequency of DR stimuli on oscillatory period. A. Relation of oscillation period to stimulation intensity (expressed as multiple of threshold intensity; *n*=12 preparations): there is a significant reduction in the period of oscillations only for high intensity (10xTh) stimuli ($p<0.02$; asterisk). Period values (usually 5-10 episodes) corresponding to each histogram are: 1.3×Th, T=2.08±0.07 s; 1.8×Th, T=2.30±0.18; 5xTh, 1.80±0.15 s; 10×Th, T=1.55±0.01 s. B: Period values for oscillations induced by different types of stimuli (intensity 2-5xTh) remain the same with low (0.5-4 Hz, T=1.72±0.15 s) or high (10-50 Hz, T=1.6±0.2 s) frequency trains (*n*=12), a single stimulus (1.56±0.15 s, *n*= 3) or patterns (*n*=5) induced by NMDA (4 μM) plus serotonin (5-HT; 5 μM, T= 1.39±0.21).C: records showing gradual lengthening of period of L2 VR oscillations during a train at 1 Hz (1.7xTh intensity). Sharp deflections are stimulus artifacts.

frequency when the stimulus intensity was ≥10×Th. The histogram in Fig. 3 B shows that there was no significant change in oscillation period when stimulating with low frequency (0.5-4 Hz) trains (T=1.55±0.05 s), high frequency (10-50 Hz) trains (T=1.6±0.2 s), or even single stimuli (T=1.56±0.15 s). Note that in only 3/12 preparations a single, high voltage (≥10×Th) stimulus was able to elicit oscillations (lasting on average 14±3 s). The histogram in Fig. 3 B also indicates that the rhythmic activity induced by the combined application of NMDA (4 μM) plus serotonin (5 μM; Beato & Nistri, 1999) had similar period of oscillation (T=1.39±0.21 s; *n*=5).

While our average period data were collected during the first 5-10 cycles of an oscillatory episode, it was clear that the oscillatory pattern usually varied during the train as shown in Fig. 3 C. Oscillations did not have a stereotypic onset and abrupt termination as the rhythm started simultaneously in left and right L2 (stimulus train applied to L5 DR; 1 Hz), built up to the fastest (2 s) cycles and became progressively longer. In the example of Fig. 3 C rhythmic oscillations lasted 55 s (on average 50±20 s, *n*=25 spinal cords) after which they failed despite continuing stimulation.

1.3 Duration of fictive locomotor patterns

Experiments were carried out to probe why the alternating pattern slowed down despite continuous stimulation. First, we quantified this phenomenon. On 12 preparations (stimulated at 0.5-4 Hz, 2-5×Th intensity) the cycle period (normalized to that of the first cycle in each episode for each spinal cord) grew to 174±15 % only after the first ten cycles with a slope of 6.1±0.4 % increment/cycle over the subsequent 11 cycles (*r*=0.98±0.21). The mechanism responsible for this delayed slowing down of oscillations was probed in tests like those depicted in Fig. 4. In this example, repetitive, weak (1.3xTh) stimuli applied to right L5 DR (to activate only low threshold afferent fibers) evoked oscillations (T=1.7 s) which lasted about 15 s and then waned even though the polarization level of the VRs remained steady. The possibility that this could have been caused by a generalized depression of synaptic activity in the spinal cord seemed unlikely since pattern loss was not associated with depression of VR reflex responses (see Fig. 4, bottom row) as indicated by the average reflex area (3.2 vs 2.9 mV×ms) recorded from left L2 VR during and after rhythmic oscillations (see corresponding records for the times indicated by open horizontal bars). Note that VR reflexes were averaged after the 4th response in the train, *i.e.* when they reached steady state

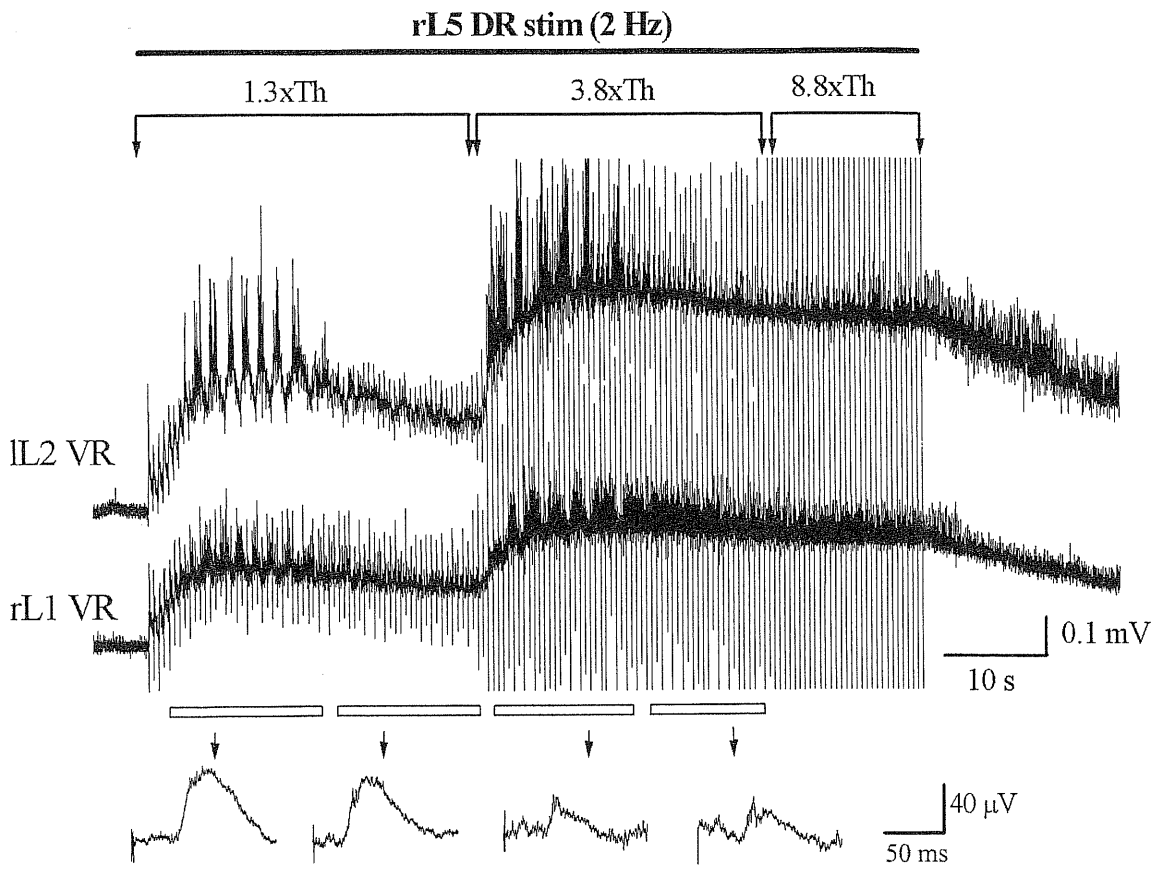

Figure 4. Failure and reappearance of locomotor-like patterns with different stimulus intensities.
Long train of stimuli delivered to the left L5 DR (2 Hz) at different intensities (1.3, 3.8 or 8.8xTh) elicits responses recorded from two contralateral VRs (lL2 and rL1): a stimulus just above threshold for activating the faster conducting fibres induces an alternating pattern (T=1.7 s) that is lost after about 15 s; the pattern is recovered (T=2.0 s) when stimulus intensity is raised above the voltage threshold for slower conducting fibres. When the pattern is lost again after about 15 s, further increase in stimulus intensity cannot re-establish the pattern. The traces in the bottom row show time-locked lL2 VR reflexes (averages of 30, 28, 28, 22 sweeps, respectively) recorded during the time indicated by the open bars: loss of locomotor-like activity is not associated with depression of VR reflex. Smaller amplitude reflexes during stronger stimuli indicate partial development of synaptic fatigue. Stimulus artifacts are fast deflections of various amplitude owing to sampling rate.

amplitude after the very early depression of monosynaptic transmission (Lev-Tov & Pinco, 1992). In the experiment shown in Fig. 4, when the intensity of the stimulus was raised (3.8xTh) presumably to recruit higher-threshold fibres, the oscillatory pattern (T=2.0 s) returned for 15 s, after which it failed again. Even if the VR reflex was smaller than the one observed with the weaker stimuli, it remained unchanged (1.1 *vs* 1.2 mV×ms) throughout the stimulation at 3.8xTh (see sample traces indicated by open bars). Baseline activity was also

enhanced by irregular spontaneous firing. Thus, the secondary loss of alternating activity was not associated with generalized, intense synaptic fatigue in the spinal network. Further increase in stimulus intensity (8.8xTh) was unable to re-establish the alternating pattern. Similar results were obtained from 8 preparations. Despite using a wide range of stimulus intensity (1-10xTh) or frequency (0.5-50 Hz) it was not possible to elicit persistent alternating patterns.

When the stimulus intensity strength was relatively large (2.5xTh) so as to activate both classes of afferent fibers from the outset, patterns emerged with gradual slow-down in period value until failure (not shown; *n*=8). Further increasing the stimulus intensity could not reinstate oscillations.

On 5 preparations we next explored if loss of patterned activity was selective for the stimulated input or whether stimulation of the contralateral root could re-establish the rhythm. Thus, the pattern recorded from L2 VRs was evoked by left DR L5 stimulation (2 Hz) first at low intensity (1.4xTh) until it disappeared and was then elicited with stronger (2.5xTh) impulses. In the latter case it lasted 12±4 s and then disappeared again. At this stage right DR L5 (or L4) was stimulated at low intensity (1.4xTh) and generated the pattern which also lasted 12±4 s (period value was 121±30% of the previous one). As usual, loss of rhythmicity occurred against a background of intense irregular firing and could not be reversed by low or high threshold stimuli applied to left or right DR L5. A period of rest (*circa* 10 min) was however sufficient to re-instate DR-stimulation induced rhythmic activity.

1.4 Intracellular recordings

Intracellular recordings with 3 M KCl-filled electrodes were performed on L2, L3 or L5 motoneurons (resting potential, V_m=-73±9 mV, *n*=21) together with DC ventral root recordings (Bracci *et al.*, 1998; Beato & Nistri, 1999) as exemplified in Fig. 5 A. Repetitive (2 Hz) stimulation of the lL5 DR (0.1 ms; 1.7xTh) induced 26 mV depolarization of an rL3 motoneuron (Fig. 5 A bottom trace) from –60 mV V_m (on average 24±6 mV, n=7 cells). With 7 s time lag from the start of the train, oscillations emerged and were out of phase between the left L2 VR (top trace in Fig. 5 A) and the right L3 cell (bottom trace of Fig. 5 A) as expected for a fictive locomotor-like pattern. Repolarizing motoneuron potential to its resting value failed to change (105±11% from control value of T=2.1±0.2 s, *n*=5) the period of these oscillations (not shown).

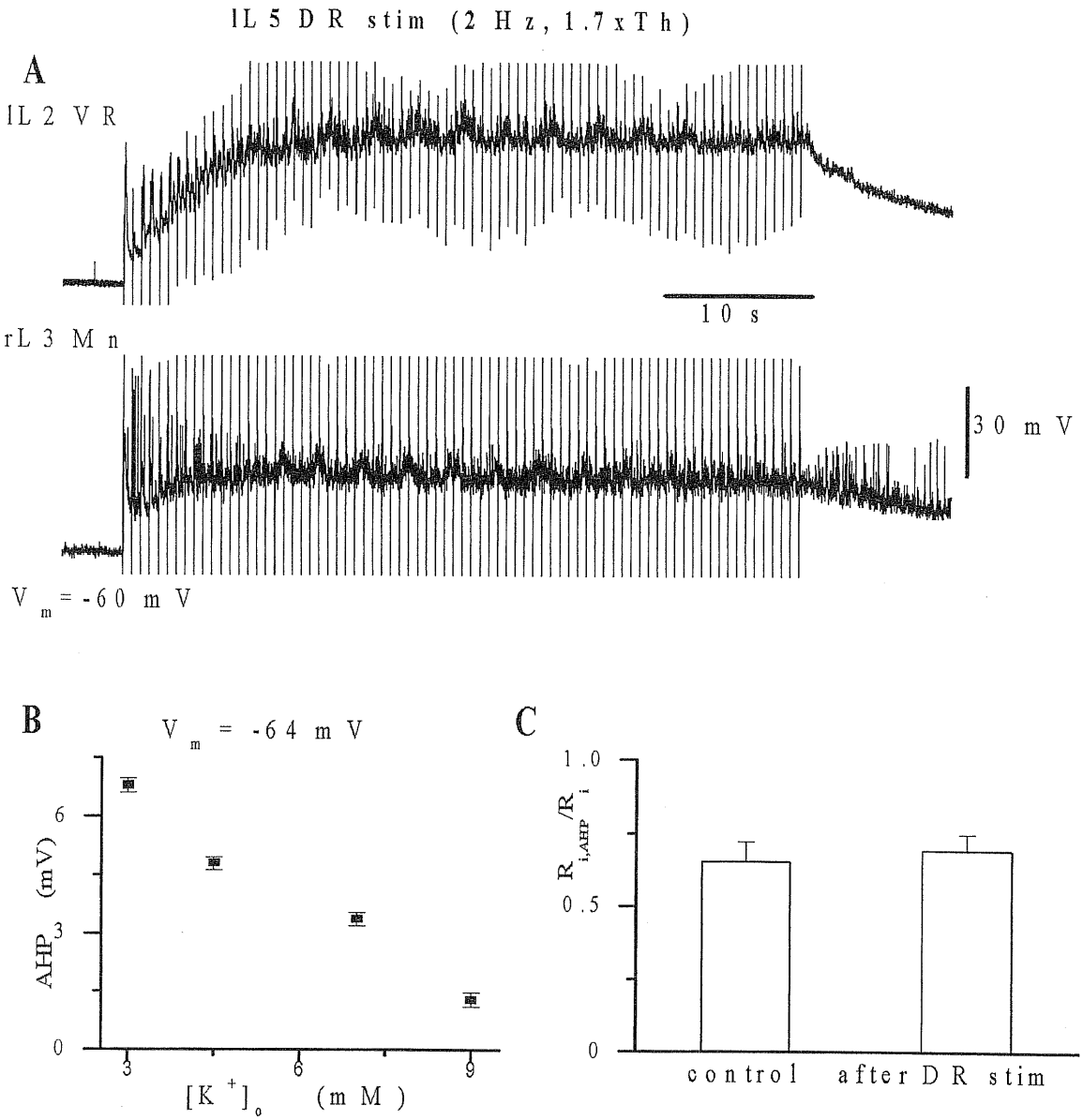

Figure 5. Intracellular and extracellular records from motoneurons. A: traces of membrane potential from right L3 motoneuron (rL3 Mn; bottom) and of left L2 VR polarization level when stimulating left L5 DR. Oscillations (2 s period) are out of phase between left VR L2 and right L3 motoneuron. Rapid deflections are stimulus artifacts of pulses applied to DRs. B: plot of AHP amplitude *vs* $[K^+]_o$. AHP, measured from antidromic spikes elicited from an L3 motoneuron at -64 mV V_m (in the presence of 1 μM strychnine), shows an almost linear decrease as a function of $[K^+]_o$ (different cell from A). C: Ratio between input resistance measured during the AHP ($R_{i,AHP}$) and membrane resistance measured right before the antidromic spike (R_i) in two conditions: absence of stimuli (control) and immediately at the end of a train of DR stimuli (2 Hz; 1.7xTh). The difference is not significant (n=4), indicating no apparent block of AHP conductance by transmitters released by DR stimuli.

1.5 K^+ Hypothesis

Since repeated stimuli to rat DRs raise extracellular K^+ ($[K^+]_o$) enough to influence neuronal excitability (Walton & Chesler, 1988) and phasic variations of $[K^+]_o$ occur during fictive swimming generated by the lamprey spinal cord (Wallen *et al.*, 1984), we hypothesized that this might be the cellular mechanism responsible for CPG activation, especially because even modest increases in $[K^+]_o$ evoke fictive locomotion (Bracci *et al.*, 1998). Ideally this notion should be tested with K^+-sensitive electrodes which, however, would have to be placed blindly in the spinal tissue, making it very difficult to identify any response as selectively due to CPG neuron activity. Furthermore, insertion of a K^+-sensitive electrode into the spinal cord is known to cause local injury with consequent rise in $[K^+]_o$ (Krnjevic & Morris, 1974). As a first approximation to investigate any $[K^+]_o$ build up, we used the afterhyperopolarization (AHP) amplitude of motoneuron antidromic spikes as a less invasive $[K^+]_o$ sensor. This approach seemed justified by the segmental co-localization of motoneurons and the neuronal networks responsible for their activation during locomotion (Tresch & Kiehn, 1999) and took advantage of the better accessibility of motoneurons for direct recording. The AHP method has long been used to measure $[K^+]_o$ changes (Baylor & Nicholls, 1969) and is applicable to rat spinal motoneurons as well (Forsythe & Redman, 1988).

In order to increase the size of the AHP of their antidromic spikes, motoneurons were usually depolarized by intracellular current injection to about V_m = -55 mV. At this membrane potential the AHP was readily contaminated by recurrent glycinergic IPSPs (Werman *et al.*, 1968). Hence, further tests for AHP measurement were done in the presence of 1 μM strychnine to avoid such a contamination. On each preparation we first established the adequacy of the DR stimulation protocol to induce alternating locomotor-like patterns; subsequently, in the presence of strychnine, we used the same DR stimuli which still evoked oscillatory patterns, though lacking alternation.

Since any excitability increase induced by strychnine *per se* might have raised motoneuronal leak conductance and thus altered the AHP, an independent check for this possibility was done by measuring the amplitude of the antidromic spike initial segment (IS). IS is due to electrotonic back propagation (to the soma) of the action potential generated at the level of the axon initial portion and is a constant current generator to measure somatic input resistance (Werman, 1969). On 7 motoneurons the IS amplitude (correct detection of the IS/SD [somato-dendritic] spike separation was confirmed by measuring the spike dV/dt) was similar

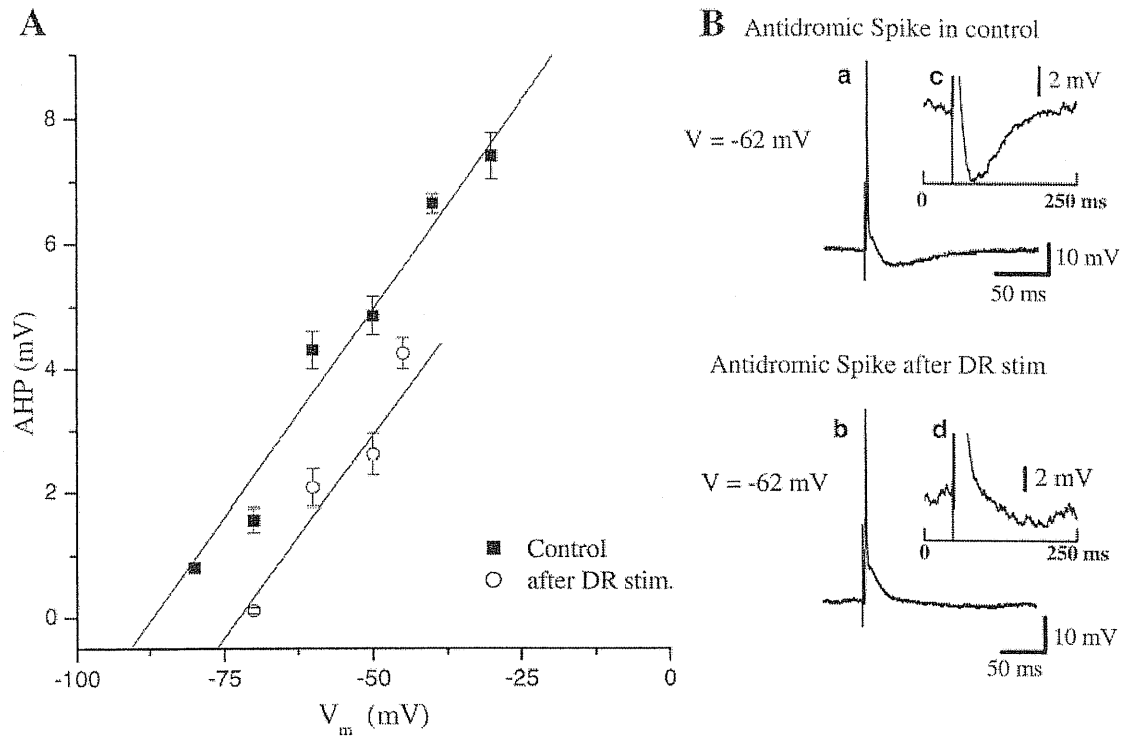

Figure 6. Changes in AHP amplitude following DR stimulus trains. A: AHP amplitude plotted *vs* V_m for a cell bathed in 4.5 mM $[K^+]_o$, in the absence of DR stimuli (control, filled squares) and immediately after DR stimuli (open circles; stimulus train: 2 Hz, 3xTh). There was a rightward, parallel shift of the line fitting the data points, indicating an AHP decrease due to DR stimuli. Ba, Bb: example of antidromic spikes from which AHP amplitude was measured. The two spikes have the same baseline potential of -62 mV. Bc, Bd show the AHPs (from Ba and Bb, respectively) with expanded voltage and time scales (stimulus artifact has been removed for illustration).

in control or in strychnine solution (22±8 mV or 18±8 mV, respectively, $p>0.05$), indicating lack of major somatic resistance shunt caused by strychnine application.

On cells manually repolarized to initial resting potential, we first established that there was a linear relation (slope value of -0.85 mV/mM $[K^+]_o$ change) between the concentration of K^+ in the bathing solution and the AHP amplitude in the absence of DR stimulation (Fig. 5 B). On 6 cells the average slope was –0.79±0.3 mV/mM which could then be used to calculate changes in AHP observed during DR stimuli as changes in $[K^+]_o$. Fig. 6 A quantifies changes in AHP amplitude (measured at different baseline potentials) in control conditions (filled squares) and immediately after DR stimulation (open circles; 2 Hz, 3xTh DR stimulation) in a single cell. The line fitting the data points was shifted rightwards with no change ($p<0.05$) in slope (0.13±0.01 without DR stimuli and 0.15±0.03 during DR stimuli; r=0.98 or 0.97,

respectively). At V_m=-60±2 mV the AHP was nearly halved (from 4.3 to 2.1 mV) following DR stimulation. The decrease in AHP size is shown in Fig. 6 Bc,d while the corresponding antidromic spikes are in Fig. 6 Ba,b (at the same -62 mV V_m). The AHP reduction corresponds to a shift in $[K^+]_o$ from 4.5 to 7.3 mM calculated from the the relation between these two variables. A similar result can also be obtained from the graph of Fig. 6 A as the extrapolated reversal potential of the AHP shifts from -87±3 mV in 4.5 mM $[K^+]_o$ to -73±4 mV in coincidence with the DR stimulation. Using the Nernst equation, the calculated $[K^+]_o$ value for the latter condition corresponds to 7.8 mM. Thus, two different approaches to estimate $[K^+]_o$ during the stimulation protocol gave values differing by 0.5 mM only. Similar $[K^+]_o$ values (7.9±0.4 mM) were calculated in 5 other preparations stimulated at 2-5xTh, 1-2 Hz. A further test for the method specificity was to explore if raising spinal excitability without reaching threshold for generating fictive locomotion might alter AHP amplitude enough to give an estimate of $[K^+]_o$ typical of fictive locomotion (≥7 mM). Hence, NMDA was applied at a concentration (2 μM) subthreshold to elicit rhythmic oscillations but still able to depolarize motoneurons by 18±3 mV. The AHP amplitude after manually repolarizing the cell membrane to control, pre-drug level (-55±8 mV) was 6.2±0.6 mV (control AHP = 7.4±3.1 mV; *n*=5 cells) and which would correspond to a rise in $[K^+]_o$ equivalent to 6.0±0.5 mM.

It was necessary to investigate if factors independent from $[K^+]_o$ might have contributed to AHP changes. For example, any AHP decrease due to DR stimuli might have been caused by large shunt in the motoneuron input resistance caused by intense transmitter release rather than by local build-up of $[K^+]_o$. On 6 cells before or immediately at the end of the stimulation protocol (at the same V_m), resting input resistance measured from hyperpolarizing electrotonic potentials (induced by -0.1,-0.2 nA) was 23±4 MΩ or 22±5 MΩ, indicating lack of large shunt. Furthermore, two parameters which critically depend on the motoneuron input resistance, like the antidromic spike amplitude (71±9 mV *vs* 65±12 mV, V_m= -58±5 mV) and the IS amplitude (18±8 mV *vs* 17±7 mV) remained the same. Finally, locomotor-like rhythmic activity evoked by 6-8.5 mM K^+ was not accompanied by large changes in resting input resistance (27±6 MΩ *vs* 30±5 MΩ observed in control solution; *n*=3; p>0.05).

Another possibility was that, during the stimulation protocol, the AHP might have been depressed by endogenously-released neurotransmitters like serotonin (Berger *et al.*, 1992; Larkman & Kelly, 1998) that could block the AHP membrane conductance. For this purpose

we measured input resistance during the AHP immediately after DR stimulation once the membrane potential was manually repolarized to resting potential level. The histograms of Fig. 5 C show that the fractional resistance fall during the AHP was the same in the absence of any DR stimuli (control) and immediately after a train of DR stimuli (n=4), suggesting no block of the underlying conductance mechanism. These results collectively indicated that changes in AHP amplitude could be used to monitor changes in $[K^+]_o$ during oscillatory patterns evoked by repetitive DR stimuli.

2. GABA or Glycine on Newborn Rat Motoneurons: Depolarizing But Inhibiting

Although GABA and glycine are inhibitory transmitters in the adult brain (Curtis & Johnston, 1974; Krnjevic, 1974), their role during early neuronal development is still debatable (see Introduction § 2.5). The present study aimed at investigating whether GABAergic or glycinergic transmission at the level of the recurrent inhibitory pathway between Renshaw cells and motoneurons inhibited excitatory synaptic inputs to spinal motoneurons.

2.1 GABA and glycine mediated synaptic potentials on spinal motoneurons

Experiments were carried out on 14 lumbar motoneurons with -70±6 mV resting potential and 90±50 MΩ input resistance. In the adult mammalian spinal cord, antidromic stimulation of motoneurons activates, via motor axon collaterals, cholinoceptive Renshaw cells which in turn make synapses on motoneurons (Renshaw, 1941) to generate a inhibitory postsysnaptic potential (recurrent IPSP) with an early glycinergic (Werman *et al.*, 1968) and a late GABAergic (Schneider & Fyffe, 1992) component (see scheme in Fig. 7 A in which Renshaw cells are shown as dark-filled neurons). We examined if recurrent PSPs of neonatal motoneurons, recorded with a sharp electrode containing $KMeSO_4$ to avoid alterations in intracellular Cl^- (Eccles, 1957), were inhibitory. Table 1 lists the average parameters of the recurrent PSP which was always depolarizing at resting potential (peak amplitude=5±3 mV, n=14). It should be noted that all our experiments were carried out on cells loaded intracellularly with the Na^+ channel blocker QX-314 to abolish somatic action potentials which would otherwise contaminate the recurrent PSP with the spike AHP.

	Rise Time (ms)	Decay Time (ms)	Half Width (ms)	Time to peak (ms)
control PSP (n=14)	1.5±0.5	14±5	11±3	5.2±0.9
PSP in strych (n=6)	3.5±2.5	18±6	20.8±0.8	15±12
PSP in bic (n=4)	10.0±1.1	25±20	21±14	11±10
PSP in kyn (n=4)	2.1±1.0	19±15	20±7	8±4
EPSP (n=9)	30±9	70±30	130±10	60±20

Table 1. Characteristics of time-course of recurrent PSP and orthodromic EPSP of lumbar motoneurons. (Strych, bic and kyn indicate strychnine, bicuculline and kynurenic acid, respectively).

We next examined the contribution by any direct afferent glutamatergic input contained within the VR (Jiang *et al.*, 1991) to the recurrent PSP by applying the broad spectrum glutamate receptor blocker kynurenic acid (1 mM). Fig. 7 B, C shows that kynurenic acid decreased the PSP area by 15 % (on average the decrease was 20±10 %; $p<0.05$; n=4; see also Table 1), indicating that afferent glutamatergic transmission made only a small contribution to the recurrent PSP (Schneider & Fyffe, 1992).

Subsequently, we tested the relative contribution by glycinergic or GABAergic transmission to the recurrent PSP. Thus, bicuculline (20 μM), applied to block $GABA_A$ receptors, decreased the PSP area by 30±20 % ($p<0.05$; n=4) as shown by the example of Fig. 7 D, E. Corresponding decreases obtained with the glycine receptor antagonist strychnine (1 μM; see example in Fig. 7 F) were 46±9 % ($p<0.01$; n=6). Table 1 lists changes in PSP parameters following application of bicuculline or strychnine.

These results confirm that the recurrent PSP was primarily mediated by glycine (Werman *et al.*, 1968) with lesser contribution by GABA (Larson, 1969; Polc & Haefely, 1982; Schneider & Fyffe, 1992) and an even smaller contamination by glutamate.

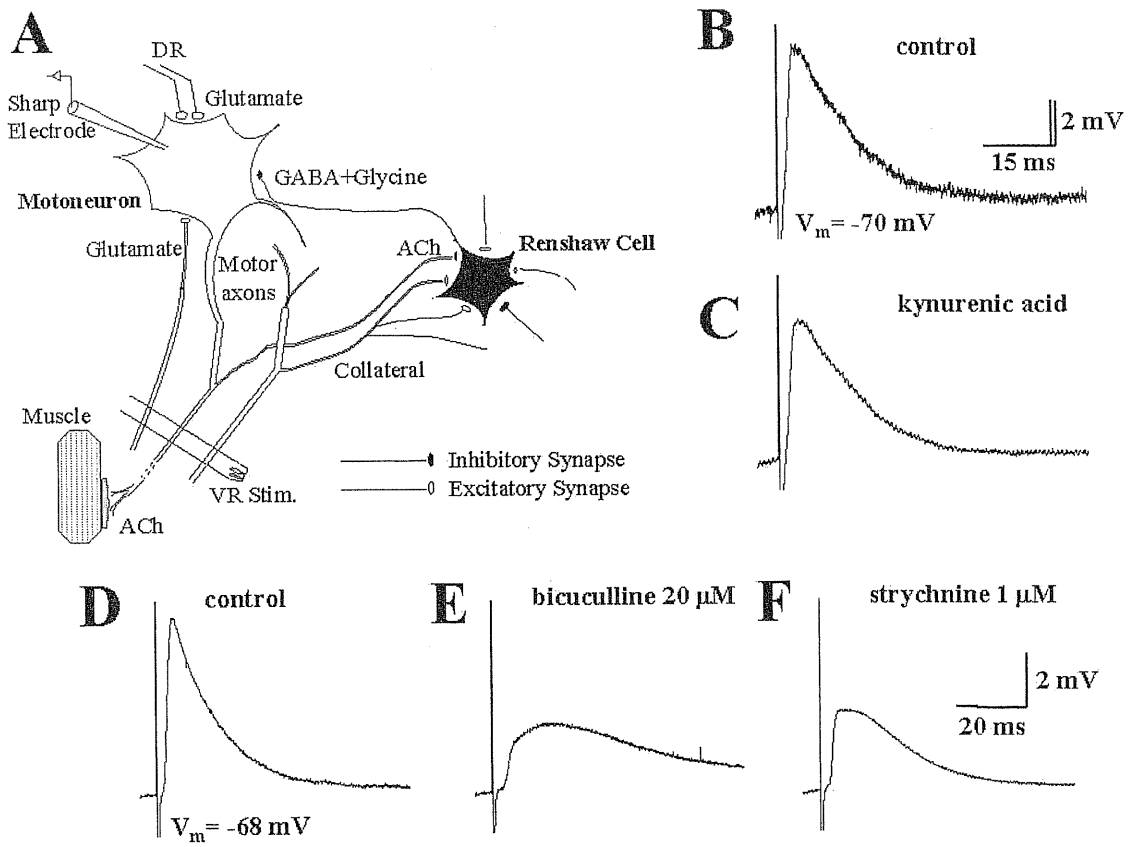

Figure 7. Glycine and GABA mediated synaptic potentials in the spinal cord. (A) Schematic representation of the recurrent inhibitory pathways in the spinal cord. Only one motoneuron is shown together with two Renshaw cells. Transmitters used by different synapses are also indicated. ACh=acetylcholine. (B) Recurrent PSP recorded from rL3 motoneuron, stimulated antidromically and recorded in control solution. PSP amplitude is 7 mV. (C) Effect of kynurenic acid (1 mM) on recurrent PSP, shown in B. The peak as well as the area are reduced by 15 %. (D) Control recurrent PSP (different cell from B) recorded from rL4 motoneuron (PSP amplitude=7 mV). (E) Recurrent PSP recorded in 20 μM bicuculline. PSP peak is reduced by 65% with respect to D, while the total area is not reduced (5 %) owing to the prolongation of the synaptic response. (F) Recurrent PSP recorded in 1 μM strychnine solution. Peak is reduced by 60%, while the area is reduced by 25 % with respect to D.

2.2 Inhibition of EPSP by recurrent Renshaw cell mediated post-synaptic potentials

To test whether the depolarizing recurrent PSP was excitatory or inhibitory, we investigated its action on the DR-evoked polysynaptic EPSP. By carefully selecting the timing of stimulation of the same segmental VR and DR, we aimed at generating the orthodromic EPSP (stimulus intensity=2-3xTh) immediately after the peak of the recurrent PSP. The peak amplitude of the EPSP was 8±5 mV (n=9, see Table 1 for other EPSP parameters). Because both recurrent PSP and EPSP were depolarizing, if these graded events did not interfere with

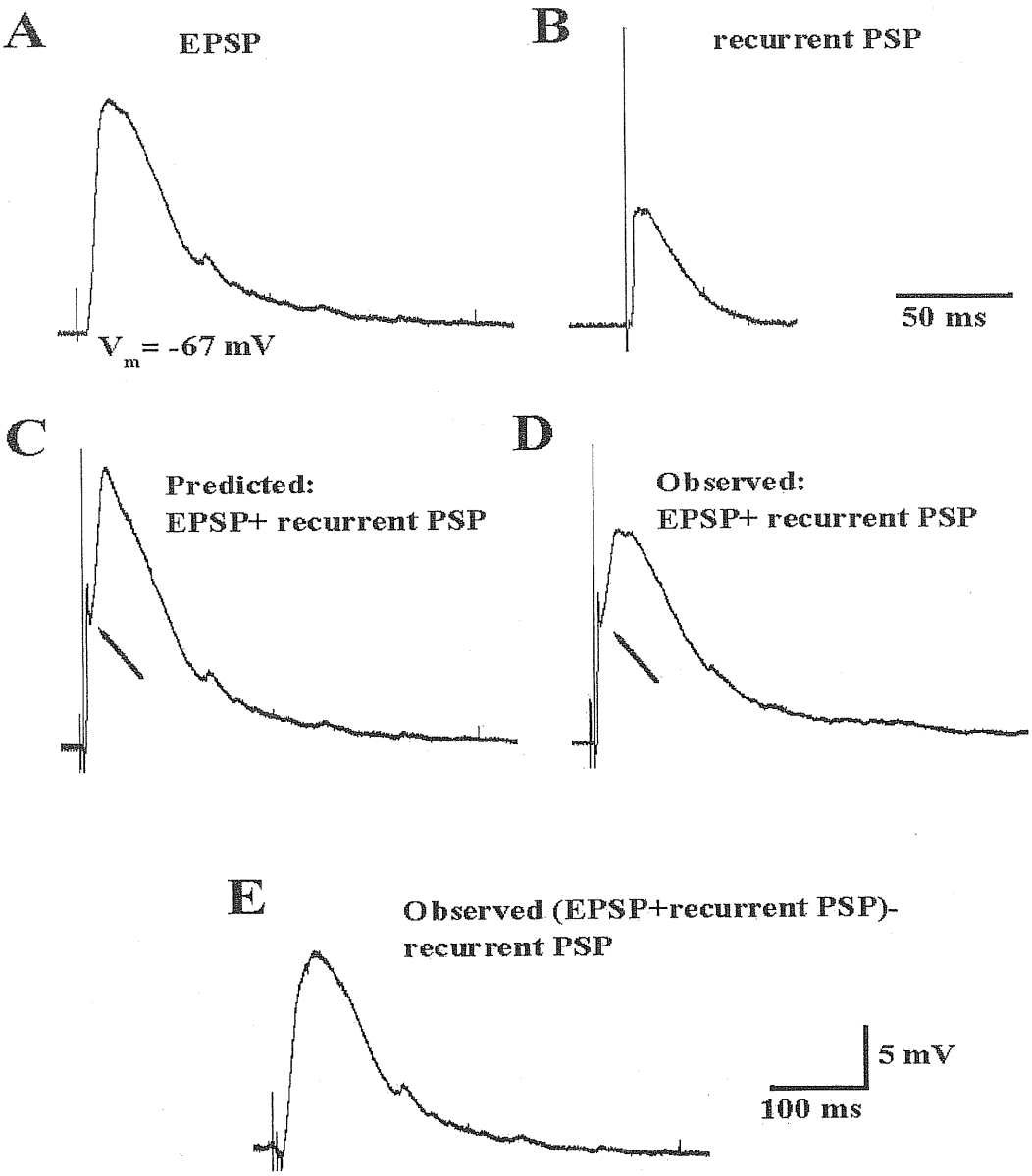

Figure 8. Inhibition by recurrent PSP of EPSP in the spinal cord. (A) EPSP recorded from rL4 motoneuron when stimulating homolateral L5 DR (stimulus intensity=3xTh). (B) Recurrent PSP recorded from the same cell when stimulating antidromically. (C) Predicted sum of EPSP (trace A) and PSP (trace B). (D) Recorded sum of EPSP and PSP. The area of the response is 83% of the predicted one (see C), indicating occlusion. (E) Difference between recorded sum (trace D) and the PSP (trace B). Voltage calibration bar in E refer to all traces while panel B has faster time calibration (as shown) with respect to all other records. Arrows point to take off of EPSP immediately after peak of PSP.

each other, they should have been summating at somatic level. This notion is illustrated in Fig. 8 in which the averaged EPSP or recurrent PSP is shown in isolation (A, B; note faster time scale in B than in A, C, D, E) while the theoretical response predicted by their linear summation is displayed in Fig. 8 C (arrow points to the start of rising phase of the EPSP). The actually observed motoneuron response during concomitant VR and DR stimulation is depicted in Fig. 8 D, which indicates 17 % area occlusion when compared with record in Fig. 8 C. On average (n=9) the occlusion amounted to 16±8% of the predicted linear summation ($p<0.01$). We then recorded the response occlusion due to concurrent generation of EPSP and recurrent PSP. To estimate the impact of the recurrent PSP on the polysynaptic EPSP, we subtracted the isolated recurrent PSP from the observed combined depolarization due to the EPSP + recurrent PSP. This seemed justified as the protocol relied on eliciting the EPSP only after the recurrent PSP had fully developed. Fig. 8 E shows that the area of the EPSP after recurrent PSP subtraction was 80% of control EPSP. On average, the EPSP reduction by the preceding recurrent PSP versus the control EPSP was 28±15 % (n=9), indicating that afferent synaptic inputs were inhibited when generated immediately after a recurrent PSP.

These results indicate that spinal motoneurons from neonatal rats were consistently inhibited by glycine or GABA despite the associated depolarization of membrane potential which should have brought these cells closer to firing threshold.

3. Neuronal Bursting Induced by NK_3 Receptor Activation

In § 4.5 of the Introduction, the hypothesis was stated that the CPG is made of local oscillators (having a rostrocaudal and segmental distribution) connected by excitatory and inhibitory synapses. The question then arises of the possibility of changing the strength of these connections, so as to couple oscillators in distinct ways and to produce rhythms with different characteristics. One way of testing this hypothesis is the experimental activation of certain classes of metabotropic receptors which, via G-protein coupled receptors, can modulate excitation or inhibition in a differential fashion, thus allowing variable functional coupling between oscillators.

The present study aimed at clarifying the basic properties of bursting evoked by NK_3 receptor activity, its segmental distribution and its potential interaction with the activity generated by the locomotor CPG of the neonatal rat spinal cord in vitro.

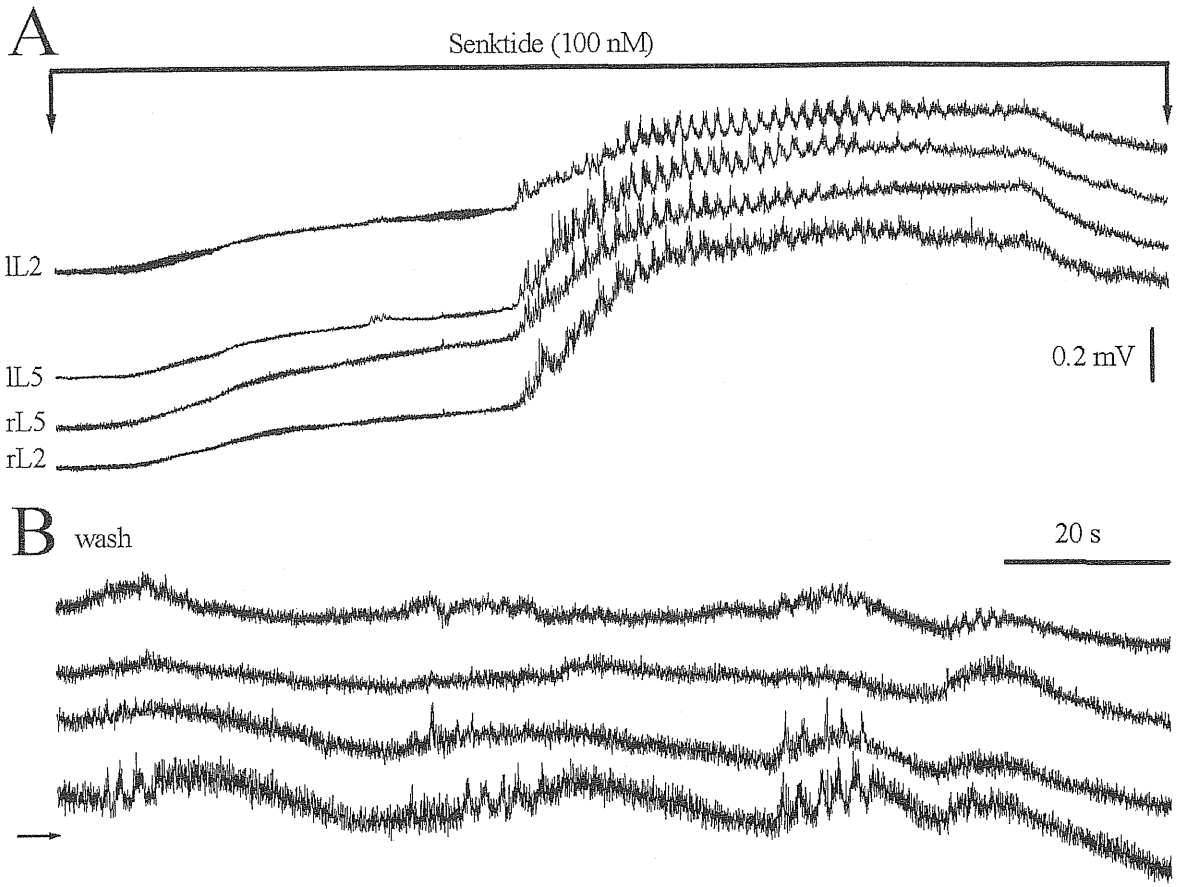

Figure 9. Effect of the NK_3 agonist senktide on the neonatal rat spinal cord. A: Effect of the NK_3 agonist senktide (100 nM) extracellularly recorded from two pairs of VRs (left and right L2 and L5: lL2, lL5, rL2, rL5). Vertical arrow indicates the start of the 4 min application of senktide. B: (continuous records from panel A; note doubling of amplifier gain) During agonist washout, rhythmic, depolarizing, bursts appear (T=43±10 s), which can include an intraburst structure consisting of oscillations with average T=1.8±0.3 s. Horizontal arrow shows control baseline of lL2 VR prior to senktide application for this level of D.C. amplification. Return to control resting activity requires 16 min (not shown).

3.1 Depolarization, fast oscillations, and delayed bursting evoked by senktide

Fig. 9 shows an example of the extracellularly recorded effect of the NK_3 agonist senktide (100 nM) on the neonatal rat spinal cord. With a 10 s latency from the start of the application (which lasted 4 min; panel A), all four VRs (right and left L2 and L5) gradually developed a depolarization which, after about 60 s, abruptly increased in amplitude and presented intense, fast oscillatory activity (T=1.7±0.04 s). Despite the continuous presence of senktide, oscillations lasted 48 s only, as VRs spontaneously begun repolarizing. Panel B of Fig. 9 (continuous records from Fig. 9 A; note doubling of amplifier gain) shows that, during

agonist washout, rhythmic depolarizing bursts appeared (T=43±10 s for the example shown in Fig. 9). Some bursts (though not all of them; see for instance last episodes of lL5 and rL5) had an intraburst structure consisting of oscillations with average T=1.8±0.3 s. These events will be further characterized below. Return to control resting activity appeared 16 min later (not shown).

All 68 preparations showed depolarization upon senktide (50-200 nM) application, although only 53% showed oscillations during agonist application. The concentrations used were large enough to saturate NK_3 receptors (Fox *et al.*, 1996, Barbieri & Nistri, 2001). The oscillations during the depolarization evoked by senktide lasted on average 52±26 s (range 16-104 s), with T= 2.8±0.8 s (range 1.6-4 s). The extent and statistical significance of phase coupling between oscillations in the four VRs is presented in Table 2 The majority (44/68) of spinal cords showed only left/right homosegmental alternation at L2 as well as L5 level. A substantial minority (20/68) presented both homosegmental and homolateral (involving flexor and extensor motor pools) alternation. The remaining eight preparations had unstable phase shifts during the oscillatory patterns.

n	lL2/rL2			lL2/lL5			rL2/rL5			rL5/lL5		
	R	ϕ	P<	R	ϕ	P<	R	ϕ	P<	R	ϕ	P<
44	0.92	192°	0.001	0.89	10°	0.001	0.84	14°	0.005	0.90	192°	0.001
20	0.94	188°	0.001	0.90	190°	0.005	0.89	189°	0.005	0.92	192°	0.001

Table 2. Circular statistics for VR oscillations during senktide applications. n=number of preparations; R is a dimensionless value (0-1 range) which indicates the concentration of phase values around the mean phase lag (ϕ; espressed as angular degrees) and provides the strength of coupling between VR oscillations. The value of P was obtained with the Rayleigh test with the small-sample modification (Drew and Doucet 1991).

3.2 Characteristics of delayed bursting activity developing after senktide washout

For 5-20 min after senktide washout, all preparations showed sustained firing as indicated by the high frequency noise recorded from VRs before reattaining baseline polarization. In most

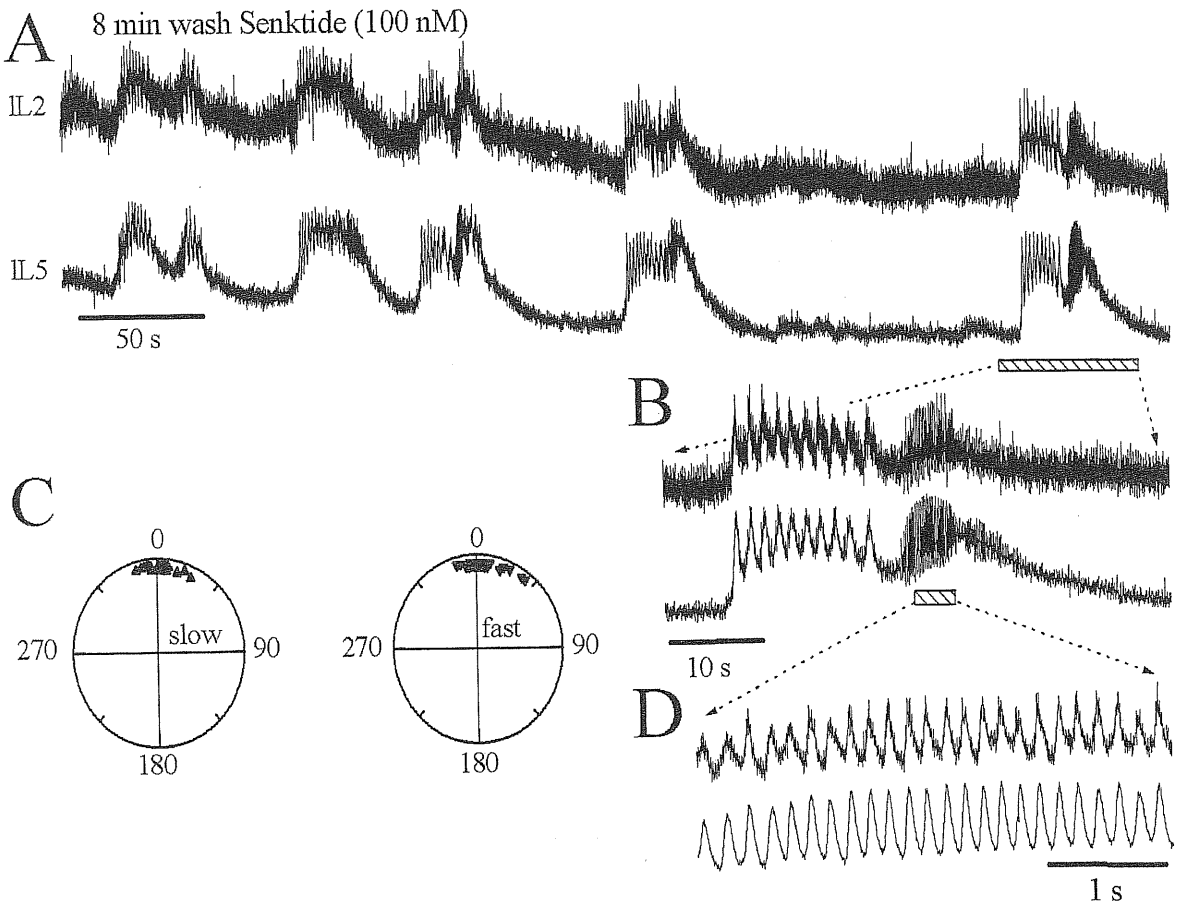

Figure 10. Characteristics of late bursting. A: Example of synchronous homolateral bursting during senktide washout recorded from lL2 and lL5 VRs. B: Polar plots of phase lags for the oscillations shown in panel A reveal full homolateral synchronicity both for "slow" (T=1.35±0.08 s) oscillations and "fast" (T=0.22±0.09 s) ones. C: Expansion of the time scale of one of the bursts recorded on washout (shown in panel A) reveals oscillatory (T=1.35±0.08 s, "slow") intraburst structure. D: Further expansion of the time scale from panel C shows, within the same burst, an additional class of faster oscillations with T=0.22±0.09 s.

cases (70%) this stage was accompanied by bursts present on at least one VR. Individual burst duration was on average 8±2 s (n=40 spinal cords) which clearly separated these late-onset bursts from the shorter lasting oscillations appearing during the application of senktide. Bursts could display either left/right alternation (with synchronous homolateral activity, 52% of preparations), or variable phase coupling (42%) or, more rarely, full synchronicity (5%). An example of the prevailing response pattern, namely synchronous homolateral bursting (L2 and L5), is shown in Fig. 10 A. Interburst interval (I.B.I.) variability was assessed by calculating the coefficient of variation (CV) of the I.B.I. for each preparation. The mean CV was 0.4±0.2, while the mean I.B.I. was 55±21 s (n=40 preparations).

We examined whether the late bursting activity appearing during senktide washout was a stereotypic response by a network locked into a patterned operation or whether it was a rhythmic program modulated by afferent synaptic inputs. For this purpose on four spinal cord preparations, after washout of senktide (100 nM), we attempted to elicit bursts by electrically stimulating (0.033 Hz; 2-3xTh) one L5 DR. Bursts could be observed on all VRs and had an average duration of 10±4 s with 1:1 entrainment. In no instance did bursts appear on DRs.

3.3 Complex intraburst oscillations during senktide washout

A considerable degree of complexity emerged when the intraburst oscillatory structure was analyzed. This is exemplified by Fig. 10 C that shows the oscillatory (T=1.35±0.08 s) structure of one spontaneous burst generated during continuous recording from two homolateral VRs (starting from 8 min senktide washout). Further expansion of the time scale (Fig. 10 D) reveals, within this burst, an additional class of faster oscillations with T=0.22±0.09 s. The slower intraburst oscillations were recorded in 25% of preparations (average T=2.0±0.5 s), while the faster oscillations (average T=0.22±0.04 s) were seen in 62% of cases. The remaining spinal cords showed only tonic firing during bursts.

It was difficult to establish whether intraburst oscillations had phase coupling because this type of analysis required synchronicity of bursts as well as presence of slow oscillations, two conditions which limited the number of samples to 10 preparations. The polar plots shown in Fig. 10 B indicate that slow as well as fast oscillations were synchronous between lL2 and lL5 VRs in the preparation illustrated in Fig. 10 A. This condition was observed in all 10 spinal cords that presented homolateral synchronicity with ϕ= 5° and ϕ= 12° for fast and slow oscillations, respectively (R=0.95 and 0.92).

3.4 Action of senktide was mimicked by [MePhe7]neurokinin B

The responses induced by senktide raised the question of receptor selectivity. Thus, we tested another NK_3 agonist, namely [MePhe7]neurokinin B (100 nM) that, as shown in Fig. 11, closely reproduced the pattern of effects evoked by senktide. In fact, a gradually developing depolarization was suddenly followed by a larger depolarization plateau containing oscillatory activity slowly waning despite sustained agonist application. During washout bursting activity emerged with intraburst oscillations. On 8 preparations, [MePhe7]neurokinin B induced VR depolarization characterized by oscillations with T=3±1s.

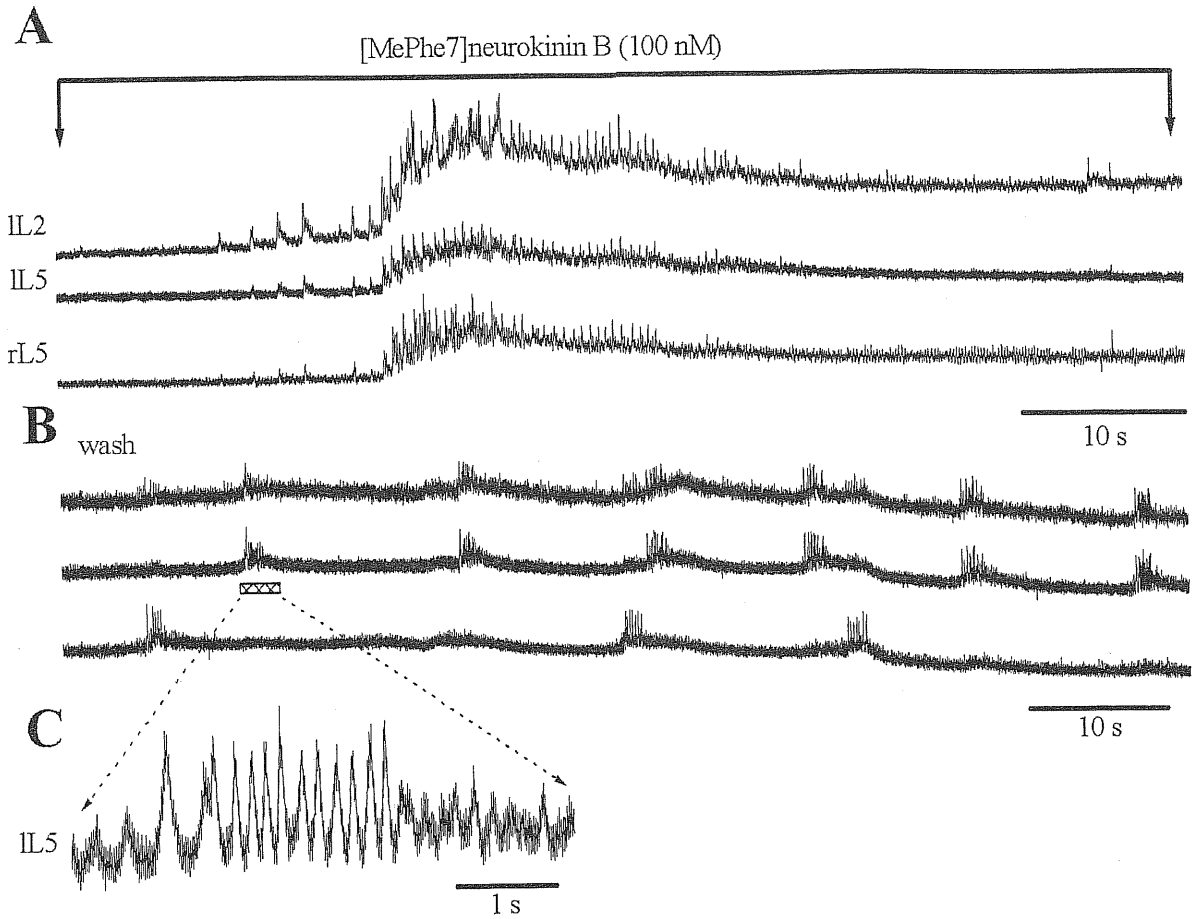

Figure 11. Effect of the NK_3 agonist [MePhe7]neurokinin B. A: Activity induced by the NK_3 agonist [MePhe7]neurokinin B (100 nM) closely reproduces the pattern evoked by senktide: depolarization first develops gradually, and more intensely after about 20 s, together with oscillatory activity. Depolarization and oscillations slowly fade away despite sustained agonist application. B: During washout, bursting activity emerges with intraburst oscillations (note doubling of amplifier gain). Bursts occur synchronously (with a period of about 15 s) on lL2 and lL5 VRs, , and with variable period on the contralateral rL5 VR. C: Intraburst structure comprises fast oscillations with T=0.23ms (3x amplifier gain with respect to A).

During washout, late bursts occurred with 44±12 s I.B.I and 9±3 s duration. Bursts comprised fast oscillations with T=0.21±0.05 ms.

3.5 Pharmacological characterization of delayed bursting induced by senktide

Delayed bursting could have been due to rhythmic network activity either caused by slow wash out of senktide persistently activating NK_3 receptors, or to a distinct pattern consequent to former NK_3 activation. Another possibility might have been that delayed bursting originated from motoneurons made hyperexcitable by previous application of senktide.

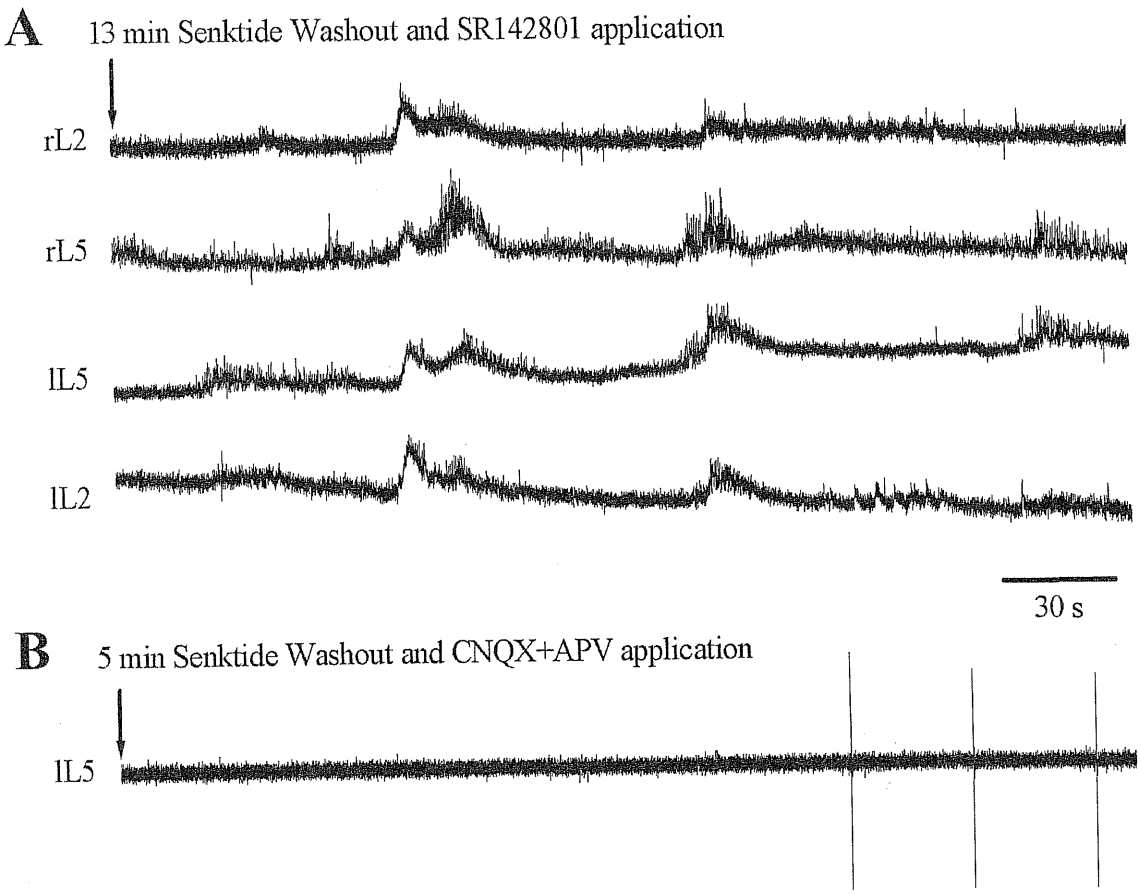

Figure 12. Delayed bursting does not require persistent NK_3 receptor activation. A: VR records from right and left L2 and L5 VRs during application of the NK_3 antagonist SR142801 (10 μM) that had started immediately after senktide washout (not shown). Traces are shown at 13 min washout (see arrow) during continuous exposure to SR142801 and present delayed bursting activity with no changes in I.B.I. or burst duration. B: Effect of CNQX (10 μM) and APV (50 μM) during senktide washout (different preparation from A) shown for lL5 VR. The record starts at 5 min senktide washout (see arrow) in the presence of CNQX and APV. Bursting is completely abolished on all four VRs (for simplicity only lL5 trace is shown here). Note that DR stimuli (see large deflection artefacts) fail to elicit polysynaptic reflexes in CNQX plus APV solution.

We designed two protocols to test these possibilities. First, we applied senktide for 4 min to generate spinal cord depolarization (with oscillations) and then washed out senktide by applying a Krebs solution containing 10 μM SR 142801, a selective NK_3 receptor antagonist (Beaujouan *et al.*, 1997; Emonds-Alt *et al.*, 1995). This approach is exemplified in Fig. 12 A where delayed bursting continued on all four VRs despite the presence of the antagonist. Similar results were obtained on 5 preparations in which the I.B.I. value for delayed bursting was 59±8 s in control solution versus 68±9 s in SR 142801 solution. The corresponding data

for mean duration of individual bursts was 10±3 s and 9±5 s, respectively. None of these differences was statistically significant.

Secondly, we tested whether delayed bursting required excitatory glutamatergic synaptic transmission. For this purpose, on five preparations (different from those tested with SR 142801), after observing senktide-evoked depolarization and oscillations for 4 min, we washed out the tachykinin agonist with a solution containing 10 μM CNQX and 50 μM APV as exemplified in Fig. 12 B. In this case, all bursting activity was eliminated and electrical stimulation of one L5 DR (2-3xTh intensity) failed to induce any response detectable from the corresponding L5 VR (see artefacts on last part of record in Fig. 12 B). Similar results were observed in the other four preparations.

These findings suggest that delayed bursting did not require persistent NK_3 receptor activity but it required network-based excitatory glutamatergic transmission.

3.6 Disinhibition as a cause for rhythmic activity caused by senktide?

As reported earlier, on the majority of preparations the senktide-induced oscillations and delayed bursting were alternating at segmental level but lacked flexor-extensor motor pool alternation on the same side. This curious phenomenon raised the possibility that, somehow, activation of NK_3 receptors functionally affected coupling between lumbar segments perhaps because their GABAergic and glycinergic connections were weakened. As a first approximation we investigated if, during the bursting stage, receptors for GABA or glycine remained responsive to application of exogenous GABA or glycine. On 7 preparations in which senktide induced late bursting developing synchronously on the same side, but alternating at segmental level, application of GABA (0.5 mM; a concentration which strongly blocks reflex activity; Rozzo *et al.*, 1999), fully eliminated late bursts as shown by the example in Fig. 13 A. This action of GABA was reversible on wash as bursts returned at a time corresponding to 10 min of senktide washout. However, in four other preparations exposed to 0.5 mM GABA, late bursting persisted with no significant changes in I.B.I. (48±13 s in control *versus* 55±20 s in GABA solution; $p>0.05$, paired *t*-test) or in single burst duration (7.9±2.1 s in control *versus* 8.5±2.4 s in GABA solution; $p>0.05$; Fig. 13 B). In this subgroup of preparations, 3 had segmental alternation and ipsilateral synchronicity before GABA application while one had synchronous activity. In the presence of GABA such

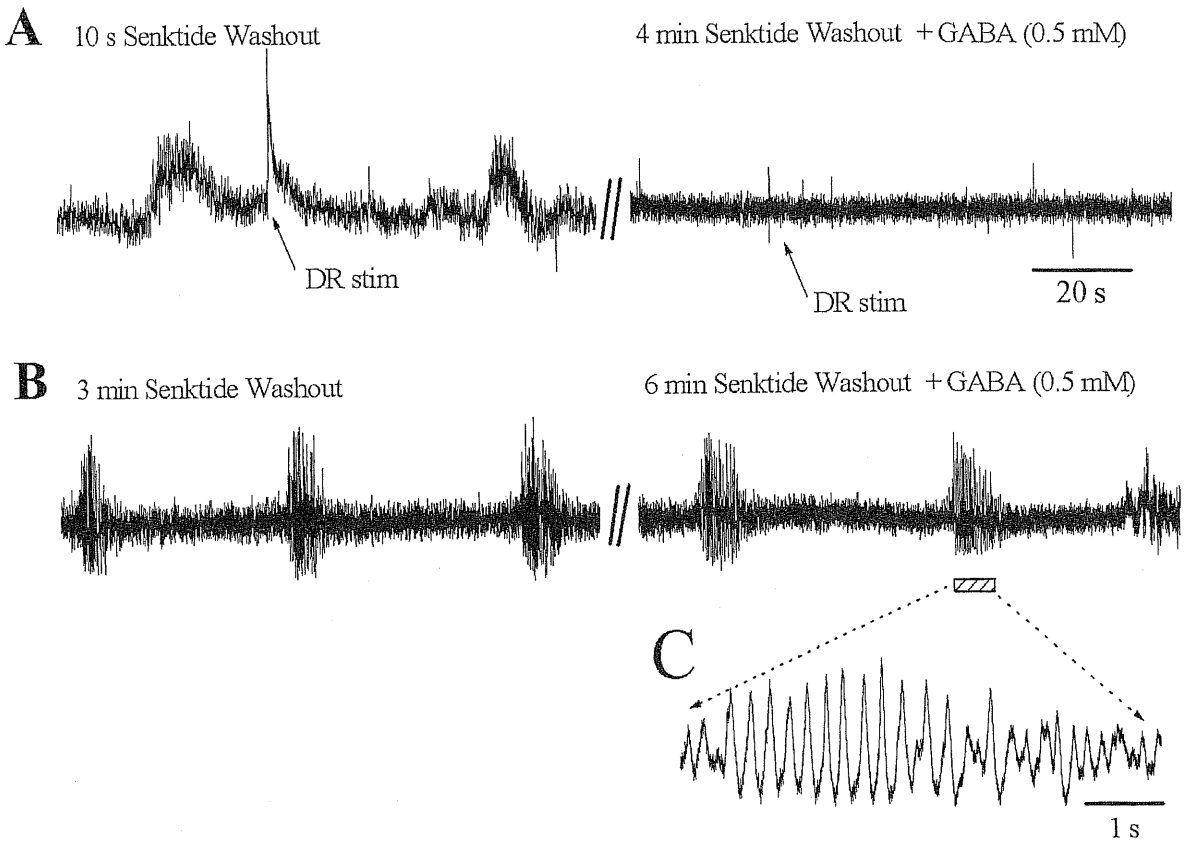

Figure 13. Complex effects of exogenous GABA on late bursting appearing during senktide washout. A, left: bursts (duration 12 s, period 45 s) recorded from rL5 VR after 10 s senktide washout. Between two bursts electrical stimulation of rL5 DR evoked burst lasting 10 s. A, right: after 4 min senktide washout and in the presence of 0.5 mM bursts are suppressed and DR stimulation becomes ineffective (see artefacts indicated by arrow).
B, left: bursts (duration 8 s, period 40 s) recorded in control solution from a rL5 VR at four min senktide washout. Different preparation from the one shown in A. B, right, shows that in the presence of GABA, bursts continue with the same duration and interburst interval. The time scale expansion below the trace demonstrates that the intraburst structure also comprises fast oscillations, with 0.26 ms period.

patterns remained unchanged. Resistance of bursting to GABA by these preparations did not involve general loss of GABA effectiveness as the DR-evoked (3xTh intensity) VR reflexes were significantly ($p<0.001$) and reversibly depressed (by 68±18%) in all preparations tested ($n=11$).

In addition to checking for the ability of exogenous GABA to suppress bursting, we sought to clarify if endogenously released GABA retained its effects at the time of senktide-induced bursting. For this purpose we monitored changes in the GABAergic DR-DRP (Dorsal Root induced Dorsal Root Potential; Curtis *et al.*, 1971; Levy, 1977; Nicoll & Alger, 1979; Nistri,

1983). DR-DRP amplitude did not significantly decline (80±10% of control; n=5; $p>0.05$) during application of senktide but it was significantly depressed (70±20%; n=5; $p<0.05$) during washout. These data indicate that a deficit in GABAergic transmission occurred during late bursting.

Application of glycine (0.5 mM) after the first 2-5 min of senktide wash blocked bursts in 7 preparations, out of which 6 demonstrated ipsilateral synchronous bursting and one fully synchronous activity. In two further preparations with ipsilateral synchronous bursting, this phenomenon continued in the presence of glycine: in fact, neither I.B.I. (44±6 s in control *versus* 54±10 s in glycine) nor burst duration (10±2 s in control *versus* 11±3 in glycine) was significantly altered. On all 9 spinal cord preparations the DR-induced VR reflex was significantly ($p<0.05$) inhibited by glycine (by 65±20%).

3.7 Senktide-induced oscillations and bursting recorded intracellularly from motoneurons

The widespread distribution of NK_3 receptors in the rat spinal cord makes it difficult to identify the cells responsible for oscillations and bursting induced by senktide. Since in each case this rhythmic activity converged on lumbar motoneurons, we recorded intracellularly from these cells to address the following issues: 1) did motoneurons actively participate in bursting? 2) what electrophysiological properties characterized the oscillatory activity? 3) were bursting and oscillations associated with changes in motoneuron recurrent inhibitory postsynaptic potentials (IPSPs)?

Two sets of intracellular experiments were performed, namely those on motoneurons with fully-blown spikes recorded with KCl or $KMeSO_4$ filled electrodes (n=22) and those on cells in which spikes were blocked by intracellularly applied QX-314 (n=14). The mean resting potential (V_m) for the first set of cells was -69±5 mV. One example of these experiments is given in Fig. 14 that shows simultaneous intracellular (bottom trace; rL5-Mn) and extracellular recordings (top three traces with VR identification indicated alongside) of a single burst (comprising a series of oscillations) appearing at 5 min washout of senktide. The intracellular record clearly shows that, at –60 mV membrane potential, the rL5-Mn (recorded with a $KMeSO_4$ filled electrode) begun depolarizing 1.2 s earlier than the onset of the first oscillation recorded extracellularly. Each oscillatory waveform of this motoneuron displayed, at its peak, a cluster of 2-5 spikes, suggesting that action potentials were generated only when the positive phase of the oscillations brought the motoneuron membrane potential to firing

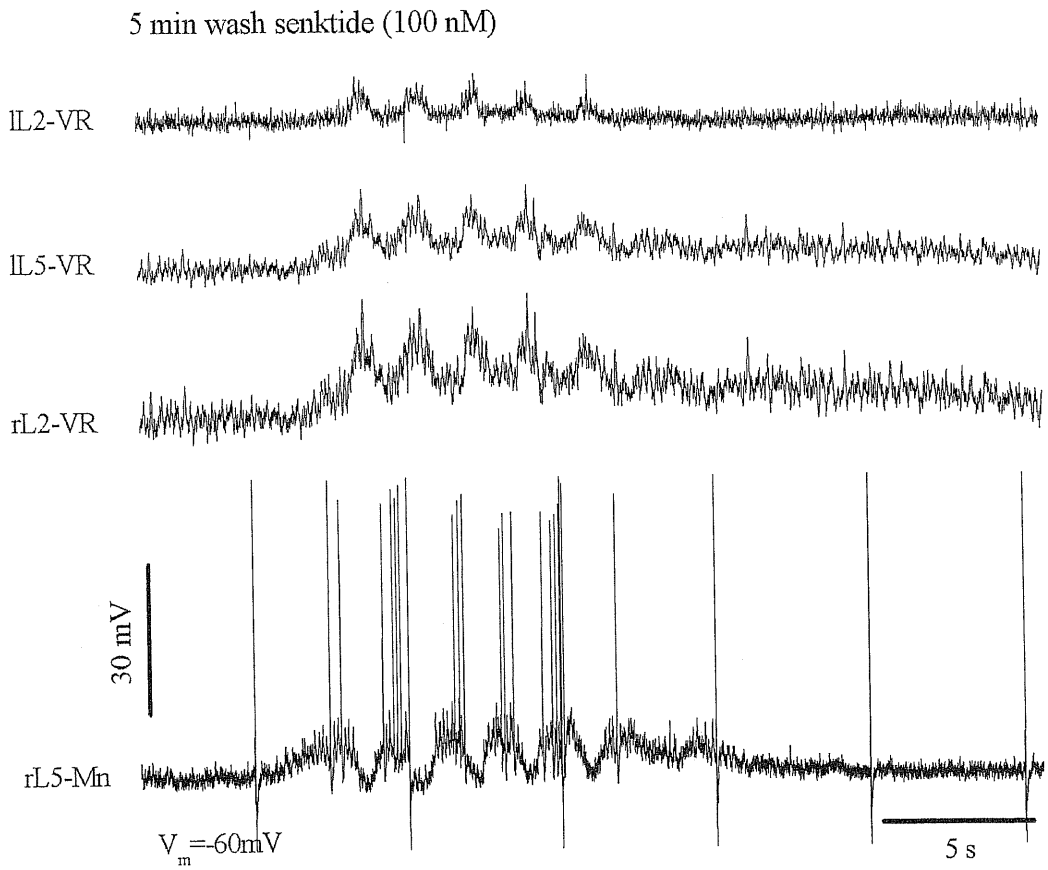

Figure 14. Intracellular and extracellular recording of a single burst. Simultaneous intracellular (bottom trace; rL5-Mn recorded with $KMeSO_4$-filled electrode) and extracellular recording (top three traces from lL2, lL5, rL2 VRs) of a single burst appearing at 5 min senktide washout. On the motoneuron the burst develops from V_m=–60 mV and comprises oscillations of T=1.8 s (starting 1.2 s earlier than the onset of the first oscillation recorded extracellularly). A cluster of 2-5 spikes is present at the peak of each oscillation. Motoneuronal oscillations appear in antiphase (R=0.71, ϕ=162°) with the extracellular activity, recorded synchronously from all three VRs. Large upward deflections appearing every 5 s are antidromic spikes (plus stimulus artefact).

threshold. Each oscillation comprised a hyperpolarization (4 mV below baseline) during which spontaneous activity was subdued.

In the example of Fig. 14 the oscillatory activity of the single motoneuron lasted longer than that recorded from the three VRs and was in antiphase (R=0.71, ϕ=162°) with the extracellular activity appearing synchronously on all three VRs (despite a modest lag for lL2 VR). Note that, unlike the pattern observed with the single cell oscillations, the oscillation troughs detected extracellularly from VRs were associated with a noisy baseline, indicating a degree of asynchrony in motoneuron pool firing behavior at each segmental level.

The mean depolarization induced by senktide (100 nM), recorded from single motoneurons, was 12±6 mV (n=22) and was associated with a significant change in input resistance (108±9%, n=14; $p<0.05$) measured by averaging at least 5 electrotonic potentials evoked every 10 s. In the presence of senktide some motoneurons (n=8) fired phasically with action potentials arising from oscillations while other motoneurons (n=4) fired irregularly (average discharge rate=5.4±4.6 Hz) or did not reach firing threshold (n=10). During 5-10 min washout of senktide in coincidence with late bursting, the average baseline input resistance (measured after rejecting electrotonic potentials during bursts) was significantly increased (115±16%, n=14, $p<0.001$) despite return of membrane potential to control level. At this stage phasic motoneurons (n=8) fired bursts of action potentials (average rate=8.8±5.5 Hz) which were usually alternated with bursts recorded extracellularly from the contralateral VR. There was no difference in responses of cells impaled with KCl or $KMeSO_4$ electrodes.

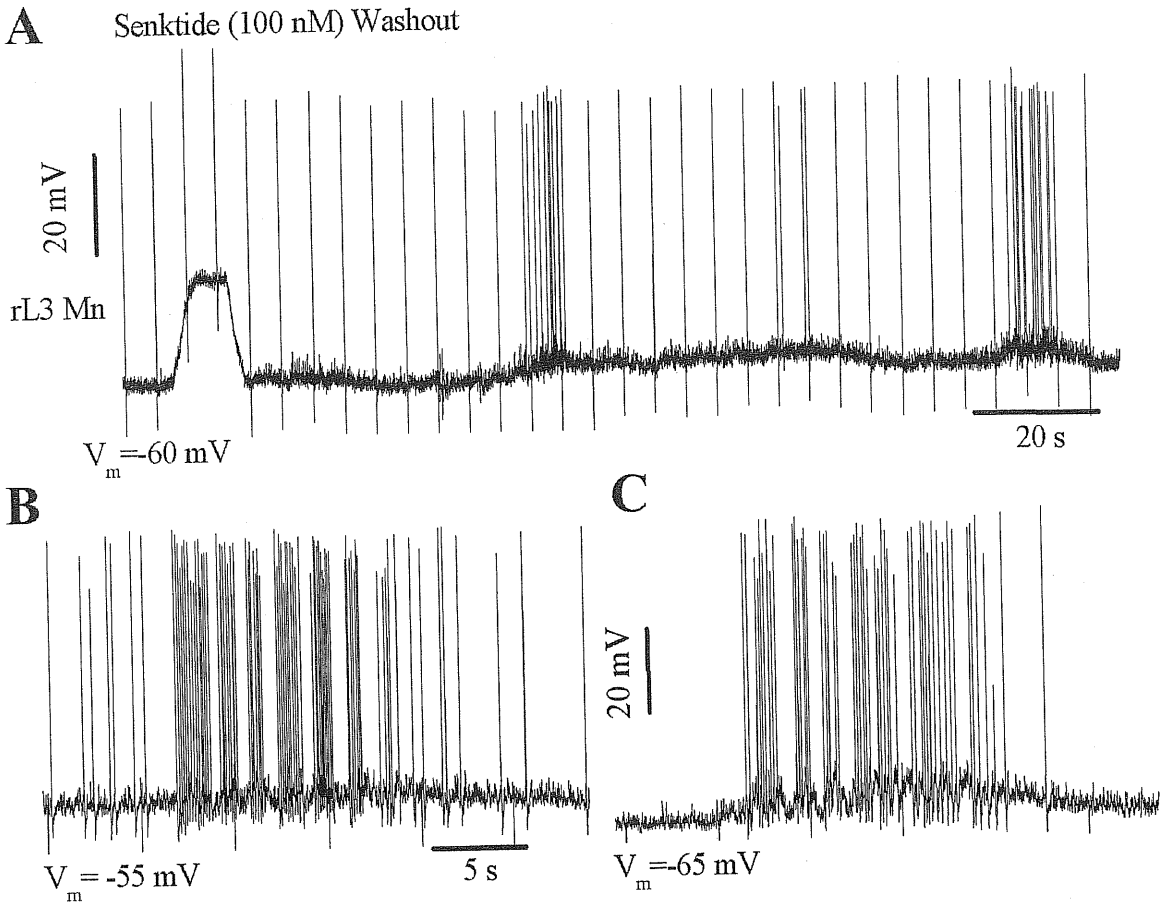

Figure 15. Bursts do not depend on motoneuron membrane potential. A: Senktide washout phase of a rL3 motoneuron; note that spontaneous bursting is present, but cannot be elicited by manually depolarizing the cell to –40 mV. B: Burst recorded intracellularly from a rL5 motoneuron at V_m =–55 mV. C: Burst recorded at V_m= –65 mV from the same motoneuron. Oscillations are still present with 30% larger amplitude.

We next examined the voltage dependence of bursting and oscillations. As indicated in Fig. 15 A, membrane depolarization to –40 mV did not elicit bursting during senktide washout whereas membrane hyperpolarization (ΔV_m= -10 mV to V_m= –65 mV) augmented the burst amplitude without suppressing it (Fig. 15 B, C). In both cases intraburst oscillations persisted with similar period. Similar observations were repeated on 7 motoneurons (V_m=-66±5 mV) depolarized by 10-20 mV or hyperpolarized by 5-15 mV. These results suggest that bursting was a network dependent phenomenon and was not due to voltage activated conductances intrinsic to the motoneuron membrane.

Intense spiking activity could actually mask the timecourse of oscillations and complicate membrane potential and input resistance changes evoked by senktide. In order to monitor oscillations more directly, five motoneurons were recorded with an intracellular solution containing QX-314 (in $KMeSO_4$ solution) to block Na^+-dependent spikes and slow inward rectifiers. On these cells senktide induced 8±4 mV depolarization associated with no significant change (3±2 %) in input resistance. The washout stage was still characterized by bursting and 12±7 % rise ($p<0.05$) in baseline input resistance. Fig. 16 C shows an example of raw data of electrotonic potentials recorded before, during and after application of senktide. Fig. 16 A exemplifies recordings from one L2 VR and a rL4 motoneuron (impaled with QX-314 filled electrode) after 3 minutes washout of senktide. Despite the fact that action potentials were suppressed, motoneuron baseline potential oscillated during bursts. In particular, the rL4 motoneuron oscillated in phase with the homolateral rL2. The trough of each oscillation did not become hyperpolarized with respect to membrane potential baseline, a phenomenon observed in all cells recorded with QX-314 electrodes (Fig. 16 B).

3.8 Recurrent IPSPs during senktide evoked bursting

On four cells impaled with QX-314 filled electrodes and stimulated antidromically, it was possible to observe a recurrent IPSP, the main component of which is believed to be mediated by glycine released by Renshaw cells (Werman *et al.*, 1968), while the late component is GABAergic (Cullheim & Kellerth, 1981; see also INTRODUCTION § 2.4 and 2.5 and RESULTS § 2). Suppression of the antidromic action potential avoided contamination of the IPSP by the spike afterhyperpolarization. The IPSP was recorded at –65 mV membrane potential and was depolarizing (amplitude 11±4 mV) regardless of the presence of KCl or $KMeSO_4$ in the electrode. The IPSP had average rise time of 1.4±0.6 ms and its decay could be fitted by a

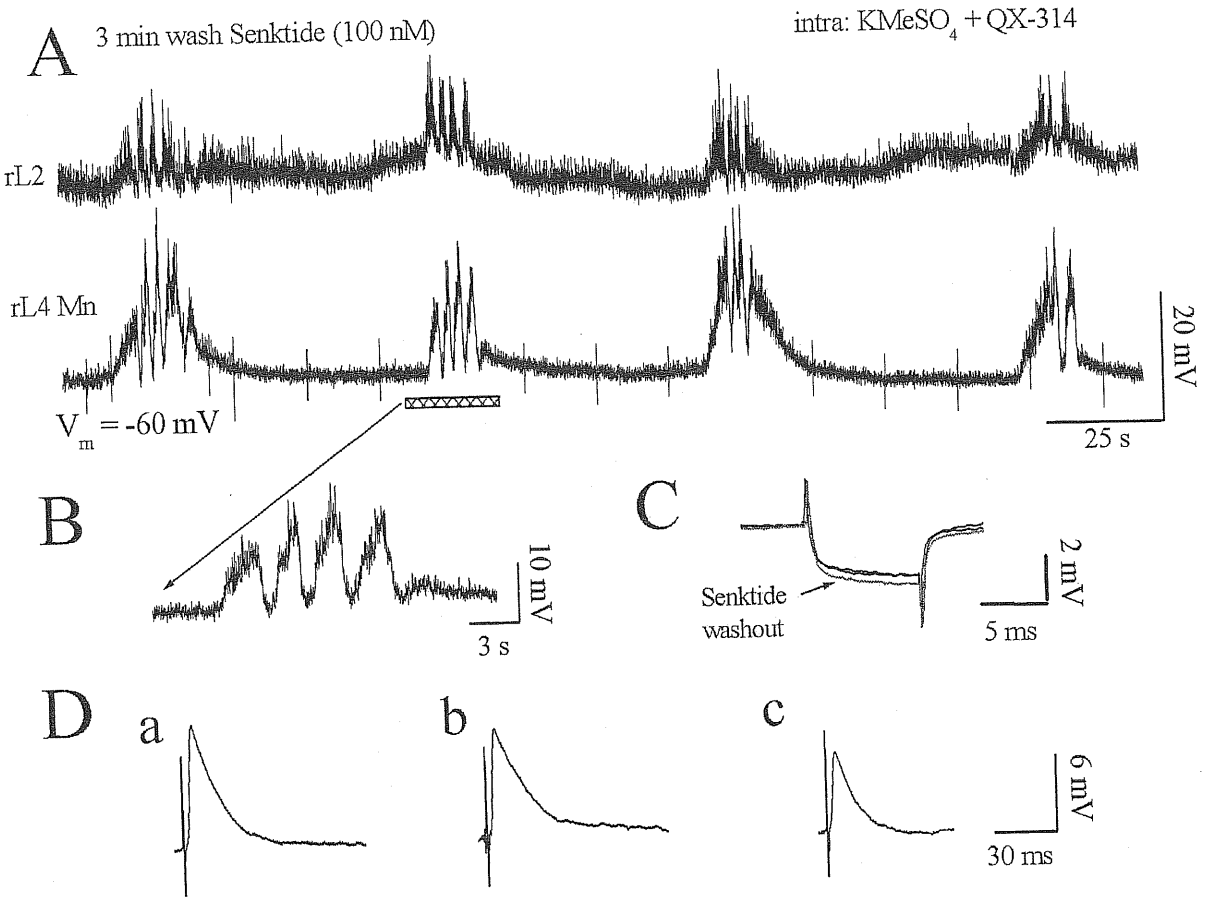

Figure 16. Bursting activity recorded intracellularly with a QX-314 filled electrode. A: Recordings from rL2 VR and rL4 motoneuron (impaled with QX-314 filled electrode) after 3 min washout of senktide. Motoneuron oscillations during bursts are present despite the fact that action potentials are suppressed. rL4 motoneuron oscillates in phase with the homolateral rL2. B: Time scale expansion of a burst recorded from rL4 motoneuron. C: superimposed records of average electrotonic potentials used to measure motoneuron input resistance (same cell as in A, B) in control solution, during senktide application and its washout (indicated by arrow). Resistance is similar in control and during senktide application, while it is increased during washout. D: average recurrent IPSP recorded from rL4 motoneuron (same as in A-C) in the absence of spike contamination (due to the presence of QX-314 in the recording electrode) in control (a), during senktide application (b) and during washout (c). Note depression of IPSP during senktide washout.

single exponential (time constant=21±9 ms). Since the peak amplitude was blocked (by 54±8%) by 1 μM strychnine, it is confirmed that the IPSP was mainly mediated by glycine. Recurrent IPSPs were studied in the presence of senktide (100 nM) or during the stage of senktide washout. As shown Fig. 16 Db, during senktide application, IPSP area and peak amplitude were not significantly changed (on average they were 105±8 and 104±5%, respectively; n=4). Nevertheless, during senktide washout (see example in Fig. 16 Dc), the IPSP area was significantly ($p<0.05$) depressed (62±20%) although the reduction in peak

amplitude was not significant (40±40 %). On these preparations bursting showed homolateral synchronicity (but left/right alternation).

3.9 Functional role for NK_3 receptors in the fictive locomotor network

The widespread distribution of NK_3 receptors does not preclude their presence also on CPG neurons responsible for generating fictive locomotor patterns. To explore this possibility, we studied if the locomotor rhythm induced by standard neurochemicals (NMDA and 5-HT; Kiehn and Kjaerulff, 1998) could be perturbed by either activating or blocking NK_3 receptors. Fig. 17 A shows irregular rhythmic activity (recorded extracellularly from L2 and L5 VRs) in the presence of low concentrations of NMDA (2 μM) and 5-HT (3 μM), clearly under the threshold for fictive locomotion. After 2 min of senktide application in the continuous presence of NMDA and 5-HT (Fig. 17 B), a regular, fictive locomotor-like rhythm (T=1.25±0.05 s) appeared with left-right alternation at segmental level and ipsilateral alternation between L2 and L5 VRs. The Rayleigh test gave significant coupling ($p<0.001$) for all pairs of VRs (lL2/rL2: R=0.93, ϕ=185°; lL2/lL5 R=0.94, ϕ=183°; lL5/rL5 R=0.91, ϕ=188°; rL2/rL5 R=0.93, ϕ=186°).

After senktide was washed out (Fig. 17 C) and NMDA and 5-HT were still continuously applied, fictive locomotor patterns faded away. Nevertheless, even when the root polarization level had returned to the value before senktide application, episodes of fictive locomotion (T=2.08±0.09) with typical homolateral and homosegmental alternation appeared during bursts (lasting in this example 20±7 s). Applying the Rayleigh test to these oscillations yielded the following values: lL2/rL2: R=0.94, ϕ=183°; lL2/lL5: R=0.95 ϕ=183°; lL5/rL5 R=0.89, ϕ=190°; rL2/rL5 R=0.92, ϕ=184° ($p<0.001$), which are very similar to those observed during the application of senktide plus NMDA and 5-HT. This result was obtained in 3 out of 4 preparations.

We also tested application of senktide during a stable fictive locomotor rhythm induced by NMDA and 5-HT. In 7/10 preparations, senktide (100 nM) raised oscillation period by 75±15% with unchanged phase lags (in the other 3 cases period did not change).

Another test for the interaction between NK_3 receptor activity and the locomotor network was done by applying the NK_3 antagonist SR142801 (10 μM) to preparations exhibiting a stable fictive locomotor rhythm. An example of this is shown in Fig. 18 A. In this preparation a stable rhythm (T=1.8 s) was induced by 6 μM NMDA and 10 μM 5-HT. After superfusing

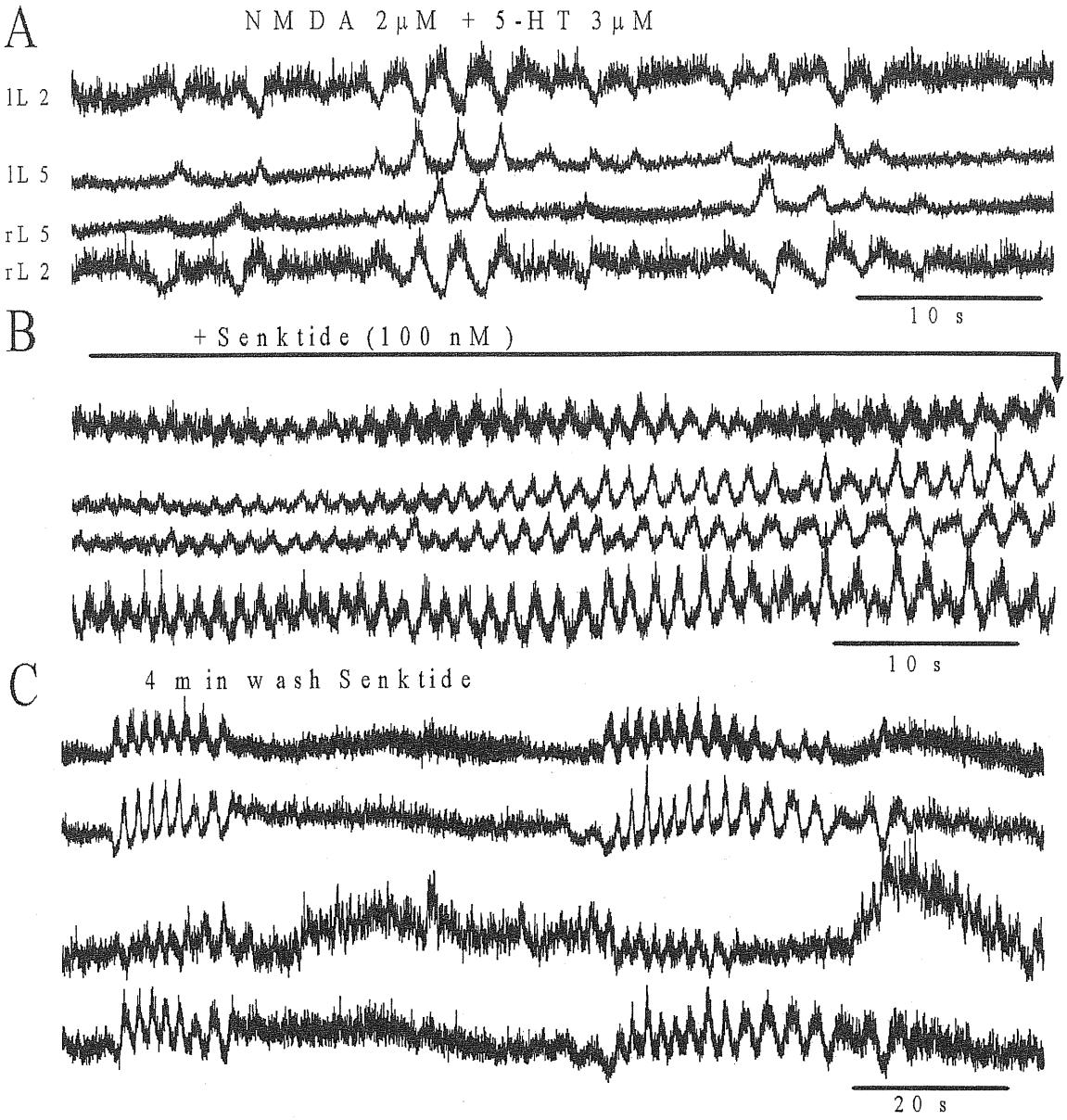

Figure 17. Facilitation of fictive locomotor patterns by activation of NK_3 receptors. A: Irregular rhythmic activity (recorded extracellularly from L2 and L5 VRs) evoked by low concentrations of NMDA (2 μM) and 5-HT (3 μM), under threshold for fictive locomotion. B: Regular, fictive locomotor-like rhythm (T=1.25±0.05 s) with left-right homosegmental alternation and ipsilateral alternation appears after 2 min of senktide co-application with NMDA and 5-HT. C: After senktide wash-out and in the continuous presence of NMDA and 5-HT, episodes of fictive locomotion (T=2.08±0.09) appear during bursts (lasting 20±7 s) and with typical homolateral and homosegmental alternation.

the spinal cord with SR142801 (in the continuous presence of NMDA and 5-HT), the rhythm became irregular, with oscillations of smaller amplitude and slower period (T=3.6 s; Fig. 18 B). After 40 min wash of SR 142801 a regular rhythm was resumed, although the oscillations

remained slow (T=3.6 s; Fig. 18 C). Analogous results were obtained in 3 other preparations, in which rhythmic activity was slowed down by 50±20%.

Collectively, these results demonstrate that coupling between local oscillators in the spinal cord can be altered by acting on G-protein coupled receptors, such as tachykinin NK_3 receptors, and this leads to novel patterns of bursting. Furthermore, these receptors play an endogenous role in the expression of fictive locomotion.

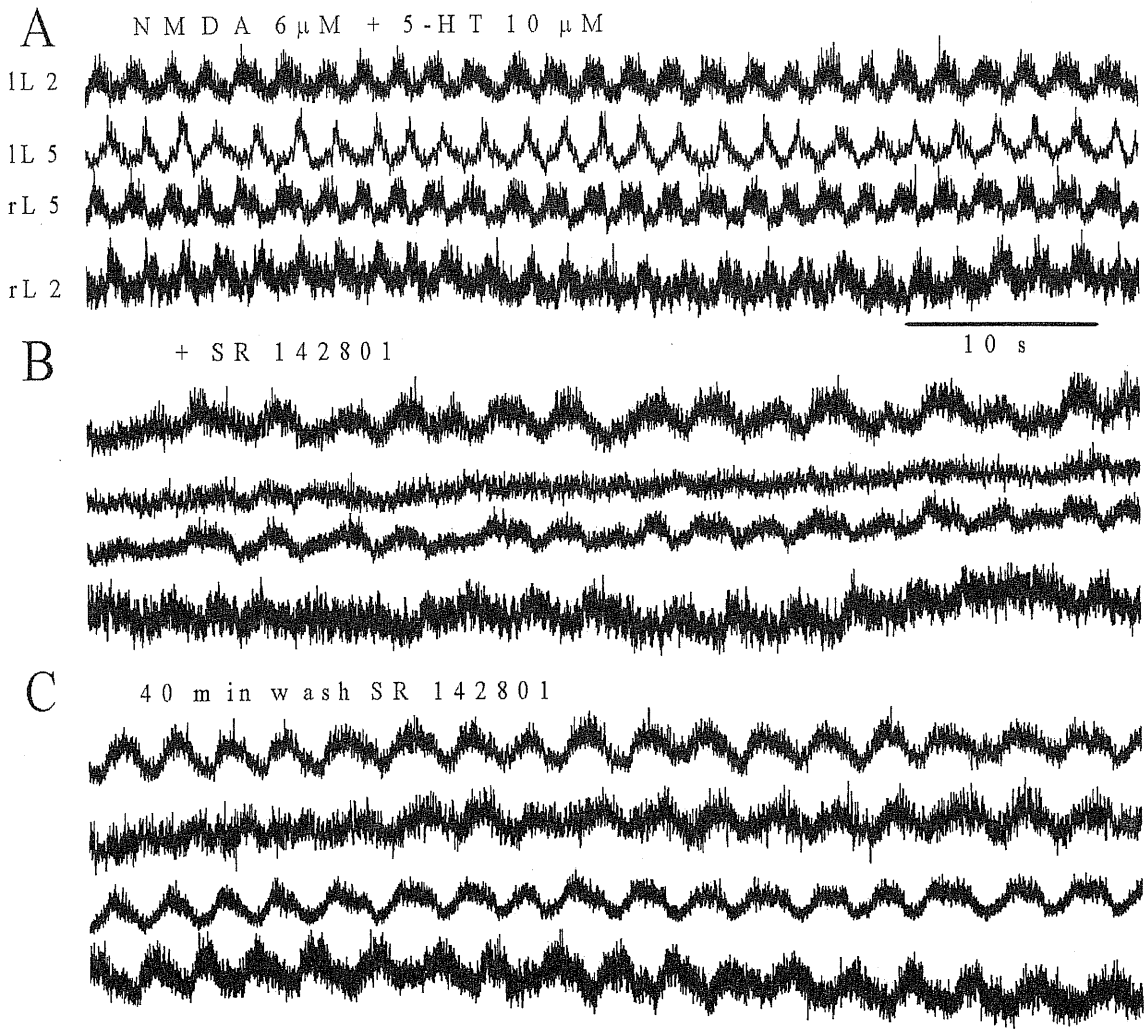

Figure 18. NK_3 antagonist application disrupts fictive locomotor patterns. A: A stable, fictive locomotion rhythm (T=1.8 s) is induced by 6 μM NMDA and 10 μM 5-HT, and it is recorded from pairs of left and right L2 and L5 VRs. B: After superfusing the spinal cord with 10 μM SR142801 for 35 min (in the continuous presence of NMDA and 5-HT), the rhythm becomes irregular, with oscillations of smaller amplitude and slower period (T=3.6 s). C: After 40 min wash of SR 142801 a regular rhythm is resumed, although the oscillations remain slow (T=3.6 s).

4. ROLE OF METABOTROPIC GLUTAMATE RECEPTORS IN SPINAL CORD RHYTHMICITY

The action of metabotropic glutamate receptors (mGluRs) is complex since they constitute a heterogeneous class comprising three subgroups (mGluR I-III), characterized by different pharmacology and transduction mechanisms (see INTRODUCTION, § 5.2). Furthermore, each group (I-III) comprises several subgroups (mGluR1-8) and their splice variants. Results will be presented first for group I mGluRs (§ 4.1-4.4). Activation of this subgroup has several actions: while on the one hand it elicits rhythmical activity (described in § 4.1), it also affects DR-evoked synaptic responses and recurrent IPSPs (described in § 4.2-4.3). In § 4.4, the role of group I mGlu receptors in drug-induced rhythmicity is described. In a parallel fashion, §4.5 will describe the action of group II and III on DR-evoked synaptic activity, recurrent IPSPs and rhythmical activity. Table 3 summarizes the compounds used for the present study. Their action and selectivity are reviewed by Schoepp *et al.*, 1999.

		AGONISTS	ANTAGONISTS
GROUP I	**mGlu1**	DHPG, t-ACPD	AIDA, MCPG
	mGlu5		MPEP, MCPG
Group III	**mGlu2,3**	DCG-IV, t-ACPD	EGLU, MCPG
GROUP II	**mGlu4,6-8**	L-AP4	CPPG

Table 3. Summary of mGluR subclasses and of compounds used for this study.

4.1 Excitatory Action of Group I Metabotropic Glutamate Receptors: rhythmic activity

4.1.1. Motoneuronal depolarization, fast oscillations, slow oscillations.

Fig. 19 shows an example of the action of the group I agonist DHPG (5 μM) recorded simultaneously from an L5 motoneuron (with a KCl filled electrode), and from the homolateral lL2 and contralateral lL5 ventral roots. Within a few seconds from the start of the application, a depolarization of about 10 mV developed with superimposed oscillatory activity and action potential firing (Fig. 19A). On 16 cells recorded in these conditions,

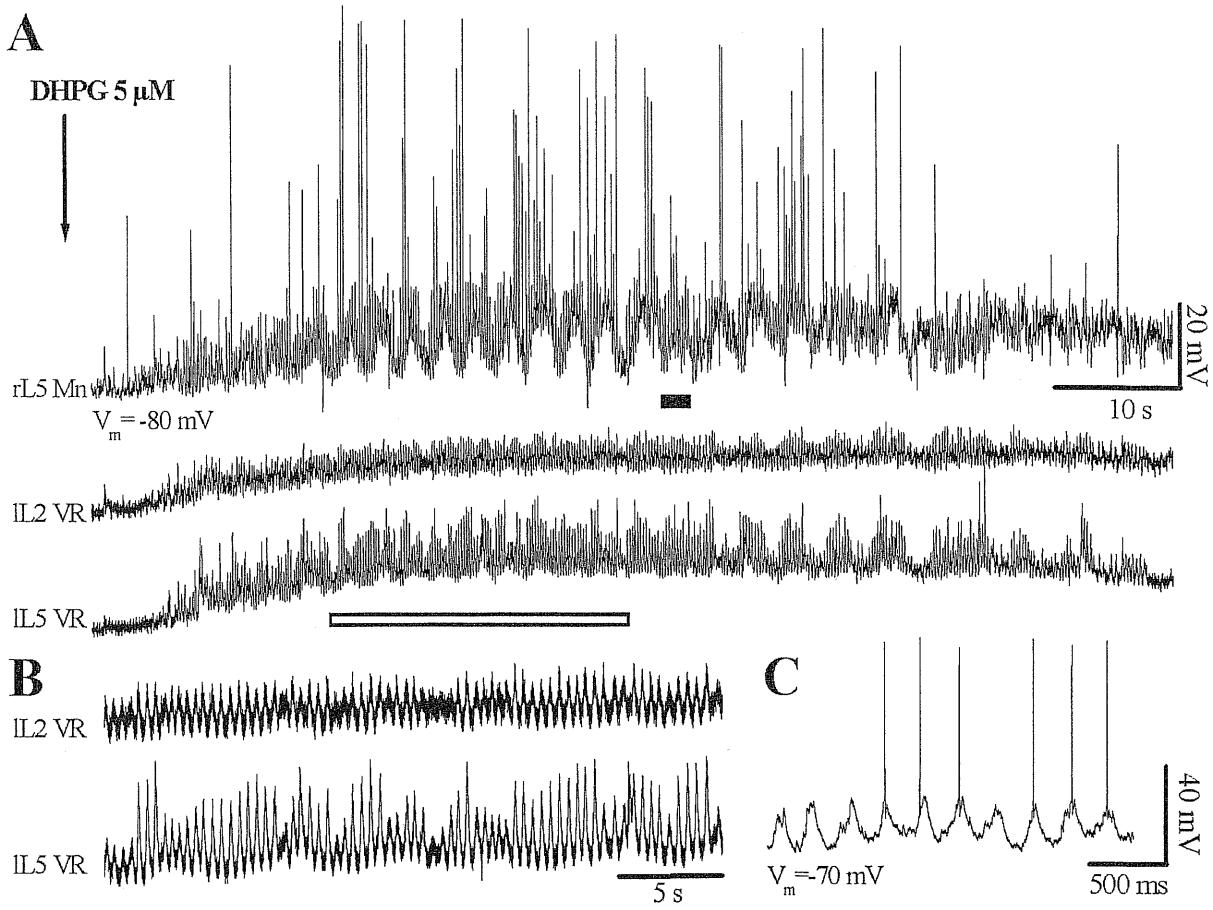

Figure 19. DHPG induces depolarization and oscillatory activity. A. Simultaneous recording from an L5 motoneuron (with a KCl filled electrode), the homolateral lL2 VR and the contralateral lL5 VR. Application of DHPG induces a depolarization of about 10 mV with superimposed synchronous oscillatory activity (on average, T_{slow}= 4.4±1.3 s) and action potential firing. B. Expansion of the time scale of panel A (open bar) reveals the presence of fast (T_{fast}= 180±90 ms) oscillations recorded extracellularly. C. Expansion of the time base of the intracellular recording (filled bar from panel A) reveals fast oscillations on single motoneuron recording.

depolarization was on average 9±3 mV (range 4-14 mV). Oscillations were fast (Fig. 19B,C for extracellular and intracellular records, respectively), with average period (T_{fast}) of 180±90 ms, and often grouped into slow ones (Fig. 19A,B), with period (T_{slow}) of 4.4±1.3 s. On a random sample of 5 cells, the amplitude of fast oscillations varied depending on whether they were occurring at the top (A_{fast} = 8±4 mV) or the trough of the slow oscillations (A_{fast} = 14±2 mV). The voltage span between top and bottom fast oscillations was around 5 mV.

The average amplitude of slow oscillations (A_{slow}) was 15.6±5.6 mV (n=5). At the top of fast oscillations, one or more spikes usually occurred (Fig. 19C). Fast and slow oscillations were

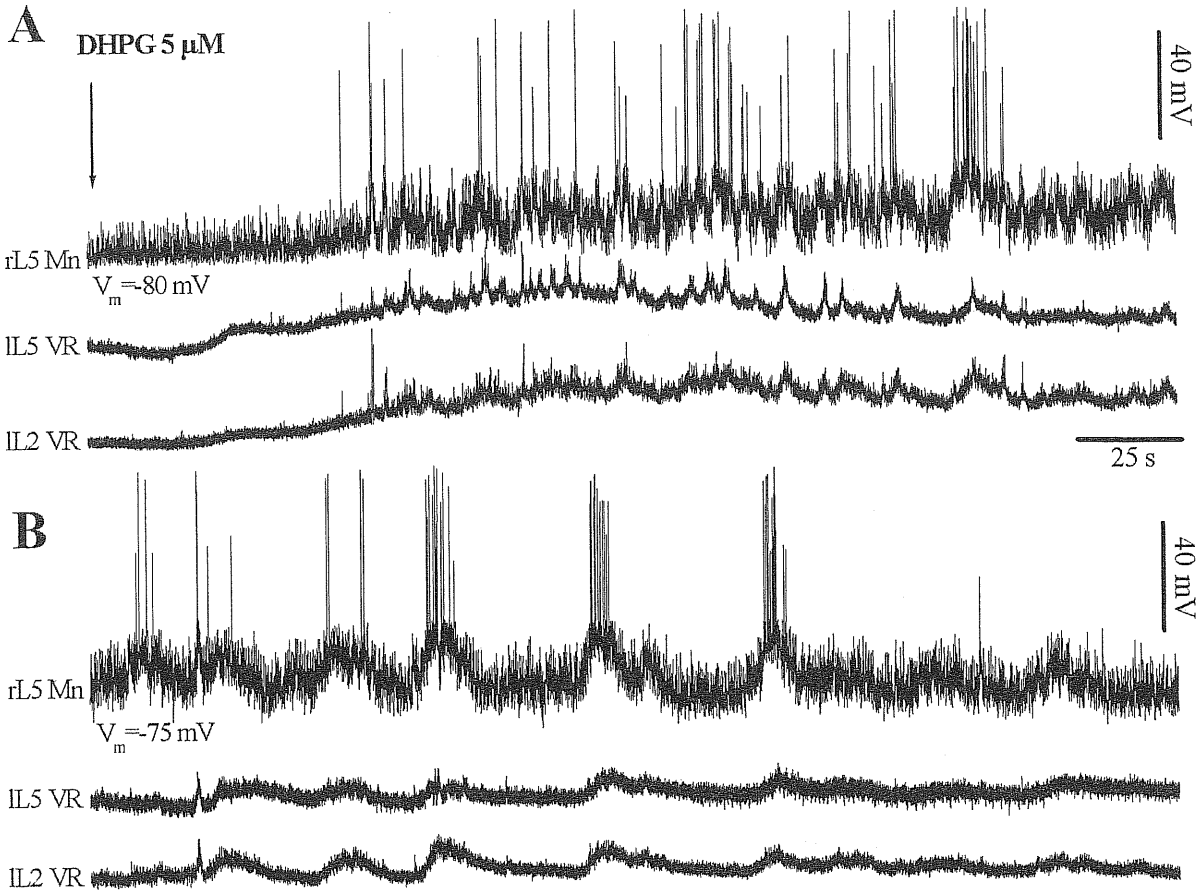

Figure 20. Time course of DHPG induced effect. A. Within one minute of DHPG (5 μM) application, the motoneuron depolarized from a resting potential of –80 mV to about –72 mV and showed fast and slow oscillatory activity. B. Continuous recording from panel A. After about 5 minutes, in the continuous presence of DHPG, cell membrane potential began to spontaneously repolarize, although increased firing persisted and a slower bursting activity appeared.

synchronous in 10 preparations out of 19, both homolaterally (lL2 vs. lL5 VRs, Fig. 19B) and homosegmentally (rL5 Mn vs. lL5 VR, Fig. 19A). On 6 preparations, our recording arrangements allowed evaluation of homolateral synchronicity only, while 3 other preparations showed out of phase oscillations (one of which completely alternated).

Fig. 20 shows the time course of the effects due to mGluR-I activation. Within one minute of DHPG (5 μM) application, the motoneuron depolarized from a resting potential of –80 mV to about –72 mV and showed fast and slow oscillatory activity. After about 5 minutes, in the continuous presence of DHPG, cell membrane potential began to spontaneously repolarize, although increased firing persisted and a slower bursting activity appeared (Fig. 20B). In all cells tested, spontaneous repolarization took place within 2 to 5 minutes from the start of DHPG application. Bursting in this later phase occurred in 13 out of 21 preparations, and

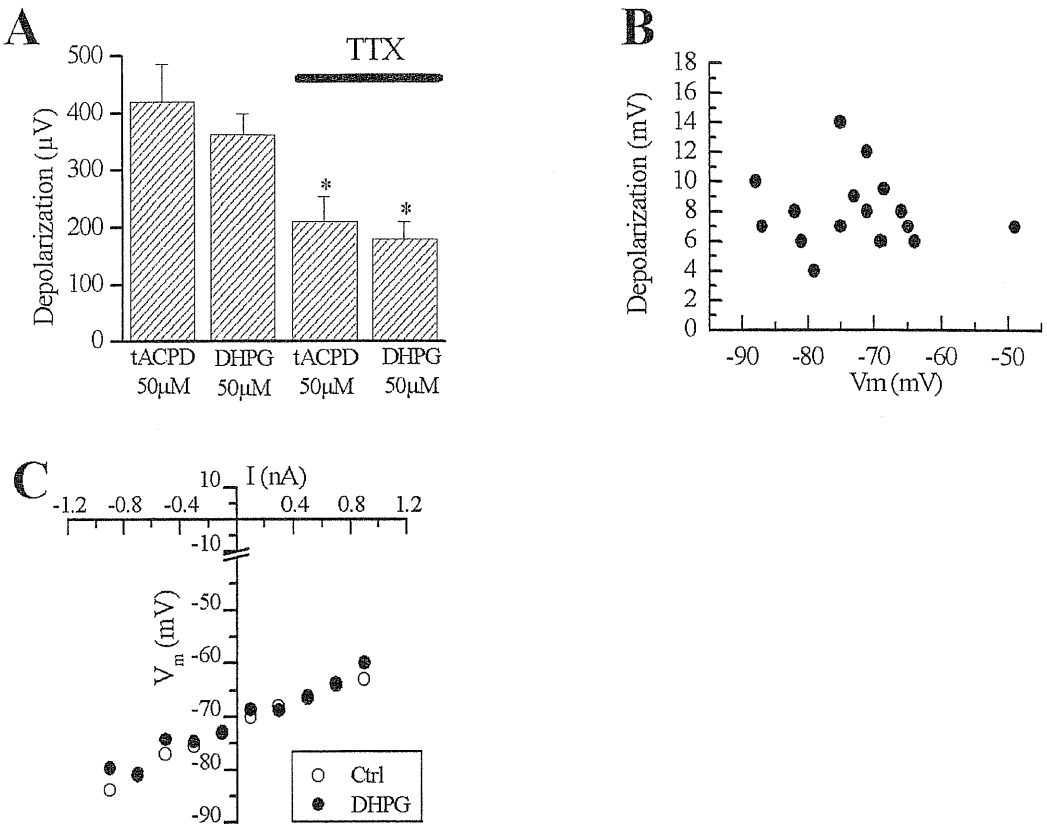

Figure 21. Dependence of DHPG induced effects on motoneuronal membrane potential. A. t-ACPD or DHPG induced motoneuronal depolarization was nearly halved in the presence of TTX. B. Membrane depolarization was independent of initial membrane potential value. C. Example of current-voltage (IV) curve for one motoneuron, obtained by injecting negative and positive currents and measuring the membrane potential, in control conditions and in the presence of DHPG (5 µM). Linear fits showed no significant changes in slope of IV curves (100±14% for 5 µM DHPG *vs.* control, n=5, r>0.99 for all linear fits), indicating that during the application of DHPG there was no apparent change in cell input resistance.

lasted 5 to 15 minutes (usually for the entire time of drug application) with a period of bursts of 37±5 s and a duration of 18±2 s. At higher DHPG concentrations (in the range of 10-50 µM), similar responses, i.e. depolarization with superimposed oscillatory activity and firing, were observed (n=4), although a stronger depolarization was induced at 50 µM (23±8 mV, n=3).

In intracellular experiments, the input resistance, calculated from the amplitude of electrotonic potentials evoked by constant current pulses (usually -0.1, -0.2 nA), was not significantly changed in the presence of 5 µM DHPG (27±15 MΩ *vs.* 27±18 MΩ in control, n=7).

Furthermore, the extent of membrane depolarization observed following DHPG application (5 μM) was unrelated with the initial resting potential, as indicated by the plot of Fig. 21B.

4.1.2 Is the effect of group I mGluR activation on motoneurons direct or network-mediated?

To explore the issue of whether motoneuronal oscillations are due to a direct effect of group I mGluRs on motoneurons or were arising as a network effect, several tests were carried out.

Experiments in TTX

First, the effect of mGluRI activation on motoneurons was investigated in the presence of TTX. In control conditions, DHPG (50 μM) or the broader mGluRI-II agonist t-ACPD elicited a comparable VR depolarization which was 360±40 μV (n=10) or 420±60 μV (n=3), respectively. In the presence of TTX, such depolarization was reduced to 210±40 μV (n=8) and 180±30 μV (n=3), respectively (Fig. 21A, $p<0.05$), showing that motoneurons and the pre-motoneuronal network contributed to the depolarization, although oscillations were completely abolished.

These observations suggest that mGluR1 activation could generate motoneuronal depolarization without the appearance of membrane oscillations. This issue was also directly examined with intracellular current injection in single motoneurons.

Current Injection

To further test whether oscillations were just a consequence of motoneuronal membrane depolarization, negative DC current was injected into motoneurons during the depolarized phase. Fig. 22A shows recording from a motoneuron that, in the presence of DHPG (5 μM), exhibited 10 mV depolarization (starting from V_m=-64 mV) with oscillatory activity (fast oscillations: T_{fast} = 130 ms, A_{fast} = 12.8 mV; slow oscillations: T_{slow}=4.4 s A_{slow}=16.5 mV) and strong firing. When the cell was repolarized to its resting level, oscillations continued, though with less firing probability (Fig. 22A, 2nd trace, continuous recording from 1st trace; negative deflections of membrane potential are due artifacts of antidromic stimulation). In 4 cells, repolarization to the same membrane potential value observed prior to DHPG application did not bring any significant changes in oscillations with respect to control (T_{fast} = 150±90%, A_{fast} = 110±10%, T_{slow}=110±30%, A_{slow}= 87±14%, n=4; $p>0.05$). Similarly, oscillations persisted with the same periodicity (T_{fast} = 110±30%, T_{slow}=75±30%, n=3) when positive current was injected to depolarize cells by 10-15 mV (see example in Fig. 22B with the corresponding VR records).

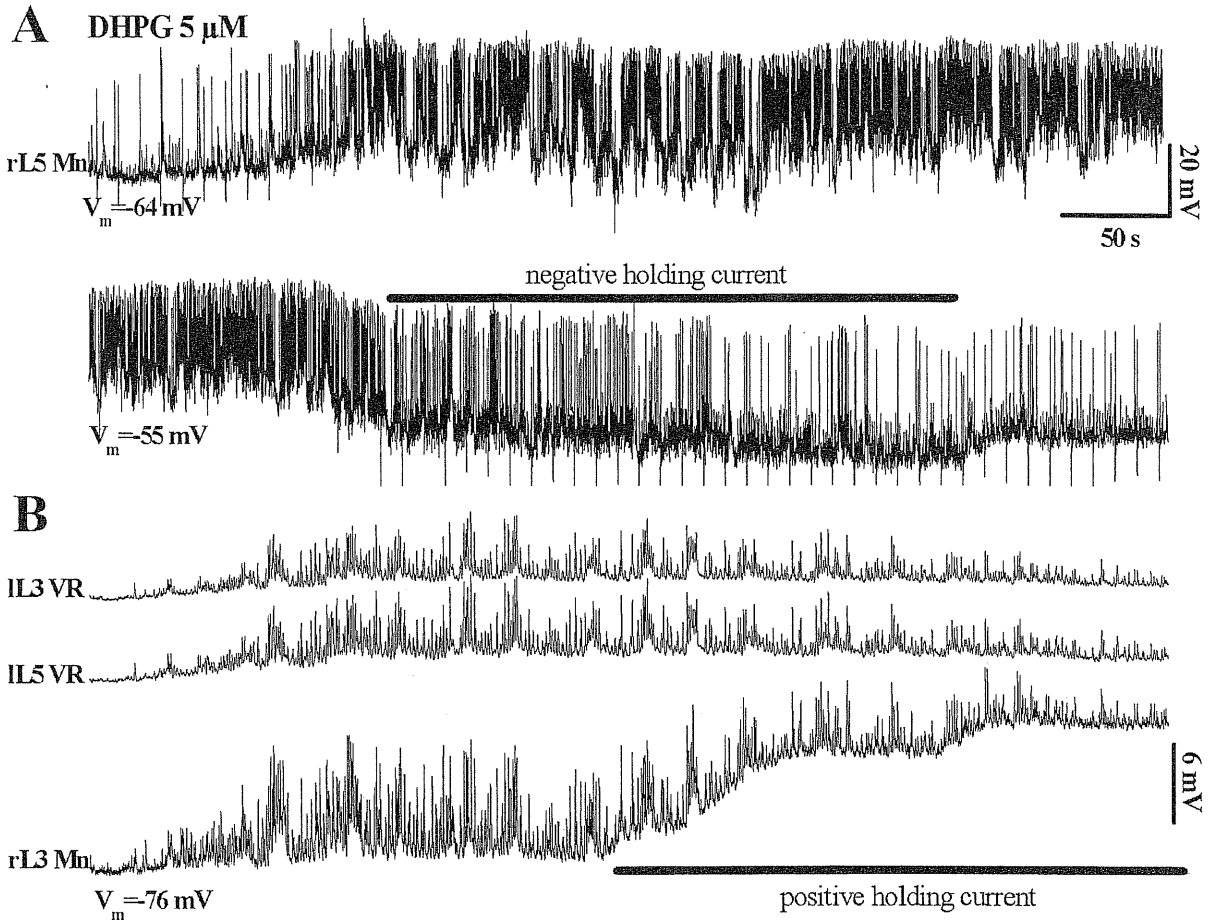

Figure 22. Dependence of DHPG induced oscillations on motoneuronal depolarization. A. DHPG induces depolarization and oscillatory activity. In the lower panel (continuous recording from top panel), when the cell is repolarized to its resting level by injection of negative DC current, oscillations continue, though with less firing probability (negative deflections of membrane potential are due artifacts of antidromic stimulation). B. Oscillations persist with the same periodicity (T_{fast} = 110±30%, T_{slow}=75±30 %, n=3) also when positive current is injected to depolarize cells by 10-15 mV.

These results show that DHPG induced oscillations were not just arising as a consequence of motoneuronal membrane depolarization.

Experiments with QX-314

The DHPG effect did not depend on the ability of motoneurons to generate spikes. In fact, when the electrode was filled with QX-314 (30 mM) (and KCl replaced with $KMeSO_4$), DHPG (5 μM)-induced depolarization was 7±1 mV (n=10), a value not significantly different from control (9±3, n=16; unpaired t-test, p>0.05). Under these recording conditions, oscillations also exhibited period of fast and slow oscillations not significantly different than control (T_{fast} = 220±80 ms, T_{slow}=3.2±1.4 s, n=4), although amplitude was significantly reduced (A_{fast} = 1.97±1.02 mV, A_{slow}=1.43 ± 1.08, p<0.001; n=4). The value of input

resistance in these experiments was 62±25 MΩ (n=7) in control conditions *versus* 60±22 MΩ (n=6) in DHPG (5 μM) solution.

The persistence of membrane depolarization and oscillations, despite intracellular application of QX-314, indicates that these responses did not require spike activity of motoneurons, although they were partly modulated in amplitude by motoneuron membrane conductances sensitive to QX-314 (I_{Na}, I_h). Furthermore, the present data allow interpreting the experiments in TTX solution as due to the block of network activity rather than to direct interference of TTX with the motoneuron ability to generate oscillations.

Voltage dependence of DHPG response

We further tested whether oscillations could arise at the level of motoneurons because of a special voltage dependence of the motoneuronal response, which could, for example, exhibit a negative slope conductance (Schwindt & Crill, 1981). To this aim, a current-voltage (I-V) curve test was performed on 5 motoneurons, by injecting negative and positive currents and measuring the membrane potential, in control conditions and in the presence of DHPG (5 μM). An example of I-V curves for one of the cells is shown in Fig. 21C. Linear fits showed no significant changes in slope of I-V curves (100±14% for 5 μM DHPG *vs.* control, n=5, r>0.99 for all linear fits). These observations also confirm that during the application of DHPG there was no apparent change in cell input resistance.

4.1.3 Subtype receptor selectivity of DHPG induced response

We tested the sensitivity of DHPG induced depolarization and oscillations to specific subgroup antagonists, namely the mGluR1 antagonist AIDA and the mGluR5 antagonist MPEP. As shown in Fig. 23A,B, AIDA (500 μM) *per se* did not affect baseline membrane potential (n=7), but, when DHPG was co-applied, depolarization was prevented (Fig. 23C,D). Lack of DHPG-induced depolarization due to AIDA was observed in 3/4 motoneurons and in all extracellular recordings from 4 preparations. In these conditions, oscillations were not abolished, although they exhibited longer periods (T_{fast}= 315±30 ms, $p<0.05$; T_{slow}=3.5±1.3 s, n=4, $p>0.05$) and smaller values for amplitude (A_{fast} = 9.4±9.0 and 3.1±2.1 mV, for oscillation occuring on top or bottom of slow oscillations, respectively, $p>0.05$; A_{slow}=4.8 ± 3.3; n=4, $p>0.05$).

On the contrary, in the presence of MPEP (100 μM, which *per se* did not change membrane potential, n=4), DHPG (5 μM) still elicited a depolarization comparable to control conditions

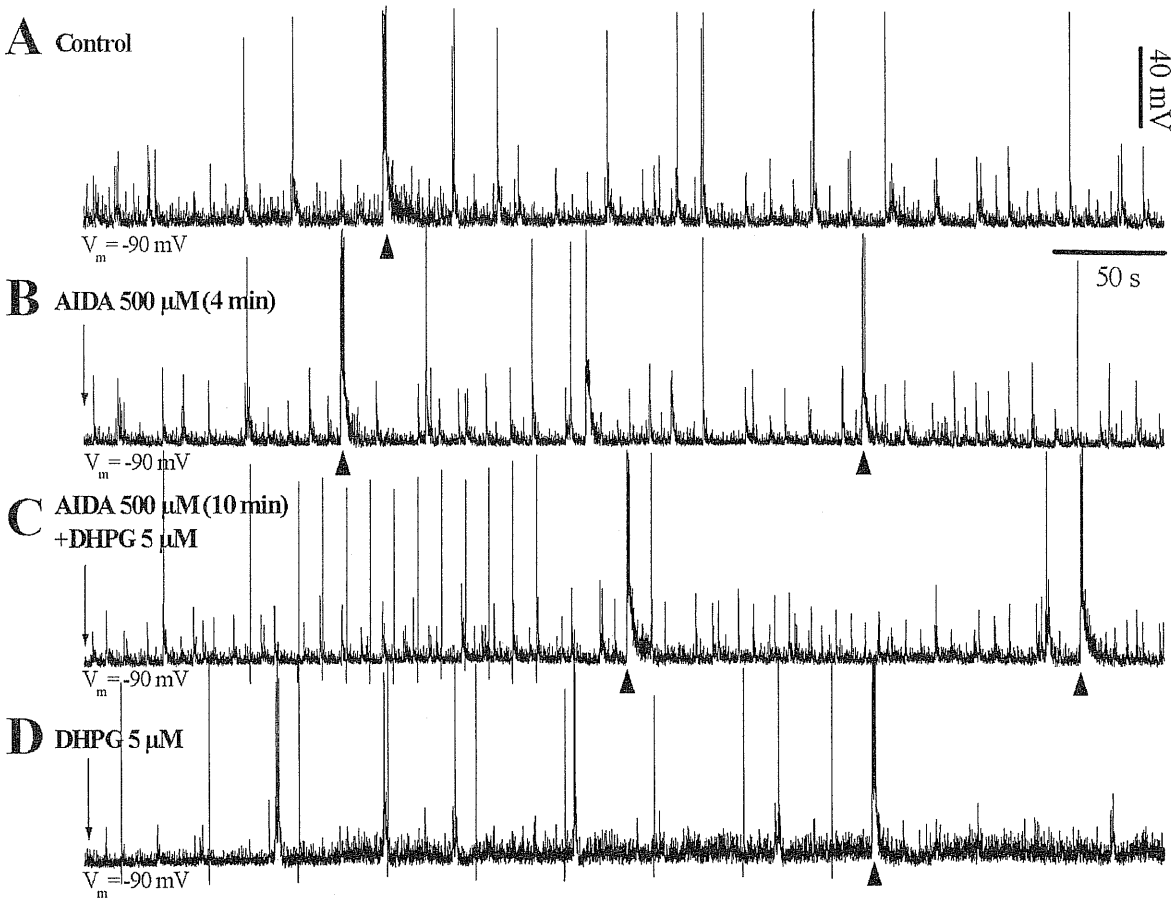

Figure 23. mGluR1 subtype receptor selectivity of DHPG induced response. A. Recording from an L5 motoneuron in control conditions. Arrows indicate responses to DR stimuli. B. AIDA (500 µM) *per se* does not affect baseline membrane potential. C. Further DHPG application prevents DHPG-induced depolarization. D. On the same preparation, application of DHPG is able to induce depolarization and some oscillatory activity.

(8±5 mV with MPEP *vs.* 7±5 mV without MPEP, n=4; paired t-test, p>0.05) while strongly reducing most oscillatory activity (Fig. 24).

These results seem to indicate that mGlu1 receptors were involved in inducing depolarization while mGlu5 receptor activation was mostly responsible for mediating oscillatory activity.

4.1.4 Is the effect of DHPG mediated by other conductances?

L-type Ca^{2+} channels

It has been shown that activation of mGluRs can unmask the bistable properties of interneurons or motoneurons (Kiehn *et al.*, 1996; Kiehn *et al.*, 1997; see also INTRODUCTION §4 and §5.2) and that this action requires activation of L-type Ca^{2+} channels

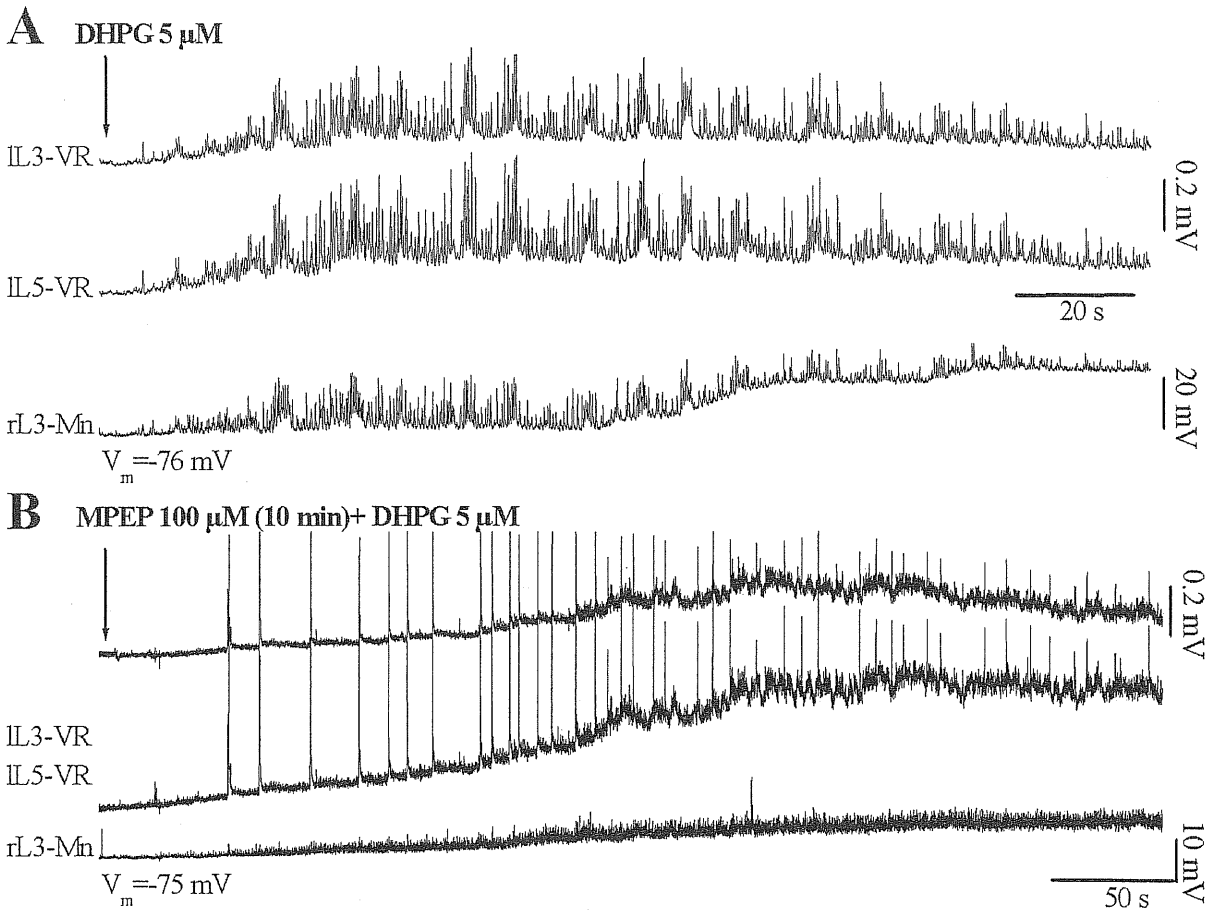

Figure 24. mGluR5 subtype receptor selectivity of DHPG induced response. A. DHPG induces depolarization and oscillatory activity (motoneuron is depolarized due to DC current injection). B. When MPEP (which *per se* did not change membrane potential) is previously applied, it strongly reduces DHPG induced oscillatory activity, while not preventing depolarization comparable to control conditions.

(Morisset & Nagy, 1999). It was then tested whether the oscillatory behavior observed in the presence of DHPG might be due to such plateau potentials, "turned on" by mGluR activation. To this aim, we applied DHPG in the presence of nifedipine (20 μM, Fig. 25A,B). Nifedipine *per se* did not affect baseline membrane potential (n=4), and further application of DHPG (5 μM) in these conditions induced a depolarization of 6.3±2.5 (n=3), a value not significantly different that the one obtained in control conditions. Likewise, oscillations persisted with characteristics similar to control (T_{fast} = 130±40 mV, $A_{fast}(1)$ = 5.5± 4.7 mV, $A_{fast}(2)$ = 10± 9 mV, T_{slow}=3.7±1.9%, A_{slow}= 7±7%, n=4; unpaired t-test, p>0.05).

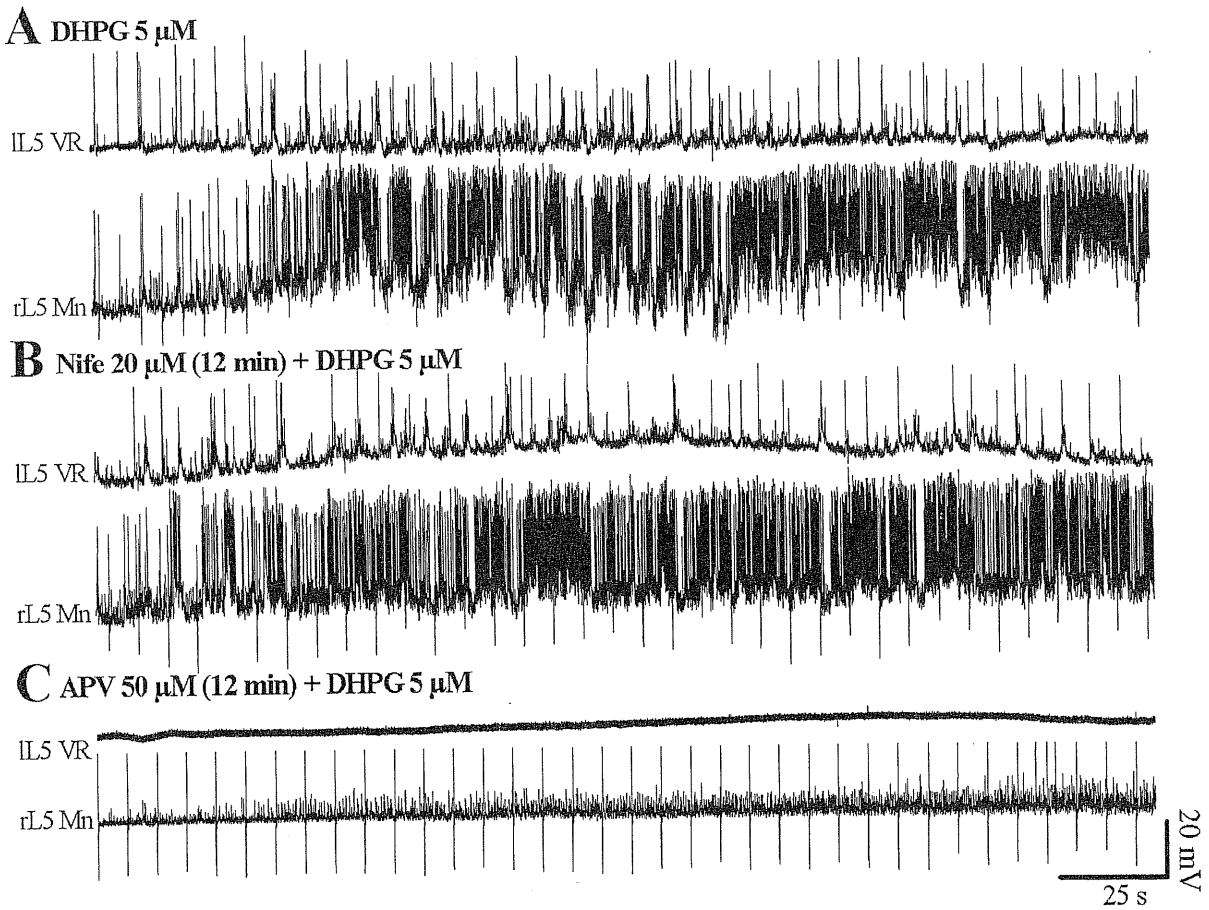

Figure 25. Role of L-Type Ca^{2+} channels and NMDA receptors in mediating DHPG induced effects. A. DHPG induces depolarization and oscillatory activity (simultaneous recording from a lL5 motoneuron and the contralateral rL5 VR). B. When, on the same cell, DHPG is applied in the presence of nifedipine (which *per se* had not affected baseline membrane potential) it induces a depolarization and oscillations comparable to the one obtained in control conditions. C. On the same cell, DHPG application in the presence of the NMDA receptor antagonist APV, induces a smaller depolarization and reduced oscillatory activity.

These results show that, under the present conditions, the membrane depolarization and oscillations due to mGluRI activity did not require activation of nifedipine sensitive Ca^{2+} channels.

Ionotropic glutamate receptors

It has also been reported that DHPG can interact with NMDA receptors (Holohean *et al.*, 1999; Ugolini *et al.*, 1999; Dang *et al.*, 2002). It was then tested whether DHPG induced oscillations also required NMDA receptor activity (Fig. 25A,C). When DHPG (5 μM) was applied in the presence of APV (50 μM; which *per se* did not alter baseline potential, n=3), depolarization was 3.3±1.5 mV (n=3), a value significantly smaller than control (unpaired t-test, $p<0.05$). Furthermore, slow oscillations were no longer visible, while fast oscillations,

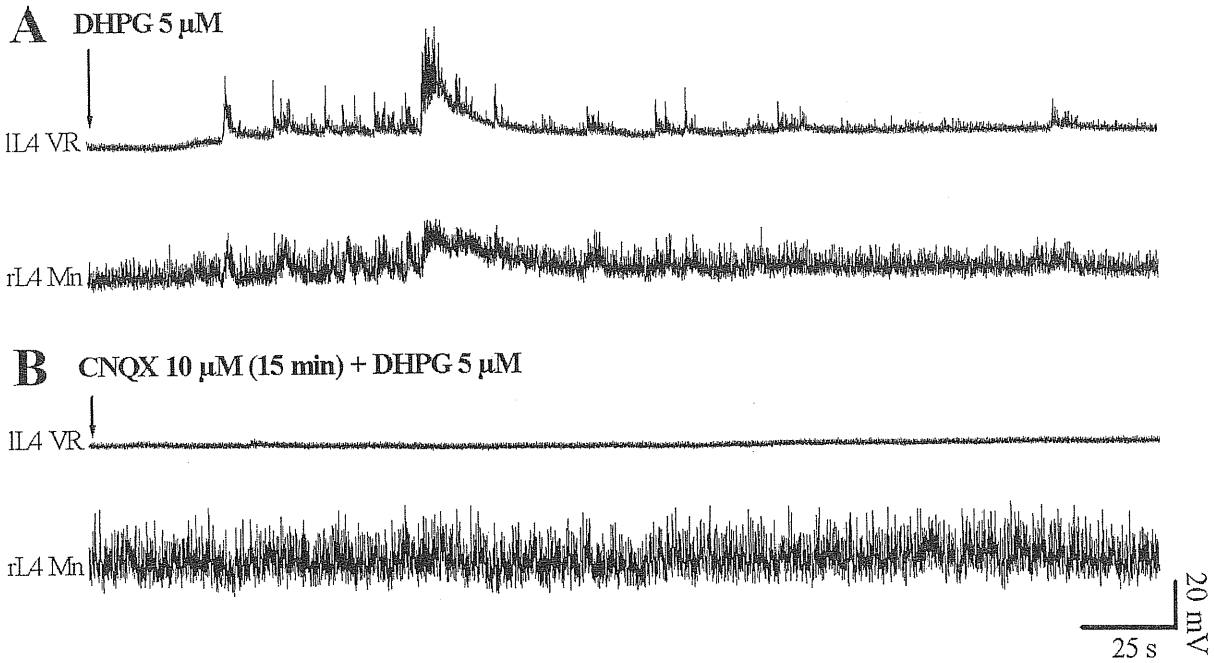

Figure 26. Role of AMPA receptors in mediating DHPG induced effects. A. DHPG induces depolarization and oscillatory activity (simultaneous recording from a lL4 motoneuron and the contralateral rL4 VR). B. On the same cell, DHPG, applied in the presence of the AMPA receptor antagonist CNQX (which *per se* had not affected baseline membrane potential), induces a smaller depolarization and reduced oscillatory activity.

though retaining a period value similar to control ones (T_{fast}= 160±40 ms, n=3, p>0.05), had significantly smaller amplitude (A_{fast}= 2.5±1.3, n=3, p<0.002). Likewise, when DHPG was applied in the presence of CNQX (10 μM), slow oscillatory activity was depressed (Fig. 26, n=2).

These observations suggest that network-based NMDA and non-NMDA receptors both contributed to the DHPG induced depolarization and oscillatory activity.

4.2 Modulation of DR-evoked responses by group I mGluRs

Action of mGluR-I on DR evoked responses

While DHPG had an excitatory action by eliciting oscillatory activity and depolarization, it also affected DR-evoked potentials, recorded either intracellularly from a single motoneuron or extracellularly from a VR. Fig. 27A show examples of responses of a rL5 motoneuron to single stimuli of intensity 2xTh and 4xTh (a and b, respectively), in control conditions (black

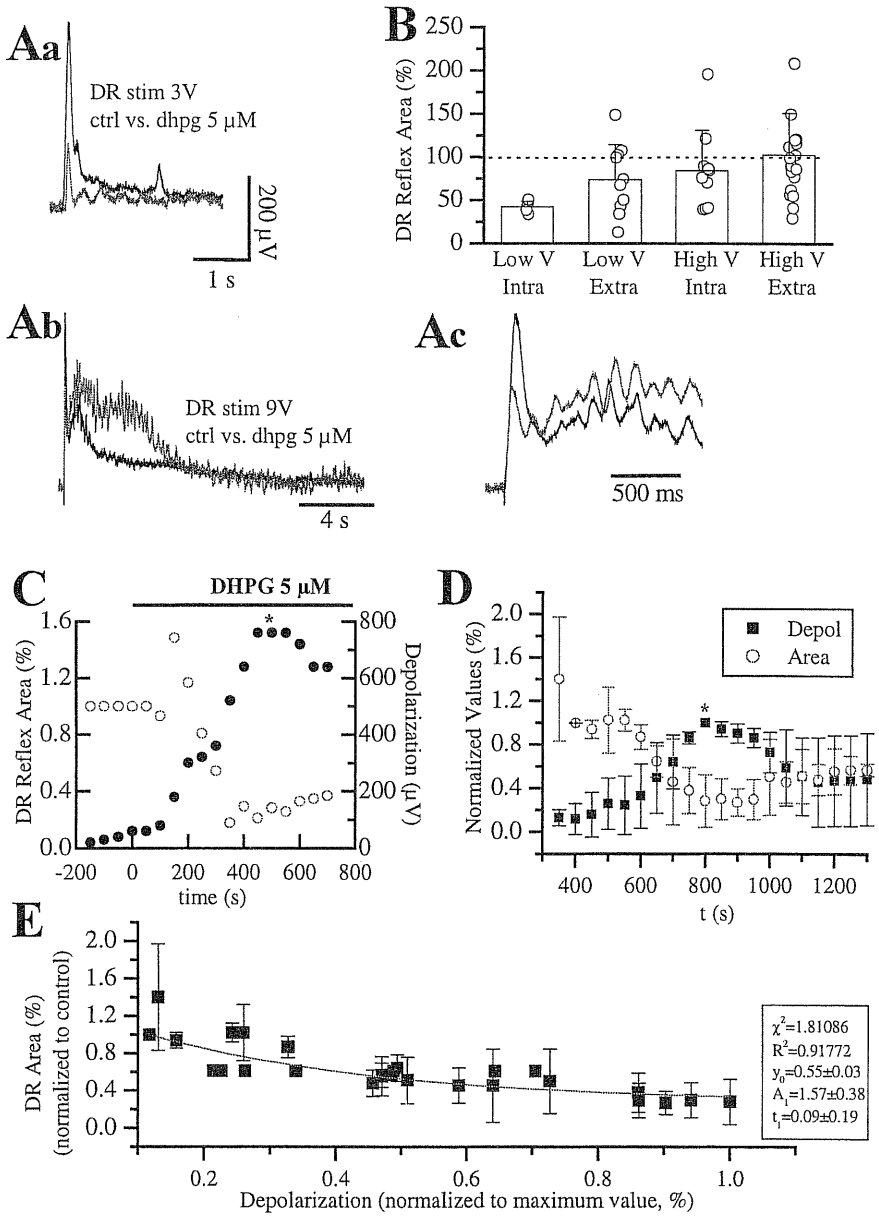

Figure 27. Action of mGluR-I on DR evoked responses. A. DHPG depresses DR evoked response (panel Aa), recorded from a rL5 motoneuron and delivered at intensity 2xTh (from the rL5 DR). On the same cell, a stronger stimulus (6xTh) increases the DR evoked response, by enhancing the late component of the reflex (Ab), while still depressing the peak (Ac). B. Percentage of DR reflex area (DHPG *vs.* control) measured for 20 preparations for low voltage (Low V) or high voltage (High V) stimulus intensity and recorded either intracellularly (Intra) or extracellularly (Extra). Each symbol represents the value for one preparation, while bars represent the means. C. Time course of DR reflex area (DHPG *vs.* control, %, hollow symbols, scale on left axis) and of depolarization (measured extracellularly, µV, black symbols, scale on right axis). Asterisk indicates maximum depolarization. D. Time course of DR reflex area (normalized to control values, hollow symbols) and of depolarization (normalized to maximum values, black symbols) *versus* time. Average for 5 cells, in which peak depolarization has been superimposed on the time base (see text for details). E. Plot of DR evoked response area (normalized values of DHPG *vs.* control, %) *versus* VR depolarization and exponential fit (see text for details).

trace) and in DHPG (5 μM) solution (gray trace). In the two cases, DHPG differentially affected those response areas, which became 67% and 210% of controls, respectively. Even when the area was increased, the peak of the response was depressed (Fig. 27Ac, 60%). The plot in Fig. 27B shows the results from 20 preparations. Each symbol (hollow circles) represents the area of DR evoked responses (averaged and then normalized to control value) for a single preparation, while the bar diagram represents the average for those preparations. In the case of low voltage stimuli (Fig. 27B, first 2 columns, for intracellular and extracellular recordings, respectively), responses were always depressed (intracellular recordings: 42±6%, n=5, $p<0.001$; extracellular recordings: 70±40%, n=10, $p<0.001$). In the case of high voltage stimuli, when recorded intracellularly, most of the responses were depressed (giving an average value of 84±47%, n=10; $p<0.01$), while only about half of the responses recorded extracellularly were reduced (the overall mean being 103±49%). In all cases of high voltage stimuli, though, the shape of the response was changed by DHPG application. In fact, while peak values were significantly reduced (60±40%, see Fig. 27Ac), response was prolonged and oscillatory activity enhanced (see Fig. 27Ab).

We explored the time dependence of the enhancement or reduction in the DR evoked response, also in view of the fact that, in the presence of DHPG, motoneurons first depolarized and then spontaneously repolarized. As can be seen from the example plotted in Fig. 27C, there was no clear correlation between depolarization (measured extracellularly; hollow symbols) and the DR evoked response area (stimulus intensity 3V, 6V, 8V; black symbols). In fact, in this case, when the motoneuron started depolarizing, the response area transiently increased, but further depolarization induced by DHPG depressed the response. We looked at the time course of DR evoked responses and of VR depolarization in 5 preparations, in which we stimulated one DR every 50 s. Their average response area (normalized to control values) and average VR depolarization (normalized to the maximum value in each preparation) are shown in Fig. 27D. To be able to average the time course of depolarization in different preparations, taking into account the different onset these might have, peaks (marked by the asterisk in the example of Fig. 27C and in Fig. 27D) were aligned with respect to the time base, so that they would superimpose. In this case, the time course was similar for all 5 preparations in the time interval shown in plot 7D. This plot indicates a loose correlation between depolarization and depression of the response. Indeed, in further experiments in which intracellularly-recorded motoneurons, in the presence of DHPG (5-10μM), were manually repolarized to resting levels prior to delivering a stimulus to the DR,

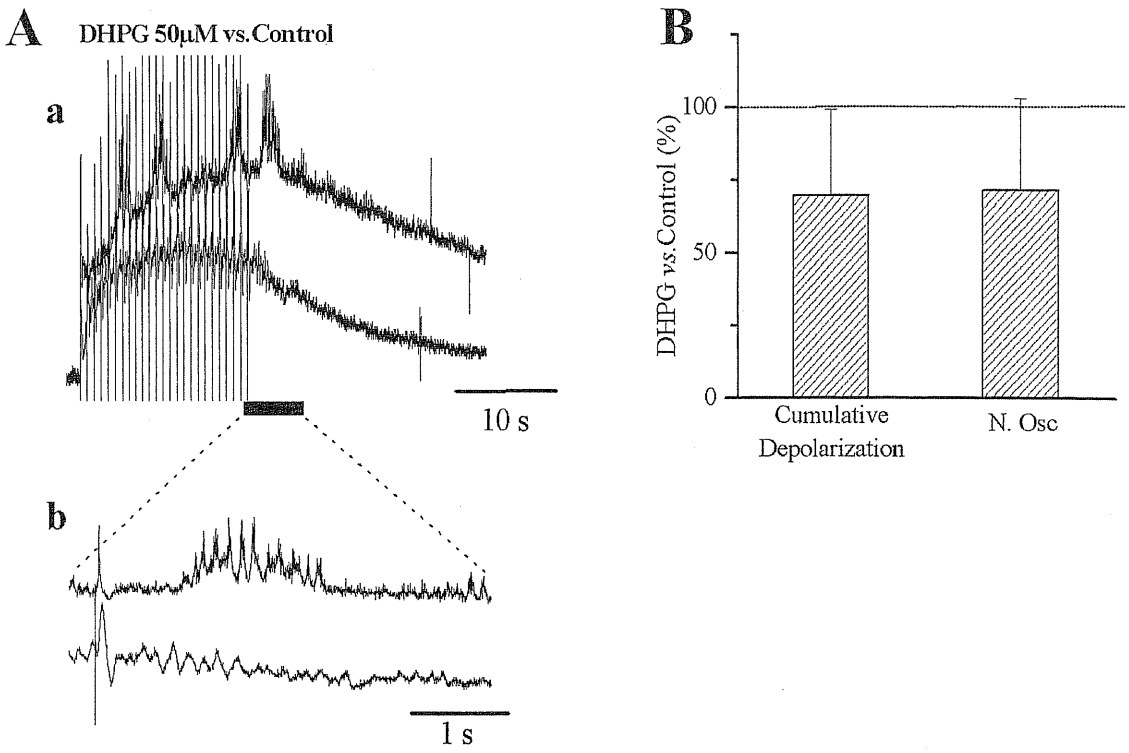

Figure 28. Effect of mGluRI agonist on responses to trains of DRstimuli. Aa. Extracellularly recorded response to a train of DR stimuli (25 stimuli, 2 Hz, 3 V) in control (black trace) and DHPG (gray trace). Ab. Expansion of trace of panel Aa reveals oscillations. Fast deflections of baseline due to stimulus artifacts. B. Histogram indicating average of cumulative depolarization and number of oscillations of responses to DR trains of stimuli in DHPG *vs.* control (%).

we found that area depression was still present, although decreased by 15±6% (n=3). Furthermore, by plotting the response area *versus* VR depolarization for data points taken during the same interval shown in Fig. 27D, we found that data could not be fitted linearly (Fig. 27E). On the other hand, an exponential curve could fit the data (values for the function $y = y_0 + A_1 e^{-x/t_1}$ are on the plot 27E), indicating complexity of processes governing depolarization and reflex reduction.

When the action of DHPG was evaluated on responses to trains of DR stimuli (Fig. 28, extracellular recording), we found area reduction in 9 out of 12 preparations. Overall, this effect was significant (75±35%, $p<0.05$, paired t-test, n=12). On 3 preparations, we also estimated a reduction in the cumulative depolarization (70±30%, n=3; $p>0.05$) and in the

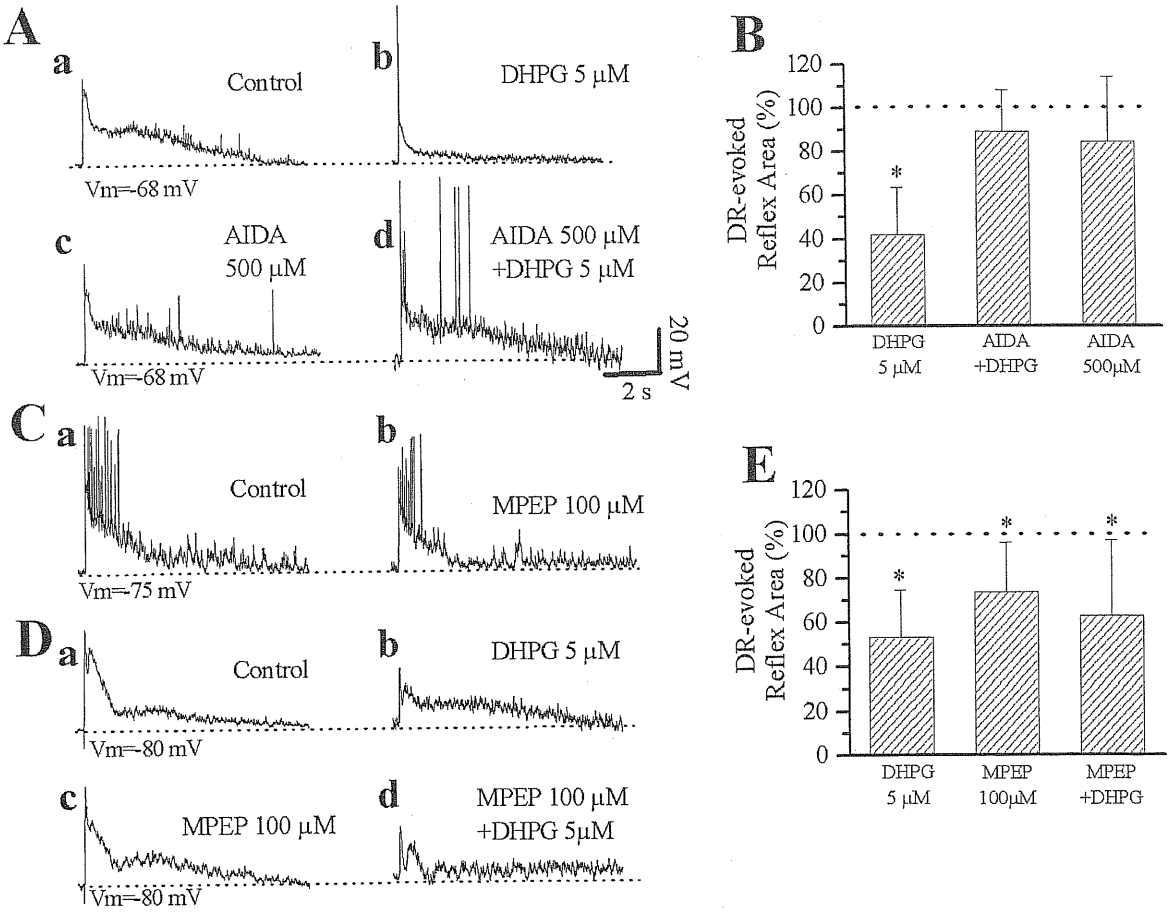

Figure 29. Subtype receptor selectivity of DHPG effect on DR evoked responses. A. DR evoked responses to stimuli of intensity 3xTh, recorded (with a KCl filled electrode) at the same membrane potential value (V_m=-68 mV): a) control; b) in the presence of DHPG (5 μM) response is depressed by 60%; c) application of AIDA (500 μM) slightly reduces the DR evoked response (10%); d) DHPG induced depression is prevented by the presence of AIDA (area 87% of control). B. Average values of DR evoked response areas (normalized to control values). C. DR evoked responses to stimuli of intensity 3xTh, recorded (with a KCl+QX-314 filled electrode) at the same membrane potential value (V_m=-75 mV): a) control; b) in the presence of MPEP response is 85% of control. D. DR evoked responses to stimuli of intensity 3xTh, recorded (with a KCl filled electrode) at the same membrane potential value (V_m=-80 mV): a) control; b) in the presence of DHPG, response is depressed; c) MPEP (100 μM) also depresses DR evoked response; d) Co-application of DHPG and MPEP further reduces DR reflex. E. Average values of DR evoked response areas (normalized to control values).

number of oscillations (measured from the last stimulus artifact to the timepoint when the trace returned to baseline; 70±30%, n=3, p>0.05; see expansion of panel Aa in panel Ab).

Subtype receptor selectivity of DHPG effect

We next tested the selectivity of DHPG dependent modulation of DR responses upon mGluRI receptor subtype. In the example shown in Fig. 29 Aa,b, a stimulus of intensity 3xTh evoked a response, at the same level of membrane potential as in control, which was depressed to 40% by DHPG. Application of the mGluR1 antagonist AIDA (500 μM) also

reduced the DR evoked response (Fig. 29Ac, 90%), but prevented further depression by DHPG (Fig. 29Ad, 87%). On average, on 4 preparations, in which both DHPG and AIDA+DHPG were applied, area reduction of the DR stimulus response by DHPG (5 μM) was 40±20% (n=4), an effect prevented (87±18%, n=4) by previous application of AIDA (500 μM). AIDA *per se* elicited responses which were 89±19% of control (n=10, p>0.05; Fig. 29B) suggesting a very slight degree of activation of mGluR1 receptors by endogenous glutamate.

DR stimuli delivered in the presence of MPEP (100 μM) gave smaller responses (74±22% of control, n=7, p<0.05; Fig. 29Ca,b for an intracellular recording with a KCl filled electrode, and Da,b for a recording with KCl+QX-314 electrode; in both cases, the membrane potential level was the same as in control). This result indicates that the DR evoked response was mediated by glutamate not only through ionotropic receptors, but also through group 5 mGluRs, which contributed to the DR reflex. When DHPG (5 μM) and MPEP (100 μM) were co-applied, DR response was further reduced to 63±34% of control (see Fig. 29Dc,d and Fig. 29E; n=3). When comparing the depression due to DHPG and to MPEP+DHPG (only in those preparations where both had been applied) we found further significant reduction (44±17% n=3, p<0.05) during the co-application, with respect to DHPG alone, indicating summation of depressant effects.

Mechanism of inhibitory action

Several hypotheses can be advanced regarding the mechanism through which DHPG might exert its inhibitory action on the DR induced reflex: a) direct action of mGluI receptors on membrane potential of certain neurons within the DR-VR pathway; b) down-modulation of excitatory synapses; c) facilitation of inhibitory transmission. The latter could in turn arise from direct modulation of Cl^- mediated conductances, or from excitation of inhibitory interneurons. We investigated whether facilitation of glycinergic or GABAergic transmission could play a role in the inhibitory action of DHPG. Fig. 30A shows an extracellular recording of a DR evoked response, in which DHPG elicited a depolarization of 240 μV and depressed the response by 60% (Fig. 30Ab *versus* Aa). In the presence of strychnine (1 μM), DHPG depolarized the ventral root by 180 μV and induced a distinctive change in the reflex shape (Fig. 30Ac,d). In this example, in fact, the reflex area was 102% of the one in strychnine alone (taken as control), but the response lasted longer and displayed intense oscillatory

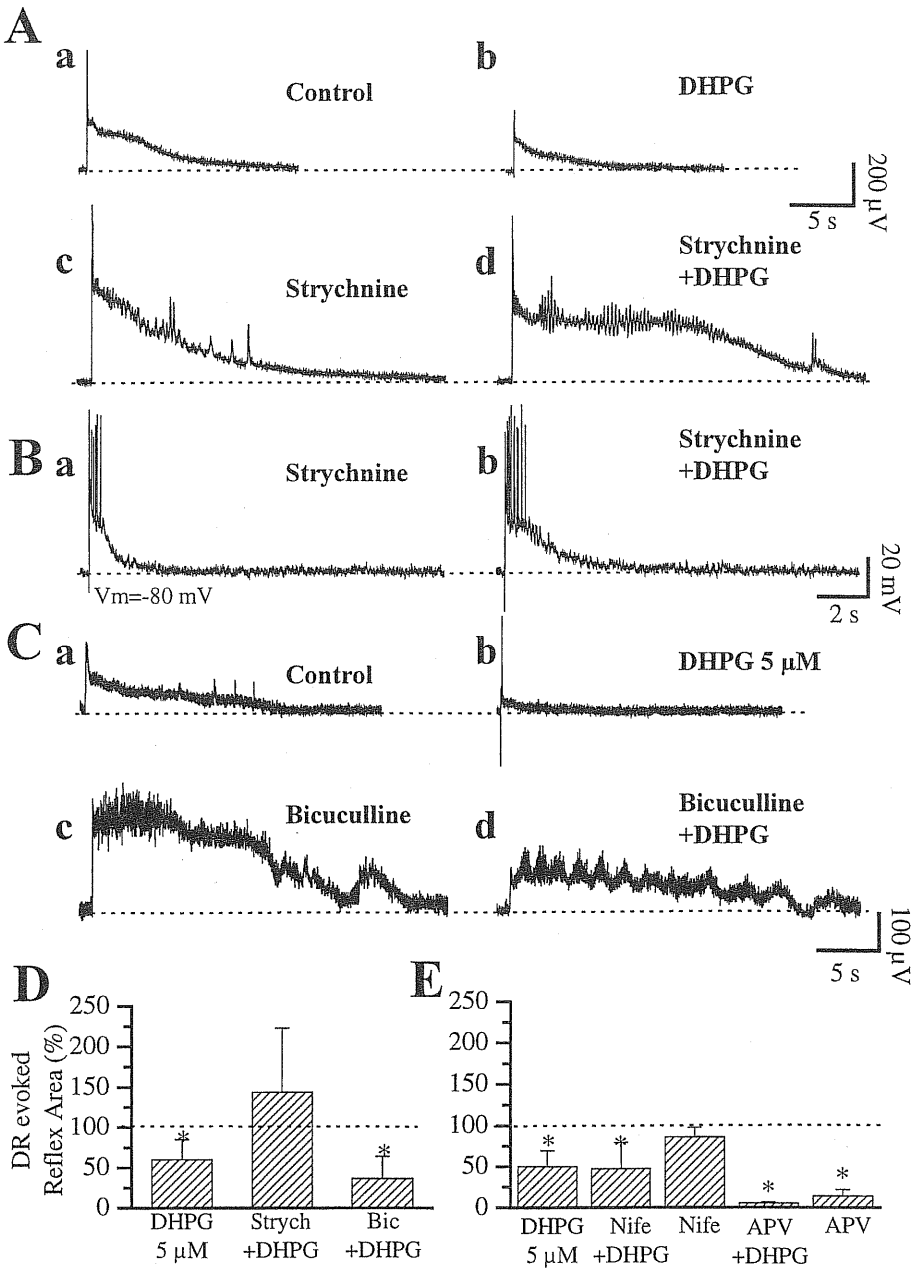

Figure 30. Mechanisms of DHPG effect on DR evoked responses. A. DR evoked responses to stimuli of intensity 2xTh, recorded extracellularly: a) control; b) in the presence of DHPG (5 µM), response is depressed; c) application of strychnine enhances DR evoked response; d) DHPG induced depression is prevented by the presence of strychnine (area is 150% of strychnine alone). B. Results are confirmed with intracellular recordings: response in the presence of strychnine and DHPG (panel Bb) is not reduced with respect to strychnine alone. C. DR evoked responses to stimuli of intensity 2xTh, recorded extracellularly (different preparation from A): a) control; b) in the presence of DHPG (5 µM), response is depressed; c) application of bicuculline enhances DR evoked response; d) DHPG induced depression is not prevented by the presence of bicuculline (area is 37% of bicuculline alone). D. Summary of pooled data, measured from 6 preparations: average DR reflex area for DHPG *vs.* control, strychnine+DHPG vs. strychnine, bicuculline+DHPG *vs.* bicuculline. E. Summary of pooled data, measured from 3 preparations: average DR reflex area (percentage *vs.* control) for DHPG, nifedipine+DHPG, nifedipine, APV+DHPG, APV.

activity. Nevertheless, the reflex peak amplitude was still depressed by DHPG (72±16 % *vs.* control in strychnine, $p<0.05$). These results were confirmed with intracellular recordings, as shown in Fig. 30B: in this case, DHPG (in the presence of strychnine) first depolarized the motoneuron by 10 mV (a value comparable to the DHPG induced depolarization in control conditions, not shown). When the cell was spontaneously repolarized in the continuous presence of strychnine and DHPG, the DR-evoked reflex area and associated firing were increased by about 50%. On all 6 preparations tested, in which DHPG had reduced the DR-evoked reflex area to 60±25%, such an effect was absent in the presence of strychnine (140±80%, Fig. 30D) because, despite reduction in the early component of the reflex, the reflex overall duration was largely increased.

On the other hand, bicuculline did not counteract the depressant action of DHPG on the VR reflex (area in Fig. 30Cd was 37% of the one in Cc) while the DHPG induced depolarization was of about 200 μV. Pooled data indicate that DHPG retained its depressant action on the reflex area in bicuculline solution (20 μM, 40±25%, n=4, Fig. 30D).

The VR depolarization evoked by DHPG was 88±23% of control in strychnine solution and 195±160% of control in bicuculline solution.

Furthermore, we could rule out the indirect involvement of L-type Ca^{2+} channels in inhibiting DR evoked response, since nifedipine did not block the depressant effect of DHPG (Fig. 30C, 47±30%, n=3). Lastly, the depressant effect of DHPG in reducing the DR evoked response was not prevented by APV (6±1% in APV+DHPG *vs.* 14±8% in APV alone, n=3).

These results show that DHPG required intact glycine receptors to exert its inhibitory action on DR-evoked reflexes. Once glycine receptors were blocked, DHPG induced long lasting reflexes.

4.3 Effect of mGluRI activation on Inhibitory Post-Synaptic Potential (IPSP)

The DHPG induced spinal rhythm was usually synchronous (see § 4.1.1). This finding suggested that either the fictive locomotion CPG was not fully activated during the network depolarization evoked by DHPG, or the CPG was switched on without emergence of alternating patterns because of concurrent impairment of inhibitory transmission at certain sites. On the other hand, data in § 4.2 appear to indicate that the DHPG inhibitory action on DR evoked responses required intact glycine receptors, a finding which would favor the hypothesis of facilitation of glycinergic transmission by DHPG. To gain more information on the relation between mGluRI activity and glycinergic transmission, we explored the effect of

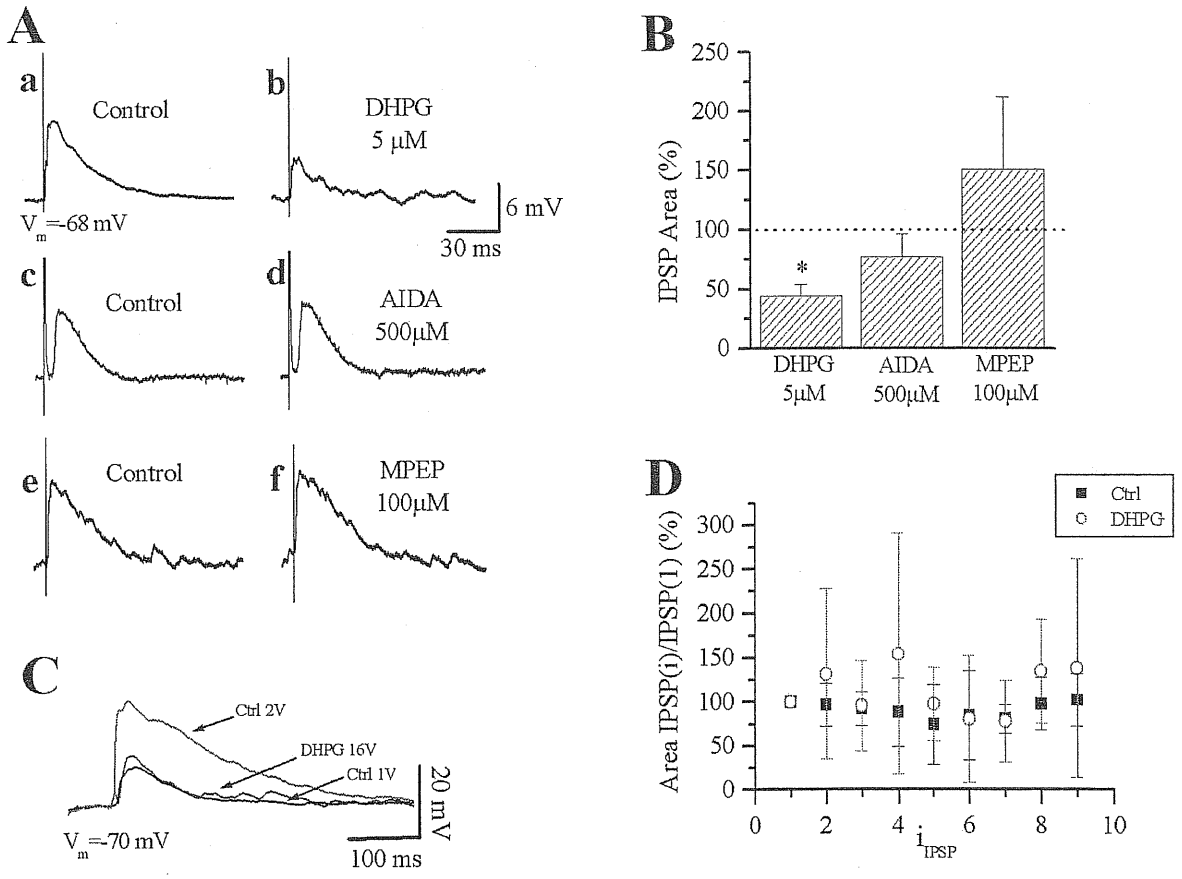

Figure 31. Effect of mGluRI activation on Inhibitory Post-Synaptic Potential. A. Recurrent IPSP recorded (with a $KMeSO_4$+QX-314 filled electrode) at the same membrane potential value (V_m=-68 mV): response is depressed in the presence of DHPG (a,b), but not in the presence of AIDA (c,d) or MPEP (e,f). B. Average from pooled data (percentage with respect to control). C. IPSPs elicited by stimuli at different intensities of VR stimulation in control (1V, 2V) and in DHPG (16V). D. Time course of IPSP area (normalized to area of first IPSP) in control (black symbols) and in DHPG (hollow symbols): i_{IPSP} indicates the number of IPSP in the sequence (i=1,...,9).

mGluR activation on the recurrent Renshaw cell mediated IPSP (Fig. 31), whose early, main component is due to glycine while the latter, smaller one, to GABA (Cullheim & Kellerth, 1981; Schneider & Fyffe, 1992; see also INTRODUCTION § 2.4, 2.5 and RESULTS § 2). In the recording shown in Fig. 31 Aa,b, DHPG depressed the IPSP by 57%. This effect was observed on 7 cells, in which, on average, IPSP area in the presence of DHPG was 44±10% of control (n=7, $p<0.05$). Furthermore peak amplitude was reduced to 53±22% ($p<0.002$), while rise time was not (93±18%), suggesting apparent lack of interference with glycine release processes. Decay time was also not altered (100±19%, $p>0.05$).

We also explored the role of endogenous mGlu1 and mGlu5 receptors in shaping the IPSP. Fig. 31c,d and e,f show examples of IPSPs measured in the presence of AIDA (500 μM, 75%) and MPEP (100 μM, 112%) respectively. On average (Fig. 31B), area reduction due to AIDA (77±19%, n=5), as well as of peak amplitude (88±24%, n=5), rise (100±50%) or decay (90±10%) time were not significantly different. Also, enhancement of IPSP area by MPEP (150±60%, n=3) was not significant with respect to control (rise time: 114±25%, peak amplitude: 109±14%, decay time: 180±140%, n=3, p>0.05 in all cases).

These experiments show that, although group I mGluRs did not seem to play an endogenous role in shaping the recurrent IPSP, exogenous application of DHPG consistently depressed these inhibitory responses on motoneurons.

Mechanisms of inihibitory action

We considered several potential mechanisms through which DHPG might have depressed the recurrent IPSP, which includes a disynaptic pathway. The first synapse (between axon collaterals and Renshaw cells) is cholinergic. One possibility might be that DHPG blocked cholinergic transmission via antagonism of acetylcholine receptors, enhancement of their desensitization, or suppression of acetylcholine release. Another possibility would be pre-synaptic depression of Renshaw cell release, as reported, for example, for the release of other transmitters by hippocampal cells (Faas *et al.*, 2002). Several of these hypotheses are not amenable to direct testing in the rat isolated spinal cord preparation. In particular, it would be rather difficult to record directly the sensitivity of Renshaw cells to exogenous acetylcholine or the occurrence of their spontaneous cholinergic events during application of DHPG. Likewise, it would be impossible to identify, on a single motoneuron, glycinergic events exclusively generated by Renshaw cells or glycine receptors associated with such synapses, as glycine is quite a ubiquitous transmitter.

A phenomenon like acetylcholine nicotinic receptor desensitization is typically increasing over time, has slow recovery and is strongly dependent on intracellular Ca^{2+} levels (Khiroug *et al.*, 1997, Khiroug *et al.*, 1998). Since DHPG increases intracellular free Ca^{2+} (Pin & Duvoisin, 1995), this phenomenon could facilitate acetylcholine receptor desensitization and eventually depress the recurrent IPSP. In such a case the IPSP should be progressively reduced by any on-going process of desensitization. The plot in Fig. 31D shows the area of the first 10 IPSPs measured in control conditions and in the presence of DHPG (the stimulation interval for each test was 3 s). The plot shows the average for 5 cells, in which the area of each IPSP was normalized to the area of the first one. There was no significantly

incrementing reduction in the IPSP with time. This observation, however, cannot completely rule out the hypothesis of desensitization since the interval of stimulation might have been too long and acetylcholine receptor desensitization complete by the time the second IPSP in each trial was measured. Protocols of paired-pulse stimulation will be helpful to further explore this issue.

We also found that inhibition of IPSPs by DHPG was not counteracted by an increase in antidromic stimulation strength, unless stimulus intensity in control was very low. In the example shown in Fig. 31C, in order to evoke a comparable response in control conditions and in DHPG solution, stimulus intensity had to be raised from 1 V (in control) to 16V in DHPG (area 130 % of control). With the stimulus intensity set at 2 V in control solution, the evoked response could not be matched in the presence of DHPG even by strongly increasing stimulus intensity.

Collectively, the present data indicate that activation of mGluRI receptors resulted in functionally distinct consequences for glycine-mediated transmission. In the case of DR-evoked reflexes, mGluRI receptors facilitated glycinergic transmission to depress motoneuron responses. However, the operation of certain glycinergic neurons, like the Renshaw cells, was depressed, a phenomenon that might be responsible for the synchronous rhythmicity associated with mGluRI receptor activity.

4.4 mGluRI activation modulates spinal rhythms

The previous results indicated that group I mGluR activation comprised excitatory as well as inhibitory effects on spinal neurons. In order to establish the extent of group I mGluR contribution to spinal network activity in terms of excitation and regulation of rhythmic patterns, and to understand the time course of such excitatory effect, experiments were carried out on the disinhibited rhythm model (see INTRODUCTION § 4.2.6). This form of spontaneous bursting (appearing after complete block of glycinergic and GABAergic inhibition) is characterized by very regular periodicity, and therefore is suitable to investigations concerning excitatory modulation by DHPG.

Studying the role of mGluR during disinhibited rhythm could then be useful for two reasons: 1) verifying the role of these receptors in shaping the rhythm and 2) exploring the action of group I mGlu receptor activation when inhibitory transmission (modulated by DHPG) is blocked.

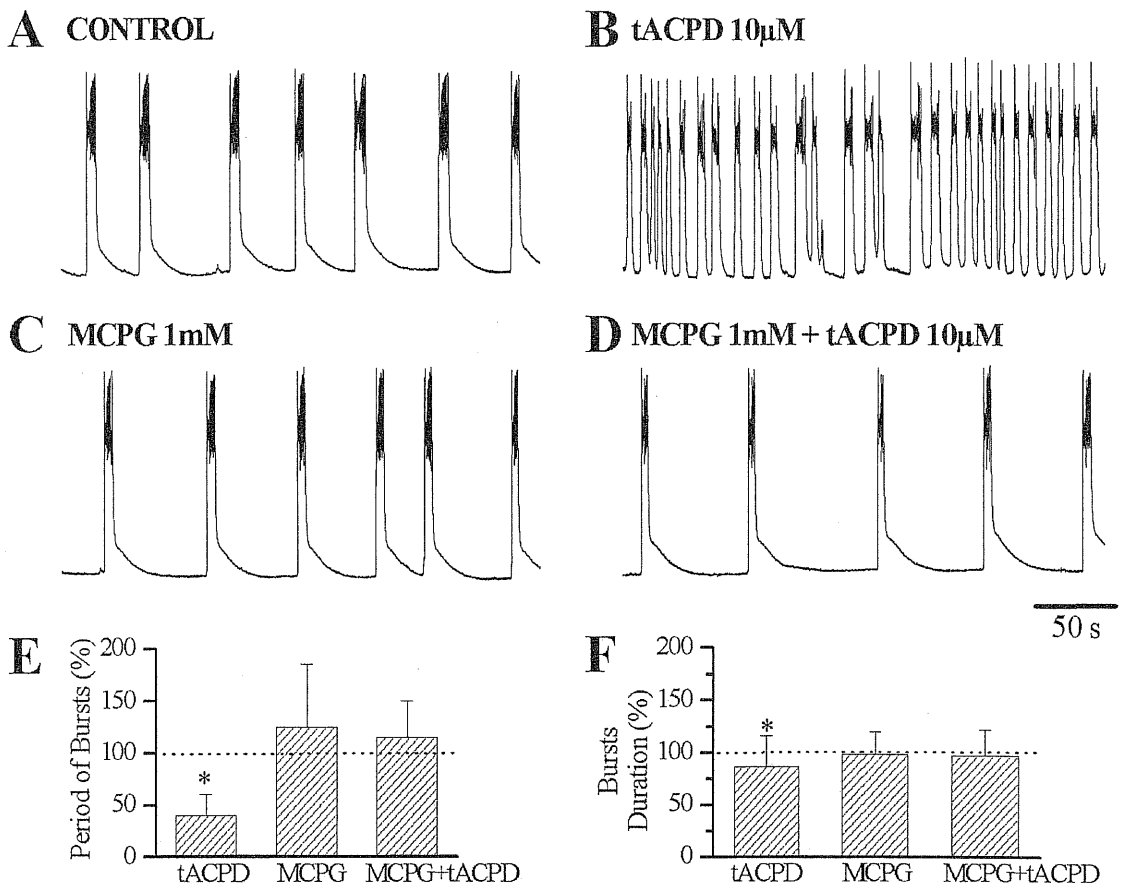

Figure 32. Action of the broad spectrum agonist of mGluRs on disinhibited rhythm. A. Example of disinhibited rhythm in control conditions. B. t-ACPD (10 μM) accelerates bursting. C. MCPG (1 mM) does not significantly alter period or burst duration; D. MCPG prevents t-ACPD induced acceleration. E. Average from pooled data for period of bursting. F. Average from pooled data for burst duration.

4.4.1 Disinhibited rhythm

We studied the role of mGlu receptors with the broad spectrum group I-II agonist and antagonist t-ACPD/MCPG and compared the effects with the selective mGluR agonists/antagonists.

Broad spectrum mGluR-I action

Fig. 32 shows the effect of t-ACPD on disinhibited rhythm: the application of t-ACPD (10 μM) accelerated bursting, leading to a reduction in period of 40±20% (n=13, $p<0.001$) with respect to control. We found that lower concentrations of t-ACPD (0.5 μM-5 μM) did not significantly alter rhythms (98±10%, n=9), while higher ones (25-50 μM) had effects comparable to 10 μM (58±22%, n=5, $p<0.001$). Burst duration was reduced to 87± 28% of control (n=23; $p<0.05$).

The broad spectrum antagonist MCPG (1 mM) did not significantly alter period (125±60%, n=12) or burst duration (98±21%), but prevented t-ACPD induced acceleration (period: 115±35%, burst duration: 97±25%, n=6; $p<0.05$ with respect to t-ACPD only). Regarding the more selective group antagonists, we found that t-ACPD induced acceleration (period being 55±18% of control) was not prevented by EGLU (200 μM; period: 52±33%, burst duration: 86±20%, n=9) and only partly by AIDA (500 μM; period: 70±40%, burst duration: 103±14%, n=11; $p>0.05$; data not shown).

Selective mGluR-I action

Since tACPD acts on classes of receptor which could yield contrasting actions, we further explored the effects of more selective agonists (see also § 4.4).

Fig. 33 summarizes the effect of mGluR-I activation. When DHPG (5 μM) was bath-applied during disinhibited rhythm, it induced VR depolarization within the first minute of application (not shown) and reduced bursting period by 40% (Fig. 33A) without eliciting oscillatory activity during the inter-burst interval. This effect was prevented when the antagonist AIDA (500 μM) was pre-applied (Fig. 33A). On average, DHPG, at the concentration of 5 μM, reduced period to 44±7% (n=11) of control (Fig. 33B). Such reduction was comparable (56±11%, n=11) at higher concentrations of DHPG (10-50 μM), while it was not present (100±16%, n=4) at lower ones (0.5-1 μM).

Time course of mGluRI action

Bath-application of DHPG during disinhibited rhythm depolarized motoneurons and accelerated bursting. We compared the time course of these effects with the action of mGluRI activation in control solution. In this latter case, in fact, the depolarizing action of DHPG waned with time despite the continuous presence of the mGluRI agonist (see § 4.1.1 and Fig. 20). In principle, this effect could be due to either a desensitization phenomenon or enhancement of inhibitory transmission which could "turn off" DHPG induced effects. We explored this issue by looking at the time course of the DHPG effect when inhibitory synaptic transmission was blocked. Fig. 33F shows time course of depolarization (measured from extracellular recordings) and period of disinhibited bursting as a function of time for one preparation. The first 400 s of the plot refer to pre-DHPG conditions, while the time window 400-800 s refers to the DHPG effect. Here, depolarization had a time course similar to control conditions (see Fig. 20), i.e. it increased, reached a plateau and then waned. On the contrary, period of oscillations remained steadily smaller than control for the whole time of the application. The same protocol was applied to 6 other preparations, which exhibited the

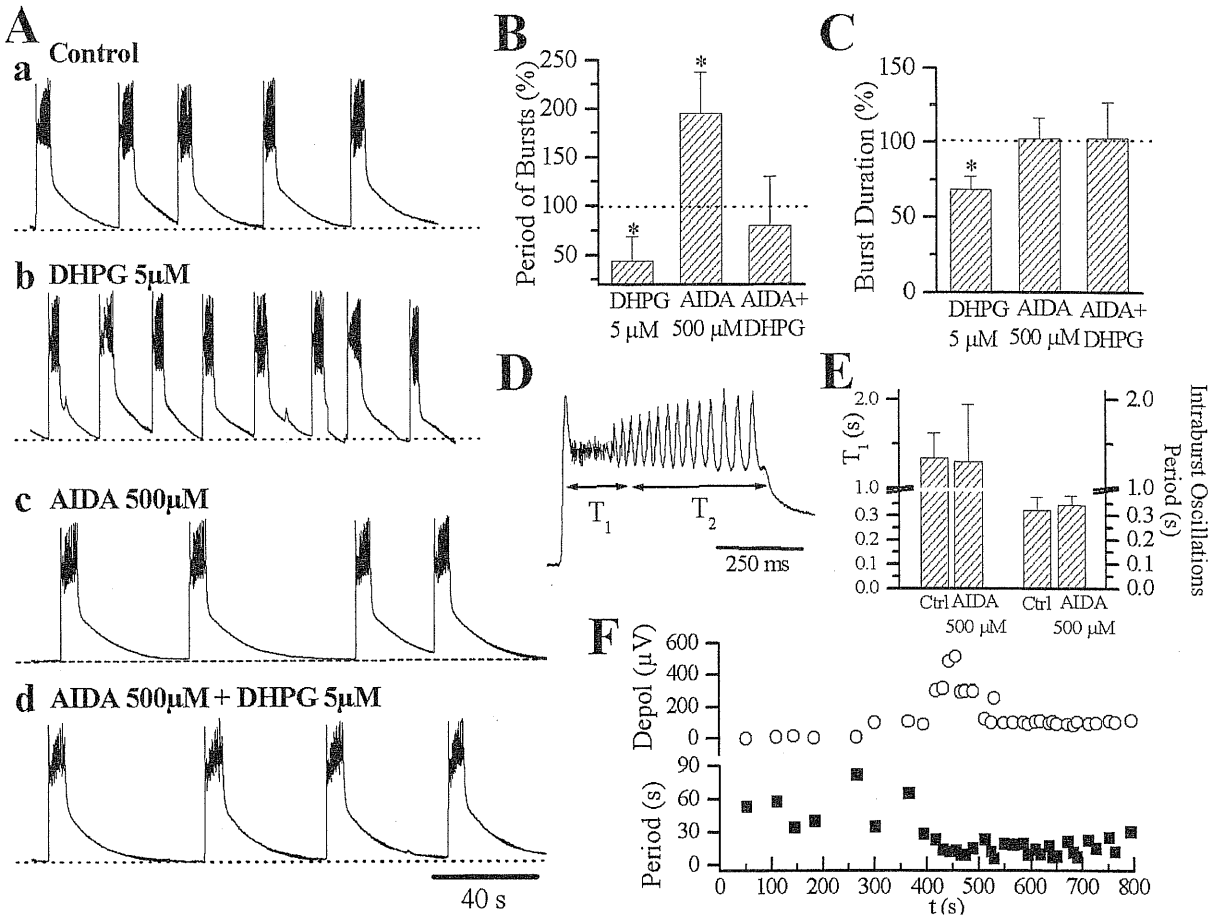

Figure 33. Action of the specific mGluRI agonist DHPG on disinhibited rhythm. A. a) Disinhibited rhythm recorded in control conditions; b) DHPG (5 μM) accelerates rhythm; c) DHPG induced acceleration is prevented AIDA application; d) AIDA *per se* does not significantly alter rhythm in terms of period and burst duration. . B. Average from pooled data for period of bursting. C. Average from pooled data for burst duration. D. Definition of parameters in a burst. E. Average from pooled data for T_1 and intraburst period calculated during the time interval T_2 for disinhibited rhythm in the presence of AIDA *vs.* control conditions. F. Example of time course of depolarization (measured extracellularly, μV) and of period of bursting for one preparation.

same behavior. These results indicate that gradual loss of depolarization occurred even when inhibitory transmission was blocked.

Endogenous role of mGluRI

To evaluate whether mGlu1 receptors were endogenously activated during disinhibited rhythm, AIDA (500 μM) was bath applied (Fig. 33A, bottom trace). In 11/16 preparations, period was almost doubled (195±140%, n=11), while in 5 other ones, period was unaltered. Furthermore, in the presence of AIDA, the DHPG induced acceleration was prevented (80±45%, n=5). As expected from the increase in burst frequency given by DHPG, duration

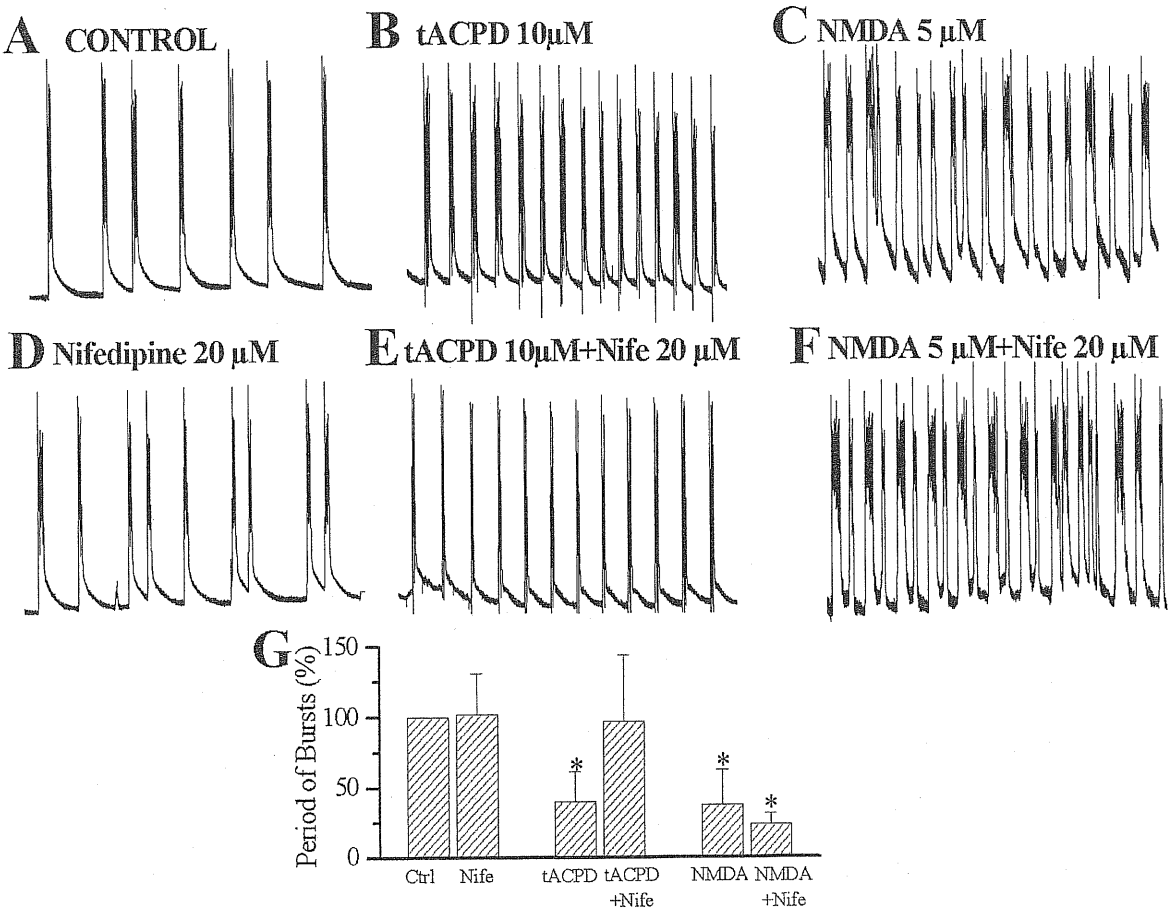

Figure 34. Involvement of L-type Ca^{2+} channels in disinhibited rhythm. A: Disinhibited rhythm recorded extracellularly in control conditions. Bath-application of t-ACPD (B) as well as of NMDA (C) accelerates rhythm. Nifedipine *per se* does not alter disinhibited rhythm (D), but slows down to control conditions t-ACPD accelerated rhythm, while not affecting NMDA accelerated rhythm, indicating specificity of effect. G. Average from pooled data for bursting period.

of bursts was also significantly shortened in these conditions (Fig. 33C). Finally, T_1, the time during a burst before oscillations appear (see Fig. 33D), and the period of intraburst oscillations were not significantly changed by AIDA (1290±650 ms *vs.* 1340±290 ms in control and 344±38 ms *vs.* 322±53 ms in control, n=14, p>0.05; Fig. 33E). These observations suggest that mGluR1 receptors could be activated to a significant extent by the release of endogenous glutamate occurring during each burst episode.

Involvement of L-type Ca^{2+} channels

mGluR activity can unmask the bistable properties of certain neurons in the spinal cord, leading to the generation of plateau potentials, through activation of L-type Ca^{2+} channels (Russo *et al.*, 1997; Svirskis & Hounsgaard, 1998; see INTRODUCTION § 5.2). Thus, we may

hypothesize that, if enough glutamate was released during disinhibited bursts to activate mGluRs (as is shown by the fact that AIDA slowed down the rhythm), these receptors might in turn activate plateau potentials, which could contribute to burst maintenance. We tested this hypothesis by blocking L-type Ca^{2+} channels with nifedipine. Experiments show that nifedipine (20 μM) did not *per se* alter bursting period (102±29%, n=7; Fig. 34A *vs.* 12D and G) or duration (not shown). Nevertheless, it brought back to control conditions the tACPD-accelerated disinhibited rhythm (97±47% vs. 40±20%, n=10; Fig. 34B *vs.* 12E and G). This effect was mGluR specific since, when rhythm was accelerated by a comparable amount (37±25%) by NMDA (5 μM), it was not slowed back down to control values by the same dose of nifedipine (23±8%, n=4; Fig. 34C *vs.* 12F and G). These results show that, during t-ACPD application to disinhibited rhythm, L-Type Ca^{2+} channels were activated.

4.4.2 Chemically induced fictive locomotion

The presence of mGluI receptors in the ventral horn of the spinal cord (Alvarez *et al.*, 2000), the importance of glutamate in fictive locomotion generation (Cazalets *et al.*, 1992; Beato *et al.*, 1997; Kiehn *et al.*, 1997), and the fact that DHPG was able to generate oscillatory activity (see § 4.1) prompted us to explore the role of mGluRs in fictive locomotion. Bath-application of DHPG to preparations exhibiting a stable, fictive locomotor pattern (Fig. 35A) induced a slow depolarization starting within the first minute of application (not shown). Within 5 minutes it also disrupted rhythm (Fig. 35B): in these conditions, although some locomotor cycles were still visible, they were much more sparse (Fig. 35B) and their amplitude reduced (78±14%, n=8, $p<0.05$; Fig. 35C). On the other hand, cycle period was not significantly different from control (100±10%, n=8; Fig. 35D) and phase alternation between homolateral and homosegmental VRs was maintained (Fig. 35B). Fast and slow oscillations typical of DHPG application were not detected during fictive locomotion.

We then investigated whether group I mGlu receptors might be endogenously activated during fictive locomotion. We found that while MPEP (100 μM) did not alter fictive locomotor patterns in terms of period (150±100%) and amplitude (83±13) of oscillations, AIDA (500 μM) increased period (112±8%, n=5) of oscillations by a small, yet significant, amount ($p<0.05$) (while also reducing the amplitude, 92±7%, n=5; Fig. 35C,D).

These results demonstrate that mGlu1 receptors were not strongly activated during fictive locomotion and certainly less so than during disinhibited rhythm, although exogenous application of DHPG could significantly affect both rhythms.

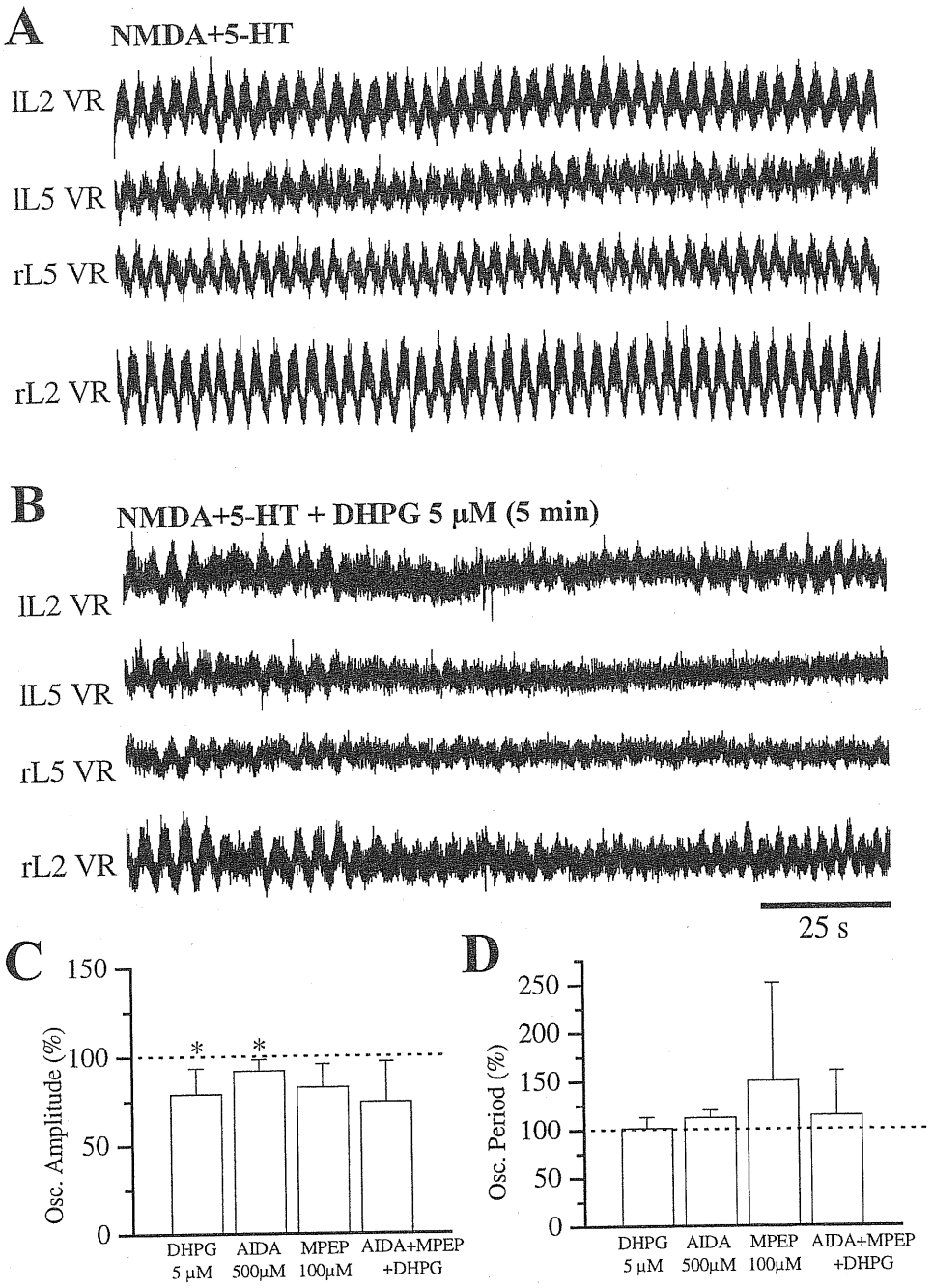

Figure 35. Role of group I mGluRs in fictive locomotion. A. Example of NMDA+5-HT induced fictive locomotor rhythm. B. Application of DHPG disrupts rhythm. C. Mean amplitude of oscillations during fictive locomotor rhythm, evoked in the presence of the group I mGluR agonist and antagonists (% with respect to control conditions). D. Mean period of oscillations during fictive locomotor rhythm, evoked in the presence of the group I mGluR agonist and antagonists (% with respect to control conditions).

4.5 Action of group II-III mGluRs on the spinal cord

In a parallel fashion, we investigated the action of group II and III mGluRs on the spinal cord. The respective agonists DCG-IV and L-AP4 did not *per se* elicit any activity. We therefore studied how their activation would affect certain pathways, such as the DR-VR reflex and the recurrent IPSP. Furthermore, their role in shaping disinhibited rhythm was explored.

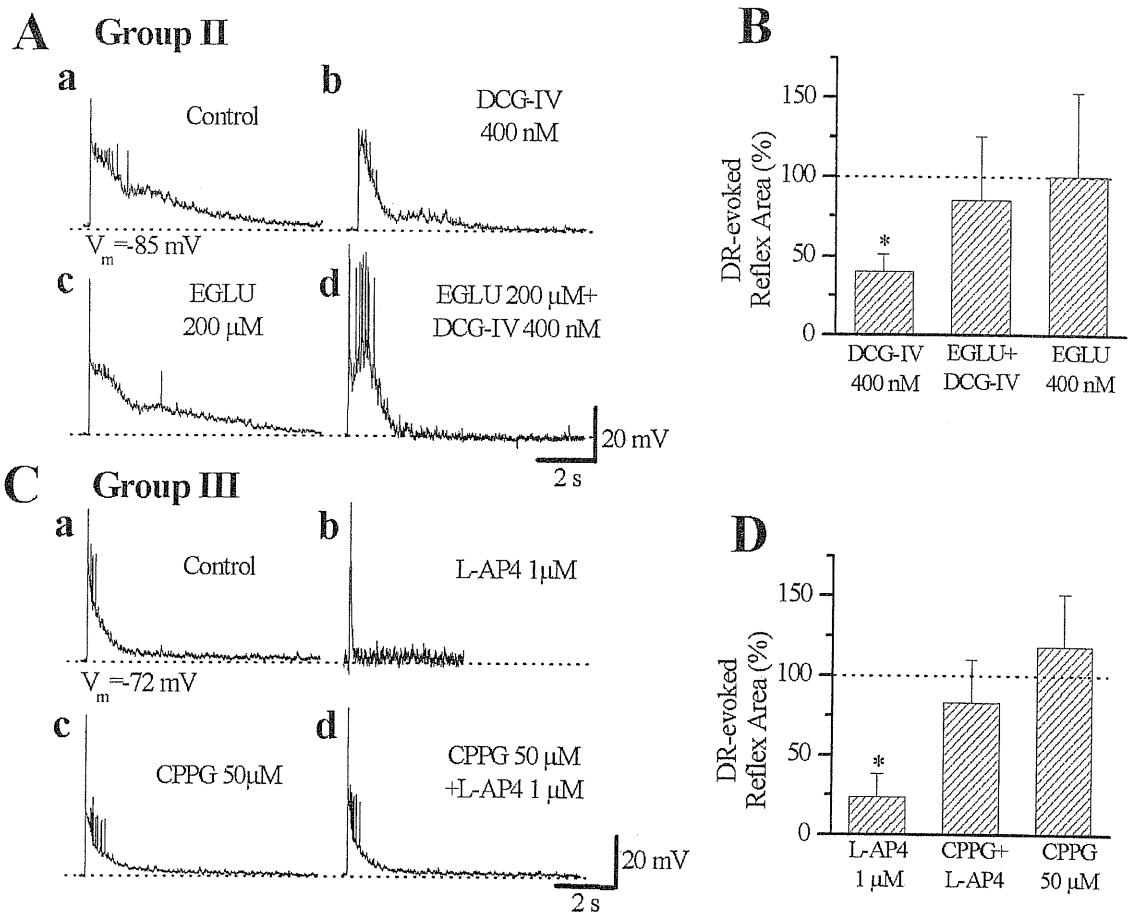

Figure 36. Action of group II and III mGluR on DR evoked responses A. Action of group II mGluR activation on DR evoked responses, recorded intracellularly, at the same membrane potential (V_m= -85 mV) and stimulus intensisty 3xTh: a) control; b) DCG-IV 400 nM depresses response; c) the group II antagonist EGLU (200 μM) does not significantly alter DR evoked response; d) EGLU prevents DCG-IV induced depression. B. Average from pooled data of DR evoked reflex area for group II agonist and antagonist. C. Action of group III mGluR activation on DR evoked responses, recorded intracellularly, at the same membrane potential (V_m= -72 mV) and stimulus intensisty 2xTh: a) control; b) L-AP4 depresses the response; c) the group III antagonist CPPG (50 μM) does not significantly alter the response; d) CPPG prevents L-AP4 induced depression. B. Average from pooled data of DR evoked reflex area for group III agonist and antagonist.

4.5.1 Action on DR evoked VR reflexes

mGluR-II action

The application of the mGluRII agonist DCG-IV depressed DR evoked responses, recorded from single motoneurons or from VRs. Fig. 36Aa,b shows the effect of DCG-IV (0.4 μM) on the potential recorded from a rL5 motoneuron when stimulating a rL5 dorsal root (4xTh stimulus intensity). On average, this depression was 40±10% (n=4, $p<0.05$; Fig. 36B) and was not dependent on stimulus intensity or DCG-IV concentration in the 0.2-2 μM range. While the mGluRII antagonist EGLU (200 μM) *per se* did not alter the response (Fig. 36Ac and B; 100±50%, n=10), it prevented DCG-IV induced depression (85±59%, n=5; Fig. 36A,d). On responses evoked by trains of DR stimuli, DCG-IV (up to 2 μM) did not show significant reduction, calculated both in terms of cumulative depolarization (92±6%, n=3) and number of oscillations (140±30%, n=3; Fig. 37A,C). On the other hand, responses to trains of DR stimuli evoked in the presence of the antagonist EGLU were significantly increased (area: 150±80%, n=6), indicating that group II metabotropic glutamate receptors are normally activated by trains of DR stimuli.

mGluR-III action

An even stronger depressant effect on the DR evoked response was elicited by the mGluR-III agonist L-AP4. Fig. 36Ca,b shows the depressant action (23%) on a rL4 motoneuron when the dorsal root was stimulated at the intensity of 6xTh. On average, L-AP4 (5 μM) depressed the response by 24±14% (Fig. 36D), an effect that was not dependent upon stimulus intensity and L-AP4 concentration (within the range 1-50μM). The mGluRIII antagonist CPPG (50 μM), while leaving unaltered the control response (118±33%, n=7), prevented L-AP4 dependent depression (84±26%, n=4).

Finally, L-AP4 also depressed responses to train of stimulation (Fig. 37B), by reducing significantly cumulative depolarization (50±10%, n=3), and almost completely abolishing oscillations (8±1%, n=3; Fig. 37C,D). On the other hand, the group III antagonist CPPG did not significantly alter responses to trains of DR stimuli (area 107±25%, n=4).

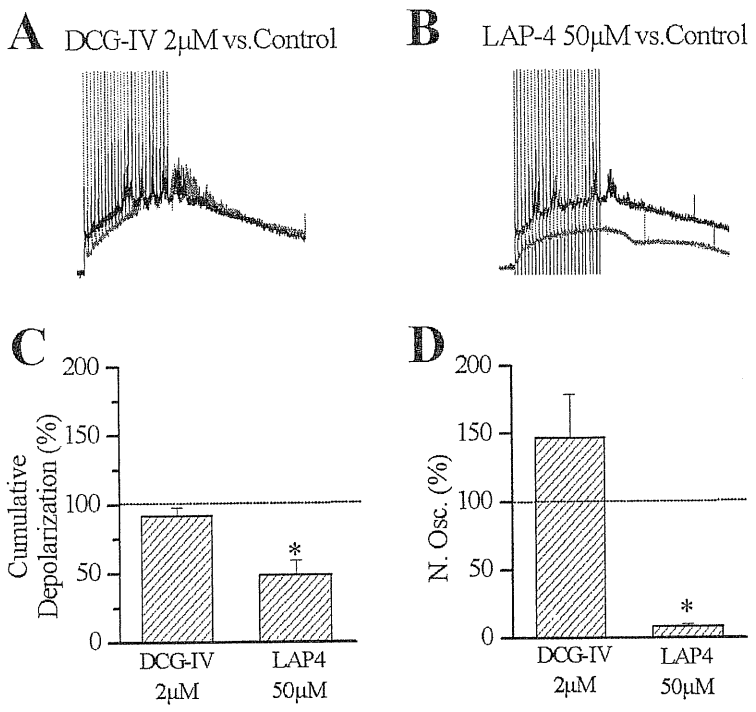

Figure 37. Action of group II and III mGluR agonists on responses to trains of DR stimuli. A. Example of responses to trains of DR stimuli (25 stimuli, 2 Hz, intensisty 3xTh) in control (black trace) and in the presence of DCG-IV (2 μM, gray trace). B. Example of responses to trains of DR stimuli (25 stimuli, 2 Hz, intensisty 3xTh) in control (black trace) and in the presence of L-AP4 (50 μM, gray trace). C. Average of cumulative depolarization for trains evoked in the presence of group II and III mGluR agonists. D. Average of number of oscillations for trains evoked in the presence of group II and III mGluR agonists.

4.5.2 Action of antagonists on IPSP

It has been reported that group II and III mGluR activation can depress GABAergic (van den Pol *et al.*, 1998; Semyanov & Kullmann, 2000; Doi *et al.*, 2002) or glycinergic (Katsurabayashi *et al.*, 2001) transmission. We therefore tested whether these receptors could play a role in modulating the recurrent IPSP on motoneurons. We found that the area of the IPSPs, measured in the presence of the mGluRII antagonist EGLU (200 μM), was 140±30% of control (n=5, paired t-test, $p>0.05$), with a small change in decay time (116±7%, paired t-test, $p<0.01$, n=5) and no significant changes in peak (104±6 %, n=5) and rise time (113±17%, n=5). On the contrary, CPPG (50 μM) did not cause any significant changes on

IPSPs in terms of area (116±26%, n=3), decay time (100±8%, n=5), peak (88±25%), and rise time (100±11%). These results show that mGluII-III receptors played little role in shaping the recurrent IPSP.

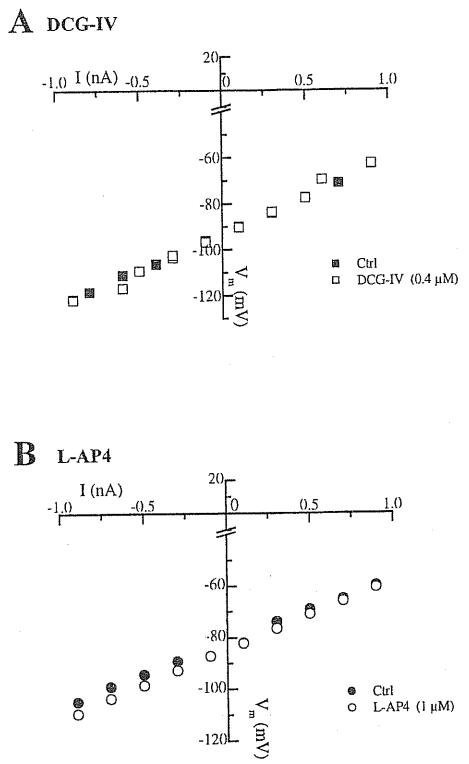

Figure 38. Voltage dependence of the response of motoneurons to DCG-IV or L-AP4. A. Example of current-voltage response curve for one cell in control conditions (filled symbols) and in the presence of the group II agonist DCG-IV (0.4 μM, hollow symbols). Linear fit gives no significant change in slope (25±11 MΩ in control *vs.* 27±12 MΩ, n=4; r>0.98 in all cases). B. Example of current-voltage response curve for one cell in control conditions (filled symbols) and in the presence of the group III agonist, L-AP4 (1 μM): in this case the slope was 18±10 MΩ vs. 19±10 MΩ (p>0.05; r>0.98 in all cases).

4.5.3 Voltage dependence

To investigate whether there was a voltage dependence of the response of motoneurons to DCG-IV or L-AP4, I-V curve tests were carried out by delivering current steps to motoneurons and recording the voltage response, in control conditions and in the presence of the mGluR agonists. Fig. 38A shows an example of I-V curve for one cell in control conditions (filled symbols) and in the presence of DCG-IV (0.4 μM, hollow symbols). There was no significant change in slope (25±11 MΩ in control *vs.* 27±12 MΩ, n=4; r>0.98 in all cases). Similar results are shown in Fig. 38B for the group III agonist, L-AP4 (1 μM): in this

case the slope was 18±10 MΩ vs. 19±10 MΩ (p>0.05; r>0.98 in all cases). Also in the case of IV curve tests performed in the presence of antagonists, no significant changes were observed (102±19% with 200 μM EGLU *vs.* control, n=4; 109±16% with 50 μM CPPG *vs.* control, n=4).

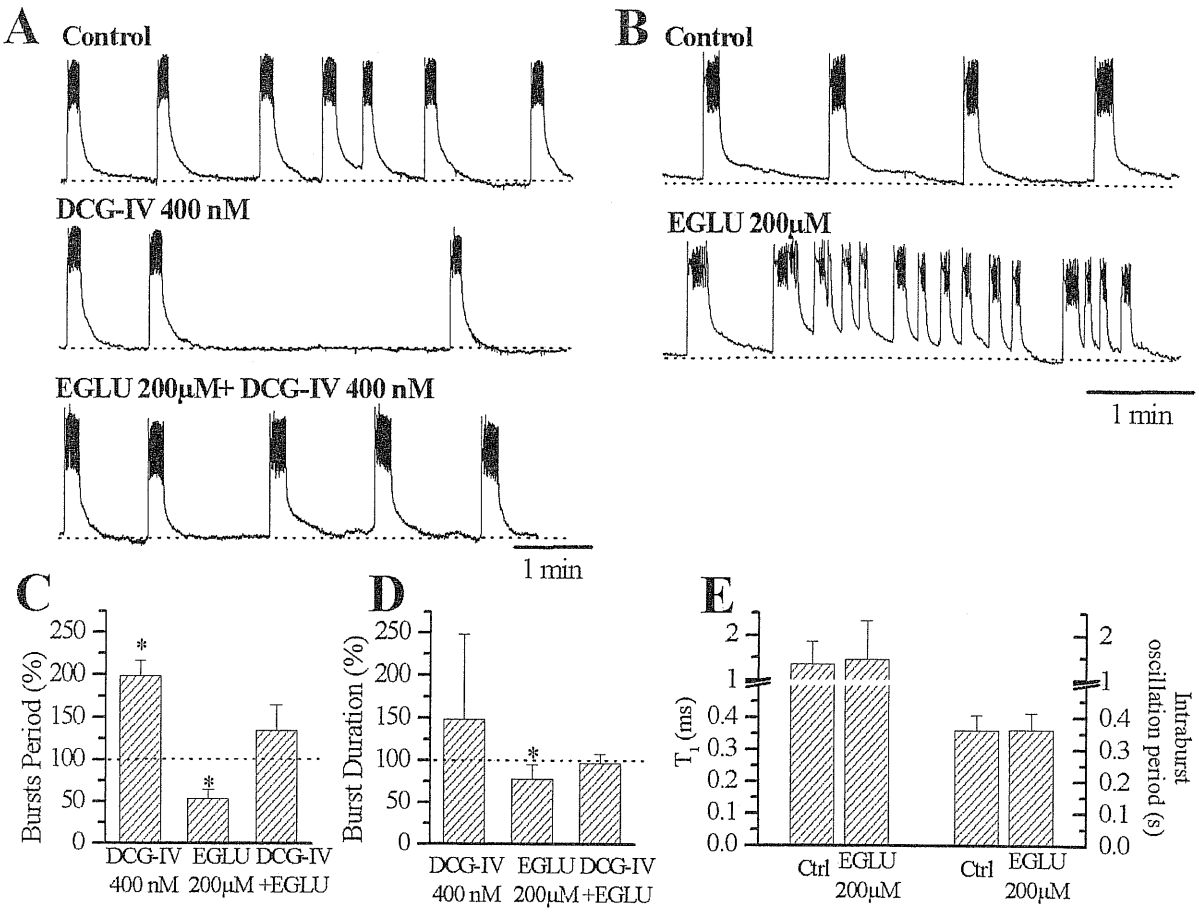

Figure 39. Group II mGluR activation modulates disinhibited rhythm. A. Effect of mGluII receptor activation in shaping disinhibited rhythm. DCG-IV (0.4 μM) slows down rhythm while no significant changes in burst duration are observed. EGLU prevents DCG-IV induced effect. B. Application of EGLU during disinhibited rhythm can accelerate bursting and decrease burst duration (different preparation from A). C. Average of bursts period during disinhibited rhythm in the presence of group II agonist and antagonist. D. Average of bursts duration during disinhibited rhythm in the presence of group II agonist and antagonist. E. Average of T_1 (see Fig. 33 for a definition) and of intraburst oscillation period in control conditions *vs.* EGLU.

4.5.4 mGluR II-III activation modulates disinhibited rhythm

We studied the role of mGluII-III receptors in shaping disinhibited rhythm. Activation of mGluII receptors by DCG-IV (0.4 μM) slowed down rhythm in 14 out of 20 preparations (Fig. 39A). On average, in these preparations, period was 200±40%, regardless of DCG-IV concentration (0.1-1 μM, n=14) while no significant changes in burst duration were observed

(Fig. 39C,D). On 6 other preparations, rhythm was abolished (0.1-0.4 μM). The effect was reversible with 10-15 minute washout. DCG-IV (0.4 μM)-induced slowing down of rhythm was prevented by application of EGLU (200 μM) in 5 out of 6 preparations (period 135±67%, n=5), while in 2/2 preparations EGLU (200 μM) did not prevent the effect of DCG-IV (1 μM). Furthermore, application of EGLU itself accelerated the rhythm in 5/8 preparations (period 54±27%, n=5; Fig. 39B,C). In those preparations where rhythm was accelerated by EGLU, the average burst duration was 78±17% of control (Fig. 39D). Furthermore, activation of mGluRII did not alter period of intraburst oscillations or T_1 (Fig. 39E, see § 4.4.1 and Fig. 33D, for a definition of T_1).

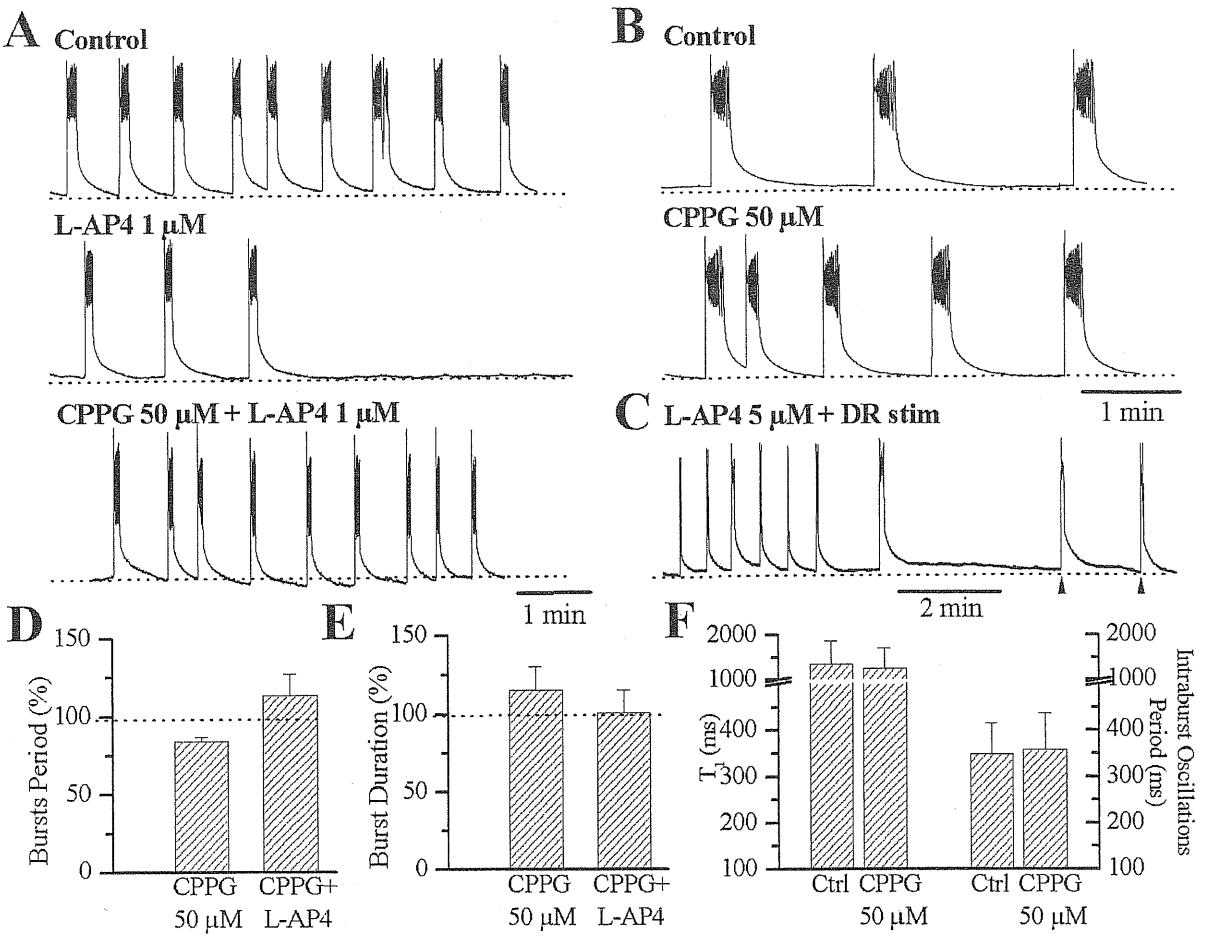

Figure 40. Group III mGluR activation modulates disinhibited rhythm. A. Effect of mGluIII receptor activation in shaping disinhibited rhythm. L-AP4 (1 μM) abolishes rhythm. CPPG (50 μM) prevents L-AP4 induced effect. B. Application of CPPG during disinhibited rhythm does not significantly alter bursting (different preparation from A). C. DR stimulation (indicated by the arrows) can trigger bursts during a period of silence induced by L-AP4. D. Average of bursts period during disinhibited rhythm in the presence of group III agonist and antagonist. E. Average of bursts duration during disinhibited rhythm in the presence of group III agonist and antagonist. F. Average of T_1 (see Fig. 33 for a definition) and of intraburst oscillation period in control conditions *vs.* EGLU.

The inhibitory effect of L-AP4 was apparently much stronger. In fact, in 9/10 preparations, rhythm was completely abolished (Fig. 40A). The dependence of the effect upon L-AP4 concentration was such that the shortest times needed to abolish rhythm were observed at 20-50 μM (2-3 minutes) while longest ones (5-10 minutes) were at 1 μM, although the dependence of effect latency upon concentration was not strict. The effect of L-AP4 was washed out in 10-15 minutes. Even when rhythm was abolished, bursts could be evoked by DR stimulation as shown in Fig. 40C: in this example, regular rhythm was abolished by L-AP4 within 2 minutes of application. After 4 minutes from the start of the last burst, a stimulus delivered to a DR evoked a burst (indicated by the black arrow, artifact of stimulation not shown due to sampling interval). Bursting could be evoked again after 1.5 minutes. The effect of L-AP4 was prevented by previous application of CPPG (Fig. 40A, bottom trace). In general, doses of L-AP4 lower than 50 μM were antagonized by 50 μM CPPG (average period 113±24%, n=6; Fig. 40A,D), while in 4/4 preparations 50 μM L-AP4 abolished rhythm even in the presence of CPPG (50 μM-200 μM).

Application of the antagonist CPPG (50-200 μM) on disinhibited rhythm accelerated bursting in 4 preparations (period 84±7%, n=4, Fig. 40B), slowed down rhythm in 2 (128±13%), and had no effect in one other case. Burst duration, T_1 and period of intraburst oscillations did not change significantly (Fig. 40E,F).

These results show that mGluII receptors partly contributed to the disinhibited rhythm and were presumably activated by endogenous glutamate during such bursts to limit burst frequency. The ability by endogenous glutamate to activate mGluIII receptors appears to be more limited and variable. Pharmacological activation of group II or III receptors was however a powerful tool to suppress bursting.

As the amount of glutamate released during bursts is probably far in excess of the one liberated during fictive locomotor patterns, the effects of those antagonists on fictive locomotion was not explored.

DISCUSSION

1. Fictive Locomotor Patterns Can Be Evoked by Dorsal Root Stimulation

The principal finding of the first part of the present study is the observation that in the neonatal rat spinal cord *in vitro* locomotor-like patterns of activity can be reliably evoked by trains of DR stimuli. This is a novel result as DR stimulation has only been reported to reset (Iizuka *et al.*, 1997) or partially entrain (Sqalli-Houssaini *et al.*, 1993) the locomotor rhythm induced by bath application of chemical substances. At the time of the publication of these results, Whelan *et al.* (Whelan *et al.*, 2000) have also shown that DR stimulation can induce alternating patterns in the neonatal mouse spinal cord. The present data thus suggest that stimulation of sensory afferent fibers can induce fictive locomotor like patterns in the neonatal rat spinal cord.

1.1 General characteristics of rhythmic activity induced by DR stimuli

A variety of stimulation protocols was used to induce patterns of rhythmic activity which were recorded from two pairs of contralateral VRs (usually L2 or L3 and L5). Such a rhythmic activity showed not only phase alternation between pairs of contralateral VRs, but also intersegmental phase alternation between VRs innervating mainly flexor and extensor muscles (L2/3 and L5, respectively). Oscillations had a period ranging from 1 to 2 s and thus were not time-locked with DR stimuli. These period properties are consistent with those of fictive locomotion induced in the neonatal spinal cord *in vitro* by bath application of agents such as NMDA (T=0.24-6.25 s, Kudo & Yamada, 1987), serotonin (T=1-4 s, Cazalets *et al.*, 1992; T=1.8-2.5 s, Beato *et al.*, 1997), or high potassium (T=0.8-2.3 s, Bracci *et al.*, 1998) and confirmed in the present study with application of NMDA plus serotonin (T=1.39±0.21 s). Furthermore, the oscillatory activity induced by DR stimulation presented the typical phase alternation at segmental and intersegmental level which is a hallmark of fictive locomotion evoked by chemical substances (Kiehn *et al.*, 1997). It is widely accepted that

these substances activate the mammalian spinal CPG responsible for driving the rhythmic firing of motoneurons (reviewed by Kiehn *et al.*, 1997). Also in our case, the oscillatory activity of motoneurons was likely to be driven by the CPG and could be regarded as a locomotor-like pattern turned on by the activation of dorsal afferents which are known to project to the CPG itself (Hultborn *et al.*, 1998).

Even relatively weak DR stimuli (1.3xTh) were very effective to induce locomotor-like patterns. Electrical pulses below 1.6xTh activated fast conducting, low threshold afferents while stronger stimuli also recruited high threshold DR fibres. Since low and high threshold afferents are expected to carry distinct sensory information, the possibility of activating the locomotor CPG even with rather low stimuli suggests that discrete inputs carried by a restricted class of sensory axons are sufficient to trigger the operation of the CPG. This condition might thus be a model to investigate in future how physiological stimuli activate and interact with the CPG. It seems that such a model would also be experimentally advantageous over the indiscriminate activation of the vast majority of spinal neurons by bath-applied substances.

1.2 How long can fictive locomotor-like patterns last?

Unlike the persistent and stable fictive locomotor pattern elicited by chemicals (Kiehn *et al.*, 1997), the DR induced one was usually transient. With a long stimulus train the oscillatory pattern waned despite persistent motoneuronal depolarization, unimpaired firing and unhindered polysynaptic reflex. When the stimulus applied to a heterosegmental root was initially weak so as to activate primarily low threshold DR fibres, it was possible to reinstate the pattern by recruiting an additional class of higher threshold fibres within the same root. Even in the latter case the pattern faded but it could be transiently rescued by weakly stimulating the contralateral DR.

The cause for the disappearance of the rhythmic pattern remains uncertain. Lack of depression of DR volleys (with stimulation protocols comparable to those used to elicit locomotor-like patterns) indicated that afferent stimuli probably continued to reach the spinal tissue. The persistence of VR reflexes equally suggests that the motoneuronal output remained operative. Synaptic fatigue, if it had played any significant role in this phenomenon, should thus have been confined to interneurons impinging upon the CPG or to CPG interneurons themselves.

CPG interneurons of the rat spinal cord can generate long episodes of locomotor-like rhythmic activity and are thus not particularly prone to fatigue. If their fatigue had been due to any excessively strong activation by afferent stimuli, it should have been possible, through fine tuning of the stimulus characteristics, to obtain a condition of stable DR-induced rhythm. This goal could not be attained by the present study despite extensive tests. This observation suggests that loss of rhythmicity was due to either fatigue in the pathway upstream of the CPG (as indeed observed with afferent impulses in the presence of strychnine and bicuculline; Bracci *et al.*, 1997) or stimulus-patterned release of some transmitters which inhibited the CPG operation. The first possibility seems more likely as recruitment of additional pathways either homolaterally (by increasing the stimulus strength) or contralaterally was temporarily sufficient to restore the oscillatory activity. Models to simulate rhythmic oscillations generated by chick embryo spinal neurons have recently been proposed to account for the episodic nature of cyclic oscillations which is thought to be due to either activation of a slow process (for example, gradual turning on of a persistent conductance or some metabolic process) or to build-up of synaptic fatigue (Tabak *et al.*, 2000). It will be interesting to apply these models to the fictive locomotor-like patterns induced by DR stimuli in the rat spinal cord.

1.3 Generation of locomotor-like patterns by DR stimuli

One hypothesis we tested is that raised $[K^+]_o$ played an important role in the activation of the CPG. In the neonatal spinal cord, in fact, single and repetitive stimuli elicit K^+ transients (Walton & Chesler, 1988) large enough to influence neuronal excitability. Moreover, phasic variations of $[K^+]_o$ have been reported to occur during fictive swimming recorded from the lamprey spinal cord *in vitro* (Wallen *et al.*, 1984). Finally, application of high $[K^+]_o$, within a certain range of concentrations, is known to induce fictive locomotion in the rat spinal cord (Bracci *et al.*, 1998). One way to test our hypothesis would have been to measure $[K^+]_o$ variations with K^+-sensitive electrodes inserted within the ventral horn where the CPG is supposed to be located (Kiehn & Kjaerulff, 1996). However, in an intact spinal cord preparation, final placement of the K^+-sensitive electrode would be blind, a fact that would make it very difficult to identify any response as due to the activity of CPG neurones which are thought to be present in various laminae (Kjaerulff *et al.*, 1994). Insertion of a K^+-sensitive electrode into the spinal cord is also known to cause local injury with consequent rise in $[K^+]_o$ (Krnjevic & Morris, 1974). Since "the interneuronal systems related to the

activity of a VR during locomotion are localized in close proximity to the motoneurons projecting in that VR" (Tresch & Kiehn, 1999), as a first approximation to investigate if there had been any $[K^+]_o$ build up, we used the AHP amplitude of motoneuron antidromic spikes as a less invasive $[K^+]_o$ sensor. The AHP method has long been used to measure $[K^+]_o$ changes (Baylor & Nicholls, 1969) and is applicable to rat spinal motoneurons as well (Forsythe & Redman, 1988).

VR stimulation is known to induce a recurrent IPSP in motoneurons due to activation of glycine and GABA receptors (Cullheim & Kellerth, 1981; Schneider & Fyffe, 1992). In the present study glycine receptors were blocked by strychine while GABA receptors were not pharmacologically inhibited by bicuculline as the combined application of these two antagonists generates strong, spontaneous rhythmic activity (Bracci *et al.*, 1996a) readily entrained by DR stimuli (Bracci *et al.*, 1997). Nevertheless, the GABAergic component of the recurrent IPSP develops with quite a delayed timecourse so as its contamination of the AHP (which is typically faster) is unlikely (Cullheim & Kellerth, 1981; Schneider & Fyffe, 1992). The use of strychnine eliminated rhythm alternation, thus depriving the locomotor-like rhythm of one of its main properties. Nevertheless, in each preparation we first tested the ability of the stimulation protocol to induce typical locomotor-like patterns before repeating it in the presence of strychnine. Furthermore, by monitoring changes in the IS size in the presence or in the absence of strychnine, we found no evidence for a large shunt in motoneuronal membrane due to strychnine-induced rise in spinal excitability. It should however be borne in mind that, because of raised network excitability, the calculated $[K^+]_o$ might be overestimated.

We first established that there was a linear relation between AHP amplitude and $[K^+]_o$. To extend the applicability of this finding to tests carried out during the DR stimulation we had to investigate potential sources of error. A major concern was the possibility that intense transmitter release shunted the motoneuronal membrane and thus attenuated the AHP size, regardless of any substantial change in $[K^+]_o$. This possibility was regarded unlikely for four reasons: 1) no concomitant reduction in spike amplitude; 2) no associated reduction in the amplitude of the IS; 3) no difference in baseline input resistance in control conditions *versus* DR stimulation; 4) no difference in resting resistance of motoneurons in control or during high K^+-induced locomotor-like patterns. Taken together these observations concur to suggest that a significant motoneuronal shunt did not limit the AHP measurement.

The leak conductance of motoneurons at rest is quite different from that of resting interneurones and includes a much smaller contribution by background network synaptic activity. In fact, applying tetrodotoxin to eliminate network mediated responses, reduces the leak of interneurones by about 1/3rd (Raastad *et al.*, 1998) while a similar treatment lowers the leak conductance of neonatal rat motoneurons by 17 % only (Fisher & Nistri, 1993a). Furthermore, the largest synaptic conductance changes recorded from spinal interneurones during fictive locomotion are predominantly due to inhibitory synapses (Raastad *et al.*, 1998) which in the present experiments were at least in part blocked by strychnine. Lack of detectable shunt in motoneurons in the present investigation might be due to the dendritic location of their excitatory synapses (Iansek & Redman, 1973) which makes excitatory synaptic potentials notoriously difficult to reverse with current injection (Flatman *et al.*, 1982). On the motoneuronal soma, a major conductance is activated by exogenously applied or locally-released glycine (unlike GABA; see Curtis & Johnston, 1974), which in the present study was blocked by strychnine.

While our data made unlikely a major shunt in cell conductance to account for the AHP depression, it was also necessary to exclude an AHP conductance block due to endogenous transmitters like serotonin (Berger *et al.*, 1992; Larkman & Kelly, 1998). This possibility was also unlikely because the fractional input resistance fall during the AHP was very similar in baseline conditions or after DR stimuli. Since in the isolated spinal cord the main serotoninergic descending inputs are severed, Schmidt (Schmidt, 1994) also concluded that endogenous release of serotonin had no role in modulating the AHP. Our own experiments on the locomotor rhythm of the isolated spinal cord show that serotonin receptor antagonists have minimal role in inhibiting the oscillations generated by NMDA or high K^+, implying that release of endogenous serotonin does not largely contribute to this phenomenon (Beato & Nistri, 1998; Bracci *et al.*, 1998).

Since the AHP in the presence of (or immediately after) DR stimuli was smaller than in control for equivalent membrane potential level, we concluded that the change in AHP amplitude was attributable to a change in the $[K^+]_o$ estimated to amount to 7.9±0.4 mM, a concentration able to induce fictive locomotion (Bracci *et al.*, 1998).

The question then arises whether the higher $[K^+]_o$ during DR-induced activity was an important manifestation of locomotor-like oscillations or a mere epiphenomenon of any enhancement in spinal electrical activity. The latter possibility is made unlikely by the data based on application of NMDA or K^+. In the rat spinal cord NMDA induces fictive locomotor

patterns associated with a clear reduction in AHP of motoneurons (Schmidt, 1994). In the present experiments concentrations of NMDA, subthreshold for inducing rhythmic oscillations but effective in depolarizing motoneurons, elicited a relatively weak depression of the AHP and a calculated small rise in $[K^+]_o$, outside the range known to trigger locomotor patterns (Bracci *et al.*, 1998). Similar observations were obtained by raising the standard $[K^+]_o$ (4.5 mM) to 5.5 mM, a concentration below threshold for inducing locomotor-like patterns (Bracci *et al.*, 1998).

1.4 Raised $[K^+]_o$: cause or consequence of locomotor-like rhythms?

While the present data are consistent with the hypothesis that DR stimuli induced an increase in $[K^+]_o$ during a locomotor-like rhythm, they could not resolve how raised $[K^+]_o$ might have caused this phenomenon. It seems likely that rhythmogenesis was caused by enhanced release of excitatory transmitters from spinal neurones activated by DR fibre stimulation. If this electrical activation was temporally restricted, like in the case of single pulses which were rarely sufficient to trigger fictive locomotion, no oscillatory activity resulted. Repetitive stimulation presumably caused persistent neuronal depolarization and high $[K^+]_o$ levels which in turn (through membrane depolarization and facilitation of transmitter release) recruited a larger population of cells up to threshold for locomotor-like electrical behaviour. The relation between build-up of $[K^+]_o$ and periodicity of locomotor-like rhythms was not investigated in view of the presence of strychnine. However, the weak dependence of locomotor-like oscillations on stimulus intensity and their lack of dependence on stimulus frequency indicate that there is strong non-linearity of the input/output operation of the CPG network. This situation might be reflected in the narrow range of high $[K^+]_o$ effective to generate oscillations (Bracci *et al.*, 1998) and the equally narrow range of $[K^+]_o$ estimated in the present study. It is likely that the strong local buffering of $[K^+]_o$ by mammalian spinal cord tissue during repetitive stimulation of primary afferents (Krnjevic & Morris, 1974; Krnjevic & Morris, 1975) contributed to this limited spectrum of $[K^+]_o$ variability.

2. Glycine or GABA on Newborn Rat Motoneurons: Depolarizing But Inhibiting

In this part of the study, we demonstrated that spinal motoneurons from neonatal rats were consistently inhibited by glycine or GABA despite the associated depolarization of membrane potential which should have brought these cells closer to firing threshold.

2.1 The action of glycine and GABA mediated synaptic potentials on spinal motoneurons

Previous studies of the action of glycine or GABA on embryonic or postnatal motoneurons have clearly shown that these transmitters mediate responses due to a large rise in Cl^- permeability (Gao & Ziskind-Conhaim, 1995; Singer & Berger, 2000). The immaturity of the Cl^- transport system presumably allows an elevated intracellular Cl^- concentration to build up with consequent Cl^- efflux (and depolarization) whenever Cl^- channels are opened by glycine or GABA. It is however noteworthy that most studies on spinal motoneurons had so far investigated the action of exogenously applied GABA or glycine.

Under our recording conditions, which attempted to minimize disturbance to intracellular Cl^- levels by filling sharp electrodes with the relatively impermeant sulphate ion (Eccles, 1957), we found that the recurrent postsynaptic potential (PSP) induced by antidromic stimuli was always depolarizing at resting membrane potential. The PSP, recorded from motoneurons after VR stimulation, was poorly sensitive to the glutamate receptor blocker kynurenic acid. Thus, under our experimental conditions, the PSP was minimally contaminated by the activation of the few glutamatergic afferent fibers contained within the VR and reputed to make direct synaptic contacts with the motoneuron soma as evidenced by their short latency (Jiang *et al.*, 1991).

The main transmitters of the recurrent PSP are believed to be glycine (for the early component; Werman *et al.*, 1968) and GABA (for the late component; Larson, 1969; Polc & Haefely, 1982; Schneider & Fyffe, 1992). In support of such studies, we found that the residual PSP after pharmacological block of $GABA_A$ receptors was larger than the one after glycine receptor antagonism, thus confirming that glycine was the principal transmitter of this PSP.

The present study focussed on examining how glycine or GABA, released to evoke the recurrent PSP, might interfere with the EPSPs in a preparation retaining its physiological

network intact. To investigate how excitatory inputs might be reduced by GABA or glycine mediated transmission, we used polysynaptic EPSPs (induced by DR stimulation) with relatively slow onset and offset, owing to summation of disparate excitatory signals generated at dendritic and somatic level of motoneurons. In this way the chance of detecting synaptic inhibition should have been higher as it was not dependent on a strict spatial coincidence of excitatory and inhibitory potentials.

It is clear that mammalian motoneurons, even at this early postnatal stage, usually exhibit strong acceleration of spike firing frequency whenever their somatic membrane is gradually depolarized (Viana *et al.*, 1995; Lape & Nistri, 2000). Likewise, depolarizing synaptic potentials might normally be expected to add up to enhance overall motoneuron excitability. This is actually a well-known phenomenon which enables summation of EPSPs to take motoneurons to firing threshold for spike generation (Eccles, 1957). Nevertheless, in the present experiments, when the recurrent PSP preceded the polysynaptic EPSP, the observed response was significantly smaller than the sum of the individual ones, indicating occlusion. Indeed, after subtracting the control recurrent PSP from the combined response, it was clear that the EPSP was significantly depressed. Thus, synaptic inhibition appeared to take place despite the depolarizing nature of both the EPSP and the recurrent PSP. It seems unlikely that the recurrent PSP might have indirectly depressed the EPSP via presynaptic inhibition for two reasons: 1) the main neurotransmitter of this PSP was glycine, which is not the transmitter of presynaptic inhibition (Eccles *et al.*, 1963), and 2) single stimuli are thought to be unable to release sufficient GABA spillover to activate GABA receptors (including $GABA_B$ ones) on primary afferent terminals (Rekling *et al.*, 2000).

Our conclusions were strengthened by experiments performed in parallel on neonatal rat hypoglossal motoneurons. In these neurons, GABA and glycine are important neurotransmitters, acting on Cl^- mediated conductances ($GABA_A$ and strychnine sensitive receptors, respectively; O'Brien & Berger, 1999; Donato & Nistri, 2000). Neonatal rat hypoglossal motoneurons were also inhibited by synaptically released or exogenously applied GABA or glycine. Obtaining similar conclusions by using two different types of neonatal motoneuron further indicated that the inhibitory function of GABA or glycine was not restricted to a particular region of the central nervous system and that there was no appreciable regional difference in GABA or glycine receptor function on motoneurons.

2.2 Factors responsible for GABA (or glycine) mediated inhibition or excitation of neonatal neurons

It might be of interest to examine why opposite functional effects of GABA are reported, for example, on hippocampal (and hypothalamic) neurons and motoneurons at the same developmental age and with similar resting potential value. The reversal potential for GABA is about –50 mV for hippocampal pyramidal cells (Ben Ari *et al.*, 1989), and about –40 mV for hypothalamic neurons (Chen *et al.*, 1996), both cell types apparently excited by GABA. These values are, however, similar to the Cl^- reversal potential of hypoglossal (Singer *et al.*, 1998) or spinal (Wu *et al.*, 1992) motoneurons and consistently positive with respect to the spike threshold. These data therefore suggest that the driving force for GABA or glycine mediated responses is comparable for different neurons and not responsible for the fact that these amino acids can be excitatory on some cells rather than others.

Another possibility is that, despite membrane depolarization, GABA inhibits certain neurons by shunting their membrane resistance (via a large increase in Cl^- permeability) to make them less responsive to excitatory signals. The single channel conductance of neonatal $GABA_A$ receptors is not dissimilar between distinct neuronal populations (mouse spinal neurons in culture: 15-28 pS, Bormann *et al.*, 1987; MacDonald *et al.*, 1989; neonatal hippocampus: 24-35 pS, Hosokawa *et al.*, 1994). Although the $GABA_A$ single channel conductance of neonatal hypoglossal motoneurons is unknown, the one for glycine (which inhibits, like GABA, via Cl^- permeability increase) is 30 pS (Singer *et al.*, 1998), that is near the data reported for GABA on other neurons.

Despite relatively similar values of reversal potential and of single channel conductance, membrane conductance during transmitter activity also depends on channel number and/or opening probability (see Nistri & Gutman, 2001) which, if differentially expressed by certain neurons, could then generate opposite functional effects of GABA (or glycine). A further factor contributing to the functional diversity of GABA (or glycine) action might be the varying distribution of their receptors with respect to the source of excitatory synaptic potentials or the site of spike generation. Even in the neonatal hippocampus a recent report describes the effect of GABA (via $GABA_A$ receptors) as inhibitory (Lamsa *et al.*, 2000) in contrast with previous studies (Ben Ari *et al.*, 1989). Perhaps the variable location of $GABA_A$ receptors might indeed be responsible for its contrasting effects even on the same hippocampal cell type. Alternatively, at least for the hippocampus, GABA-mediated excitation might require activation of a distinct membrane receptor class ($GABA_C$ receptor;

Martina *et al.*, 1995; Bormann, 2000). It is noteworthy that, in the P3-P8 neonatal rat spinal cord, motoneurons possess very low $GABA_C$ receptor activity (Rozzo *et al.*, 1999).

3. Neuronal Bursting Induced by NK_3 Receptor Activation

One main finding of the present study was the persistent oscillatory activity induced by NK_3 receptors in the neonatal rat spinal cord *in vitro*. In the majority of preparations, oscillations were alternating between left and right homosegmental motor pools but synchronous between different segments on the same side. This novel pattern thus differs from the fully alternating fictive locomotor rhythm or the fully synchronous discharges evoked by block of synaptic inhibition. Despite washout of the NK_3 agonist, delayed bursts with superimposed fast oscillations emerged in coincidence with weakening of GABAergic transmission and of recurrent IPSPs of motoneurons.

3.1 Distribution and action of NK_3 receptors in the rat spinal cord

Tachykinin receptors comprise a heterogeneous family of G-protein coupled receptors (Regoli *et al.*, 1994) mainly concentrated to the deep laminae of the spinal dorsal horn. Nevertheless, recent studies of NK_3 receptors have indicated their widespread distribution in central and ventral areas of the spinal gray matter (Beresford *et al.*, 1992; Linden *et al.*, 2000; Mileusnic *et al.*, 1999; Seybold *et al.*, 1997). Interestingly, ultrastructural investigations have shown NK_3 receptors of the rat spinal cord to be closely associated with glomeruli of dendritic spines, making those receptors potentially capable of influencing synaptic transmission (Zerari *et al.*, 1997).

While the precise mechanism of action mediating NK_3 receptor activity remains unclear, it seems probable that they operate on neonatal rat spinal neurons in a fashion similar to other tachykinin receptors, namely depression of a leak K^+ conductance (Fisher & Nistri, 1993b) or of a Ca^{2+} dependent K^+ conductance (Phenna *et al.*, 1996) or activation of non-selective cationic channels (Inoue *et al.*, 1995). Because intracellular recording from QX-314 injected motoneurons indicated no resistance change during application of senktide, this result suggests that senktide depolarizations were generated either remotely from motoneurons or were due to concurrent activation and depression of motoneuron intrinsic conductances. As

TTX eliminates motoneuron responses to NK_3 receptor agonists, the second possibility seems most unlikely (Fisher *et al.*, 1994).

The sparse location of NK_3 receptors implies activation of interneurons widely distributed within the spinal cord, a condition which makes difficult to unravel the mechanism of action of such receptors merely through bath application of pharmacological substances known to activate or block intracellular second messengers or ion channels. Indeed, the bath superfusion method used for NK_3 agonists in the present study included widespread distribution of these substances rather than their discrete application to selected regions (see INTRODUCTION § 3.2.2). Further work aimed at clarifying the precise mechanisms responsible for the action of senktide should perhaps be based on simplified network preparations like organotypic slice cultures with focal drug application.

3.2 Oscillations and bursting due to NK_3 receptor activation

Although electrophysiological studies of NK_3 receptor activity at cellular level in the spinal cord are sparse, our laboratory briefly noted that NK_3 agonists surprisingly elicited tetrodotoxin-sensitive bursting activity much more intense than that observed with activation of other tachykinin receptors (Barbieri & Nistri, 2001; Fisher *et al.*, 1994). The present study examined in more detail the rhythmic activity induced by NK_3 receptors. The NK_3 agonists senktide or [MePhe7]neurokinin B evoked a slow depolarization comprising oscillations with relatively fast period and with phase alternation at segmental level but lacking, in most cases, synchronicity between L2 and L5 motor pools of the same side. In a minority of preparations oscillations displayed the fully alternating pattern typically observed during fictive locomotion evoked by excitatory agents like NMDA and 5-HT. Even if oscillations often disappeared near the end of agonist application (see for example Fig. 1 A), the washout phase was accompanied by the emergence of late bursts with a complex oscillatory structure.

3.3 Factors controlling oscillations and delayed bursting

The senktide-evoked responses recorded from motoneurons or VRs were network based phenomena as they are known to be suppressed by TTX (Fisher *et al.*, 1994) and their periodicity was independent from motoneuron membrane potential. Detailed investigation into the nature of oscillations and bursting was limited by a major experimental difficulty, namely the desensitization of NK_3 receptors that develops rapidly and prevents, for ≥ 30 min, responses to further agonist application (Barbieri & Nistri, 2001). The mechanism

responsible for desensitization is not fully understood but, in the case of the endogenous ligand, namely substance P, it is known to involve rapid internalization of membrane NK_1 receptors (75 % of receptors can be internalized within 8 min) with consequent loss of neuronal responsiveness for extended time (Honoré *et al.*, 1999). Return of responses to tachykinins thus implies receptor trafficking to the neuronal membrane, an inherently slow phenomenon. These findings also indicate that it was unlikely that the delayed bursting emerging after senktide washout, was caused by differential redistribution of this agent between superficial and deep layers of the spinal cord, because virtually all cells should have been desensitized by long-lasting application of a saturating concentration of senktide. Further evidence shows that delayed bursting did not involve sustained occupation and activation of NK_3 receptors in the spinal cord. In fact, the NK_3 antagonist SR 142801 did not block late bursting which required intact glutamatergic transmission at network level as indicated by its full suppression by CNQX and APV. Further studies should address the issue of whether AMPA or NMDA receptor activity is preferential to support late bursting.

The ability of the neonatal spinal cord to generate persistent bursting after senktide washout suggests that the excitability of the spinal network remained elevated long after the agonist had been removed and when the NK_3 receptors were still desensitized. Such an upregulation of excitability, downstream of receptor occupancy, is certainly a novel phenomenon for the neonatal rat spinal cord. Nevertheless, it has been reported that hippocampal neurons after washing out metabotropic glutamate receptor agonists (Aniksztejn *et al.*, 1995) or muscarinic receptor agonists (Chapman & Lacaille, 1999; Kouznetsova & Nistri, 2000) generate sustained rhythmic discharges. It is worth noting that, in the hippocampus, persistent spontaneous discharges are typical of immature postnatal neurons as they do not appear on adult cells and are proposed to be due to a particular homeostasis of intracellular free Ca^{2+} (Aniksztejn *et al.*, 1995).

Despite the experimental constraints of the present study, it is possible to outline some general characteristics of oscillations and late bursting. Even though oscillations could first emerge during depolarization, they were indistinguishable from those present during late bursts. Indeed, in the majority of preparations, oscillations and late bursting, despite their different periodicity, had analogous phase coupling consisting of homosegmental alternation and homolateral synchronicity between upper and lower lumbar segments. The most parsimonious explanation is that the same network was responsible for these distinct forms of neuronal rhythmicity. Curiously though, this NK_3 agonist-induced bursting is somewhat

intermediate between the full alternation expressed by the locomotor network (Kiehn & Kjaerulff, 1998; Nishimaru & Kudo, 2000) and the complete synchronicity typical of the disinhibited pattern (Bracci *et al.*, 1996a). This realization prompted further tests to study whether synaptic inhibition was fully operative as a consequence of NK_3 receptor activity.

3.4 Inhibitory synaptic mechanisms following NK_3 receptor activity

The onset and maintenance of late bursting were particularly prominent phenomena whose magnitude might have been partly due to tissue immaturity since at a later age bursting does not persist as much as found in the present study (Barbieri & Nistri, 2001). One possible explanation for this phenomenon might have been some reversible depression of synaptic inhibition especially in view of the absence of ipsilateral rhythm alternation, which requires reciprocal synaptic inhibition (Beato & Nistri, 1999). Thus, synchronous activity observed after senktide application was reminiscent of the effects elicited by the $GABA_A$ antagonist bicuculline (Cowley & Schmidt, 1995; Kremer & Lev-Tov, 1997). In our previous scheme for locomotor network operation we envisaged variable strength of intersegmental excitatory connections (Beato & Nistri, 1999). The present data therefore raised the possibility that the strength of inhibitory synaptic connections could also be varied.

To explore potential changes in synaptic inhibition strength, three approaches were adopted: 1) testing the effectiveness of exogenous GABA or glycine; 2) monitoring the DR-DRP which is the expression of GABAergic presynaptic inhibition (Curtis *et al.*, 1971; Levy, 1977; Nicoll & Alger, 1979; Nistri, 1983); 3) examining the motoneuron recurrent IPSP which is due to Renshaw cell activity and mediated by glycine for its main (and early) component (Werman *et al.*, 1968) and by GABA for its late phase (Cullheim & Kellerth, 1981; Polc & Haefely, 1982).

On most preparations, bath-applied GABA or glycine reversibly suppressed bursting. This result does not rule out concomitant depression of GABAergic or glycinergic inhibition as, at least in the case of exogenous GABA, burst suppression could have been caused by widespread activation of extrasynaptic receptors or of additional receptor classes not modulated by NK_3 receptor activity. On a few preparations bursting was not blocked by exogenous GABA (or glycine) even though these amino acids always depressed VR reflexes induced by DR stimulation. The preferential location of NK_3 receptors in relation to the pathways mediating bursting rather than those involved in VR reflexes (note that the NK_3

antagonist SR 142801 does not affect VR reflexes; Barbieri & Nistri, 2001) might account for this discrepancy.

While data with exogenously applied transmitters were not conclusive, impairment of GABAergic transmission (as indicated by reduction in DR-DRPs) appeared after strong activation of NK_3 receptors. The depression of the recurrent IPSP is consistent with this interpretation especially because a reduction in IPSP area (to which the late, GABA-mediated, phase contributes) rather than peak amplitude was manifested with consequent fall in the inhibitory charge across the cell membrane. Decrease in glycine mediated inhibition might have also contributed to this phenomenon although it was more difficult to demonstrate it experimentally. Of course, the efficacy of synaptic inhibition at various stations within the complex polysynaptic network mediating bursting remains untested and can only be inferred from studies on recurrent IPSPs or DR-DRPs. It is worth noting that intense sensory stimulation of spinal neurons has been found to be associated with reduction in the inhibition mediated by GABA or glycine (Lin *et al.*, 1996), lending support to the notion that the strength of synaptic inhibition can change quite rapidly.

The reason why GABAergic inhibition seemed impaired remains uncertain. NK_3 receptors are G-protein coupled units transducing the operation of intracellular second messengers, especially those belonging to the inositol triphosphate (IP_3) cycle (Buell *et al.*, 1992). It is plausible that in the present experiments NK_3 receptor activity could have raised intracellular IP_3 and thus internal Ca^{2+} ($[Ca^{2+}]_i$) (Pinnock *et al.*, 1994) high enough to impair $GABA_A$ receptor function which crucially depends on $[Ca^{2+}]_i$ (Inoue *et al.*, 1986). It should be noted that the broad spectrum tachykinin agonist substance P strongly depresses $GABA_A$ receptor function via a Ca^{2+} dependent protein kinase C mechanism (Brandon *et al.*, 2000; Yamada & Akasu, 1996). Any reduction in GABA-mediated transmission would be expected to be a transitory phenomenon receding once $[Ca^{2+}]_i$ homeostasis is re-established. The rise in motoneuron input resistance during delayed bursting might reflect depression of tonic GABAergic transmission and might have facilitated integration of inputs into bursting signals.

It seems also likely that "physiological" activation of NK_3 receptors by endogenous ligands may not necessarily involve late weakening of GABA mediated inhibition. In fact, on a consistent number of preparations, rhythmic activity with fully alternating patterns was preserved. Furthermore, activation of NK_3 receptors must have occurred during the fully

alternating rhythms of fictive locomotion evoked by NMDA and 5-HT, as this pattern was readily disrupted by the NK_3 antagonist.

3.5 Can NK_3 receptors modulate locomotor rhythms?

Senktide transformed irregular oscillations induced by NMDA and 5-HT concentrations subthreshold for fictive locomotion into fully alternating, stable, motor patterns. Interestingly, during senktide washout and in the continuous presence of NMDA plus 5-HT, bursts developed with alternating (left/right and rostral/caudal) oscillations typical of fictive locomotion. Furthermore, senktide accelerated but did not disrupt fictive locomotor patterns. These data suggest that NK_3 receptor activity could concur to activate the locomotor CPG, without making its patterns prevail over those induced by NMDA and 5-HT. This result accords with recent work on the neonatal mouse spinal cord showing that alternating motor rhythms were of larger amplitude than the non alternating ones, indicating that the operation of the locomotor network functionally switched off other rhythmic patterns (Whelan *et al.*, 2000). Notwithstanding the resolution of the signal transduction processes mediating the action of NK_3 receptor agonists, tachykinin receptors are known to upregulate glutamatergic transmission (Rusin *et al.*, 1992; for review see Urban *et al.*, 1994). This action of NK_3 receptors on rat spinal cord neurons (Cumberbatch *et al.*, 1995) could account for the facilitation of fictive locomotor patterns evoked by NMDA and 5-HT. An alternative explanation is that NK_3 receptor activation (or the delayed bursting consequent to it) could generate sufficient interneuronal depolarization to facilitate fictive locomotion.

The ability of the NK_3 antagonist SR 142801 to disrupt the NMDA and 5-HT evoked patterns suggests that during the operation of the locomotor CPG there was endogenous release of ligands acting on NK_3 receptors.

4. Role of metabotropic glutamate receptors in spinal cord rhythmicity

Metabotropic glutamate receptors are known to modulate spinal cord activity through excitatory and inhibitory actions (Anwyl, 1999). The present study resolved the contribution by subclasses of such receptors to excitation and inhibition and demonstrated their

participation to rhythmic patterns arising either directly via activation of metabotropic receptors or induced by neurochemicals.

In particular, activation of group I mGluRs induced depolarization of motoneurons, with superimposed oscillatory activity, which, in the majority of preparations, was synchronous. Thus, the overall manifestation of this effect was excitation mediated by mGlu1 receptors in terms of depolarization and by mGlu5 receptors in terms of oscillations. One possible reason for lack of pattern alternation could be decreased inhibitory activity, although direct evidence for this was obtained only for the Renshaw cell mediated IPSP. DR evoked responses could be inhibited through facilitation of glycinergic transmission via mGlu1 receptors, though enhancement of the late polysynaptic component of the response was observed. During fictive locomotor rhythm there was weak activation of metabotropic glutamate receptors, while during disinhibited rhythm such receptors appeared to play a more prominent role, presumably because the strong and long lasting release of glutamate associated with bursting was adequate to activate them. The action of group II or III mGluRs was always inhibitory, as demonstrated by their action on DR evoked responses and on disinhibited rhythm.

4.1 Excitatory action of DHPG

Activation of group I mGluRs excited spinal networks and was observed as motoneuron output either at single cell level or as integrated VR responses. The first issue was how much of this effect, which undoubtedly included mGluR-rich spinal interneurons (see INTRODUCTION § 5.2.1), was generated by motoneurons themselves and/or modulated by their intrinsic membrane properties.

Once the action of mGluR activation was restricted to motoneurons by application of TTX, it became clear that motoneuron depolarization was substantially depressed and that oscillations were absent. The simplest interpretation was that premotoneurons and interneurons made a major contribution to the response observed from motoneurons intra or extracellularly. However, this is a complex problem because under certain circumstances motoneurons do generate intrinsic oscillations (Kiehn *et al.*, 2000): this realization prompted further tests to validate the genesis of oscillatory activity found in our experiments.

Our observations support the conclusion that oscillations did not arise as a mere consequence of motoneuronal depolarization for a number of reasons. (1) When single motoneurons were recorded with QX-314 filled electrodes to block I_{Na} and I_h currents, the excitatory effect induced by DHPG persisted in terms of depolarization and comprised oscillations with

similar periodicity. Such data confirm that block of DHPG-induced excitatory action, in the presence of TTX, was due to a block of network activity rather than to a direct interference of TTX with the motoneuron ability to generate oscillations. (2) Injection of negative or positive DC current during appearance of oscillatory activity did not disrupt oscillations or alter their period. (3) It was possible to dissect out pharmacologically depolarization (mediated by mGlu1 receptors) from oscillations (mediated by mGlu5 receptors). These two components could therefore be independently manifested at the level of motoneurons. In conclusion, all these data point to a strong activity of pre-motoneuronal and interneuronal network induced by DHPG.

4.2 Membrane effectors of metabotropic glutamate receptors

Substantial evidence shows that mGluRI activity is associated with neosynthesis of IP_3 and intracellular free calcium mobilization. mGluRII and III receptors conversely depress the formation of c-AMP (Pin & Duvoisin, 1995). Ideally it would be most useful to examine how these metabolic processes are transduced into modulation of existing membrane proteins important to control excitability of selected populations of spinal neuron. Unfortunately, there are several limitations to this aim. Access to the interneuronal populations which may be the main target for metabotropic receptor activity is restricted when using the isolated spinal cord. Thus, the present study lacked the visual identification of single cells in various laminae as slice preparations can provide. Furthermore, no attempt was made to record intracellularly from single interneurons as the isolated preparation was unsuitable to characterize such cells on the basis of selective peripheral inputs and to assign them a certain neuronal function. Moreover, the strong response induced by metabotropic receptor activity suggests that several classes of interneurons were activated, making difficult to choose a particular cell type for investigation. Considerable help to interpreting the present data can however be obtained from the demonstration of the location of metabotropic receptor distribution within the spinal cord (see INTRODUCTION § 5.2.1).

Even if direct data from interneurons are lacking, it is still possible to address other questions like the potential interaction between metabotropic and ionotropic glutamate receptors at network level. Are the former simply operating by modulating the function of the latter? In fact, it has been suggested that, in the spinal cord, both mGlu1 and mGlu5 receptors can enhance the activity of ionotropic glutamate receptors (Bleakman *et al.*, 1992; Jones & Headley, 1995; Holohean *et al.*, 1999; Ugolini *et al.*, 1999; Dang *et al.*, 2002). In a variety of

spinal neurons of the lamprey spinal cord, activation of postsynaptic group I mGluRs potentiates NMDA-induced currents through a G-protein dependent mechanism and NMDA-induced calcium responses (Krieger *et al.*, 2000). Nevertheless, this mechanism might not be due to a specific interaction between NMDA/AMPA receptors with mGluRs, but rather to overall changes in membrane potential and cell input resistance (Jones & Headley, 1995). On dorsal horn neurons of the rat, group I mGlu receptor agonists produce a direct, persistent excitatory postsynaptic effect consisting of a slow membrane depolarization, associated with increase in input resistance and an intense neuronal discharge, independent of AMPA or NMDA receptor activation (Zhong *et al.*, 2000).

We investigated whether the excitatory action of mGluI receptors might actually be mediated by NMDA and AMPA receptors. In extracellular experiments, comparable reduction in the amplitude of motoneuronal depolarization and of oscillatory activity in response to DHPG was observed in either APV or CNQX solution. Likewise, results obtained with intracellular experiments from motoneurons under similar conditions indicated attenuation of membrane potential and fast oscillatory activity, plus disappearance of slow oscillations. These observations suggest that network-based NMDA and non-NMDA receptors both contributed to the DHPG induced depolarization without the need for a preferential (or special) contribution by either of them. Hence, the extent of oscillatory activity seemed to depend on network depolarization rather than on the activation of a specific class of ionotropic glutamate receptors. It should be noted that this notion has been inferred from single motoneurons or VRs and that it would need validation with direct recordings from interneurons. It should also be considered that, unlike the widespread distribution of ionotropic glutamate receptors, the more discrete distribution of class I mGluRs in the rat spinal cord may be responsible for their ability to induce peculiar patterns of oscillatory activity.

The present experiments did not allow to actually distinguish whether mGluRs directly modulate NMDA (or AMPA) receptors. Future experiments should elucidate this issue by examining the action of metabotropic receptor agonists at single cell level after blocking all known ionotropic receptors. The present experiments did however show that activation of L-type calcium channels was not a prerequisite for eliciting depolarization and oscillations by metabotropic receptor group I activation because the calcium channel antagonist nifedipine did not influence their action. Only in certain conditions the role of such calcium channels became apparent (see DISCUSSION § 4.8).

4.3 Time course of DHPG action

Within 5 minutes of DHPG application, motoneuron depolarization waned and oscillatory action was less pronounced, despite continuous application of the drug. This phenomenon could be due to several mechanisms. It could, in fact, be caused by decrease of excitation, for example due to gradual receptor desensitization, or by progressive enhancement of inhibitory transmission.

In the hippocampus, an activity-dependent switch from facilitation to inhibition of excitatory synaptic transmission has been reported, as a result of group I receptor desensitization (Rodriguez-Moreno *et al.*, 1998). The authors suggest that DHPG-activated mGluRs potentiate glutamate release via their coupling to a pathway that shows full desensitization within about 5 min. During the period in which the facilitatory response is desensitized, the receptor becomes coupled to another response pathway, which in turn results in inhibition of glutamate release. Furthermore, mGluRI activation may either facilitate or attenuate NMDA excitotoxicity depending upon how long before and to what extent metabotropic receptors have been activated (Bruno *et al.*, 2001).

We investigated whether inhibitory transmission rather than a functional receptor switch could have a role in determining the evolutionary change in the effect induced by mGluRI activation. To this end, we studied the time course of the effect of DHPG application to the spinal cord, when ionotropic inhibitory transmission was blocked, i.e. during disinhibited rhythm. This is a very useful model for this task since it is characterized by very regular periodicity. We found that, in these conditions, DHPG induced a depolarization and an increase in bursting period (see Fig. 33F) with the same time course as in control conditions with intact inhibitory transmission, indicating that glycine and GABA receptors were not involved in the modification of DHPG effects with time. These results suggest that receptor desensitization (or a functional switch of receptor activity) was perhaps implicated in the changing outcome of metabotropic receptor activation. In keeping with this hypothesis, we found that, in control conditions, any depression of DR evoked responses persisted throughout the action of DHPG.

4.4 Inhibition due to mGluR-I activation

The previous section concluded that the faltering excitation during persistent administration of DHPG was probably caused by an intrinsic change in mGluI receptors as observed in other preparations (Rodriguez-Moreno *et al.*, 1998). It is however clear that certain effects

originating from mGluRI activation required a different explanation, namely the hypothesis that some spinal neurons were inhibited right from the early part of DHPG application. One example of this is provided by the fact that DHPG depressed reflexes induced by relatively weak DR stimuli. This action of DHPG on reflex responses was complex. In fact, although the peak of the response was always inhibited, a noticeable prolongation of the reflex was manifested in the case of high voltage stimulation in the presence of DHPG. In this case, any oscillatory activity evoked by the stimulus and superimposed on synaptic depolarization, was enhanced, sometimes giving rise to an increase in the overall area of the reflex (calculated from the onset of the response to membrane potential return to baseline). It is interesting that, in spinal slices, monosynaptic EPSPs on dorsal interneurons were depressed by mGluRI activation while polysynaptic EPSP evoked by strong DR stimuli were potentiated (Zhong *et al.*, 2000). In the present experiments potentiation was, however, an occasional phenomenon only.

Several hypotheses can be advanced regarding the mechanism through which DHPG might have exerted its inhibitory action on the DR induced reflex: a) direct action of mGluRI on membrane potential of certain neurons within the DR-VR pathway; b) down-modulation of excitatory synapses; c) facilitation of inhibitory transmission. The latter could in turn arise from direct modulation of Cl^- mediated conductances, or from excitation of inhibitory interneurons.

Concerning the first hypothesis, one cause might have been membrane depolarization associated with fall in the driving force for excitatory transmitters. However, the reflex depression was consistently present at different degree of depolarization recorded from VRs, and, in the case of intracellular recording from motoneurons, at membrane potential values close to rest. Another possibility is that inhibition might have been due to shunting of the membrane by depolarization and activation of intrinsic conductances: this is an unlikely hypothesis in view of the fact that input resistance of motoneurons was not significantly altered in the presence of DHPG. Furthermore, the dependence of depression upon intensity of stimulation argues against shunting inhibition.

Since, in the presence of nifedipine or APV, DHPG could still depress reflexes, it seems unlikely that there was any generalized downregulation of excitation. Moreover, the mGluR1 antagonist AIDA depressed fictive locomotion induced by NMDA and 5-HT, suggesting that there was background facilitatory rather than depressant activity of mGluR1 receptors on glutamate receptors.

We thus investigated whether mGluRI activation might have reduced DR evoked responses by enhancing the activity of inhibitory neurons. Indeed, application of strychnine (but not of bicuculline) prevented the inhibitory effect of DHPG, thus indicating that facilitation of glycinergic transmission was probably involved in DR reflex depression by mGluR-I activation. In the presence of strychnine, reflexes were considerably prolonged possibly because the excitatory actions by DHPG were unopposed by concurrent inhibitory effects.

When DR fibers were stimulated repeatedly with strong stimuli at 2 Hz to generate sensitization of afferent inputs, the overall result was strong depression of the cumulative depolarization and associated oscillations. Hence, even if single reflex responses became longer, they lost the ability to produce non-linear summation of inputs typically associated with slow synaptic potentials (Baranauskas & Nistri, 1998). Chen *et al.* (Chen *et al.*, 2000) have also reported long lasting depression of afferent inputs by metabotropic receptor activity. We propose that, under these circumstances, intense release of inhibitory transmitters was facilitated and sustained by DHPG and it therefore prevented non-linear summation. This notion could not be tested in strychnine or bicuculline solution because of the associated excitability increase which prevented repeated high frequency stimulation.

The precise mechanism through which glycinergic facilitation took place, i.e. through increase in the releasing probability or in the efficacy of postsynaptic receptors, remains unknown. Previous results on this issue are controversial. For example, Zhong *et al.* (Zhong *et al.*, 2000) found that strychnine *and* bicuculline were necessary to remove the depressant action by DHPG on EPSPs of lamina II interneurons. On the other hand, on dorsal horn neurons, mGluR-I activation could induce sustained depression at sensory synapses even in the presence of strychnine and bicuculline, therefore indipendent of glycinergic and GABAergic transmission (Chen *et al.*, 2000).

Potentiation of glycinergic transmission was mediated by mGlu1 receptors since AIDA reverted this effect, while application of the mGlu5 receptor antagonist MPEP did not prevent DHPG induced depression of DR evoked responses. On the contrary, MPEP *per se* depressed responses, indicating that mGluR5 receptors were endogenously activated during a DR stimulus and contributed to the excitation of the DR reflex. Interestingly, in the presence of MPEP, the reflex depressant action by DHPG became significantly larger.

We suspect that reflex depression could be simply explained by assuming that a group of glycinergic interneurons was depolarized by mGluR1 activation and released their transmitter to inhibit reflex responses. With strong stimuli, excitatory transmission could apparently

overcome enhanced glycinergic transmission. In this sense, the fact that DHPG could produce overall excitation or inhibition depended on the location of its receptors rather than on different membrane mechanisms. In keeping with our view is the finding that the excitatory action of DHPG can enhance the activity of inhibitory neurons (Dang *et al.*, 2002), thus leading to increased inhibition in specific areas of the network.

4.5 Inhibition of IPSPs

Several issues prompted us to investigate the action of DHPG on the Renshaw-cell mediated IPSP. This is a dysynaptic potential evoked by activation of recurrent collaterals of motor axons. Renshaw cells were traditionally identified as glycinergic (Werman *et al.*, 1968) although in subsequent studies it was clear that their synaptic input also comprised a late GABAergic component. There are few analogous examples of functionally identifiable glycinergic transmission sites. Thus, Renshaw cell mediated inhibition seemed to be an appropriate model to study how DHPG could modulate inhibitory transmission.

On the one hand, the finding that DHPG induced a synchronous rhythm suggested that inhibitory transmission was altered. On the other hand, DHPG seemed to exert its inhibitory action on DR evoked responses through a mechanism involving facilitation of glycinergic transmission.

Our experiments showed that DHPG depressed the peak amplitude of recurrent IPSPs on motoneurons, thereby preferentially affecting their glycinergic component.

We considered several mechanisms by which this depression might have taken place. As the IPSP is based on a disynaptic pathway, depression could occur either at the level the cholinergic synapse or of the glycinergic one. For instance, DHPG could antagonize acetylcholine receptors, enhance their desensitization, or suppress acetylcholine release. To the best of our knowledge, DHPG is actually reported to enhance acetylcholine release from brain synaptosomes (Marti *et al.*, 2001). Acetylcholine nicotinic receptor desensitization is typically slowly developing with delayed recovery and is strongly dependent on intracellular Ca^{2+} levels (Khiroug *et al.*, 1997, Khiroug *et al.*, 1998). Since DHPG increases intracellular free Ca^{2+} (Pin & Duvoisin, 1995), this phenomenon could facilitate acetylcholine receptor desensitization, especially if accompanied by larger acetylcholine release, and eventually depress the recurrent IPSP by impairing the input to the Renshaw cells. In such a case the IPSP should be progressively reduced by any on-going process of desensitization. The advantage of this hypothesis would be that it might account for Renshaw cell depression

using a unitary explanation based on postsynaptic depolarization (in this case of the Renshaw cell) with associated elevation in intracellular Ca^{2+}. Again, the metabotropic receptor location rather than distinct mechanisms could account for the multifarious phenomena emerging after mGluR-I activation.

In the presence of DHPG there was no consistent reduction of the IPSP area with time, suggesting that increased desensitization was unlikely to be the main mechanism through which IPSPs were depressed by mGluRI activation. This observation, however, cannot completely rule out the hypothesis of increased desensitization caused by DHPG. In fact, the inter-pulse interval might have been long enough for desensitization to completely recover before the second IPSP was evoked, or saturation of desensitization might have already occurred by the time the first stimulus was applied. Protocols of paired-pulse stimulation, with a smaller time interval between two pairs of stimuli, would be needed to further elucidate issue.

Another possibility would be pre-synaptic depression of Renshaw cell release, as reported, for example, for the release of other transmitters by hippocampal cells (Fitzjohn *et al.*, 2001; Faas *et al.*, 2002). This hypothesis is not liable to direct testing in the rat isolated spinal cord preparation as Renshaw cells are sparsely located and very rarely encountered (Dourado & Sargent, 2002). In particular, it would be rather difficult to record directly the sensitivity of Renshaw cells to exogenous acetylcholine or the occurrence of their spontaneous cholinergic events during application of DHPG. Likewise, it would be impossible to identify, on a single motoneuron, glycinergic events exclusively generated by Renshaw cells or glycine receptors associated with such synapses, as glycine is quite a ubiquitous transmitter.

Collectively, the present data indicate that the operation of certain glycinergic neurons, like the Renshaw cells, was depressed. Although it is unclear whether Renshaw cell activity can effectively contribute to the pattern alternation of fictive locomotion in mammals (for chick spinal cord, see Wenner & O'Donovan, 2001), it seems reasonable that Renshaw cell depression might be paradigmatic for the synchronous rhythmicity associated with mGluRI receptor activity. This issue will be further explored in the next paragraph.

4.6 Origin of DHPG induced oscillations

Fast or slow oscillations evoked by DHPG were most often synchronous. If the only action by DHPG was to depolarize CPG neurons, like for instance application of high K^+ (Bracci *et al.*, 1997), one should have observed alternating patterns especially because the degree of

depolarization was adequate to generate network based oscillations. It is therefore necessary to assume that either DHPG oscillations did not involve the fictive locomotion CPG, or that they did so while in the presence of impaired operating mechanisms so that pattern generation was triggered, but it lost its alternation.

In the lamprey spinal cord, a slow dorsal-ventral rhythm, induced by mGluRs, can be observed superimposed on a fast NMDA-induced locomotor rhythm. In the present study, there was no coexistence of DHPG and fictive locomotor patterns, an observation suggesting that the rhythmicity induced by DHPG could not coexist with locomotor CGP operation. This effect was not however exclusive for the locomotor CPG because metabotropic receptor activation can elicit oscillations in superficial areas of the dorsal horn normally outside the locomotor CGP (Zhong *et al.*, 2000). Thus, it is possible that lack of coexistence was due to the fact that the locomotor pattern can be so strong as to switch off other spinal rhythms (Whelan *et al.*, 2000).

Assuming that the locomotor CPG was at least in part activated by DHPG, any decrease in inhibition versus the level of excitation would lead to impairment of alternation (Cowley & Schmidt, 1995; Kremer & Lev-Tov, 1997; see also INTRODUCTION § 4.3). Thus, synchronicity could depend on altered inhibitory transmission or, more generally, on an altered equilibrium between the level of excitation and inhibition. Our experiments showed that both excitatory and inhibitory transmission systems were enhanced. This could lead to several hypotheses. One is that enhancement of excitation was stronger than enhancement of inhibition. One way to explore this issue would have been to decrease the level of excitation, but application of APV or CNQX abolished oscillations, making it impossible to evaluate whether synchronous oscillations would turn into alternated ones (see, for example, Kremer & Lev-Tov, 1997). On the other hand, if excitation were not strong enough to fully activate the CPG, this might lead to generation of synchronous activity (Bracci *et al.*, 1997). The hypothesis of prevailing excitation over inhibition is however inconsistent with data from stimulus trains. In those conditions, reflexes were depressed apparently because of facilitation of glycinergic inhibition, yet DHPG prevented the onset of rhythmic patterns, whether synchronous or alternating. These results indicate that a major synaptic input to motoneurons was curtailed during metabotropic receptor activity and that, despite continuous afferent volley stimulation, the locomotor CPG could not generate patterns.

4.7 Role of group I mGluRs in fictive locomotion

Our results show that bath-application of DHPG to preparations exhibiting a stable, fictive locomotor pattern induced slow depolarization and rhythm disruption. In the presence of NMDA, 5-HT and DHPG, although some locomotor cycles were still visible, they were sparse and with reduced amplitude, though retaining the same cycle period and phase alternation between homolateral and homosegmental VRs. This condition is clearly different from the results obtained with the lamprey spinal cord, in which DHPG increases burst frequency of NMDA induced fictive swimming, presumably through an increase in network depolarization and potentiation of NMDA receptor function (Krieger *et al.*, 1998). In the rat spinal cord, the depolarization induced by DHPG during fictive locomotion indicated overall excitation coupled to rhythm suppression. These findings seem to indicate that mere activation of mGluI receptors could not be sufficient to trigger locomotor CPG operation.

A different issue is whether during fictive locomotion the CPG relies on activation of certain metabotropic receptors. Experiments testing selective antagonists of mGlu1 and mGlu5 receptors indicated them weakly active during fictive locomotion. In the lamprey spinal cord, on the other hand, mGlu5 receptors seem to be activated by endogenous glutamate during fictive swimming, thus participating in burst frequency regulation (Krieger *et al.*, 1998). This phenomenon is apparently brought about by synaptically released glutamate binding to presynaptic group I mGluRs (autoreceptors) to raise $[Ca^{2+}]_i$ and to facilitate excitatory transmitter release (Takahashi & Alford, 2002).

4.8 Role of group I mGluRs in disinhibited rhythm

The disinhibited rhythm was useful to understand the nature and duration of DHPG action on spinal networks once synaptic inhibition had been blocked. Disinhibited bursts, lasting several seconds and occurring at regular interval, are mainly dependent on non-NMDA receptor activity (Bracci *et al.*, 1996a). mGluRI activation clearly accelerated such a rhythm without changing the intraburst structure. Network compensation for faster bursting meant concurrent decrease in individual burst duration in analogy with entrainment experiments in which burst duration occurred in parallel to burst frequency rise (Bracci *et al.*, 1997).

It is noteworthy that the DHPG-induced depolarization gradually disappeared while the rhythm acceleration persisted, indicating the two phenomena apparently had separate origin. The rhythm facilitation induced by metabotropic glutamate receptors was accompanied by activation of L-type Ca^{2+} channels because this action was prevented by nifedipine.

Moreover, a large degree of activation of metabotropic glutamate receptors by endogeneous glutamate was demonstrated by the rhythm slowdown observed after antagonism of mGluR1 receptors.

While in other experimental conditions, mGlu receptor antagonists or nifedipine had little effect on rhythmic activities, these data suggest that disinhibited bursts were long events during which there was presumably substantial release of endogeneous glutamate to strongly activate metabotropic receptors which in turn operated *via* nifedipine-sensitive conductances when additional receptor activation was provided by exogenous compounds.

Cooperation between metabotropic agonists and endogenous glutamate was seemingly necessary to switch on nifedipine sensitive channels as, in the absence of exogenous agonists, nifedipine was ineffective on disinhibited rhythms. Thus, it looks likely that endogenous glutamate could activate mGluI receptors with functional consequences independent from Ca^{2+} channel activity.

4.9 Role of group II and III mGluRs in the spinal cord

The present data indicate that mGlu receptors from both group II and group III have the ability to provide powerful inhibition of synaptic transmission in the spinal cord. In fact, activation of group II or III metabotropic glutamate receptors by the exogenous agonists DCG-IV or L-AP4 were able to reversibly depress DR evoked responses. Likewise, activation of these receptors during disinhibited rhythm slowed down or abolished bursting. Furthermore, the application of the group II antagonist EGLU, and to a lesser extent, the group III antagonist CPPG, accelerated bursting, indicating that these receptors were endogenously activated, but obviously not saturated, during disinhibited rhythm.

4.9.1 Localization, effects and mode of action of mGlu II-III receptors

Although we did not identify the specific mGlu receptor subtype(s) within the II and III groups present in the neonatal rat spinal cord, studies of mGluR subtype expression can cast some light on this issue. Levels of mRNA for mGlu2 and mGlu4 receptors are very low in the spinal cord (Boxall *et al.*, 1998; Berthele *et al.*, 1999; Jia *et al.*, 1999; Ohishi *et al.*, 1993; Ohishi *et al.*, 1995), with moderate signal for mGlu3 receptor in the dorsal horn (Berthele *et al.*, 1999; Jia *et al.*, 1999). No mRNA labeling for mGlu6 and mGlu8 receptors has been detected in the rat spinal cord (Valerio *et al.*, 1997; Boxall *et al.*, 1998; Berthele *et al.*, 1999). Thus, it seems likely that mGluR3 as well as mGluR7 (Li *et al.*, 1997) make up most of the

spinal metabotropic receptors of group II and III. Evidence supports the presence of autoreceptors belonging to groups II-III of metabotropic glutamate receptors on central endings of primary afferents in the spinal cord (Valerio *et al.*, 1997; Jia *et al.*, 1999).

Furthermore, on lamprey spinal motoneurons the proposed presynaptic co-localization of group II and group III mGlu receptors on a single reticulospinal axon is in accordance with their role as glutamatergic autoreceptors to limit reticulospinal-mediated excitation (Krieger *et al.*, 1996). There is also suggestive evidence that group II and group III presynaptic mGlu receptors are co-localized on the same primary afferent terminals impinging upon motoneurons of the immature rat spinal ventral horn (Cao *et al.*, 1995; Cao *et al.*, 1997; Jane *et al.*, 1994; Jane *et al.*, 1995).

In the brain, inhibition of synaptic transmission by group II and group III metabotropic glutamate receptors is a common phenomenon (Pin & Duvoisin, 1995; Conn & Pin, 1997; Anwyl, 1999). Group II and III metabotropic glutamate receptors are negatively coupled to adenylyl cyclase and thus inhibit cyclic AMP formation (Pin & Duvoisin, 1995). DCG-IV is a specific agonist on mGlu 2 and mGlu 3 receptors (Ishida *et al.*, 1993a; Hayashi *et al.*, 1994). L-AP4 is known to be a group III agonist acting on a glutamate autoreceptor operating via negative feedback to decrease excitatory transmitter release (Pin & Duvoisin, 1995). The reversal of the depressant effect of L-AP4 by CPPG, a potent group III mGlu receptor antagonist, has been consistently observed (Toms *et al.*, 1996).

4.9.2 Synaptic depression mediated by mGluR II and III receptors in the rat spinal cord

Studies of rat spinal cord preparations report reduction in synaptic events by DCG-IV which preferentially decreases the amplitude of the early monosynaptic component over the polysynaptic components of the ventral root potential (Ishida *et al.*, 1993b). Like DCG-IV, the group II agonists (1*S*–3*R*)-ACPD and l-CCG-1 depress the monosynaptic and polysynaptic components of the ventral root potential (Pook *et al.*, 1992; Eaton *et al.*, 1993; Ishida *et al.*, 1993b; Jane *et al.*, 1994) as well as the EPSPs evoked by low or high intensity dorsal root stimulation (King & Liu, 1996). EGLU is a selective group II mGlu receptor antagonist that preferentially blocks presynaptic mGlu receptors and has little or no antagonist activity at postsynaptic metabotropic glutamate receptors and ionotropic glutamate receptors (Jane *et al.*, 1996). On dorsal horn neurons, DCG-IV attenuates mono and polysynaptic EPSPs evoked by primary afferent stimulation (Gerber *et al.*, 2000). Interestingly, IPSPs are also depressed.

The potent depressant action of L-AP4 has been observed on ventral root responses (Evans *et al.*, 1982) and excitatory and inhibitory transmission on dorsal horn neurons (Davies & Watkins, 1982; Gerber *et al.*, 2000).

In the present investigation, although both L-AP4 and DCG-IV reversibly depressed reflex responses evoked by single DR stimuli, their effect on cumulative depolarization due to pulse trains was different. In fact, the depression of the first few reflexes by DCG-IV could be gradually overcome by subsequent pulses in the train (see Fig. 37), yielding a final global response not significantly different from controls. Conversely, the depressant effect by L-AP4 was maintained throughout the stimulus train (Fig. 37). It seems probable that, in the case of DCG-IV, progressively larger amounts of released glutamate acting postsynaptically overcame the presynaptic depression. However, it appears likely that this was a dynamic condition in which the processes of sensitization of inputs and depression of reflex were in fine balance because the mGluR II antagonist EGLU *per se* strongly enhanced cumulative depolarization. Perhaps at low concentrations of extracellular glutamate, the higher affinity of group II receptors over ionotropic receptors (Schoepp *et al.*, 1999) favored depression. When there was more free glutamate available owing to high frequency stimulation, the lower affinity ionotropic receptors prevailed.

As far as group III receptors were concerned, they could strongly suppress single or repeated reflexes but were little accessible to endogenous glutamate as their pharmacological antagonism could not augment synaptic responses. The depressant effect of L-AP4 or DCG-IV was presumably mediated presynaptically at terminals of interneurons in the pre-motoneuronal network because no action by either compound on resting membrane potential and input resistance of motoneurons was detected.

4.9.3 Disinhibited Rhythm

The role of group II and III receptors in spinal rhythmicity was studied taking as a model the disinhibited rhythm. In fact, our investigation regarding group I receptors showed that these receptors played an important role in this type of rhythmicity rather than in fictive locomotion. Because of the overall inhibitory action of group II and III receptors, it seemed interesting to explore whether they contributed to rhythm generation and maintenance. Future studies will be required to examine their potential action on fictive locomotor patterns.

DCG-IV slowed down the rhythm, or even completely arrested it, effects that were blocked by the selective antagonist EGLU indicating receptor specificity. A curious observation was

that, despite a ten fold range of test concentrations of DCG-IV, the resultant effect on the rhythm periodicity was not clearly related to the agonist dose. Either the rhythm was slowed down to a certain, consistent value or was fully suppressed. We interpret this phenomenon as due to the fact that any direct modulation of glutamatergic transmission could occur within a limited spectrum to remain compatible with bursting. Spinal networks could still support stereotypic bursting if glutamate release was maintained within certain limits below which, even if glutamate release could continue albeit at lower rate, a significant number of neurons fell below threshold for burst onset and propagation of excitation (Darbon *et al.*, 2002). This hypothesis accords with the all-or-none nature of disinhibited bursts (Darbon *et al.*, 2002).

Conversely, in the majority of preparations, EGLU accelerated bursting and decreased burst duration. We interpret this finding as evidence to support autoregulation by endogenous glutamate of glutamate release during a burst episode. Hence, in the absence of fast, Cl^- mediated inhibition spontaneous rhythmicity was likely to be regulated by the concomitant operation of glutamate metabotropic receptors (together with a modest contribution by $GABA_C$ receptors; Rozzo *et al.*, 1999) plus gradual activation of the electrogenic sodium pump (Ballerini *et al.*, 1997). These factors would curtail bursts because of depression of glutamate release (mGluRII activation), inhibition of network interneurons ($GABA_C$ receptors) and hyperpolarization of the membrane potential throughout the spinal network (sodium pump). It should be interesting to test, in future experiments, if the very slow and irregular bursting emerging after block of the sodium pump (Rozzo *et al.*, 2002b) might be eliminated by EGLU.

The action of the group III agonist L-AP4 on the disinhibited rhythm was also a suppressant one and readily antagonized by the selective blocker CPPG. However, CPPG per se could not significantly change bursting, indicating that group III receptors were not normally activated by endogenous glutamate during bursts.

CONCLUSIONS

The present project has contributed to clarify the operating mechanisms of the neonatal rat spinal cord as far as certain aspects of synaptic transmission and rhythmicity are concerned. Repeated activation of synaptic inputs could activate the locomotor CPG, apparently via a rise in extracellular K^+ and network neuron depolarization. In this case the locomotor pattern presented the expected alternation typical of such an activity even in an isolated preparation of the spinal cord.

Previous work has established how ionotropic receptors for glutamate, GABA and glycine all concur to ensure synaptic transmission from dorsal root afferents as well as to generate alternating spinal patterns. The present work considered that the extended duration of locomotor-like cycles could imply the recruitment of metabotropic receptors for tachykinins and glutamate itself. Activation of the NK_3 class of tachykinin receptors increased spinal cord excitability for periods beyond the application of the agonists and triggered the onset of curious oscillatory patterns which often preserved segmental alternation but were synchronous at heterosegmental level. The phenomenon appeared to be due to weakening of GABAergic synapses at certain sites within the spinal cord. However, during fictive locomotion, NK_3 receptors were normally activated and provided part of the excitatory drive necessary to support this activity.

Parallel experiments had demonstrated the effective inhibitory nature of GABA on spinal motoneurons even at this very early postnatal age. Activation of glutamate metabotropic receptors unveiled a wide complexity of effects. Group I receptors mediated depolarization and onset of oscillatory activity (via the subclasses mGluR1 and 5, respectively). While their role in fictive locomotor patterns was quite limited, it is clear they were important for the regular bursting emerging spontaneously after blocking GABA and glycine mediated inhibition (disinhibited bursting). However, in addition to excitation and facilitation, group I receptors also largely depressed reflex responses, at least in part via stimulation of endogenous glycine release. The oscillatory patterns induced by group I activation were usually synchronous and seemed to represent another example of rhythmicity that spinal cord networks could generate in addition to previously reported patterns. Group II and III

receptors were always exerting an inhibitory function on spinal neurons and their bursting behaviour. On the basis of experiments with selective agonists and antagonists, it was proposed that group II receptors were involved in controlling the duration and frequency of disinhibited bursts.

The present study thus outlines a repertoire of rhythmicity that spinal cord networks can produce with different properties in terms of phase, frequency and duration. A challenge for future studies will be to establish if these various patterns can be associated with different functions and/or distinct networks, or whether they simply highlight the complex range of programs which developing networks can generate.

REFERENCES

Alvarez, F. J., Villalba, R. M., Carr, P. A., Grandes, P., & Somohano, P. M. (2000). Differential distribution of metabotropic glutamate receptors 1a, 1b, and 5 in the rat spinal cord. *J.Comp Neurol.* **422**, 464-487.

Aniksztejn, L., Sciancalepore, M., Ben Ari, Y., & Cherubini, E. (1995). Persistent current oscillations produced by activation of metabotropic glutamate receptors in immature rat CA3 hippocampal neurons. *J.Neurophysiol.* **73**, 1422-1429.

Anwyl, R. (1999). Metabotropic glutamate receptors: electrophysiological properties and role in plasticity. *Brain Res.Brain Res.Rev.* **29**, 83-120.

Aoki, F., Wannier, T., & Grillner, S. (2001). Slow dorsal-ventral rhythm generator in the lamprey spinal cord. *J.Neurophysiol.* **85**, 211-218.

Aronica, E., Catania, M. V., Geurts, J., Yankaya, B., & Troost, D. (2001). Immunohistochemical localization of group I and II metabotropic glutamate receptors in control and amyotrophic lateral sclerosis human spinal cord: upregulation in reactive astrocytes. *Neuroscience* **105**, 509-520.

Atsuta, Y., Garcia-Rill, E., & Skinner, R. D. (1988). Electrically induced locomotion in the in vitro brainstem-spinal cord preparation. *Brain Res.* **470**, 309-312.

Atsuta, Y., Garcia-Rill, E., & Skinner, R. D. (1990). Characteristics of electrically induced locomotion in rat in vitro brain stem-spinal cord preparation. *J.Neurophysiol.* **64**, 727-735.

Baldissera, F., Hultborn, H., & Illert, M. Integration in spinal neuronal systems. Brooks, V. B. Handbook of physiology, Section 1: The nervous system, Vol. II, Motor Control, Part 1. 509-595. 1981. Bethesda: American Physiology Society.

Ballerini, L., Bracci, E., & Nistri, A. (1997). Pharmacological block of the electrogenic sodium pump disrupts rhythmic bursting induced by strychnine and bicuculline in the neonatal rat spinal cord. *J.Neurophysiol.* **77**, 17-23.

Ballerini, L. & Galante, M. (1998). Network bursting by organotypic spinal slice cultures in the presence of bicuculline and/or strychnine is developmentally regulated. *Eur.J.Neurosci.* **10**, 2871-2879.

Ballerini, L., Galante, M., Grandolfo, M., & Nistri, A. (1999). Generation of rhythmic patterns of activity by ventral interneurones in rat organotypic spinal slice culture. *J.Physiol* **517 (Pt 2)**, 459-475.

Baranauskas, G. & Nistri, A. (1998). Sensitization of pain pathways in the spinal cord: cellular mechanisms. *Prog.Neurobiol.* **54**, 349-365.

Baranauskas, G., Traversa, U., Rosati, A. M., & Nistri, A. (1995). An NK1 receptor-dependent component of the slow excitation recorded intracellularly from rat motoneurons following dorsal root stimulation. *Eur.J.Neurosci.* **7**, 2409-2417.

Barbeau, H. & Rossignol, S. (1991). Initiation and modulation of the locomotor pattern in the adult chronic spinal cat by noradrenergic, serotonergic and dopaminergic drugs. *Brain Res.* **546**, 250-260.

Barbieri, M. & Nistri, A. (2001). Depression of windup of spinal neurons in the neonatal rat spinal cord in vitro by an NK3 tachykinin receptor antagonist. *J.Neurophysiol.* **85**, 1502-1511.

Barry, M. J. & O'Donovan, M. J. (1987). The effects of excitatory amino acids and their antagonists on the generation of motor activity in the isolated chick spinal cord. *Brain Res.* **433**, 271-276.

Barthe, J. Y. & Clarac, F. (1997). Modulation of the spinal network for locomotion by substance P in the neonatal rat. *Exp.Brain Res.* **115**, 485-492.

Baylor, D. A. & Nicholls, J. G. (1969). Changes in extracellular potassium concentration produced by neuronal activity in the central nervous system of the leech. *J.Physiol* **203**, 555-569.

Beato, M., Bracci, E., & Nistri, A. (1997). Contribution of NMDA and non-NMDA glutamate receptors to locomotor pattern generation in the neonatal rat spinal cord. *Proc.R.Soc.Lond B Biol.Sci.* **264**, 877-884.

Beato, M. & Nistri, A. (1998). Serotonin-induced inhibition of locomotor rhythm of the rat isolated spinal cord is mediated by the 5-HT1 receptor class. *Proc.R.Soc.Lond B Biol.Sci.* **265**, 2073-2080.

Beato, M. & Nistri, A. (1999). Interaction between disinhibited bursting and fictive locomotor patterns in the rat isolated spinal cord. *J.Neurophysiol.* **82**, 2029-2038.

Beaujouan, J. C., Saffroy, M., Torrens, Y., & Glowinski, J. (1997). Potency and selectivity of the tachykinin NK3 receptor antagonist SR 142801. *Eur.J.Pharmacol.* **319**, 307-316.

Ben Ari, Y., Cherubini, E., Corradetti, R., & Gaiarsa, J. L. (1989). Giant synaptic potentials in immature rat CA3 hippocampal neurones. *J.Physiol* **416**, 303-325.

Ben Ari, Y., Khazipov, R., Leinekugel, X., Caillard, O., & Gaiarsa, J. L. (1997). GABAA, NMDA and AMPA receptors: a developmentally regulated 'menage a trois'. *Trends Neurosci.* **20**, 523-529.

Beresford, I. J., Ireland, S. J., Stables, J., & Hagan, R. M. (1992). Ontogeny and characterization of [125I]Bolton Hunter-eledoisin binding sites in rat spinal cord by quantitative autoradiography. *Neuroscience* **46**, 225-232.

Berger, A. J., Bayliss, D. A., & Viana, F. (1992). Modulation of neonatal rat hypoglossal motoneuron excitability by serotonin. *Neurosci.Lett.* **143**, 164-168.

Berthele, A., Boxall, S. J., Urban, A., Anneser, J. M., Zieglgansberger, W., Urban, L., & Tolle, T. R. (1999). Distribution and developmental changes in metabotropic glutamate receptor messenger RNA expression in the rat lumbar spinal cord. *Brain Res.Dev.Brain Res.* **112**, 39-53.

Bleakman, D., Rusin, K. I., Chard, P. S., Glaum, S. R., & Miller, R. J. (1992). Metabotropic glutamate receptors potentiate ionotropic glutamate responses in the rat dorsal horn. *Mol.Pharmacol.* **42**, 192-196.

Bolea, S., Avignone, E., Berretta, N., Sanchez-Andres, J. V., & Cherubini, E. (1999). Glutamate controls the induction of GABA-mediated giant depolarizing potentials through AMPA receptors in neonatal rat hippocampal slices. *J.Neurophysiol.* **81**, 2095-2102.

Bormann, J. (2000). The 'ABC' of GABA receptors. *Trends Pharmacol.Sci.* **21**, 16-19.

Bormann, J., Hamill, O. P., & Sakmann, B. (1987). Mechanism of anion permeation through channels gated by glycine and gamma-aminobutyric acid in mouse cultured spinal neurones. *J.Physiol* **385**, 243-286.

Boxall, S. J., Berthele, A., Laurie, D. J., Sommer, B., Zieglgansberger, W., Urban, L., & Tolle, T. R. (1998). Enhanced expression of metabotropic glutamate receptor 3 messenger RNA in the rat spinal cord during ultraviolet irradiation induced peripheral inflammation. *Neuroscience* **82**, 591-602.

Boxall, S. J., Thompson, S. W., Dray, A., Dickenson, A. H., & Urban, L. (1996). Metabotropic glutamate receptor activation contributes to nociceptive reflex activity in the rat spinal cord in vitro. *Neuroscience* **74**, 13-20.

Bracci, E., Ballerini, L., & Nistri, A. (1996a). Spontaneous rhythmic bursts induced by pharmacological block of inhibition in lumbar motoneurons of the neonatal rat spinal cord. *J.Neurophysiol.* **75**, 640-647.

Bracci, E., Ballerini, L., & Nistri, A. (1996b). Localization of rhythmogenic networks responsible for spontaneous bursts induced by strychnine and bicuculline in the rat isolated spinal cord. *J.Neurosci.* **16**, 7063-7076.

Bracci, E., Beato, M., & Nistri, A. (1997). Afferent inputs modulate the activity of a rhythmic burst generator in the rat disinhibited spinal cord in vitro. *J.Neurophysiol.* **77**, 3157-3167.

Bracci, E., Beato, M., & Nistri, A. (1998). Extracellular K+ induces locomotor-like patterns in the rat spinal cord in vitro: comparison with NMDA or 5-HT induced activity. *J.Neurophysiol.* **79**, 2643-2652.

Bragin, A., Jando, G., Nadasdy, Z., Hetke, J., Wise, K., & Buzsaki, G. (1995). Gamma (40-100 Hz) oscillation in the hippocampus of the behaving rat. *J.Neurosci.* **15**, 47-60.

Brandon, N. J., Delmas, P., Kittler, J. T., McDonald, B. J., Sieghart, W., Brown, D. A., Smart, T. G., & Moss, S. J. (2000). GABAA receptor phosphorylation and functional modulation in cortical neurons by a protein kinase C-dependent pathway. *J.Biol.Chem.* **275**, 38856-38862.

Brocard, F., Clarac, F., & Vinay, L. (1997). What is the contribution of the deveopment of ventral descending pathways to the ontogeny of motor activities in the neonatal rat? *Soc.Neurosci.Abstract* 410.16..

Brown, T. G. (1911). The intrinsic factors in the act of progression in the mammal. *Proc.R.Soc.Lond.(Biol.)* **84**, 308-319.

Bruno, V., Battaglia, G., Copani, A., Cespedes, V. M., Galindo, M. F., Cena, V., Sanchez-Prieto, J., Gasparini, F., Kuhn, R., Flor, P. J., & Nicoletti, F. (2001). An activity-dependent switch from facilitation to inhibition in the control of excitotoxicity by group I metabotropic glutamate receptors. *Eur.J.Neurosci.* **13**, 1469-1478.

Buell, G., Schulz, M. F., Arkinstall, S. J., Maury, K., Missotten, M., Adami, N., Talabot, F., & Kawashima, E. (1992). Molecular characterisation, expression and localisation of human neurokinin-3 receptor. *FEBS Lett.* **299**, 90-95.

Burke R.E (1990). Spinal cord: ventral horn. In *The synaptic organziation of the brain*, ed. Sheperd, G. M., pp. 88-132. Oxford University Press.

Burke R.E & Rudomin, P. (1977) Spinal Neurons and synapses. Kandel, E. R. Handbook of physiology, Section 1: The nervous system. [I: The Cellular Biology of Neurons], 877-944. Bethesda, American Physiological Society.

Burke, R. E. (1981). Motor Units: Anatomy, physiology and functional organization. In: Handbook of physiology, Section 1, Vol. II: Motor Control, Part 1. 345-422. Brooks, V.B. ed. Bethesda, American Physiological Society.

Buzsaki, G. (2002). Theta oscillations in the hippocampus. *Neuron* **33**, 325-340.

Cao, C. Q., Evans, R. H., Headley, P. M., & Udvarhelyi, P. M. (1995). A comparison of the effects of selective metabotropic glutamate receptor agonists on synaptically evoked whole cell currents of rat spinal ventral horn neurones in vitro. *Br.J.Pharmacol.* **115**, 1469-1474.

Cao, C. Q., Tse, H. W., Jane, D. E., Evans, R. H., & Headley, P. M. (1997). Metabotropic glutamate receptor antagonists, like $GABA_B$ antagonists, potentiate dorsal root-evoked excitatory synaptic transmission at neonatal rat spinal motoneurons in vitro. *Neuroscience* **78**, 243-250.

Cartmell, J. & Schoepp, D. D. (2000). Regulation of neurotransmitter release by metabotropic glutamate receptors. *J.Neurochem.* **75**, 889-907.

Cazalets, J. R. & Bertrand, S. (2000). Ubiquity of motor networks in the spinal cord of vertebrates. *Brain Res.Bull.* **53**, 627-634.

Cazalets, J. R., Grillner, P., Menard, I., Cremieux, J., & Clarac, F. (1990). Two types of motor rhythm induced by NMDA and amines in an in vitro spinal cord preparation of neonatal rat. *Neurosci.Lett.* **111**, 116-121.

Cazalets, J. R., Sqalli-Houssaini, Y., & Clarac, F. (1992). Activation of the central pattern generators for locomotion by serotonin and excitatory amino acids in neonatal rat. *J.Physiol* **455**, 187-204.

Cazalets, J. R., Sqalli-Houssaini, Y., & Clarac, F. (1994). GABAergic inactivation of the central pattern generators for locomotion in isolated neonatal rat spinal cord. *J.Physiol* **474**, 173-181.

Chapman, C. A. & Lacaille, J. C. (1999). Cholinergic induction of theta-frequency oscillations in hippocampal inhibitory interneurons and pacing of pyramidal cell firing. *J.Neurosci.* **19**, 8637-8645.

Chen, G., Trombley, P. Q., & van den Pol, A. N. (1996). Excitatory actions of GABA in developing rat hypothalamic neurones. *J.Physiol* **494 (Pt 2)**, 451-464.

Chen, J., Heinke, B., & Sandkuhler, J. (2000). Activation of group I metabotropic glutamate receptors induces long-term depression at sensory synapses in superficial spinal dorsal horn. *Neuropharmacology* **39**, 2231-2243.

Cherubini, E., Gaiarsa, J. L., & Ben Ari, Y. (1991). GABA: an excitatory transmitter in early postnatal life. *Trends Neurosci.* **14**, 515-519.

Chub, N. & O'Donovan, M. J. (1998). Blockade and recovery of spontaneous rhythmic activity after application of neurotransmitter antagonists to spinal networks of the chick embryo. *J.Neurosci.* **18**, 294-306.

Chub, N. & O'Donovan, M. J. (2001). Post-episode depression of GABAergic transmission in spinal neurons of the chick embryo. *J.Neurophysiol.* **85**, 2166-2176.

Cohen, A. H. & Harris-Warrick, R. M. (1984). Strychnine eliminates alternating motor output during fictive locomotion in the lamprey. *Brain Res.* **293**, 164-167.

Conn, P. J. & Pin, J. P. (1997). Pharmacology and functions of metabotropic glutamate receptors. *Annu.Rev.Pharmacol.Toxicol.* **37**, 205-237.

Conway, B. A., Hultborn, H., Kiehn, O., & Mintz, I. (1988). Plateau potentials in alpha-motoneurones induced by intravenous injection of L-dopa and clonidine in the spinal cat. *J.Physiol* **405**, 369-384.

Cowley, K. C. & Schmidt, B. J. (1994a). A comparison of motor patterns induced by N-methyl-D-aspartate, acetylcholine and serotonin in the in vitro neonatal rat spinal cord. *Neurosci.Lett.* **171**, 147-150.

Cowley, K. C. & Schmidt, B. J. (1994b). Some limitations of ventral root recordings for monitoring locomotion in the in vitro neonatal rat spinal cord preparation. *Neurosci.Lett.* **171**, 142-146.

Cowley, K. C. & Schmidt, B. J. (1995). Effects of inhibitory amino acid antagonists on reciprocal inhibitory interactions during rhythmic motor activity in the in vitro neonatal rat spinal cord. *J.Neurophysiol.* **74**, 1109-1117.

Cowley, K. C. & Schmidt, B. J. (1997). Regional distribution of the locomotor pattern-generating network in the neonatal rat spinal cord. *J.Neurophysiol.* 77, 247-259.

Cullheim, S., Fleshman, J. W., Glenn, L. L., & Burke, R. E. (1987). Membrane area and dendritic structure in type-identified triceps surae alpha motoneurons. *J.Comp Neurol.* **255**, 68-81.

Cullheim, S. & Kellerth, J. O. (1981). Two kinds of recurrent inhibition of cat spinal alpha-motoneurones as differentiated pharmacologically. *J.Physiol* **312**, 209-224.

Cumberbatch, M. J., Chizh, B. A., & Headley, P. M. (1995). Modulation of excitatory amino acid responses by tachykinins and selective tachykinin receptor agonists in the rat spinal cord. *Br.J.Pharmacol.* **115**, 1005-1012.

Curtis, D. R., Duggan, A. W., Felix, D., & Johnston, G. A. (1971). Bicuculline, an antagonist of GABA and synaptic inhibition in the spinal cord of the cat. *Brain Res.* **32**, 69-96.

Curtis, D. R. & Johnston, G. A. (1974). Amino acid transmitters in the mammalian central nervous system. *Ergeb.Physiol* **69**, 97-188.

Dai, X., Douglas, J.R., Nagy, J.J., Noga, B. R. & Jordan, L. M. (1990).Localization of spinal neurons activated during treadmill locomotion using the c-fos immunohistochemical method. *Soc.Neurosci.Abstract* 16.88.

Dale, N. (1995). Experimentally derived model for the locomotor pattern generator in the Xenopus embryo. *J.Physiol* **489 (Pt 2)**, 489-510.

Dang, K., Naeem, S., Walker, K., Bowery, N. G., & Urban, L. (2002). Interaction of group I mGlu and NMDA receptor agonists within the dorsal horn of the spinal cord of the juvenile rat. *Br.J.Pharmacol.* **136**, 248-254.

Darbon, P., Scicluna, L., Tscherter, A., & Streit, J. (2002). Mechanisms controlling bursting activity induced by disinhibition in spinal cord networks. *Eur.J.Neurosci.* **15**, 671-683.

Davies, J. & Watkins, J. C. (1982). Actions of D and L forms of 2-amino-5-phosphonovalerate and 2-amino-4- phosphonobutyrate in the cat spinal cord. *Brain Res.* **235**, 378-386.

de Leon, R., Hodgson, J. A., Roy, R. R., & Edgerton, V. R. (1994). Extensor- and flexor-like modulation within motor pools of the rat hindlimb during treadmill locomotion and swimming. *Brain Res.* **654**, 241-250.

Delgado-Lezama, R., Perrier, J. F., Nedergaard, S., Svirskis, G., & Hounsgaard, J. (1997). Metabotropic synaptic regulation of intrinsic response properties of turtle spinal motoneurones. *J.Physiol* **504 (Pt 1)**, 97-102.

Delvolve, I., Branchereau, P., Dubuc, R., & Cabelguen, J. M. (1999). Fictive rhythmic motor patterns induced by NMDA in an in vitro brain stem-spinal cord preparation from an adult urodele. *J.Neurophysiol.* **82**, 1074-1077.

Doi, A., Ishibashi, H., Jinno, S., Kosaka, T., & Akaike, N. (2002). Presynaptic inhibition of GABAergic miniature currents by metabotropic glutamate receptor in the rat CNS. *Neuroscience* **109**, 299-311.

Donato, R. & Nistri, A. (2000). Relative contribution by GABA or glycine to Cl^--mediated synaptic transmission on rat hypoglossal motoneurons in vitro. *J.Neurophysiol.* **84**, 2715-2724.

Dong, X. W. & Feldman, J. L. (1999). Distinct subtypes of metabotropic glutamate receptors mediate differential actions on excitability of spinal respiratory motoneurons. *J.Neurosci.* **19**, 5173-5184.

Douglas, J. R., Noga, B. R., Dai, X., & Jordan, L. M. (1993). The effects of intrathecal administration of excitatory amino acid agonists and antagonists on the initiation of locomotion in the adult cat. *J.Neurosci.* **13**, 990-1000.

Dourado, M. & Sargent, P. B. (2002). Properties of nicotinic receptors underlying Renshaw cell excitation by alpha-motor neurons in neonatal rat spinal cord. *J.Neurophysiol.* **87**, 3117-3125.

Drew, T. & Doucet, S. (1991). Application of circular statistics to the study of neuronal discharge during locomotion. *J.Neurosci.Methods* **38**, 171-181.

Durand, D. & Greenwood J.A. (1958). Modifications of the Rayleigh test for uniformity in analysis of two-dimensional orientation data. *The Journal of Geology* **66**, 229-238.

Eaton, S. A., Jane, D. E., Jones, P. L., Porter, R. H., Pook, P. C., Sunter, D. C., Udvarhelyi, P. M., Roberts, P. J., Salt, T. E., & Watkins, J. C. (1993). Competitive antagonism at metabotropic glutamate receptors by (S)-4-carboxyphenylglycine and (RS)-alpha-methyl-4-carboxyphenylglycine. *Eur.J.Pharmacol.* **244**, 195-197.

Eccles, J. C. (1957). *The Physiology of Nerve Cells* Oxford University press, London.

Eccles, J. C., Fatt, P., & Koketsu, K. (1954). Cholinergic and inhibitory synapses in a pathway from motor axon collaterals in motoneurons. *J.Physiol* **126**, 524-562.

Eccles, J. C., Schmidt, R. F., & Willis, W. D. (1963). Pharmacological studies on presynaptic inhibition. *J.Physiol* **168**, 500-530.

Edgerton V.R., Grillner, S., Sjostrom A., & Zangger P. (1976). Central generation of locomotion in vertebrates. In *Neural Control of Locomotion*, eds. Herman R., Grillner S., Sjostrom A., & Zangger P., pp. 439-464. Plenum Press, New York.

Elliott, P. & Wallis, D. I. (1992). Serotonin and L-norepinephrine as mediators of altered excitability in neonatal rat motoneurons studied in vitro. *Neuroscience* **47**, 533-544.

Emonds-Alt, X., Bichon, D., Ducoux, J. P., Heaulme, M., Miloux, B., Poncelet, M., Proietto, V., Van Broeck, D., Vilain, P., Neliat, G., & . (1995). SR 142801, the first potent non-peptide antagonist of the tachykinin NK3 receptor. *Life Sci.* **56**, L27-L32.

Evans, R. H., Francis, A. A., Jones, A. W., Smith, D. A., & Watkins, J. C. (1982). The effects of a series of omega-phosphonic alpha-carboxylic amino acids on electrically evoked and excitant amino acid-induced responses in isolated spinal cord preparations. *Br.J.Pharmacol.* **75**, 65-75.

Faas, G. C., Adwanikar, H., Gereau, R. W., & Saggau, P. (2002). Modulation of presynaptic calcium transients by metabotropic glutamate receptor activation: a differential role in acute depression of synaptic transmission and long-term depression. *J.Neurosci.* **22**, 6885-6890.

Fedirchuk, B., Wenner, P., Whelan, P. J., Ho, S., Tabak, J., & O'Donovan, M. J. (1999). Spontaneous network activity transiently depresses synaptic transmission in the embryonic chick spinal cord. *J.Neurosci.* **19**, 2102-2112.

Feller, M. B. (1999). Spontaneous correlated activity in developing neural circuits. *Neuron* **22**, 653-656.

Feller, M. B., Wellis, D. P., Stellwagen, D., Werblin, F. S., & Shatz, C. J. (1996). Requirement for cholinergic synaptic transmission in the propagation of spontaneous retinal waves. *Science* **272**, 1182-1187.

Fisher, N. D., Baranauskas, G., & Nistri, A. (1994). Multiple types of tachykinin receptor mediate a slow excitation of rat spinal motoneurones in vitro. *Neurosci.Lett.* **165**, 84-88.

Fisher, N. D. & Nistri, A. (1993a). A study of the barium-sensitive and -insensitive components of the action of thyrotropin-releasing hormone on lumbar motoneurons of the rat isolated spinal cord. *Eur.J.Neurosci.* **5**, 1360-1369.

Fisher, N. D. & Nistri, A. (1993b). Substance P and TRH share a common effector pathway in rat spinal motoneurones: an in vitro electrophysiological investigation. *Neurosci.Lett.* **153**, 115-119.

Fisher, R. S. & Alger, B. E. (1984). Electrophysiological mechanisms of kainic acid-induced epileptiform activity in the rat hippocampal slice. *J.Neurosci.* **4**, 1312-1323.

Fitzgerald, M. (1988). The development of activity evoked by fine diameter cutaneous fibres in the spinal cord of the newborn rat. *Neurosci.Lett.* **86**, 161-166.

Fitzjohn, S. M., Palmer, M. J., May, J. E., Neeson, A., Morris, S. A., & Collingridge, G. L. (2001). A characterisation of long-term depression induced by metabotropic glutamate receptor activation in the rat hippocampus in vitro. *J.Physiol* **537**, 421-430.

Flatman, J. A., Engberg, I., & Lambert, J. D. (1982). Reversibility of Ia EPSP investigated with intracellularly iontophoresed QX-222. *J.Neurophysiol.* **48**, 419-430.

Forssberg, H. & Grillner, S. (1973). The locomotion of the acute spinal cat injected with clonidine i.v. *Brain Res.* **50**, 184-186.

Forsythe, I. D. & Redman, S. J. (1988). The dependence of motoneurone membrane potential on extracellular ion concentrations studied in isolated rat spinal cord. *J.Physiol* **404**, 83-99.

Fox, A. J., Naeem, S., Patel, I. A., Walpole, C., & Urban, L. (1996). Receptors mediating tachykinin-evoked depolarisations of neurons in the neonatal rat spinal cord. *Acta Biol.Hung.* **47**, 129-144.

Fulton, B. P. & Walton, K. (1986). Electrophysiological properties of neonatal rat motoneurones studied in vitro. *J.Physiol* **370**, 651-678.

Gaiarsa, J. L., Corradetti, R., Ben Ari, Y., & Cherubini, E. (1990). GABA mediated synaptic events in neonatal rat CA3 pyramidal neurons in vitro: modulation by NMDA and non-NMDA receptors. *Adv.Exp.Med.Biol.* **268**, 151-159.

Galli, L. & Maffei, L. (1988). Spontaneous impulse activity of rat retinal ganglion cells in prenatal life. *Science* **242**, 90-91.

Gao, B. X., Cheng, G., & Ziskind-Conhaim, L. (1998). Development of spontaneous synaptic transmission in the rat spinal cord. *J.Neurophysiol.* **79**, 2277-2287.

Gao, B. X. & Ziskind-Conhaim, L. (1995). Development of glycine- and GABA-gated currents in rat spinal motoneurons. *J.Neurophysiol.* **74**, 113-121.

Gao, X. B. & van den Pol, A. N. (2001). GABA, not glutamate, a primary transmitter driving action potentials in developing hypothalamic neurons. *J.Neurophysiol.* **85**, 425-434.

Gao, Z. & Peet, N. P. (1999). Recent advances in neurokinin receptor antagonists. *Curr.Med.Chem.* **6**, 375-388.

Garaschuk, O., Hanse, E., & Konnerth, A. (1998). Developmental profile and synaptic origin of early network oscillations in the CA1 region of rat neonatal hippocampus. *J.Physiol* **507 (Pt 1)**, 219-236.

Garcia-Rill, E., Skinner, R. D., & Fitzgerald, J. A. (1985). Chemical activation of the mesencephalic locomotor region. *Brain Res.* **330**, 43-54.

Gerber, G., Zhong, J., Youn, D., & Randic, M. (2000). Group II and group III metabotropic glutamate receptor agonists depress synaptic transmission in the rat spinal cord dorsal horn. *Neuroscience* **100**, 393-406.

Grillner, S. (1981). Control of locomotion in bipeds, tetrapods, and fish. In *Handbook of Physiology*, ed. Brooks, V. B., pp. 1179-1236. American Physiological Society.

Grillner, S. (2000). From egg to action. *Brain Res.Bull.* **53**, 473-477.

Grillner, S., Deliagina, T., Ekeberg, O., El Manira, A., Hill, R. H., Lansner, A., Orlovsky, G. N., & Wallen, P. (1995). Neural networks that co-ordinate locomotion and body orientation in lamprey. *Trends Neurosci.* **18**, 270-279.

Grillner, S., Parker, D., & El Manira, A. (1998). Vertebrate locomotion--a lamprey perspective. *Ann.N.Y.Acad.Sci.* **860**, 1-18.

Grillner, S., Wallen, P., Brodin, L., & Lansner, A. (1991). Neuronal network generating locomotor behavior in lamprey: circuitry, transmitters, membrane properties, and simulation. *Annu.Rev.Neurosci.* **14**, 169-199.

Gruner, J. A. & Altman, J. (1980). Swimming in the rat: analysis of locomotor performance in comparison to stepping. *Exp.Brain Res.* **40**, 374-382.

Guertin, P. A. & Hounsgaard, J. (1998). NMDA-Induced intrinsic voltage oscillations depend on L-type calcium channels in spinal motoneurons of adult turtles. *J.Neurophysiol.* **80**, 3380-3382.

Hayashi, Y., Sekiyama, N., Nakanishi, S., Jane, D. E., Sunter, D. C., Birse, E. F., Udvarhelyi, P. M., & Watkins, J. C. (1994). Analysis of agonist and antagonist activities of phenylglycine derivatives for different cloned metabotropic glutamate receptor subtypes. *J.Neurosci.* **14**, 3370-3377.

Ho, S. & O'Donovan, M. J. (1993). Regionalization and intersegmental coordination of rhythm-generating networks in the spinal cord of the chick embryo. *J.Neurosci.* **13**, 1354-1371.

Hochman, S., Jordan, L. M., & MacDonald, J. F. (1994b). N-methyl-D-aspartate receptor-mediated voltage oscillations in neurons surrounding the central canal in slices of rat spinal cord. *J.Neurophysiol.* **72**, 565-577.

Hochman, S., Jordan, L. M., & Schmidt, B. J. (1994a). TTX-resistant NMDA receptor-mediated voltage oscillations in mammalian lumbar motoneurons. *J.Neurophysiol.* **72**, 2559-2562.

Holohean, A. M., Hackman, J. C., & Davidoff, R. A. (1999). Mechanisms involved in the metabotropic glutamate receptor-enhancement of NMDA-mediated motoneurone responses in frog spinal cord. *Br.J.Pharmacol.* **126**, 333-341.

Honoré, P., Menning, P. M., Rogers, S. D., Nichols, M. L., Basbaum, A. I., Besson, J. M., & Mantyh, P. W. (1999). Spinal substance P receptor expression and internalization in acute, short-term, and long-term inflammatory pain states. *J.Neurosci.* **19**, 7670-7678.

Hornby, T. G., McDonagh, J. C., Reinking, R. M., & Stuart, D. G. (2002). Effects of excitatory modulation on intrinsic properties of turtle motoneurons. *J.Neurophysiol.* **88**, 86-97.

Hosokawa, Y., Sciancalepore, M., Strata, F., Martina, M., & Cherubini, E. (1994). Developmental changes in spontaneous GABAA-mediated synaptic events in rat hippocampal CA3 neurons. *Eur.J.Neurosci.* **6**, 805-813.

Hounsgaard, J. & Kiehn, O. (1989). Serotonin-induced bistability of turtle motoneurones caused by a nifedipine-sensitive calcium plateau potential. *J.Physiol* **414**, 265-282.

Hultborn, H., Conway, B. A., Gossard, J. P., Brownstone, R., Fedirchuk, B., Schomburg, E. D., Enriquez-Denton, M., & Perreault, M. C. (1998). How do we approach the locomotor network in the mammalian spinal cord? *Ann.N.Y.Acad.Sci.* **860**, 70-82.

Hultborn, H. & Kiehn, O. (1992). Neuromodulation of vertebrate motor neuron membrane properties. *Curr.Opin.Neurobiol.* **2**, 770-775.

Iansek, R. & Redman, S. J. (1973). The amplitude, time course and charge of unitary excitatory post-synaptic potentials evoked in spinal motoneurone dendrites. *J.Physiol* **234**, 665-688.

Iizuka, M., Kiehn, O., & Kudo, N. (1997). Development in neonatal rats of the sensory resetting of the locomotor rhythm induced by NMDA and 5-HT. *Exp.Brain Res.* **114**, 193-204.

Inoue, K., Nakazawa, K., Inoue, K., & Fujimori, K. (1995). Nonselective cation channels coupled with tachykinin receptors in rat sensory neurons. *J.Neurophysiol.* **73**, 736-742.

Inoue, M., Oomura, Y., Yakushiji, T., & Akaike, N. (1986). Intracellular calcium ions decrease the affinity of the GABA receptor. *Nature* **324**, 156-158.

Ishida, M., Saitoh, T., & Shinozaki, H. (1993a). A new metabotropic glutamate receptor agonist: developmental change of its sensitivity to receptors in the newborn rat spinal cord. *Neurosci.Lett.* **160**, 156-158.

Ishida, M., Saitoh, T., Shimamoto, K., Ohfune, Y., & Shinozaki, H. (1993b). A novel metabotropic glutamate receptor agonist: marked depression of monosynaptic excitation in the newborn rat isolated spinal cord. *Br.J.Pharmacol.* **109**, 1169-1177.

Jane, D. E., Jones, P. L., Pook, P. C., Tse, H. W., & Watkins, J. C. (1994). Actions of two new antagonists showing selectivity for different sub-types of metabotropic glutamate receptor in the neonatal rat spinal cord. *Br.J.Pharmacol.* **112**, 809-816.

Jane, D. E., Pittaway, K., Sunter, D. C., Thomas, N. K., & Watkins, J. C. (1995). New phenylglycine derivatives with potent and selective antagonist activity at presynaptic glutamate receptors in neonatal rat spinal cord. *Neuropharmacology* **34**, 851-856.

Jane, D. E., Thomas, N. K., Tse, H. W., & Watkins, J. C. (1996). Potent antagonists at the L-AP4- and (1S,3S)-ACPD-sensitive presynaptic metabotropic glutamate receptors in the neonatal rat spinal cord. *Neuropharmacology* **35**, 1029-1035.

Jankowska, E. (1992). Interneuronal relay in spinal pathways from proprioception. *Prog.Neurobiol.* **38**, 335-378.

Jankowska, E. (2001). Spinal interneuronal systems: identification, multifunctional character and reconfigurations in mammals. *J.Physiol* **533**, 31-40.

Jefferys, J. G., Traub, R. D., & Whittington, M. A. (1996). Neuronal networks for induced '40 Hz' rhythms. *Trends Neurosci.* **19**, 202-208.

Jia, H., Rustioni, A., & Valtschanoff, J. G. (1999). Metabotropic glutamate receptors in superficial laminae of the rat dorsal horn. *J.Comp Neurol.* **410**, 627-642.

Jiang, Z. G., Shen, E., Wang, M. Y., & Dun, N. J. (1991). Excitatory postsynaptic potentials evoked by ventral root stimulation in neonate rat motoneurons in vitro. *J.Neurophysiol.* **65**, 57-66.

Jonas, P., Bischofberger, J., & Sandkuhler, J. (1998). Corelease of two fast neurotransmitters at a central synapse. *Science* **281**, 419-424.

Jones, M. W. & Headley, P. M. (1995). Interactions between metabotropic and ionotropic glutamate receptor agonists in the rat spinal cord in vivo. *Neuropharmacology* **34**, 1025-1031.

Jordan, L. M. (1998). Initiation of locomotion in mammals. *Ann.N.Y.Acad.Sci.* **860**, 83-93.

Katsurabayashi, S., Kubota, H., Wang, Z. M., Rhee, J. S., & Akaike, N. (2001). cAMP-dependent presynaptic regulation of spontaneous glycinergic IPSCs in mechanically dissociated rat spinal cord neurons. *J.Neurophysiol.* **85**, 332-340.

Katz, L. C. & Shatz, C. J. (1996). Synaptic activity and the construction of cortical circuits. *Science* **274**, 1133-1138.

Kettunen, P., Krieger, P., Hess, D., & El Manira, A. (2002). Signaling mechanisms of metabotropic glutamate receptor 5 subtype and its endogenous role in a locomotor network. *J.Neurosci.* **22**, 1868-1873.

Khalilov, I., Khazipov, R., Esclapez, M., & Ben Ari, Y. (1997). Bicuculline induces ictal seizures in the intact hippocampus recorded in vitro. *Eur.J.Pharmacol.* **319**, R5-R6.

Khiroug, L., Giniatullin, R., Sokolova, E., Talantova, M., & Nistri, A. (1997). Imaging of intracellular calcium during desensitization of nicotinic acetylcholine receptors of rat chromaffin cells. *Br.J.Pharmacol.* **122**, 1323-1332.

Khiroug, L., Sokolova, E., Giniatullin, R., Afzalov, R., & Nistri, A. (1998). Recovery from desensitization of neuronal nicotinic acetylcholine receptors of rat chromaffin cells is modulated by intracellular calcium through distinct second messengers. *J.Neurosci.* **18**, 2458-2466.

Kiehn, O. (1991). Plateau potentials and active integration in the 'final common pathway' for motor behaviour. *Trends Neurosci.* **14**, 68-73.

Kiehn, O. & Eken, T. (1998). Functional role of plateau potentials in vertebrate motor neurons. *Curr.Opin.Neurobiol.* **8**, 746-752.

Kiehn, O., Hounsgaard, J., & Sillar, K. T. (1997). Basic building blocks of vertebrate spinal central pattern generators. In *Neurons, Networks, and Motor Behavior*, eds. Stein, P. S. G., Grillner, S., Selverston, A. I., & Stuart, D. G., pp. 47-59. The MIT Press, Cambridge, Massachusetts, USA.

Kiehn, O., Iizuka, M., & Kudo, N. (1992). Resetting from low threshold afferents of N-methyl-D-aspartate-induced locomotor rhythm in the isolated spinal cord-hindlimb preparation from newborn rats. *Neurosci.Lett.* **148**, 43-46.

Kiehn, O., Johnson, B. R., & Raastad, M. (1996). Plateau properties in mammalian spinal interneurons during transmitter-induced locomotor activity. *Neuroscience* **75**, 263-273.

Kiehn, O. & Kjaerulff, O. (1996). Spatiotemporal characteristics of 5-HT and dopamine-induced rhythmic hindlimb activity in the in vitro neonatal rat. *J.Neurophysiol.* **75**, 1472-1482.

Kiehn, O. & Kjaerulff, O. (1998). Distribution of central pattern generators for rhythmic motor outputs in the spinal cord of limbed vertebrates. *Ann.N.Y.Acad.Sci.* **860**, 110-129.

Kiehn, O., Kjaerulff, O., Tresch, M. C., & Harris-Warrick, R. M. (2000). Contributions of intrinsic motor neuron properties to the production of rhythmic motor output in the mammalian spinal cord. *Brain Res.Bull.* **53**, 649-659.

King, A. E. & Liu, X. H. (1996). Dual action of metabotropic glutamate receptor agonists on neuronal excitability and synaptic transmission in spinal ventral horn neurons in vitro. *Neuropharmacology* **35**, 1673-1680.

Kjaerulff, O., Barajon, I., & Kiehn, O. (1994). Sulphorhodamine-labelled cells in the neonatal rat spinal cord following chemically induced locomotor activity in vitro. *J.Physiol* **478 (Pt 2)**, 265-273.

Kjaerulff, O. & Kiehn, O. (1996). Distribution of networks generating and coordinating locomotor activity in the neonatal rat spinal cord in vitro: a lesion study. *J.Neurosci.* **16**, 5777-5794.

Kjaerulff, O. & Kiehn, O. (1997). Crossed rhythmic synaptic input to motoneurons during selective activation of the contralateral spinal locomotor network. *J.Neurosci.* **17**, 9433-9447.

Kouznetsova, M. & Nistri, A. (2000). Facilitation of cholinergic transmission by substance P methyl ester in the mouse hippocampal slice preparation. *Eur.J.Neurosci.* **12**, 585-594.

Kremer, E. & Lev-Tov, A. (1997). Localization of the spinal network associated with generation of hindlimb locomotion in the neonatal rat and organization of its transverse coupling system. *J.Neurophysiol.* **77**, 1155-1170.

Krieger, P., El Manira, A., & Grillner, S. (1996). Activation of pharmacologically distinct metabotropic glutamate receptors depresses reticulospinal-evoked monosynaptic EPSPs in the lamprey spinal cord. *J.Neurophysiol.* **76**, 3834-3841.

Krieger, P., Grillner, S., & El Manira, A. (1998). Endogenous activation of metabotropic glutamate receptors contributes to burst frequency regulation in the lamprey locomotor network. *Eur.J.Neurosci.* **10**, 3333-3342.

Krieger, P., Hellgren-Kotaleski, J., Kettunen, P., & El Manira, A. J. (2000). Interaction between metabotropic and ionotropic glutamate receptors regulates neuronal network activity. *J.Neurosci.* **20**, 5382-5391.

Krnjevic, K. (1974). Chemical nature of synaptic transmission in vertebrates. *Physiol.Rev.* **54**, 540.

Krnjevic, K. & Morris, M. E. (1974). Extracellular accumulation of K+ evoked by activity of primary afferent fibers in the cuneate nucleus and dorsal horn of cats. *Can.J.Physiol Pharmacol.* **52**, 852-871.

Krnjevic, K. & Morris, M. E. (1975). Factors determining the decay of K+ potentials and focal potentials in the central nervous system. *Can.J.Physiol Pharmacol.* **53**, 923-934.

Kudo, N., Ozaki, S., & Yamada, T. (1991). Ontogeny of rhythmic activity in the spinal cord of the rat. In *Neurobiological basis of human locomotion*, eds. Shimamura M, Grillner S., & Edgerton V.R., pp. 127-136. Japan Scientific Societies Press, Tokyo.

Kudo, N. & Yamada, T. (1987). N-methyl-D,L-aspartate-induced locomotor activity in a spinal cord-hindlimb muscles preparation of the newborn rat studied in vitro. *Neurosci.Lett.* **75**, 43-48.

Lamsa, K., Palva, J. M., Ruusuvuori, E., Kaila, K., & Taira, T. (2000). Synaptic $GABA_A$ activation inhibits AMPA-kainate receptor-mediated bursting in the newborn (P0-P2) rat hippocampus. *J.Neurophysiol.* **83**, 359-366.

Landmesser, L. T. & O'Donovan, M. J. (1984a). Activation patterns of embryonic chick hind limb muscles recorded in ovo and in an isolated spinal cord preparation. *J.Physiol* **347**, 189-204.

Landmesser, L. T. & O'Donovan, M. J. (1984b). The activation patterns of embryonic chick motoneurones projecting to inappropriate muscles. *J.Physiol* **347**, 205-224.

Lape, R. & Nistri, A. (2000). Current and voltage clamp studies of the spike medium afterhyperpolarization of hypoglossal motoneurons in a rat brain stem slice preparation. *J.Neurophysiol.* **83**, 2987-2995.

Larkman, P. M. & Kelly, J. S. (1998). Characterization of 5-HT-sensitive potassium conductances in neonatal rat facial motoneurones in vitro. *J.Physiol* **508 (Pt 1)**, 67-81.

Larson, M. D. (1969). An analysis of the action of strychnine on the recurrent IPSP and amino acid induced inhibitions in the cat spinal cord. *Brain Res.* **15**, 185-200.

Latham, P. E., Richmond, B. J., Nelson, P. G., & Nirenberg, S. (2000a). Intrinsic dynamics in neuronal networks. I. Theory. *J.Neurophysiol.* **83**, 808-827.

Latham, P. E., Richmond, B. J., Nirenberg, S., & Nelson, P. G. (2000b). Intrinsic dynamics in neuronal networks. II. experiment. *J.Neurophysiol.* **83**, 828-835.

Lee, R. H. & Heckman, C. J. (1996). Influence of voltage-sensitive dendritic conductances on bistable firing and effective synaptic current in cat spinal motoneurons in vivo. *J.Neurophysiol.* **76**, 2107-2110.

Legendre, P., McKenzie, J. S., Dupouy, B., & Vincent, J. D. (1985). Evidence for bursting pacemaker neurones in cultured spinal cord cells. *Neuroscience* **16**, 753-767.

Lev-Tov, A. & Delvolve, I. (2000). Pattern generation in non-limb moving segments of the mammalian spinal cord. *Brain Res.Bull.* **53**, 671-675.

Lev-Tov, A., Delvolve, I., & Kremer, E. (2000). Sacrocaudal afferents induce rhythmic efferent bursting in isolated spinal cords of neonatal rats. *J.Neurophysiol.* **83**, 888-894.

Lev-Tov, A. & Pinco, M. (1992). In vitro studies of prolonged synaptic depression in the neonatal rat spinal cord. *J.Physiol* **447**, 149-169.

Levy, R. A. (1977). The role of GABA in primary afferent depolarization. *Prog.Neurobiol.* **9**, 211-267.

Li, H., Ohishi, H., Kinoshita, A., Shigemoto, R., Nomura, S., & Mizuno, N. (1997). Localization of a metabotropic glutamate receptor, mGluR7, in axon terminals of presumed nociceptive, primary afferent fibers in the superficial layers of the spinal dorsal horn: an electron microscope study in the rat. *Neurosci.Lett.* **223**, 153-156.

Lin, Q., Peng, Y. B., & Willis, W. D. (1996). Inhibition of primate spinothalamic tract neurons by spinal glycine and GABA is reduced during central sensitization. *J.Neurophysiol.* **76**, 1005-1014.

Linden, D. R., Reutter, M. A., McCarson, K. E., & Seybold, V. S. (2000). Time-dependent changes in neurokinin(3) receptors and tachykinins during adjuvant-induced peripheral inflammation in the rat. *Neuroscience* **98**, 801-811.

Liu, H., Brown, J. L., Jasmin, L., Maggio, J. E., Vigna, S. R., Mantyh, P. W., & Basbaum, A. I. (1994). Synaptic relationship between substance P and the substance P receptor: light and electron microscopic characterization of the mismatch between neuropeptides and their receptors. *Proc.Natl.Acad.Sci.U.S.A* **91**, 1009-1013.

Lukasiuk, K. & Pitkanen, A. (2000). $GABA_A$-mediated toxicity of hippocampal neurons in vitro. *J.Neurochem.* **74**, 2445-2454.

MacDonald, R. L., Rogers, C. J., & Twyman, R. E. (1989). Kinetic properties of the $GABA_A$ receptor main conductance state of mouse spinal cord neurones in culture. *J.Physiol* **410**, 479-499.

MacLean, J. N., Hochman, S., & Magnuson, D. S. (1995). Lamina VII neurons are rhythmically active during locomotor-like activity in the neonatal rat spinal cord. *Neurosci.Lett.* **197**, 9-12.

MacLean, J. N., Schmidt, B. J., & Hochman, S. (1997). NMDA receptor activation triggers voltage oscillations, plateau potentials and bursting in neonatal rat lumbar motoneurons in vitro. *Eur.J.Neurosci.* **9**, 2702-2711.

Maeda, E., Robinson, H. P., & Kawana, A. (1995). The mechanisms of generation and propagation of synchronized bursting in developing networks of cortical neurons. *J.Neurosci.* **15**, 6834-6845.

Maggio, J. E. (1988). Tachykinins. *Annu.Rev.Neurosci.* **11**, 13-28.

Magnuson, D. S., Schramm, M. J., & MacLean, J. N. (1995). Long-duration, frequency-dependent motor responses evoked by ventrolateral funiculus stimulation in the neonatal rat spinal cord. *Neurosci.Lett.* **192**, 97-100.

Magnuson, D. S. & Trinder, T. C. (1997). Locomotor rhythm evoked by ventrolateral funiculus stimulation in the neonatal rat spinal cord in vitro. *J.Neurophysiol.* **77**, 200-206.

Marti, M., Paganini, F., Stocchi, S., Bianchi, C., Beani, L., & Morari, M. (2001). Presynaptic group I and II metabotropic glutamate receptors oppositely modulate striatal acetylcholine release. *Eur.J.Neurosci.* **14**, 1181-1184.

Martina, M., Strata, F., & Cherubini, E. (1995). Whole cell and single channel properties of a new GABA receptor transiently expressed in the Hippocampus. *J.Neurophysiol.* **73**, 902-906.

McClellan, A. D. (1984). Descending control and sensory gating of 'fictive' swimming and turning responses elicited in an in vitro preparation of the lamprey brainstem/spinal cord. *Brain Res.* **302**, 151-162.

Meister, M., Wong, R. O., Baylor, D. A., & Shatz, C. J. (1991). Synchronous bursts of action potentials in ganglion cells of the developing mammalian retina. *Science* **252**, 939-943.

Mileusnic, D., Lee, J. M., Magnuson, D. J., Hejna, M. J., Krause, J. E., Lorens, J. B., & Lorens, S. A. (1999). Neurokinin-3 receptor distribution in rat and human brain: an immunohistochemical study. *Neuroscience* **89**, 1269-1290.

Moore, L. E., Chub, N., Tabak, J., & O'Donovan, M. (1999). NMDA-induced dendritic oscillations during a soma voltage clamp of chick spinal neurons. *J.Neurosci.* **19**, 8271-8280.

Morisset, V. & Nagy, F. (1999). Ionic basis for plateau potentials in deep dorsal horn neurons of the rat spinal cord. *J.Neurosci.* **19**, 7309-7316.

Nicoll, R. A. & Alger, B. E. (1979). Presynaptic inhibition: transmitter and ionic mechanisms. *Int.Rev.Neurobiol.* **21**, 217-258.

Nishimaru, H., Iizuka, M., Ozaki, S., & Kudo, N. (1996). Spontaneous motoneuronal activity mediated by glycine and GABA in the spinal cord of rat fetuses in vitro. *J.Physiol* **497 (Pt 1)**, 131-143.

Nishimaru, H. & Kudo, N. (2000). Formation of the central pattern generator for locomotion in the rat and mouse. *Brain Res.Bull.* **53**, 661-669.

Nistri, A. (1983). Spinal cord pharamacology of GABA and related amino acids. Davidoff, R. A. In *Handbook of the spinal cord.* [1 Pharmacology], 45-104. New York, Dekker.

Nistri, A. & Gutman, A. (2001). Basic properties of excitable cells at rest. In *Cellular and Molecular Neurobiology*, ed. Hammond, C., pp. 57-68. Academic Press, London.

Noga, B. R., Cowley, K. C., Huang, A., Jordan, L. M., & Schmidt, B. J. (1993).Effects of inhibitory amino acids antagonist on locomotor rhythm in the decerebrate cat. *Soc.Neurosci.Abstract* 19.540.

O'Brien, J. A. & Berger, A. J. (1999). Cotransmission of GABA and glycine to brain stem motoneurons. *J.Neurophysiol.* **82**, 1638-1641.

O'Donovan, M., Ho, S., & Yee, W. (1994). Calcium imaging of rhythmic network activity in the developing spinal cord of the chick embryo. *J.Neurosci.* **14**, 6354-6369.

O'Donovan, M. J. & Rinzel, J. (1997). Synaptic depression: a dynamic regulator of synaptic communication with varied functional roles. *Trends Neurosci.* **20**, 431-433.

O'Donovan, M. J., Wenner, P., Chub, N., Tabak, J., & Rinzel, J. (1998). Mechanisms of spontaneous activity in the developing spinal cord and their relevance to locomotion. *Ann.N.Y.Acad.Sci.* **860**, 130-141.

Ogawa, T., Kanazawa, I., & Kimura, S. (1985). Regional distribution of substance P, neurokinin alpha and neurokinin beta in rat spinal cord, nerve roots and dorsal root ganglia, and the effects of dorsal root section or spinal transection. *Brain Res.* **359**, 152-157.

Ohishi, H., Akazawa, C., Shigemoto, R., Nakanishi, S., & Mizuno, N. (1995). Distributions of the mRNAs for L-2-amino-4-phosphonobutyrate-sensitive metabotropic glutamate receptors, mGluR4 and mGluR7, in the rat brain. *J.Comp Neurol.* **360**, 555-570.

Ohishi, H., Shigemoto, R., Nakanishi, S., & Mizuno, N. (1993). Distribution of the messenger RNA for a metabotropic glutamate receptor, mGluR2, in the central nervous system of the rat. *Neuroscience* **53**, 1009-1018.

Otsuka, M. & Konishi, S. (1974). Electrophysiology of mammalian spinal cord in vitro. *Nature* **252**, 733-734.

Otsuka, M. & Yoshioka, K. (1993). Neurotransmitter functions of mammalian tachykinins. *Physiol. Rev.* **73**, 229-308.

Parker, D., Zhang, W., & Grillner, S. (1998). Substance P modulates NMDA responses and causes long-term protein synthesis-dependent modulation of the lamprey locomotor network. *J.Neurosci.* **18**, 4800-4813.

Phenna, S., Carpenter, E., Peers, C., Maudsley, S., & Gent, J. P. (1996). Inhibition of Ca^{2+}-sensitive K+ currents in NG 108-15 cells by substance P and related tachykinins. *Br.J.Pharmacol.* **119**, 315-320.

Pin, J. P. & Duvoisin, R. (1995). The metabotropic glutamate receptors: structure and functions. *Neuropharmacology* **34**, 1-26.

Pinco, M. & Lev-Tov, A. (1993a). Modulation of monosynaptic excitation in the neonatal rat spinal cord. *J.Neurophysiol.* **70**, 1151-1158.

Pinco, M. & Lev-Tov, A. (1993b). Synaptic excitation of alpha-motoneurons by dorsal root afferents in the neonatal rat spinal cord. *J.Neurophysiol.* **70**, 406-417.

Pinnock, R. D., Suman-Chauhan, N., Chung, F. Z., Webdale, L., Madden, Z., Hill, D. R., & Woodruff, G. N. (1994). Characterization of tachykinin mediated increases in $[Ca^{2+}]_i$ in Chinese hamster ovary cells expressing human tachykinin NK_3 receptors. *Eur.J.Pharmacol.* **269**, 73-78.

Polc, P. & Haefely, W. (1982). Benzodiazepines enhance the bicuculline-sensitive part of recurrent Renshaw inhibition in the cat spinal cord. *Neurosci.Lett.* **28**, 193-197.

Pook, P. C., Sunter, D. C., Udvarhelyi, P. M., & Watkins, J. C. (1992). Evidence for presynaptic depression of monosynaptic excitation in neonatal rat motoneurones by (1S,3S)- and (1S,3R)-ACPD. *Exp.Physiol* **77**, 529-532.

Pratt, C. A. & Jordan, L. M. (1987). Ia inhibitory interneurons and Renshaw cells as contributors to the spinal mechanisms of fictive locomotion. *J.Neurophysiol.* **57**, 56-71.

Prime, L., Pichon, Y., & Moore, L. E. (1999). N-Methyl-D-aspartate-induced oscillations in whole cell clamped neurons from the isolated spinal cord of Xenopus laevis embryos. *J.Neurophysiol.* **82**, 1069-1073.

Raastad, M., Enriquez-Denton, M., & Kiehn, O. (1998). Synaptic signaling in an active central network only moderately changes passive membrane properties. *Proc.Natl.Acad.Sci.U.S.A* **95**, 10251-10256.

Raastad, M., Johnson, B. R., & Kiehn, O. (1996). The number of postsynaptic currents necessary to produce locomotor-related cyclic information in neurons in the neonatal rat spinal cord. *Neuron* **17**, 729-738.

Raastad, M., Johnson, B. R., & Kiehn, O. (1997). Analysis of EPSCs and IPSCs carrying rhythmic, locomotor-related information in the isolated spinal cord of the neonatal rat. *J.Neurophysiol.* **78**, 1851-1859.

Regoli, D., Boudon, A., & Fauchere, J. L. (1994). Receptors and antagonists for substance P and related peptides. *Pharmacol.Rev.* **46**, 551-599.

Reichling, D. B., Kyrozis, A., Wang, J., & MacDermott, A. B. (1994). Mechanisms of GABA and glycine depolarization-induced calcium transients in rat dorsal horn neurons. *J.Physiol* **476** , 411-421.

Rekling, J. C., Funk, G. D., Bayliss, D. A., Dong, X. W., & Feldman, J. L. (2000). Synaptic control of motoneuronal excitability. *Physiol Rev.* **80**, 767-852.

Renshaw, B. (1941). Influence of discharge of motoneurons upon excitation of neighbouring motoneurons. *J.Neurophysiol.* **4**, 167-183.

Rexed, B. (1952). The cytoarchitectonic organization of the spinal cord of the cat. *J.Comp Neurol.* **96**, 415-495.

Richter, D. W. (1996). Neural regulation of respiration: rhythmogenesis and afferent control. In *Comprehensive human physiology* , ed. Greger, R. W. U., pp. 2079-2095. Springer, Heidelberg.

Ritter, A., Wenner, P., Ho, S., Whelan, P. J., & O'Donovan, M. J. (1999). Activity patterns and synaptic organization of ventrally located interneurons in the embryonic chick spinal cord. *J.Neurosci.* **19**, 3457-3471.

Rivera, C., Voipio, J., Payne, J. A., Ruusuvuori, E., Lahtinen, H., Lamsa, K., Pirvola, U., Saarma, M., & Kaila, K. (1999). The K^+/Cl^- co-transporter KCC2 renders GABA hyperpolarizing during neuronal maturation. *Nature* **397**, 251-255.

Roberts, A., Soffe, S. R., Wolf, E. S., Yoshida, M., & Zhao, F. Y. (1998). Central circuits controlling locomotion in young frog tadpoles. *Ann.N.Y.Acad.Sci.* **860**, 19-34.

Rodriguez-Moreno, A., Sistiaga, A., Lerma, J., & Sanchez-Prieto, J. (1998). Switch from facilitation to inhibition of excitatory synaptic transmission by group I mGluR desensitization. *Neuron* **21**, 1477-1486.

Rose, P. K. & Richmond, F. J. R. (1981). White-matter dendrites in the upper cervical spinal cord of the adult cat: a light and electron microscopy study. *J.Comp Neurol.* **199**, 191-203.

Rossignol, S. (1996). Neural control of stereotypic limb movement. In *Handbook of physiology*, eds. Rowell, L. B. & Sheperd J.T., pp. 173-216. American Physiological Society.

Rozzo, A., Ballerini, L., & Nistri, A. (1999). Antagonism by (1,2,5,6-tetrahydropyridine-4-yl) methylphosphinic acid of synaptic transmission in the neonatal rat spinal cord in vitro: an electrophysiological study. *Neuroscience* **90**, 1085-1092.

Rozzo, A., Ballerini, L., Abbate, G., & Nistri, A. (2002a). Experimental and modeling studies of novel bursts induced by blocking Na^+ pump and synaptic inhibition in the rat spinal cord. *J.Neurophysiol.* **88**, 676-691.

Rozzo, A., Armellin, M., Franzot, J., Chiaruttini, C., Nistri, A., & Tongiorgi, E. (2002b). Expression and dendritic mRNA localization of GABAC receptor rho1 and rho2 subunits in developing rat brain and spinal cord. *Eur.J.Neurosci.* **15**, 1747-1758.

Rusin, K. I., Ryu, P. D., & Randic, M. (1992). Modulation of excitatory amino acid responses in rat dorsal horn neurons by tachykinins. *J.Neurophysiol.* **68**, 265-286.

Russo, R. E., Nagy, F., & Hounsgaard, J. (1997). Modulation of plateau properties in dorsal horn neurones in a slice preparation of the turtle spinal cord. *J.Physiol* **499 (Pt 2)**, 459-474.

Sanchez-Vives, M. V. & McCormick, D. A. (2000). Cellular and network mechanisms of rhythmic recurrent activity in neocortex. *Nat.Neurosci.* **3**, 1027-1034.

Schmidt, B. J. (1994). Afterhyperpolarization modulation in lumbar motoneurons during locomotor-like rhythmic activity in the neonatal rat spinal cord in vitro. *Exp.Brain Res.* **99**, 214-222.

Schmidt, B. J., Hochman, S., & MacLean, J. N. (1998). NMDA receptor-mediated oscillatory properties: potential role in rhythm generation in the mammalian spinal cord. *Ann.N.Y.Acad.Sci.* **860**, 189-202.

Schneider, S. P. & Fyffe, R. E. (1992). Involvement of GABA and glycine in recurrent inhibition of spinal motoneurons. *J.Neurophysiol.* **68**, 397-406.

Schoepp, D. D., Jane, D. E., & Monn, J. A. (1999). Pharmacological agents acting at subtypes of metabotropic glutamate receptors. *Neuropharmacology* **38**, 1431-1476.

Schwindt, P. C. & Crill, W. E. (1981). Negative slope conductance at large depolarizations in cat spinal motoneurons. *Brain Res.* **207**, 471-475.

Sejnowski, T. J. & Destexhe, A. (2000). Why do we sleep? *Brain Res.* **886**, 208-223.

Semyanov, A. & Kullmann, D. M. (2000). Modulation of GABAergic signaling among interneurons by metabotropic glutamate receptors. *Neuron* **25**, 663-672.

Senn, W., Wannier, T., Kleinle, J., Luscher, H. R., Muller, L., Streit, J., & Wyler, K. (1998). Pattern generation by two coupled time-discrete neural networks with synaptic depression. *Neural Comput.* **10**, 1251-1275.

Sernagor, E., Chub, N., Ritter, A., & O'Donovan, M. J. (1995). Pharmacological characterization of the rhythmic synaptic drive onto lumbosacral motoneurons in the chick embryo spinal cord. *J.Neurosci.* **15**, 7452-7464.

Seybold, V. S., Grkovic, I., Portbury, A. L., Ding, Y. Q., Shigemoto, R., Mizuno, N., Furness, J. B., & Southwell, B. R. (1997). Relationship of NK_3 receptor-immunoreactivity to subpopulations of neurons in rat spinal cord. *J.Comp Neurol.* **381**, 439-448.

Sherrington, C. (1898). Decerebrate rigidity and reflex coordination of movements. *J.Physiol* **22**, 319-332.

Shik, M. L., Severin F.L, & Orlovskii, G. N. (1966). Control of walking and running by means of elecetrical stimulation of the mid-brain. *Biophysics* **11**, 756-765.

Silos-Santiago, I. & Snider, W. D. (1992). Development of commissural neurons in the embryonic rat spinal cord. *J.Comp Neurol.* **325**, 514-526.

Singer, J. H. & Berger, A. J. (2000). Development of inhibitory synaptic transmission to motoneurons. *Brain Res.Bull.* **53**, 553-560.

Singer, J. H., Talley, E. M., Bayliss, D. A., & Berger, A. J. (1998). Development of glycinergic synaptic transmission to rat brain stem motoneurons. *J.Neurophysiol.* **80**, 2608-2620.

Sivilotti, L. & Nistri, A. (1991). GABA receptor mechanisms in the central nervous system. *Prog.Neurobiol.* **36**, 35-92.

Smith, J. C. (1997). Integration of cellular and network mechanisms in mammalian oscillatory motor circuits: insights from the respiratory oscillator. In *Neurons, Networks, and Motor Behavior*, eds. Stein, P. S. G., Grillner, S., Selverston, A. I., & Stuart, D. G., The MIT Press, Cambridge, Massachusetts, USA.

Smith, J. C., Butera, R. J., Koshiya, N., Del Negro, C., Wilson, C. G., & Johnson, S. M. (2000). Respiratory rhythm generation in neonatal and adult mammals: the hybrid pacemaker-network model. *Respir.Physiol* **122**, 131-147.

Soffe, S. R. (1987). Ionic and pharmacological properties of reciprocal inhibition in Xenopus embryo motoneurones. *J.Physiol* **382**, 463-473.

Soffe, S. R. (1989). Roles of glycinergic inhibition and n-methyl-d-aspartate receptor mediated excitation in the locomotor rhythmicity of one half of the *Xenopus* embryo central nervous system. *Eur.J.Neurosci.* **1**, 561-571.

Soffe, S. R. (1991). Triggering and gating of motor responses by sensory stimulation: behavioural selection in Xenopus embryos. *Proc.R.Soc.Lond B Biol.Sci.* **246**, 197-203.

Sqalli-Houssaini, Y., Cazalets, J. R., & Clarac, F. (1993). Oscillatory properties of the central pattern generator for locomotion in neonatal rats. *J.Neurophysiol.* **70**, 803-813.

Staley, K. J., Longacher, M., Bains, J. S., & Yee, A. (1998). Presynaptic modulation of CA3 network activity. *Nat.Neurosci.* **1**, 201-209.

Staley, K. J. & Mody, I. (1992). Shunting of excitatory input to dentate gyrus granule cells by a depolarizing GABAA receptor-mediated postsynaptic conductance. *J.Neurophysiol.* **68**, 197-212.

Steriade, M. (1994). Sleep oscillations and their blockage by activating systems. *J.Psychiatry Neurosci.* **19**, 354-358.

Steriade, M. (2000). Corticothalamic resonance, states of vigilance and mentation. *Neuroscience* **101**, 243-276.

Streit, J., Luscher, C., & Luscher, H. R. (1992). Depression of postsynaptic potentials by high-frequency stimulation in embryonic motoneurons grown in spinal cord slice cultures. *J.Neurophysiol.* **68**, 1793-1803.

Streit, J., Tscherter, A., Heuschkel, M. O., & Renaud, P. (2001). The generation of rhythmic activity in dissociated cultures of rat spinal cord. *Eur.J.Neurosci.* **14**, 191-202.

Stuart, G. J. & Redman, S. J. (1992). The role of $GABA_A$ and $GABA_B$ receptors in presynaptic inhibition of Ia EPSPs in cat spinal motoneurones. *J.Physiol* **447**, 675-692.

Svirskis, G. & Hounsgaard, J. (1997). Depolarization-induced facilitation of a plateau-generating current in ventral horn neurons in the turtle spinal cord. *J.Neurophysiol.* **78**, 1740-1742.

Svirskis, G. & Hounsgaard, J. (1998). Transmitter regulation of plateau properties in turtle motoneurons. *J.Neurophysiol.* **79**, 45-50.

Tabak, J., Rinzel, J., & O'Donovan, M. J. (2001). The role of activity-dependent network depression in the expression and self-regulation of spontaneous activity in the developing spinal cord. *J.Neurosci.* **21**, 8966-8978.

Tabak, J., Senn, W., O'Donovan, M. J., & Rinzel, J. (2000). Modeling of spontaneous activity in developing spinal cord using activity-dependent depression in an excitatory network. *J.Neurosci.* **20**, 3041-3056.

Takahashi, M. & Alford, S. (2002). The requirement of presynaptic metabotropic glutamate receptors for the maintenance of locomotion. *J.Neurosci.* **22**, 3692-3699.

Toms, N. J., Jane, D. E., Kemp, M. C., Bedingfield, J. S., & Roberts, P. J. (1996). The effects of (RS)-alpha-cyclopropyl-4-phosphonophenylglycine ((RS)-CPPG), a potent and selective metabotropic glutamate receptor antagonist. *Br.J.Pharmacol.* **119**, 851-854.

Tresch, M. C. & Kiehn, O. (1999). Coding of locomotor phase in populations of neurons in rostral and caudal segments of the neonatal rat lumbar spinal cord. *J.Neurophysiol.* **82**, 3563-3574.

Tresch, M. C. & Kiehn, O. (2000). Motor coordination without action potentials in the mammalian spinal cord. *Nat.Neurosci.* **3**, 593-599.

Tscherter, A., Heuschkel, M. O., Renaud, P., & Streit, J. (2001). Spatiotemporal characterization of rhythmic activity in rat spinal cord slice cultures. *Eur.J.Neurosci.* **14**, 179-190.

Ugolini, A., Corsi, M., & Bordi, F. (1999). Potentiation of NMDA and AMPA responses by the specific mGluR5 agonist CHPG in spinal cord motoneurons. *Neuropharmacology* **38**, 1569-1576.

Urban, L., Thompson, S. W., & Dray, A. (1994). Modulation of spinal excitability: co-operation between neurokinin and excitatory amino acid neurotransmitters. *Trends Neurosci.* **17**, 432-438.

Valerio, A., Paterlini, M., Boifava, M., Memo, M., & Spano, P. (1997). Metabotropic glutamate receptor mRNA expression in rat spinal cord. *Neuroreport* **8**, 2695-2699.

van den Pol, A. N., Gao, X. B., Patrylo, P. R., Ghosh, P. K., & Obrietan, K. (1998). Glutamate inhibits GABA excitatory activity in developing neurons. *J.Neurosci.* **18**, 10749-10761.

Viana, F., Bayliss, D. A., & Berger, A. J. (1995). Repetitive firing properties of developing rat brainstem motoneurones. *J.Physiol* **486 (Pt 3)**, 745-761.

Wallen, P. (1997). Spinal networks and sensory feedback in the control of undulatory swimming in the lamprey. In *Neurons, Networks, and Motor Behavior*, eds. Stein, P. S. G., Grillner, S., Selverston, A. I., & Stuart, D. G., pp. 75-81. The MIT Press, Cambridge, Massachusetts, USA.

Wallen, P., Grafe, P., & Grillner, S. (1984). Phasic variations of extracellular potassium during fictive swimming in the lamprey spinal cord in vitro. *Acta Physiol Scand.* **120**, 457-463.

Wallen, P. & Grillner, S. (1987). N-methyl-D-aspartate receptor-induced, inherent oscillatory activity in neurons active during fictive locomotion in the lamprey. *J.Neurosci.* **7**, 2745-2755.

Walton, K. D. & Chesler, M. (1988). Activity-related extracellular potassium transients in the neonatal rat spinal cord: an in vitro study. *Neuroscience* **25**, 983-995.

Wang, J., Reichling, D. B., Kyrozis, A., & MacDermott, A. B. (1994). Developmental loss of GABA- and glycine-induced depolarization and Ca^{2+} transients in embryonic rat dorsal horn neurons in culture. *Eur.J.Neurosci.* **6**, 1275-1280.

Wenner, P. & O'Donovan, M. J. (2001). Mechanisms that initiate spontaneous network activity in the developing chick spinal cord. *J.Neurophysiol.* **86**, 1481-1498.

Werman, R. (1969). An electrophysiological approach to drug-receptor mechanisms. *Comp Biochem.Physiol* **30**, 997-1017.

Werman, R., Davidoff, R. A., & Aprison, M. H. (1968). Inhibitory of glycine on spinal neurons in the cat. *J.Neurophysiol.* **31**, 81-95.

Whelan, P., Bonnot, A., & O'Donovan, M. J. (2000). Properties of rhythmic activity generated by the isolated spinal cord of the neonatal mouse. *J.Neurophysiol.* **84**, 2821-2833.

Wu, W. L., Ziskind-Conhaim, L., & Sweet, M. A. (1992). Early development of glycine- and GABA-mediated synapses in rat spinal cord. *J.Neurosci.* **12**, 3935-3945.

Yamada, K. & Akasu, T. (1996). Substance P suppresses $GABA_A$ receptor function via protein kinase C in primary sensory neurones of bullfrogs. *J.Physiol* **496 (Pt 2)**, 439-449.

Zerari, F., Karpitskiy, V., Krause, J., Descarries, L., & Couture, R. (1997). Immunoelectron microscopic localization of NK-3 receptor in the rat spinal cord. *Neuroreport* **8**, 2661-2664.

Zhong, J., Gerber, G., Kojic, L., & Randic, M. (2000). Dual modulation of excitatory synaptic transmission by agonists at group I metabotropic glutamate receptors in the rat spinal dorsal horn. *Brain Res.* **887**, 359-377.

ABBREVIATIONS

ACSF: Artificial Cerebrospinal Fluid

AHP: Afterhyperpolarization

CNS: Central Nervous System

CPG: Central Pattern Generator

DC: Direct Current

DR: Dorsal Root

DRP: Dorsal Root Potential

EAA: Excitatory Aminoacids

EPSP: Excitatory Postsynaptic Potential

I.B.I.: Interburst Interval

IP_3: inositol 1,4,5-trisphosphate

IPSP: Inhibitory Postsynaptic Potential

I-V: Current-Voltage

mGluR: Metabotropic Glutamate Receptor

PAD: Primary Afferent Depolarization

PSP: Post-synaptic Potential

rPSP: recurrent Post-synaptic Potential

SD: Standard Deviation

Th: Threshold

V_m: Membrane Potential

VR: Ventral Root

Abbreviations for Substances

5-HT: 5-hydroxytryptamine

AIDA: (*RS*)-1-Aminoindan-1,5-dicarboxylic acid

AMPA: α-Amino-3-hydroxy-5-methyl-4-isoxazolepropionic acid

CNQX: 6-Cyano-7-nitroquinoxaline-2,3-dione

CPPG: (*RS*)-*a*-Cyclopropyl-4-phosphonophenylglycine

DCG-IV: (2*S*,2'*R*,3'*R*)-2-(2',3'-Dicarboxycyclopropyl)glycine

DHPG: (*RS*)-3,5-Dihydroxyphenylglycine

EGLU: (2*S*)-*α*-Ethylglutamic acid

GABA: γ-aminobutyric acid

L-AP4: L-(+)-2-Amino-4-phosphonobutyric acid

MCPG: (*RS*)-α-Methyl-4-carboxyphenylglycine

MPEP: 2-Methyl-6-(phenylethynyl)pyridine hydrochloride

NMDA: N-Methyl-D-Aspartate

t-ACPD: (±)-1-Aminocyclopentane-trans-1,3-dicarboxylic acid

TTX: Tetrodotoxin

ACKNOWLEDGEMENTS

I would like to deeply thank Prof. Andrea Nistri for his constant and careful supervision during all these years. His dedication to neuroscience and trust in me were often encouraging and fundamental for my growth in this field. I would also like to thank Dr. Marco Beato, for his precious teaching, and from whom it was a real pleasure to learn. My gratitude goes to Dr. Laura Ballerini, for always being present and helpful whenever I asked her help. A special thank goes to Dr. Giuliano Taccola, for having shared with me the study of "the monster" (!), something I wouldn't have survived to by myself. I would also like to thank all the people in the Bellavista that have been helpful in many ways (not only work!) and that have made my work a lot more pleasant.

Finally, thank you to my family, for always being supportive, and a very special thanks to all my friends here and away: each one of them, for a special reason, really 'made the difference'.